

Abstract

Virological measurements are often interpreted as reporting direct properties of virions, such as structure, stiffness, mobility, dielectric response, infectivity, or titer. In practice, however, an experiment rarely observes the full latent virion–environment ensemble. It reports a protocol-conditioned observed ensemble shaped by sample preparation, surfaces, fields, structured media, timing, biological selection, amplification, detection thresholds, and readout. This paper develops a mathematical framework for this process, termed *experimental collapse*, within a protocol-resolved virophysics. The central object is a null-inclusive protocol observation operator,

$$P_{\text{obs},t}^{\varnothing}(\cdot | E) = \mathcal{M}_E^{\varnothing} P_{\text{ref},t},$$

which maps a reference latent ensemble to the observed ensemble generated by a specified protocol E , including possible null outcomes. This formulation separates latent-state transformation, survival or detection weighting, readout, and non-observation, allowing protocol effects to be treated as explicit components of the measurement rather than as informal sources of bias.

The framework defines protocol-conditioned latent ensembles, observed ensembles, detection yields, collapse functionals, protocol blindness, observation equivalence, Fisher-information observability, inverse inference, and multi-protocol consistency. It also provides a mechanism-resolved language for common collapse channels, including preparation and interface effects, geometric projection, reconstruction, surface immobilization, mechanical loading, field steering, medium filtering, time-window selection, biological amplification, neutralization, endpoint censoring, and detection thresholds. In this view, protocol dependence is not only a limitation of measurement. It is also the forward mechanism by which latent virion–environment mechanics becomes experimentally inferable.

As a worked example, the plaque assay is developed as a classical instance of experimental collapse. A plaque count is shown to estimate an effective protocol-conditioned infectious concentration,

$$\Lambda_{\text{PFU}} = \int_{\Psi} \pi_{\text{PFU}}(x; E_{\text{PFU}}) n_{\text{ref}}(x) dx,$$

rather than the total physical particle concentration. In the dilute, well-mixed, non-overlapping regime, this quantity recovers the standard Poisson plaque-count model and PFU titer formula. Extensions to overdispersed counts, zero inflation, plaque merging, endpoint dilution, neutralization, and morphology-augmented readouts show how deviations from the ideal model can be interpreted as protocol-conditioned information rather than as merely statistical noise. Overall, the paper argues that virological data are most precisely interpreted as outputs of explicit protocol kernels. This perspective clarifies what a measurement reports, what it leaves unresolved, and how complementary protocols can be designed to recover otherwise hidden latent structure.

Experimental Collapse in Virophysics

Protocol-Resolved Observation, Inference, and Plaque-Assay Blindness

Lillian St. Kleess

May 27, 2026

Contents

1	Introduction & Conceptual Overview	4
1.1	Latent, Protocol-Conditioned, and Observed Ensembles	6
1.2	Protocol Blindness	7
1.3	Collapse as an Inverse Problem	9
1.4	Multi-Protocol Consistency	10
1.5	Plaque Assays as a Worked Example of Experimental Collapse	12
2	Experimental Collapse: Concept and Mathematical Formulation	29
2.1	Experimental Protocols	30
2.2	Latent and Observed State Spaces	30
2.3	Protocol Transformation Kernels	31
2.4	Survival, Detection, and Null Observations	33
2.5	Readout Kernels and Observed Ensembles	34
2.6	Collapse Functionals	36
2.7	Protocol Blindness and Fisher-Information Observability	38
3	Latent, Protocol-Conditioned, and Observed Ensembles	42
3.1	Reference Latent Ensembles	42
3.2	Protocol-Conditioned Latent Ensembles	43
3.3	Survival, Detection, and Null Observations	45
3.4	Readout Kernels and Observed Ensembles	46
3.5	Latent versus Observed Virion State	48
3.6	Protocol Observation Operators	54
3.7	Protocol-Lifted Observables	56
3.8	Mechanism-Resolved Collapse Channels	58
3.9	Quantifying Experimental Collapse	61
3.10	Modal and Dynamical Collapse	65
3.11	Collapse Severity Classes	66
3.12	Experimental Collapse and Inverse Inference	68

3.13	Protocol Identifiability	71
3.14	Fisher-Information Observability	73
3.15	Multi-Protocol Consistency	78
3.16	Inverse Environmental Inference	80
3.17	Worked Example Template: Comparing Protocols	83
3.18	Section Reference: Core Objects and Equations	85
	Section Reference: Core Objects and Equations	85
4	Mechanisms of Experimental Collapse	89
4.1	Mechanism-Resolved Factorization	90
4.2	Preparation and Interface Collapse	91
4.3	Geometric Projection and Reconstruction Collapse	93
4.4	Medium Filtering and Adhesive Collapse	97
4.5	Time-Window and Persistence Collapse	99
4.6	Detection, Rejection, and Null-Channel Collapse	107
4.7	Mechanism-Level Identifiability and Fisher-Information Observability	116
4.8	Multi-Protocol Inference after Mechanism-Resolved Collapse	121
4.9	Section Reference: Mechanisms, Inference, and Protocol Design	136
	Section Reference: Mechanisms, Inference, and Protocol Design	136
5	Worked Example: The Plaque Assay as Experimental Collapse	141
5.1	Plaque-Assay Protocol as a Collapse Map	142
5.2	Plaque-Forming Probability as a Protocol Weight	143
5.3	Plaque-Count Statistics in the Dilute Regime	145
5.4	Single-Unit Readout Kernel and Null Channel	148
5.5	Plaque-Assay Protocol Blindness	150
5.6	Two-Subpopulation Reduction	152
	Section Reference: Plaque Assay as Experimental Collapse	165
6	Conclusion	168

1 Introduction & Conceptual Overview

Virological experiments often appear to answer direct questions. How many infectious particles are present in a sample? What is the structure of the virion? How stiff is the capsid or envelope? How does a particle move through mucus, gel, or extracellular matrix? How does it respond to an applied electric field? These questions are experimentally well defined, but each contains an important theoretical distinction. A measurement does not usually report the full microscopic state of a virion population. It reports the part of that state made visible, stable, selectable, amplifiable, or readable under a particular experimental protocol.

This paper develops that distinction into a framework called *protocol-resolved virophysics*. The central idea is that a virological measurement should not be treated as a protocol-free window onto a virion population, but as a protocol-conditioned map from latent virion–environment states to observed data. In its most compact form,

$$\boxed{\text{Latent virion–environment ensemble} \xrightarrow{\text{Experimental protocol}} \text{Observed ensemble.}} \quad (1.1)$$

The observed ensemble is genuine experimental data. The purpose of this distinction is not to weaken the status of such data, but to identify what kind of object it is: the output of a specified preparation, conditioning, selection, transformation, amplification, and readout procedure.

We call this protocol-conditioned reduction *experimental collapse*. The term is used here in a classical statistical and biophysical sense, *not* as a claim about quantum measurement. Experimental collapse refers to the way a high-dimensional latent virion–environment ensemble is transformed, selected, projected, amplified, or partially erased by an experimental procedure before it becomes reported data.

At the level of measures, the organizing equation of the paper is

$$\boxed{P_{\text{obs},t}^{\varnothing}(\cdot | E) = \mathcal{M}_{E,t}^{\varnothing} P_{\text{ref},t}.} \quad (1.2)$$

Here $P_{\text{ref},t}$ is a reference latent ensemble, $\mathcal{M}_{E,t}^{\varnothing}$ is the null-inclusive observation operator associated with protocol E , and $P_{\text{obs},t}^{\varnothing}(\cdot | E)$ is the observed ensemble, including possible null outcomes. Equation (1.2) is deliberately compact. It plays the same introductory role that $H = T + V$ often plays in mechanics: it states the structure of the theory first, before the detailed components are unfolded.

To write the same idea more explicitly, let Ψ denote the latent state space and let \mathcal{Y} denote the non-null observed data space. The null-enlarged observation space is

$$\mathcal{Y}^{\varnothing} = \mathcal{Y} \cup \{\varnothing\}, \quad (1.3)$$

where \varnothing denotes the event that no accepted datum is reported. For any measurable set $A \subseteq \mathcal{Y}^{\varnothing}$,

$$\boxed{P_{\text{obs},t}^{\varnothing}(A | E) = \int_{\Psi} K_E^{\varnothing}(A | x) P_{\text{ref},t}(dx).} \quad (1.4)$$

The kernel K_E^{\varnothing} is the protocol’s observation kernel. It collects the transformations between a latent

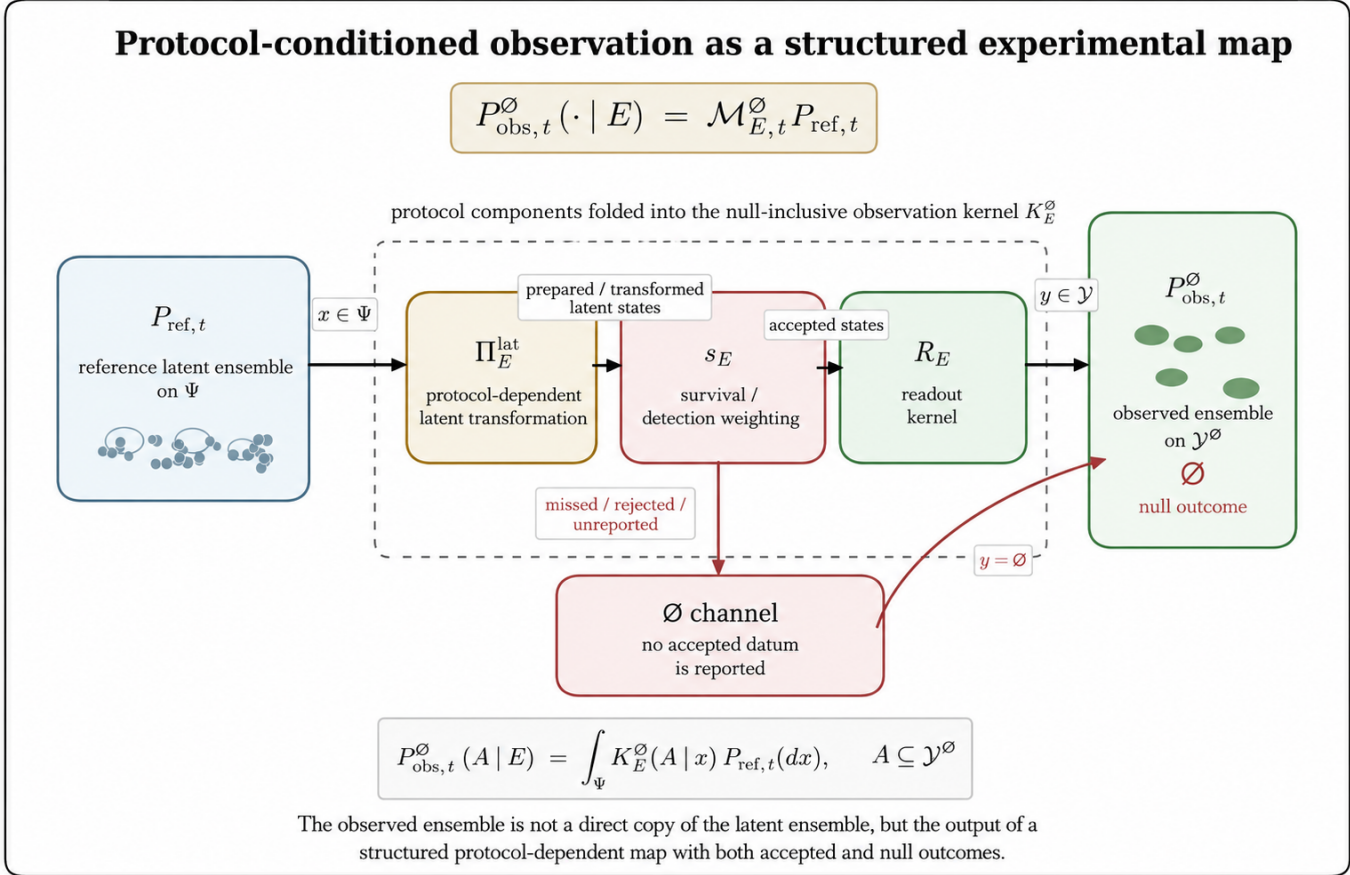


Figure 1. Protocol-conditioned observation as a structured experimental map. A reference latent ensemble $P_{\text{ref},t}$ on the latent state space Ψ is acted on by protocol-dependent components, including a latent transformation Π_E^{lat} , survival or detection weighting s_E , and a readout kernel R_E . These components are absorbed into the null-inclusive observation kernel K_E^{\emptyset} , which maps latent states either to reported observations in \mathcal{Y} or to the null outcome \emptyset . The observed ensemble $P_{\text{obs},t}^{\emptyset}$ is therefore not a direct copy of the latent ensemble, but the output of a structured, protocol-conditioned experimental map.

state $x \in \Psi$ and a reported datum $y \in \mathcal{Y}$, including physical conditioning, biological filtering, selection, loss, readout, and the possibility that no accepted datum is reported at all.

The need for this framework is visible across virology. In cryo-EM and cryo-ET, the final density map or tomogram depends not only on virion structure, but also on grid preparation, air–water interface exposure, ice thickness, vitrification, particle orientation, particle picking, alignment, classification, and reconstruction [1, 3, 4, 5, 33, 47]. In AFM, a reported height, rupture force, or indentation stiffness is conditioned by surface attachment, hydration, tip geometry, loading rate, indentation depth, and the mechanical model used to interpret the force–deformation curve [50, 6, 7, 8, 9]. In dielectrophoresis and electrorotation, the observed trajectory, trapping behavior, crossover frequency, or rotation rate depends on the imposed electric field, medium conductivity, permittivity, hydrodynamic drag, and particle polarizability [10, 11, 12, 13]. In mucus or gel tracking, a reported diffusivity or trajectory class is a joint property of the virion and the structured medium, including mesh scale, mucin interactions, adhesion, antibody-mediated immobilization, local rheology, and tracking thresholds [14, 35, 15, 24, 23]. Even the plaque assay, one of the most classical and useful measurements in virology, has this structure.

A plaque count is not a direct count of physical particles. It is a count of visible infectious lesions produced under a specified cell line, adsorption time, overlay, incubation time, staining method, and counting rule [16, 36, 17, 18, 60]. A structurally intact particle, a defective particle, a damaged particle, an aggregate, a neutralized particle, a cell-line-incompatible particle, and an entry-competent but replication-incompetent particle may all produce the same observed result: no plaque. Conversely, a single visible plaque reports a successful biological pathway, not a full microscopic history. The plaque assay therefore provides a particularly clear example of experimental collapse: a biological protocol converts a heterogeneous latent particle population into a countable set of visible lesions.

The purpose of this paper is not to argue that protocol-conditioned measurements are unreliable. On the contrary, protocol-conditioned measurements are the foundation of experimental virology. Cryo-EM is powerful because it preserves and reconstructs structure. AFM is powerful because it applies force. Field-driven assays are powerful because they couple to electrical and hydrodynamic response. Tracking is powerful because it records motion through specified environments. Plaque assays are powerful because they amplify infectious activity into countable lesions. The point is more precise: each protocol asks a particular question of the virion–environment system, and the observed ensemble is the answer to that question.

This distinction matters because protocol-conditioned observations can be misread in two opposite ways. The first mistake is to treat the observed ensemble as if it were a direct, protocol-free sample of the latent virion population. The second is to dismiss protocol-conditioned data as mere artifact. The framework developed here avoids both mistakes. It treats the observed ensemble as valid, but valid as the output of a specified experimental map.

1.1 Latent, Protocol-Conditioned, and Observed Ensembles

The basic mathematical object of the paper is a chain of ensembles:

$$\boxed{P_{\text{ref},t} \xrightarrow{\Pi_E^{\text{lat}}} \tilde{P}_{E,t}^{\text{lat}} \xrightarrow{s_E, R_E, \emptyset} P_{\text{obs},t}^{\emptyset}(\cdot | E)}. \quad (1.1.1)$$

The reference latent ensemble $P_{\text{ref},t}$ describes the distribution of virion or virion–environment states before the additional conditioning imposed by the experimental protocol. The latent transformation kernel Π_E^{lat} describes how preparation, surfaces, fields, loading, media, timing, or biological conditions transform the latent state before readout. The survival or detection weight s_E describes which protocol-conditioned states remain visible to the accepted readout channel. The readout kernel R_E describes how surviving states become reported data. The null outcome \emptyset records states that are present in the latent ensemble but produce no accepted observation under protocol E .

A useful expanded form of the observation kernel is

$$K_E^{\emptyset}(A | x) = \int_{\Psi_E} \left[s_E(z) R_E(A \cap \mathcal{Y} | z) + (1 - s_E(z)) \mathbf{1}_A(\emptyset) \right] \Pi_E^{\text{lat}}(dz | x), \quad (1.1.2)$$

where $z \in \Psi_E$ denotes a protocol-conditioned latent state, $s_E(z) \in [0, 1]$ is the probability or weight that the state survives into the accepted readout channel, and $R_E(\cdot | z)$ is the non-null readout kernel. This expression separates three effects that are often conflated in informal experimental language: latent transformation, survival or detection weighting, and readout.

Component	Interpretation
Π_E^{lat}	Physical or biological transformation of the latent ensemble before readout; examples include adsorption, field steering, dilution, mechanical loading, incubation, or passage through a structured medium.
s_E	Survival, visibility, detectability, infectivity, localization, or acceptance weighting; this determines which conditioned states remain in the reported data channel.
R_E	Instrumental, computational, or biological readout; examples include image reconstruction, force-curve fitting, trajectory estimation, fluorescence thresholding, or plaque counting.
\emptyset	Null channel for states that are present in the latent ensemble but produce no accepted observation under protocol E .

Table 1. Interpretation of the main components of the null-inclusive observation kernel in Eq. (1.1.2).

This separation is important because different parts of a protocol have different meanings. Surface adsorption may physically transform the state. Particle picking may select which states are reported. Finite resolution may project a surviving state into a lower-dimensional representation. A plaque assay may biologically amplify some states while sending others into the null channel. These effects are not interchangeable. They are distinct components of the observation operator.

1.2 Protocol Blindness

Once measurement is written as a map from latent states to observed data, it becomes possible to ask a precise complementary question: what does a given protocol fail to distinguish? This failure is not necessarily an experimental mistake. It is a structural property of the protocol. A protocol can only report distinctions to which its preparation, selection, transformation, and readout channels are sensitive.

At the state level, two latent states $x_1, x_2 \in \Psi$ are *observation-equivalent* under protocol E if they induce the same null-inclusive distribution over observed outcomes:

$$\boxed{x_1 \sim_E x_2 \iff K_E^\emptyset(\cdot | x_1) = K_E^\emptyset(\cdot | x_2).} \quad (1.2.1)$$

No amount of repeated observation under protocol E alone can distinguish states in the same equivalence class, unless additional assumptions, additional measurements, or protocol variation are introduced. In this sense, the protocol defines a quotient of the latent state space:

$$\boxed{\Psi \longrightarrow \Psi / \sim_E.} \quad (1.2.2)$$

The quotient Ψ / \sim_E is the part of the latent state space that remains distinguishable after the protocol has acted. Distinctions that survive the map are observable under E ; distinctions identified by the equivalence relation are collapsed by E .

This is the basic meaning of *protocol blindness*. A protocol is blind to a latent distinction when

different latent states, mechanisms, or parameter values produce the same observed distribution under that protocol. Protocol blindness therefore does not mean that the hidden distinction is physically absent. It means that the distinction is not resolved by the experimental map being used. At the parameter level, protocol blindness can be expressed through Fisher information.

Let

$$p_E^\varnothing(y | \theta)$$

be a protocol-conditioned likelihood, with density or mass taken with respect to a common dominating measure on \mathcal{Y}^\varnothing , including the atom at \varnothing . The Fisher-information matrix is

$$\mathcal{I}_E(\theta) = \mathbb{E}_{Y \sim p_E^\varnothing(\cdot | \theta)} \left[\nabla_\theta \log p_E^\varnothing(Y | \theta) \nabla_\theta \log p_E^\varnothing(Y | \theta)^\top \right]. \quad (1.2.3)$$

A parameter direction v is locally blind under protocol E when the likelihood does not change to first order in that direction. Equivalently, under the usual regularity assumptions,

$$\boxed{v \in \mathcal{B}_E(\theta) \iff v^\top \mathcal{I}_E(\theta) v = 0,} \quad (1.2.4)$$

where $\mathcal{B}_E(\theta)$ is the local blind subspace of the protocol at parameter value θ . Thus, $\mathcal{I}_E(\theta)$ identifies which parameter combinations are locally visible to the protocol and which parameter combinations lie in directions of vanishing statistical sensitivity.

This gives a local, information-theoretic form of protocol blindness. If $v^\top \mathcal{I}_E(\theta) v = 0$, then infinitesimal changes in θ along v do not produce a first-order change in the observed likelihood. Such a direction may correspond to a genuine physical parameter, but one that is not coupled to the protocol, is selected away, is averaged over, is below threshold, or is mapped into the same observed category as other states.

Mode of blindness	Interpretation
Uncoupled sector	The latent variable exists, but the protocol does not couple to it. For example, an electrical assay may be insensitive to a mechanical parameter if the parameter does not affect polarizability, charge distribution, or hydrodynamic response.
Selection blindness	The protocol preferentially admits some states and excludes others before readout. The excluded states enter the null channel or are absent from the accepted data set.
Projection or averaging	Distinct latent states are mapped to the same lower-dimensional observable, such as a scalar intensity, fitted stiffness, apparent diffusivity, or plaque count.
Threshold blindness	The relevant distinction changes the observed distribution, but only below the resolution, detection, counting, or classification threshold of the experiment.
Confounding	Two or more latent parameters affect the observed likelihood in nearly the same direction, making their individual contributions difficult or impossible to separate under protocol E alone.

Table 2. Common mechanisms by which a protocol can become blind to latent distinctions. These mechanisms are not mutually exclusive; a single experimental procedure can combine selection, projection, thresholding, and confounding.

The experimental consequence is important. Absence of a signal under one protocol is not automatically evidence of absence in the latent mechanics. It may instead mean that the relevant sector is not coupled to the protocol, is removed by selection, is averaged over by the readout, falls below threshold, or is statistically confounded with another parameter. Protocol-resolved interpretation therefore asks not only what a measurement reports, but also what distinctions the measurement is structurally unable to resolve.

1.3 Collapse as an Inverse Problem

Experimental collapse is not only a limitation. It is also the forward map that makes inference possible. If the protocol kernel is known, calibrated, estimated, or parametrized, then observed data can be used to infer latent virion parameters, environmental parameters, and protocol parameters. In this sense, collapse is not merely distortion or loss. It is also signal generation: the protocol perturbs, selects, amplifies, or reads out the system in a way that makes certain latent properties experimentally accessible.

Let the full parameter vector be decomposed as

$$\theta = (\theta_{\text{vir}}, \theta_{\text{env}}, \theta_E), \quad (1.3.1)$$

where θ_{vir} denotes virion parameters, θ_{env} denotes environmental parameters, and θ_E denotes protocol

parameters. A protocol-resolved forward model then has the compact form

$$\theta \longmapsto P_{\text{obs},t}^{\varnothing}(\cdot | E, \theta) = \mathcal{M}_{E,t}^{\varnothing}(\theta_E) P_{\text{ref},t}(\cdot | \theta_{\text{vir}}, \theta_{\text{env}}). \quad (1.3.2)$$

This is the forward model for a protocol-resolved inverse problem [28, 29, 56]. The inverse problem asks which values of θ are compatible with the observed ensemble, given the experimental map that produced it. The same relation can be summarized schematically as

$$\boxed{\text{Observed protocol-conditioned data} \longrightarrow \left\{ \begin{array}{c} \text{Virion parameters} \\ \text{Environmental parameters} \\ \text{Protocol parameters} \end{array} \right\}.} \quad (1.3.3)$$

The arrow in Eq. (1.3.3) should not be read as a direct algebraic inversion. It represents an inference problem constrained by the forward operator $\mathcal{M}_{E,t}^{\varnothing}$, the latent ensemble model $P_{\text{ref},t}$, the data likelihood, and any prior physical, biological, or experimental information.

This formulation is especially useful for strongly conditioning protocols. AFM loading is inferentially useful because it makes mechanical compliance visible. Dielectrophoresis and electrorotation are useful because applied fields make dielectric response, charge asymmetry, hydrodynamic drag, and polarizability visible. Mucus and gel tracking are useful because the medium makes transport, adhesion, immobilization, and local rheological response visible. Plaque assays are useful because biological amplification makes infectious activity visible. In each case, the protocol changes the ensemble, but if that change is modeled, calibrated, or statistically constrained, it can be used to infer properties that would otherwise remain hidden.

The central practical question is therefore not whether the protocol perturbs the system. It does. The question is whether the perturbation is characterized well enough to be used as part of the inference. A protocol-resolved theory treats the experiment and the virion–environment system together: the observed data are not a direct copy of the latent population, but neither are they merely artifact. They are the output of a structured forward map, and that map determines both what can be inferred and what remains blind.

1.4 Multi-Protocol Consistency

Different experimental protocols generally collapse different latent sectors of the same virion–environment ensemble. Accordingly, multi-protocol comparison should not be formulated as a demand for raw observational agreement. A density map, a force–indentation curve, a field–response spectrum, a trajectory ensemble, and a plaque count are not expected to be identical objects, because they are not the same kind of measurement. They live in different observation spaces, are produced by different physical or biological transformations, and are filtered through different selection and readout mechanisms.

The relevant question is therefore not whether the raw observables look the same. The relevant question is whether these different observables can be explained by a *common latent model* viewed through different protocol-conditioned observation kernels. Multi-protocol consistency is thus a statement about shared latent explanation, not raw equality of measured outputs.

At the level of the present framework, suppose that M protocols E_1, \dots, E_M are applied to comparable virion–environment systems. The observed ensemble associated with protocol E_j is written as $P_{\text{obs},t}^{(j),\varnothing}$. Multi-protocol consistency asks whether each observed ensemble can be approximated by applying its own protocol-conditioned observation operator to the same underlying latent model:

$$\boxed{P_{\text{obs},t}^{(j),\varnothing}(\cdot) \approx \mathcal{M}_{E_j,t}^{\varnothing}(\lambda_j) P_{\text{ref},t}(\cdot \mid \theta), \quad j = 1, \dots, M.} \quad (1.4.1)$$

Here θ denotes the shared latent parameter vector, while λ_j collects protocol-specific nuisance parameters associated with protocol E_j . These nuisance parameters may represent calibration constants, instrument settings, background effects, detection thresholds, preparation artifacts, analysis choices, or other protocol-local quantities that influence the observation map without belonging to the common latent virion model itself.

The approximation symbol in Eq. (1.4.1) is important. In practice, one does not expect exact equality between an empirical dataset and an idealized forward model. Finite-sample variation, measurement noise, model error, biological heterogeneity, imperfect calibration, and residual protocol uncertainty all contribute to discrepancies. The question is whether the discrepancies are compatible with a single latent explanation once each protocol has been passed through its own observation map.

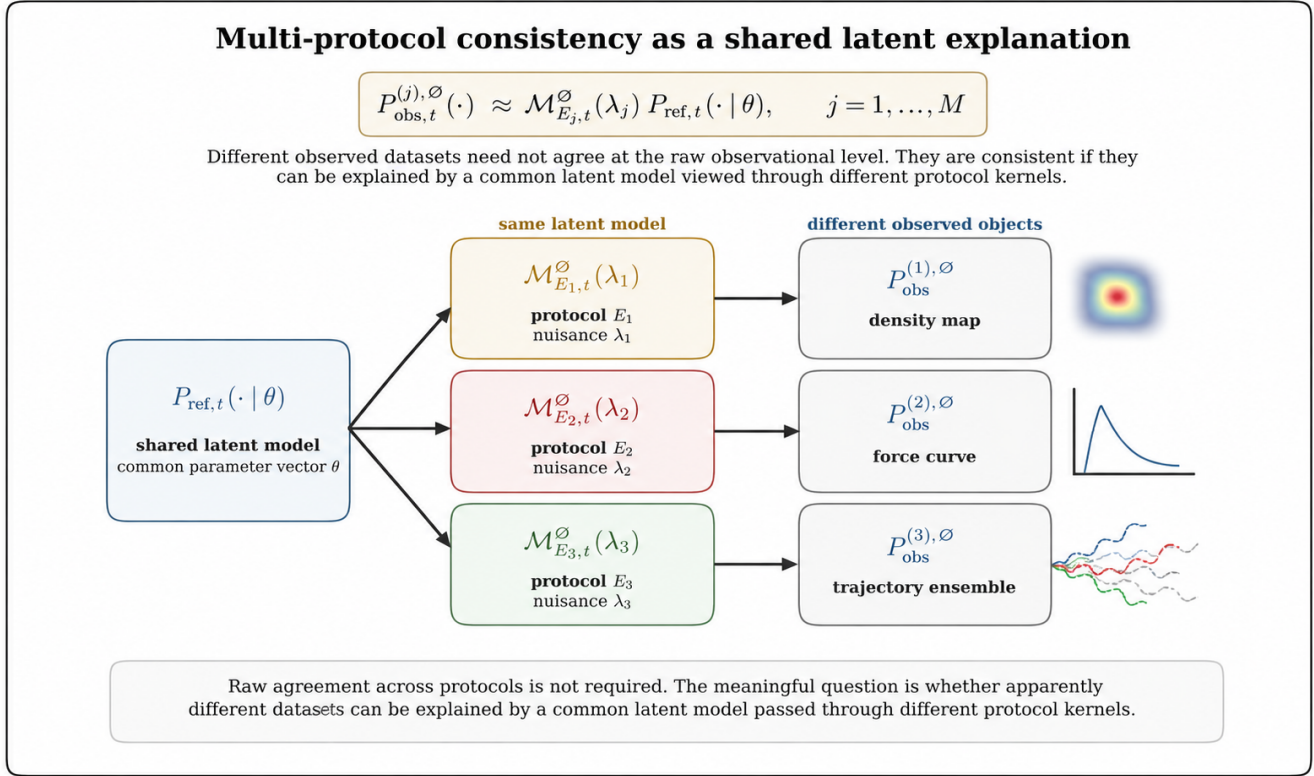


Figure 2. Multi-protocol consistency as a shared latent explanation. A single reference latent ensemble, $P_{\text{ref},t}(\cdot | \theta)$, is mapped through distinct protocol-specific observation operators $\mathcal{M}_{E_j,t}^{\varnothing}(\lambda_j)$, each with its own protocol-local nuisance parameters λ_j . The resulting observed ensembles, $P_{\text{obs},t}^{(j),\varnothing}$, need not agree at the raw observational level: one protocol may report a density map, another a force curve, and another a trajectory ensemble. In the protocol-resolved formulation, the relevant consistency question is not whether these observed data objects are identical, but whether they can be explained by a common latent virion–environment model after each protocol kernel has transformed, selected, projected, or nulled the latent ensemble. Apparent disagreement between protocols can therefore reflect complementary protocol-conditioned projections rather than incompatibility of the underlying latent model.

Equivalently, multi-protocol inference separates two kinds of variation: *latent variation*, which belongs to the virion–environment system itself, and *protocol-local variation*, which belongs to the experimental map. The shared parameter vector θ describes the former. The nuisance parameters $\lambda_1, \dots, \lambda_M$ describe the latter. A successful multi-protocol explanation is one in which the same latent model can generate the different observed ensembles after the appropriate protocol-specific conditioning has been applied.

1.5 Plaque Assays as a Worked Example of Experimental Collapse

The plaque assay provides a concrete worked example of the framework developed above. It is experimentally familiar, quantitative, and biologically meaningful: a virus-containing sample is diluted, applied to a susceptible cell monolayer, allowed to adsorb, constrained by an overlay, incubated, stained or otherwise visualized, and finally reported as a plaque count [16, 36, 17, 18, 60]. Yet the final observable is far lower-dimensional than the latent process that produces it. A plaque assay does not

directly report total physical particles, total genomes, antigen abundance, virion orientation, aggregation history, mechanical state, receptor-binding competence, entry probability, replication competence, or local spread efficiency. It reports the number of infection-competent units that successfully pass through a specified cell-line, adsorption, overlay, incubation, staining, detection, and counting protocol.

This distinction makes the plaque assay a useful anchor for protocol-resolved virophysics. The assay is not a noisy particle counter. It is a functional readout: it asks how much of the plated sample can generate visible, countable infectious lesions under the chosen experimental conditions. Thus, the relevant object is not a protocol-free property called “infectiousness,” but a protocol-conditioned probability of producing a visible plaque.

The central protocol-resolved quantity is the plaque-forming probability of a latent state:

$$\boxed{\pi_{\text{PFU}}(x; E_{\text{PFU}}) = \Pr \left(\begin{array}{c} \text{latent state } x \text{ generates a visible, countable plaque} \\ \text{under plaque-assay protocol } E_{\text{PFU}} \end{array} \right)}. \quad (1.5.1)$$

Here E_{PFU} denotes the full plaque-assay protocol, including the cell line, adsorption time, inoculum volume, overlay composition, incubation time, staining or reporter method, plaque-detection threshold, and counting rule. The probability $\pi_{\text{PFU}}(x; E_{\text{PFU}})$ is therefore not a context-free property of the particle alone. It belongs to the state-protocol pair (x, E_{PFU}) . A particle may be physically intact but non-plaque-forming under one cell line, overlay, incubation time, or detection threshold, while becoming plaque-forming under a different protocol. Plaque competence is therefore a protocol-conditioned functional property, not merely a structural label.

In the language of the observation-kernel formalism, the individual latent state x is mapped either into the visible-plaque channel or into the null channel:

$$\boxed{K_{E_{\text{PFU}}}^{\{\text{plaque}\}}(\{\text{plaque}\} | x) = \pi_{\text{PFU}}(x; E_{\text{PFU}}), \quad K_{E_{\text{PFU}}}^{\{\emptyset\}}(\{\emptyset\} | x) = 1 - \pi_{\text{PFU}}(x; E_{\text{PFU}})}. \quad (1.5.2)$$

This binary reduction is deliberately simplified, but it captures the key collapse: many physically distinct latent states may be mapped to the same observed outcome, especially the null outcome \emptyset . A structurally intact but cell-line-incompatible virion, a neutralized virion, a defective particle, a damaged particle, an aggregate that fails to initiate a countable lesion, and a particle that enters but fails to spread can all contribute the same observed result: no plaque.

The corresponding effective plaque-forming concentration is

$$\boxed{\Lambda_{\text{PFU}}(E_{\text{PFU}}) = \int_{\Psi} \pi_{\text{PFU}}(x; E_{\text{PFU}}) n_{\text{ref}}(x) dx.} \quad (1.5.3)$$

Here $n_{\text{ref}}(x)$ is the latent number-density distribution over the state space Ψ . Depending on the modeling resolution, the latent object x may represent an individual physical particle, an aggregate, an infection-competent unit, a damaged or defective particle, or another assay-relevant object. More generally, if the latent population is represented by a number measure $N_{\text{ref}}(dx)$, then Eq. (1.5.3) may be written as

$$\Lambda_{\text{PFU}}(E_{\text{PFU}}) = \int_{\Psi} \pi_{\text{PFU}}(x; E_{\text{PFU}}) N_{\text{ref}}(dx).$$

The density notation is used here for readability. Equation (1.5.3) is the central collapse equation for the plaque assay. It states that PFU is not the total physical particle concentration,

$$C_{\text{part}} = \int_{\Psi} n_{\text{ref}}(x) dx, \quad (1.5.4)$$

but a protocol-weighted infectious projection of that concentration. The plaque assay therefore maps a high-dimensional latent ensemble into one scalar functional: the expected concentration of visible plaque-forming events under the specified protocol.

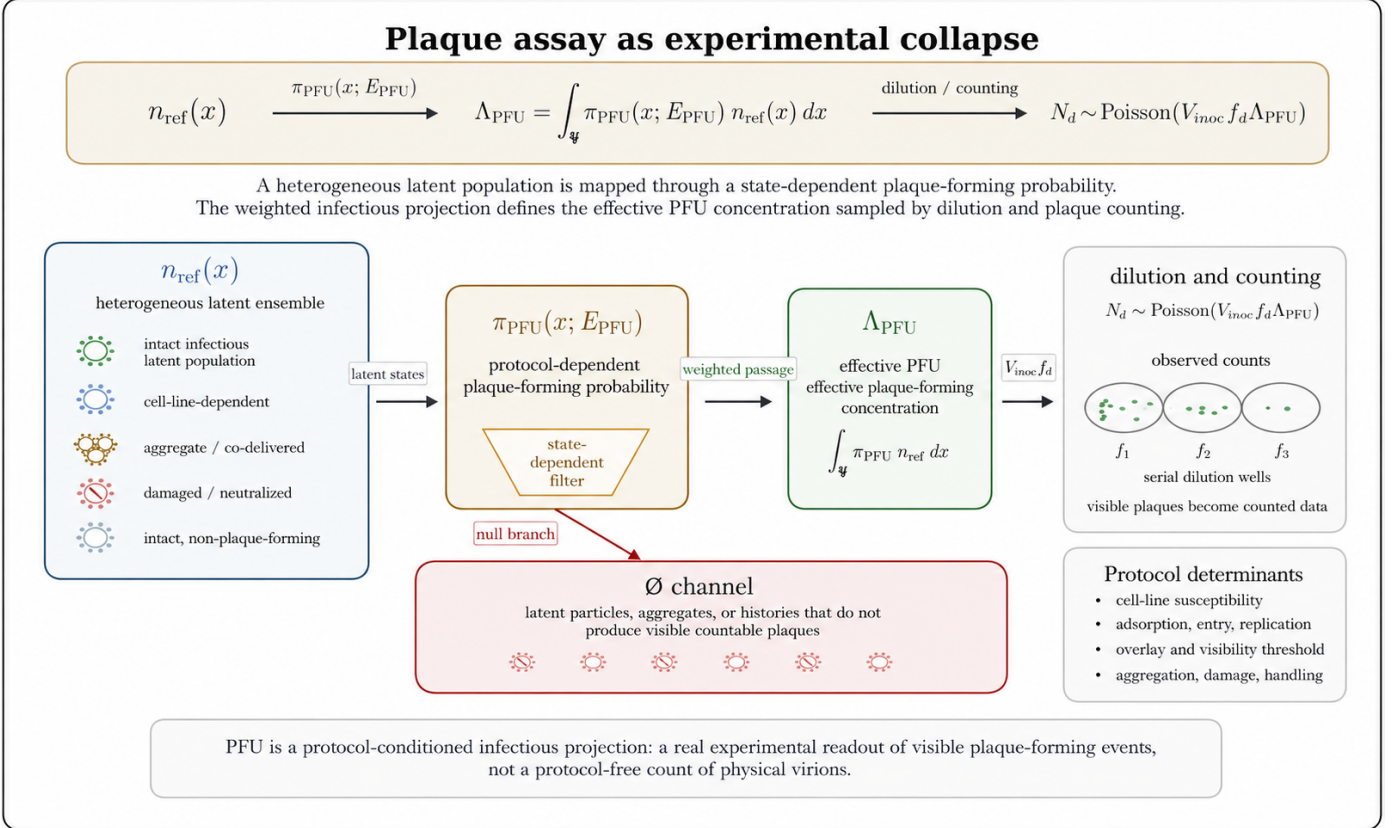


Figure 3. Plaque assay as experimental collapse. A heterogeneous latent virion or infectious-unit population is mapped through the protocol-dependent plaque-forming probability $\pi_{\text{PFU}}(x; E_{\text{PFU}})$. This state-dependent filter assigns different plaque-forming weights to intact infectious particles, cell-line-dependent particles, aggregates or co-delivered units, damaged or neutralized particles, and intact but non-plaque-forming particles. The weighted population defines the effective plaque-forming concentration Λ_{PFU} , which is then sampled through dilution and plaque counting to produce the observed count N_d . The null channel contains latent particles, aggregates, or assay histories that fail to produce visible countable plaques under the selected protocol. Thus PFU is a protocol-conditioned infectious projection of the latent ensemble, not a protocol-free count of total physical virions.

This observation also clarifies the meaning of particle-to-PFU or genome-to-PFU ratios. Such ratios are not merely measures of experimental inefficiency. They are coarse summaries of how much latent material is mapped into the visible plaque-forming channel under a specified protocol. Two samples with similar particle counts can have different plaque titers if their latent distributions place

different weight on plaque-forming states. Conversely, two samples with different latent compositions can produce similar plaque counts if their protocol-weighted plaque-forming concentrations agree. The plaque-forming probability $\pi_{\text{PFU}}(x; E_{\text{PFU}})$ can be understood as the probability that a latent virion, aggregate, or infectious unit passes through a sequence of protocol-dependent biological and observational stages. Plaque formation is therefore not a single intrinsic binary property of a particle. It is a terminal readout of a staged assay pathway.

Schematically, the pathway begins with a latent assay input and proceeds through delivery, adsorption, attachment and entry, productive replication, local spread, visibility, and counting. Failure at any required stage sends the latent state into the null channel for the plaque assay: no visible countable plaque is reported. This null outcome may reflect handling loss, poor delivery, failed adsorption, receptor incompatibility, failed entry, nonproductive replication, spread limitation under the overlay, subthreshold visibility, plaque merging, or a counting rule that excludes the event. This staged view is useful because different protocol variations act on different parts of the pathway. Adsorption time primarily perturbs delivery and cell contact. Cell line or receptor condition perturbs attachment, entry, and intracellular permissiveness. Neutralization can alter binding, entry, or aggregation. Overlay composition and incubation time affect local spread and visibility. Staining threshold and counting criteria act near the final readout. Thus changing a plaque-assay condition changes the biological observation kernel, not merely the numerical value of the final titer.

A low plaque count does not identify a unique failure mechanism by itself. It may arise because few competent particles are present, because competent particles are poorly coupled to the chosen cell line, because adsorption or entry is inefficient, because replication or spread is weak, or because the final lesion does not cross the visibility or counting threshold. Treating plaque formation as a staged biological pathway turns a scalar PFU readout into a structured set of possible bottlenecks that can be probed by controlled protocol variation.

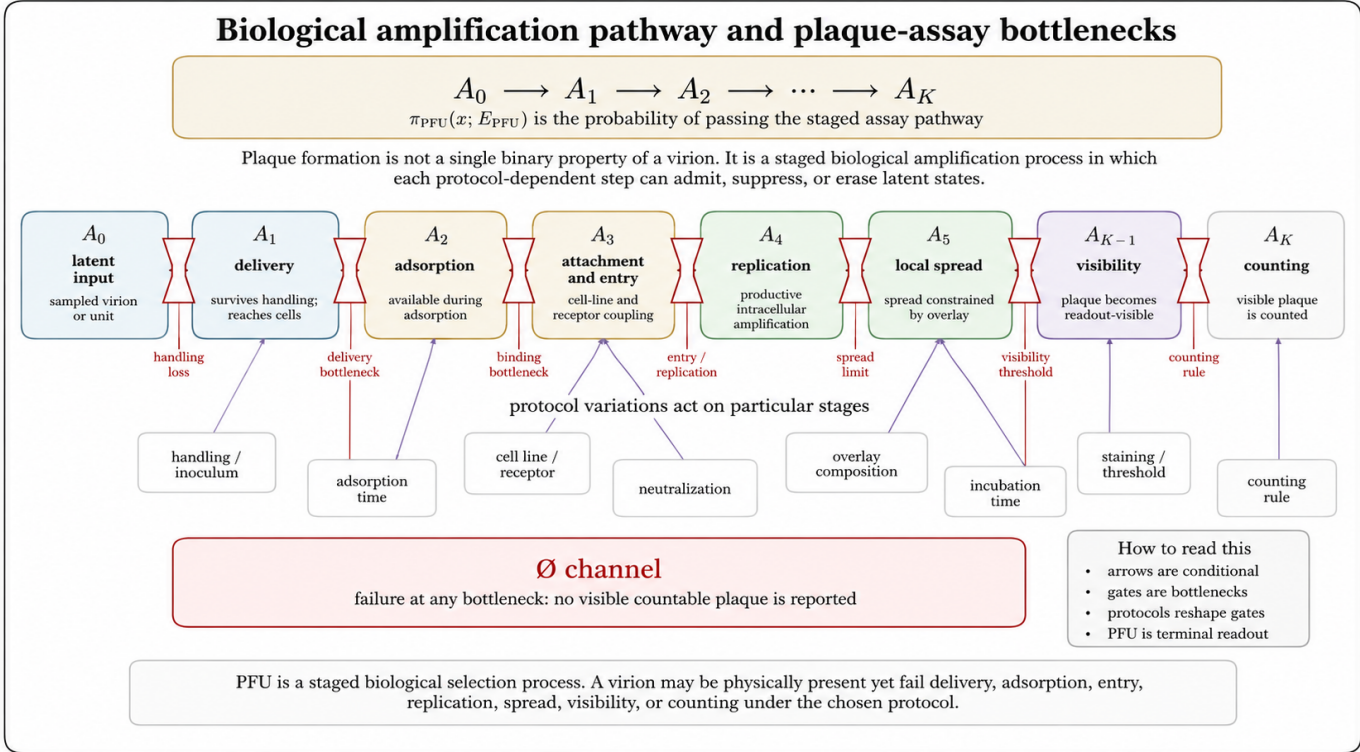


Figure 4. Biological amplification pathway and plaque-assay bottlenecks. Plaque formation is represented as a staged biological selection process rather than as a single intrinsic property of a virion. A latent virion, aggregate, or infectious unit must pass through delivery, adsorption, attachment and entry, productive replication, local spread, visibility, and final counting before it contributes to the PFU readout. Failure at any stage sends the event into the plaque-assay null channel, meaning no visible countable plaque is reported. The figure also indicates where common protocol variations act: inoculum handling, adsorption time, cell line or receptor condition, neutralization, overlay composition, incubation time, staining threshold, and counting rule. In this view, $\pi_{\text{PFU}}(x; E_{\text{PFU}})$ is the probability that a latent state passes the full staged assay pathway under the specified protocol.

Protocol component	Interpretation
E_{mod}	Measurement modality, such as cryo-EM, cryo-ET, AFM, DEP, electrorotation, particle tracking, plaque assay, focus assay, or endpoint dilution assay.
E_{prep}	Sample preparation pipeline, including dilution, purification, vitrification, staining, fixation, labeling, buffer exchange, or other pre-observation processing.
E_{field}	Externally imposed fields or forcing, including electric fields, mechanical loading, hydrodynamic flow, optical forcing, or other active perturbations.
E_{surf}	Substrate, confinement, adsorption, grid, interface, or surface-contact conditions.
E_{medium}	Surrounding medium, such as buffer, gel, mucus, extracellular fluid, aerosol droplet, overlay, or cellular environment.
E_{time}	Temporal window, incubation time, sampling cadence, exposure time, or duration of forcing.
E_{sel}	Selection, rejection, survival, detectability, thresholding, particle picking, or acceptance criteria.
E_{read}	Instrumental readout, reconstruction, fitting, counting, classification, or post-processing rule.

Table 3. Schematic components of an experimental protocol. The tuple in Eq. (2.1.1) is not meant to impose a unique decomposition on every experiment; rather, it identifies the main channels through which a protocol can transform, select, reweight, or project a latent virion ensemble.

The abstract protocol variable E includes, for example:

- (i) Cryo-electron microscopy or cryo-electron tomography, where sample preparation, vitrification, air–water interface exposure, support interaction, particle orientation, particle picking, and reconstruction determine which configurations are preserved and how they are represented [1, 2, 3, 4, 5, 33];
- (ii) Atomic force microscopy, where virions or virus-like particles are imaged, indented, or mechanically interrogated under surface-contact and probe-loading conditions [6, 7, 8, 9];
- (iii) Dielectrophoresis or electrorotation, where nonuniform or rotating electric fields actively drive polarization, translation, trapping, reorientation, or frequency-dependent response [10, 11, 12, 13];
- (iv) Single-particle tracking in mucus or gel-like media, where observed trajectories are shaped jointly by virion size, surface chemistry, glycoprotein binding, medium microstructure, adhesion, confinement, and the instrumental time window [14, 35, 15];
- (v) Plaque, focus-forming, or endpoint dilution assays, where the reported quantity is not the total number of physical virions but a protocol-conditioned measure of infectious activity under specified host-cell, overlay, incubation, staining, endpoint, and counting conditions [16, 17, 18].

The probability π_{PFU} may be interpreted as the probability of passing the assay pathway. Schematically,

plaque formation requires survival through handling, delivery to the monolayer, productive adsorption, entry, replication, local spread under the overlay, and visibility under the final readout criterion. A useful reduced representation is

$$\begin{aligned} \pi_{\text{PFU}}(x; E_{\text{PFU}}) &= p_{\text{surv}}(x) p_{\text{deliv}}(x \mid \text{surv}) p_{\text{ads}}(x \mid \text{deliv}) p_{\text{entry}}(x \mid \text{ads}) \\ &\times p_{\text{rep}}(x \mid \text{entry}) p_{\text{spread}}(x \mid \text{rep}) p_{\text{vis}}(x \mid \text{spread}). \end{aligned} \quad (1.5.5)$$

This expression should be read as a schematic conditional factorization of the assay pathway, not as a claim that the microscopic events are independent. A particle may be present in the sample and yet fail any one of these filters. Such a particle contributes to the latent physical population, but not to the final visible plaque count.

Assay stage	Protocol-conditioned interpretation
Handling and dilution	Particles may be lost, damaged, aggregated, disaggregated, diluted, inactivated, or unevenly delivered before contacting the monolayer.
Adsorption and entry	The cell line, receptor availability, temperature, adsorption time, and medium conditions determine which particles enter the productive infection pathway.
Replication and local spread	A particle that enters a cell must still generate progeny and spread locally through the overlay-restricted environment to form a visible lesion.
Visualization and counting	Staining, reporter expression, incubation time, plaque morphology, thresholding, and counting rules determine which lesions are accepted as countable plaques.
Null channel	Any state that fails to generate an accepted visible plaque is mapped to \emptyset , even if it was physically present in the original sample.

Table 4. Protocol-conditioned stages of plaque-assay collapse. Each stage acts as a filter or transformation between the latent particle population and the final visible plaque count.

In the dilute, independent, non-overlapping-plaque regime, the effective plaque-forming concentration enters the usual count model through the Poisson mean:

$$\boxed{N_d \mid \Lambda_{\text{PFU}} \sim \text{POISSON}(V_{\text{inoc}} f_d \Lambda_{\text{PFU}}(E_{\text{PFU}}))}, \quad (1.5.6)$$

where N_d is the observed plaque count at dilution fraction f_d , and V_{inoc} is the plated inoculum volume. The assumptions behind Eq. (1.5.6) are themselves protocol-dependent: plaques must be sufficiently rare to avoid strong overlap, the counted lesions must be approximately independent, and the dilution and plating process must be well mixed enough for the Poisson approximation to be appropriate.

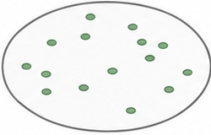
Assay nonidealities: from ideal Poisson plaques to real plaque data

$$N_d \sim \text{Poisson}(V_{\text{inoc}} f_d \Lambda_{\text{PFU}})$$

the ideal dilute count model is a useful baseline, but real assays add biological and observational structure

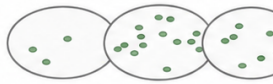
Plaque-count data can depart from the ideal Poisson model through heterogeneity, aggregation, null-channel enrichment, plaque merging, censoring, and morphology-dependent readout.

A Ideal dilute Poisson plaques



separated,
countable plaques
 $\text{Var}(N) \approx E[N]$

B Overdispersion

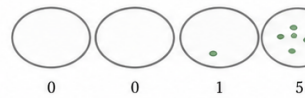


well-to-well heterogeneity
or aggregation

$$\text{Var}(N) > E[N]$$

clustered input

C Zero inflation



excess empty wells from
null-channel enrichment

$\text{Pr}(N=0)$
larger than
Poisson

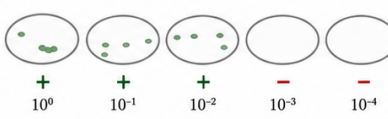
D Plaque merging



high inoculum or
long incubation

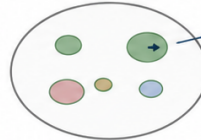
true events merge
into fewer visible plaques

E Endpoint dilution



binary or censored readout:
positive / negative rather than plaque count

F Plaque morphology



radius
size, shape,
opacity, texture

more information than
count alone

The Poisson model is the clean dilute limit. Real plaque data may require overdispersed, zero-inflated, censored, merging-aware, or morphology-aware observation models.

Figure 5. Assay nonidealities beyond the ideal Poisson plaque-count model. The dilute Poisson model provides a useful baseline for plaque counting when infectious events are independent, spatially separated, and directly countable. Real plaque-assay data, however, may depart from this ideal regime through biological, spatial, and observational structure. The panels summarize common deviations: ideal separated plaques with approximately Poisson variance; overdispersion from well-to-well heterogeneity, aggregation, or clustered input; zero inflation from null-channel enrichment and excess empty wells; plaque merging at high inoculum or long incubation; endpoint dilution as a binary or censored readout rather than a direct plaque count; and plaque morphology as an enriched observation carrying information about size, shape, opacity, texture, and growth behavior. These nonidealities do not invalidate the plaque assay. Rather, they indicate when the readout model should be expanded beyond the clean dilute limit to include overdispersed, zero-inflated, censored, merging-aware, or morphology-aware observation kernels.

Thus, the standard plaque-titer calculation is recovered as an estimator of Λ_{PFU} , not of C_{part} :

$$\hat{\Lambda}_{\text{PFU},d} = \frac{N_d}{V_{\text{inoc}} f_d}. \quad (1.5.7)$$

Replicate wells and dilution series improve the statistical precision of this scalar estimate, but they do not by themselves reveal the latent composition of the sample. Increasing the number of replicate plaque counts reduces uncertainty in Λ_{PFU} ; it does not automatically identify how that effective concentration decomposes into particle integrity, receptor compatibility, replication competence, neutralization state, aggregation state, or visibility under the counting rule.

The inverse problem becomes especially transparent in a two-subpopulation reduction. Suppose the latent ensemble is decomposed into a plaque-competent sector with concentration C_C and a plaque-

incompetent, weakly competent, damaged, defective, neutralized, aggregated, or assay-incompatible sector with concentration C_I . If the subpopulation-averaged plaque-forming probabilities are \bar{p}_C and \bar{p}_I , then

$$\boxed{\Lambda_{\text{PFU}} = \bar{p}_C C_C + \bar{p}_I C_I.} \quad (1.5.8)$$

This expression states exactly what a plaque count identifies: a weighted sum over latent sectors. A low plaque titer may reflect a small competent fraction, a low plaque-forming probability of otherwise competent particles, weak coupling between the virus and the chosen cell line, suppression by the overlay, insufficient incubation time, a stringent readout threshold, or loss at adsorption, entry, replication, local spread, or visibility. PFU alone cannot distinguish these mechanisms without additional measurements, controlled protocol variation, or prior biological assumptions.

The same point can be written as an identifiability statement. A single scalar measurement of Λ_{PFU} cannot determine the four quantities $(C_C, C_I, \bar{p}_C, \bar{p}_I)$ without additional constraints:

$$\Lambda_{\text{PFU}} = \bar{p}_C C_C + \bar{p}_I C_I \quad \text{is one equation for several latent unknowns.} \quad (1.5.9)$$

This is not a failure of the plaque assay. It is the mathematical statement of what the plaque assay is designed to report. The assay collapses a heterogeneous latent population into a countable functional measure of infectious lesion formation under specified conditions.

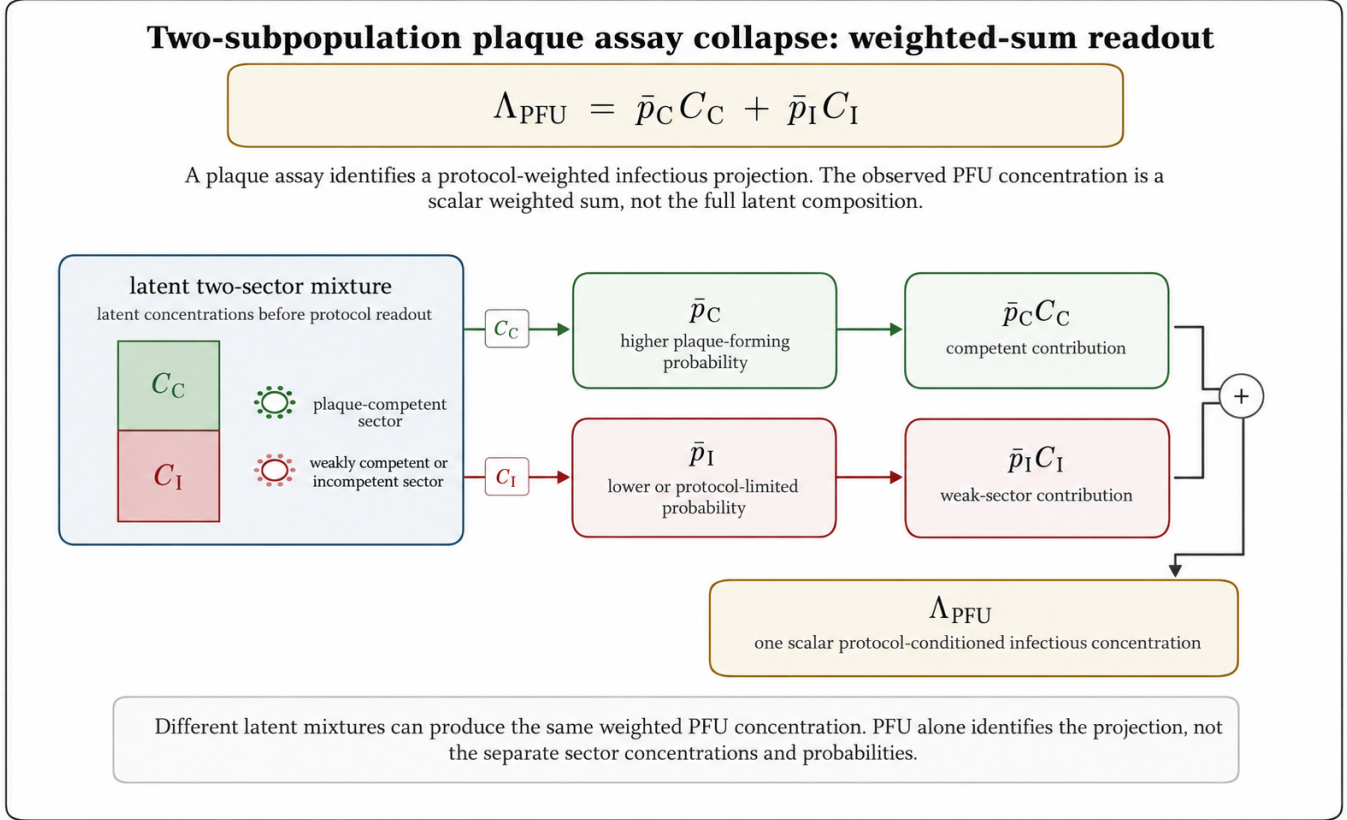


Figure 6. Plaque-assay collapse as a weighted projection of a latent two-subpopulation ensemble. The latent population is represented by two concentration sectors: a plaque-competent sector C_C and a weakly competent or incompetent sector C_I . Under a fixed plaque-assay protocol, these sectors are not observed as independent latent concentrations. Instead, each sector is weighted by its protocol-conditioned plaque-forming probability, \bar{p}_C or \bar{p}_I , and the assay reports the scalar infectious readout. The figure emphasizes that PFU concentration is a weighted projection of the latent ensemble rather than a direct measurement of the full latent composition. Distinct combinations of C_C , C_I , \bar{p}_C , and \bar{p}_I can produce the same observed Λ_{PFU} . PFU alone therefore does not identify the separate sector concentrations or their underlying protocol-conditioned plaque-forming probabilities.

Equivalently, under the constant-probability approximation, let

$$C_{\text{part}} = C_C + C_I, \quad \varphi_C = \frac{C_C}{C_{\text{part}}}, \quad \varphi_I = 1 - \varphi_C.$$

Here C_{part} is the total latent particle concentration in the two-sector reduction, and φ_C is the fraction of that population assigned to the plaque-competent sector. If the sector-averaged plaque-forming probabilities are written as p_C and p_I , then

$$\Lambda_{\text{PFU}} = C_{\text{part}} \left[p_I + (p_C - p_I) \varphi_C \right]. \quad (1.5.10)$$

This form separates physical abundance from plaque-forming efficiency. The factor C_{part} describes how much latent material is present, whereas the bracketed term describes how effectively that latent

material is mapped into the visible plaque-forming channel under the specified protocol.

Equation (1.5.10) also makes the non-identifiability explicit. A plaque assay alone identifies the combined quantity

$$C_{\text{part}} \left[p_{\text{I}} + (p_{\text{C}} - p_{\text{I}}) \varphi_{\text{C}} \right],$$

not the separate latent factors C_{part} , φ_{C} , p_{C} , and p_{I} . Consequently, a large particle-to-PFU ratio may arise from several distinct mechanisms: a small competent fraction, poor assay coupling to the competent sector, a weakly competent sector with low plaque-forming probability, or a protocol that suppresses one or more stages of plaque development. These possibilities are biologically different, but they can collapse to the same scalar PFU readout.

A short numerical example makes the distinction concrete. Suppose two viral preparations have the same total latent particle concentration,

$$C_{\text{part}} = 10^8 \text{ mL}^{-1},$$

but differ in the fraction of particles assigned to the plaque-competent sector. Let the plaque protocol have sector-averaged plaque-forming probabilities

$$p_{\text{C}} = 0.80, \quad p_{\text{I}} = 10^{-3},$$

and consider two preparations with

$$\varphi_{\text{C}}^{(A)} = 0.10, \quad \varphi_{\text{C}}^{(B)} = 0.01.$$

Using

$$\Lambda_{\text{PFU}} = C_{\text{part}} \left[p_{\text{I}} + (p_{\text{C}} - p_{\text{I}}) \varphi_{\text{C}} \right],$$

the corresponding effective plaque-forming concentrations are

$$\Lambda_{\text{PFU}}^{(A)} = 10^8 \left[10^{-3} + (0.80 - 10^{-3})(0.10) \right] \approx 8.09 \times 10^6 \text{ PFU/mL}, \quad (1.5.11)$$

$$\Lambda_{\text{PFU}}^{(B)} = 10^8 \left[10^{-3} + (0.80 - 10^{-3})(0.01) \right] \approx 8.99 \times 10^5 \text{ PFU/mL}. \quad (1.5.12)$$

If 0.1 mL is plated at dilution fraction 10^{-4} , the expected plaque counts are therefore

$$\mathbb{E}[N_d^{(A)}] = 0.1 \times 10^{-4} \times 8.09 \times 10^6 \approx 80.9, \quad (1.5.13)$$

$$\mathbb{E}[N_d^{(B)}] = 0.1 \times 10^{-4} \times 8.99 \times 10^5 \approx 9.0. \quad (1.5.14)$$

Thus, two preparations with the same physical particle concentration can fall into very different plaque-count regimes under the same dilution and plating conditions. In this example, the difference is not the amount of latent material present, but the protocol-conditioned projection of that material into the visible plaque-forming channel. The implied particle-to-PFU ratios also differ: approximately 12.4 for preparation A and 111.2 for preparation B. The particle-to-PFU ratio is therefore not, in this formulation, an intrinsic constant of the virus alone; it is a compressed readout of latent composition

and protocol-conditioned plaque-forming probabilities.

The same non-identifiability appears in Fisher-information form. For one plaque protocol and one dilution, let

$$\theta = \begin{pmatrix} C_C \\ C_I \end{pmatrix}, \quad \mathbf{p} = \begin{pmatrix} p_C \\ p_I \end{pmatrix}. \quad (1.5.15)$$

The Poisson mean can then be written compactly as

$$\mu_d = V_{\text{inoc}} f_d \mathbf{p}^\top \theta. \quad (1.5.16)$$

For a Poisson count with mean μ_d , the Fisher information for the two latent concentrations is

$$\mathcal{I}_E(\theta) = \frac{(V_{\text{inoc}} f_d)^2}{\mu_d} \mathbf{p} \mathbf{p}^\top. \quad (1.5.17)$$

This matrix is rank one whenever $\mathbf{p} \neq 0$. The protocol is locally informative only along the sensitivity direction \mathbf{p} . It is blind to directions v satisfying

$$\mathbf{p}^\top v = 0. \quad (1.5.18)$$

For example, in the two-sector case, a local blind direction is proportional to

$$v_\perp = \begin{pmatrix} p_I \\ -p_C \end{pmatrix}, \quad \mathbf{p}^\top v_\perp = 0.$$

Motion in this direction changes the latent sector concentrations while leaving the scalar combination

$$p_C C_C + p_I C_I$$

unchanged to first order. This is the Fisher-information form of plaque-assay protocol blindness.

Multiple dilutions and replicate wells increase precision along the same sensitivity direction, but they do not by themselves rotate that direction in latent subpopulation space. If the same protocol is repeated across dilution levels $d = 1, \dots, D$, the information takes the form

$$\mathcal{I}_E^{\text{rep}}(\theta) = \left[\sum_{d=1}^D \frac{(V_{\text{inoc}} f_d)^2}{\mu_d} \right] \mathbf{p} \mathbf{p}^\top. \quad (1.5.19)$$

Thus, repeated plaque counts under the same protocol reduce uncertainty in $\mathbf{p}^\top \theta$, but they do not identify the components of θ separately. This is a precise mathematical version of the statement that replication improves precision but does not automatically resolve latent composition.

Protocol variation can reduce this blindness when it changes the probability vector. For independent

plaque-count data from protocols E_1, \dots, E_M , define

$$\mathbf{p}_m = \begin{pmatrix} p_C^{(m)} \\ p_I^{(m)} \end{pmatrix}, \quad \mu_m = V_m f_m \mathbf{p}_m^\top \theta. \quad (1.5.20)$$

The multi-protocol Fisher information becomes

$$\mathcal{I}_{\text{multi}}(\theta) = \sum_{m=1}^M \frac{(V_m f_m)^2}{\mu_m} \mathbf{p}_m \mathbf{p}_m^\top. \quad (1.5.21)$$

Each term is rank one, but the sum can have higher rank if the protocol probability vectors point in different directions. In the two-sector case, the rank can increase from one to two only if at least two protocol vectors are not collinear:

$$\text{rank } \mathcal{I}_{\text{multi}}(\theta) = 2 \iff \exists m, n \text{ such that } \det \begin{pmatrix} p_C^{(m)} & p_I^{(m)} \\ p_C^{(n)} & p_I^{(n)} \end{pmatrix} \neq 0, \quad (1.5.22)$$

up to the usual requirements that the corresponding means are finite and the protocols provide nonzero information. This is the plaque-assay version of the general multi-protocol principle: complementary protocols are valuable not because their raw observables are identical, but because their observation kernels probe different latent directions.

Changing the cell line, adsorption time, overlay composition, incubation time, temperature, neutralization condition, receptor availability, or readout threshold may rotate the protocol sensitivity direction by changing the probability vector \mathbf{p}_m . When this rotation is large enough, controlled protocol variation can expose latent sectors that are collapsed by the original assay.

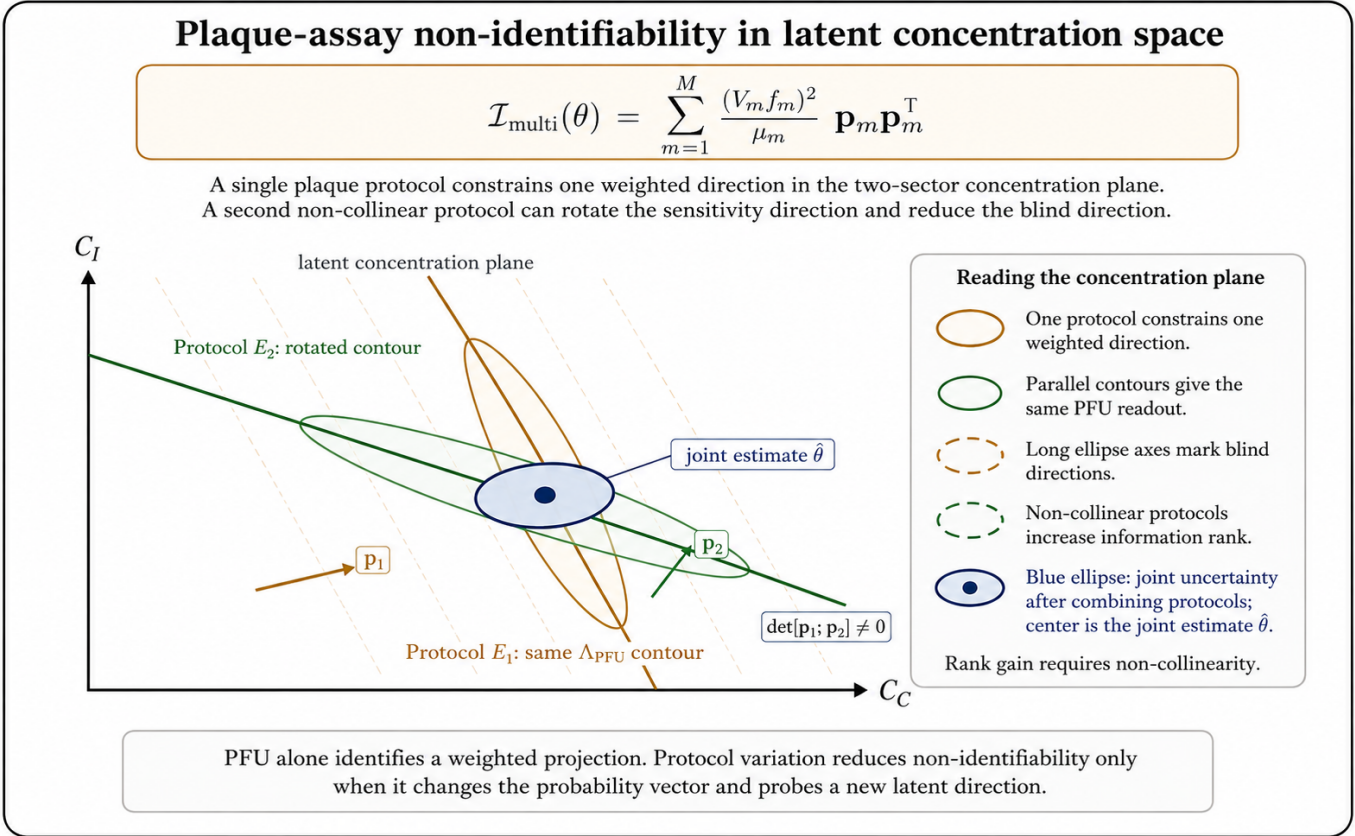


Figure 7. Plaque-assay non-identifiability in the two-sector latent concentration plane. The latent state is reduced to two concentration coordinates: C_C , the plaque-competent sector, and C_I , the weakly competent or incompetent sector. A single plaque protocol constrains only one weighted direction in this plane. All points lying on the same Λ_{PFU} contour produce the same scalar PFU readout and are therefore indistinguishable under that protocol alone. The elongated uncertainty ellipses indicate that each individual protocol leaves a blind or weakly constrained direction approximately parallel to its equal-readout contour. Introducing a second protocol increases the identifiable rank only if the new protocol has a non-collinear probability vector \mathbf{p}_m , thereby rotating the sensitivity direction in latent concentration space.

The worked example therefore translates experimental collapse into the language of an everyday virological assay. A plaque count is real experimental data, but it is not a protocol-free census of virions. It is the visible count generated after a latent population has been filtered through survival, delivery, adsorption, entry, replication, local spread, visibility, and counting rules. This interpretation preserves the practical value of PFU while clarifying its target: PFU estimates a protocol-conditioned infectious projection.

Additional particle counts, genome counts, antigen measurements, structural imaging, neutralization assays, receptor-binding assays, tracking assays, or controlled plaque-protocol variations add complementary observation kernels. These additional kernels can help separate physical abundance from plaque-forming efficiency and can constrain latent sectors that the plaque assay alone cannot resolve. The general mathematical development below formalizes this logic for arbitrary protocol-conditioned observation maps, of which the plaque assay is one biologically familiar example.

This perspective leads to a practical criterion for protocol complementarity. A new protocol is especially

valuable when it contributes information in a direction that is blind, weakly resolved, or nuisance-confounded under the existing protocol set. In other words, the goal of multi-protocol inference is not redundancy for its own sake. The goal is to reduce protocol blindness by combining experimental maps that are sensitive to different latent sectors.

This can be expressed at the level of likelihoods. If D_j denotes the data obtained under protocol E_j , then a protocol-resolved joint inference problem has the schematic form

$$p(D_1, \dots, D_M \mid \theta, \lambda_1, \dots, \lambda_M) = \prod_{j=1}^M p_{E_j}^{\otimes}(D_j \mid \theta, \lambda_j), \quad (1.5.23)$$

when the datasets are conditionally independent given the shared latent parameters and the protocol-specific nuisance parameters. This factorization is not a claim that the observed datasets are the same kind of object. Rather, it states that each dataset provides a different view of the same latent model, conditioned through its own protocol.

Under the same conditional-independence assumption, and when nuisance parameters are fixed, calibrated, marginalized, or appropriately profiled, the informational contributions of the separate protocols combine through Fisher information:

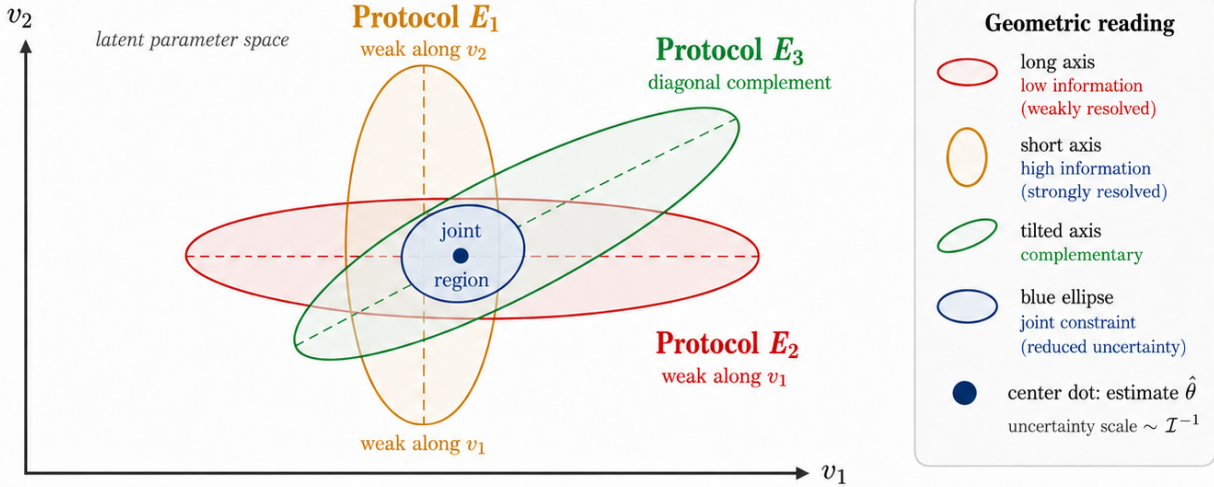
$$\boxed{\mathcal{I}_{\text{multi}}(\theta) = \sum_{j=1}^M \mathcal{I}_{E_j}(\theta).} \quad (1.5.24)$$

Equation (1.5.24) gives a compact expression of why complementary protocols are powerful. Each protocol constrains some directions in parameter space more strongly than others. A direction that is nearly blind under one protocol may be visible under another. Their combination can therefore shrink the joint uncertainty region even when no single protocol is individually sufficient.

Complementary protocols and additive Fisher information

$$\mathcal{I}_{\text{multi}}(\theta) = \sum_{j=1}^M \mathcal{I}_{E_j}(\theta)$$

Each protocol resolves some latent directions better than others.
Complementary protocols reduce blindness by constraining different directions
in the same latent parameter space.



- ✓ **Ellipses encode information geometry.** Each ellipse shows the uncertainty (covariance) induced by one protocol.
- ✓ **Axes indicate resolution.** Dashed major axes = poorly resolved directions; short axes = well-resolved.
- ✓ **Complementarity shrinks uncertainty.** Combining protocols with different orientations reduces the joint uncertainty region.

Figure 8. Complementary protocols and additive Fisher information. Protocol-specific Fisher information constrains different directions in the latent parameter space. In this schematic, the axes v_1 and v_2 represent local parameter directions in the shared latent virion–environment model. Each colored ellipse represents the uncertainty region associated with one protocol: long axes indicate weakly resolved directions, while short axes indicate strongly resolved directions. Protocol E_1 , protocol E_2 , and protocol E_3 provide distinct sensitivity directions, so their combination reduces the joint uncertainty region. The blue ellipse represents the combined multi-protocol constraint. The figure illustrates why additional data from one protocol mainly improves precision along directions that the protocol already sees, whereas adding a genuinely complementary protocol can reduce protocol blindness by constraining a previously weak or unresolved parameter direction.

A corresponding local blind subspace for the combined protocol set may be written as

$$\mathcal{B}_{\text{multi}}(\theta) = \ker \mathcal{I}_{\text{multi}}(\theta). \quad (1.5.25)$$

When the individual Fisher-information matrices probe different parameter directions, the kernel of the sum can be smaller than the kernels associated with the separate protocols. In this sense, multi-protocol inference reduces blindness not by forcing measurements to look the same, but by combining different observation kernels that resolve different directions of the same latent model.

This is the sense in which disagreement between protocols must be interpreted carefully. Apparent

disagreement may indicate a genuine inconsistency in the latent model, but it may also indicate that the protocols are sensitive to different latent sectors, that a nuisance parameter has been miscalibrated, or that one of the observation operators is misspecified. Conversely, apparent agreement can be misleading if multiple protocols share the same blind direction or the same selection bias. Multi-protocol consistency is therefore not merely a comparison of outputs; it is a test of whether a shared latent explanation can survive multiple, differently conditioned experimental views.

This point motivates the more detailed examples developed below. The plaque assay is especially useful as an introductory case because its output is simple and familiar—a count of visible lesions—while its protocol-conditioned structure is rich. It combines adsorption, entry, replication, spread through a cell layer, biological amplification, incubation, staining, thresholding, and counting. For that reason, it provides a clear example of how a classical virological measurement can be understood as a null-inclusive observation operator acting on a heterogeneous latent particle population.

2 Experimental Collapse: Concept and Mathematical Formulation

The preceding discussion motivates a more explicit mathematical formulation. The central object is no longer an isolated measurement outcome, but a map between ensembles: a reference latent ensemble, a protocol-conditioned latent ensemble, and an observed ensemble. This section defines these objects and the operations that connect them.

A virological measurement does not generally report the full physical state of a virion or virion population. The latent state may include position, velocity, orientation, angular velocity, deformation state, spike or surface configuration, charge distribution, binding state, local medium variables, and collective mechanical mode amplitudes. Only some of these degrees of freedom are made accessible by a given experiment. Which variables become visible depends on the preparation, forcing, selection, survival, detection, and readout operations of the protocol.

This is the mathematical content of *experimental collapse*. A protocol may preserve some latent distinctions, transform others, eliminate some states from the accepted data channel, reweight the surviving population, or project many distinct latent states onto the same observed output. The experimentally reported ensemble is therefore not, in general, a direct sample from the reference latent ensemble. It is the ensemble produced after the reference population has passed through a specified experimental map.

In compact form, the structure is

$$\begin{array}{c}
 \boxed{
 \begin{array}{ccc}
 P_{\text{ref},t} & \xrightarrow{\mathcal{C}_{E,t}} & P_{E,t} & \xrightarrow{\mathcal{M}_{E,t}^{\otimes}} & P_{\text{obs},t}^{\otimes}(\cdot | E) \\
 \text{reference latent ensemble} & & \text{protocol-conditioned latent ensemble} & & \text{observed ensemble}
 \end{array}
 }
 \end{array}
 \tag{2.1}$$

The term *reference* is important. The reference latent ensemble is not an absolute, context-free state of a virion. It is the ensemble associated with a specified biological or physical environment before the additional conditioning introduced by the measurement protocol. Thus, the reference ensemble may already be specific to a buffer, mucus layer, extracellular fluid, aerosol droplet, surface microenvironment, temperature, ionic condition, or host-tissue context. Experimental collapse describes the further conditioning imposed by the measurement procedure itself.

In what follows, a protocol is represented by three mathematical operations: a latent-state transformation kernel, a survival or detection weight, and a readout kernel. Together, these operations define how a latent ensemble becomes an observed ensemble, including the possibility of null observation.

Remark 2.1 (Why this is mechanical, not merely epistemic). Experimental collapse is not introduced merely to say that measurements are incomplete. Incompleteness alone would be an epistemic limitation. The stronger claim is that many virological protocols act as additional physical, chemical, mechanical, or biological environments. They can alter forces, torques, boundary conditions, accessible orientations, adhesion states, deformation pathways, survival probabilities, biological amplification pathways, and detectable subpopulations. The discrepancy between the reference latent ensemble and the observed ensemble is therefore not only informational. It can be dynamical, mechanical, biochemical,

or assay-dependent.

The concept prevents two opposite errors. The first is to treat every observed configuration as a faithful sample from an unconstrained or biologically natural ensemble. The second is to dismiss protocol-conditioned observations as mere artifacts. A better interpretation is that each experiment reports a real ensemble, but one produced by a specified mechanical and observational map. Once that map is represented explicitly, different experiments can be compared as distinct protocol-conditioned projections of a shared latent system.

2.1 Experimental Protocols

Definition 2.2 (Experimental protocol). An *experimental protocol* is the collection of experimental choices, physical conditions, biological conditions, selection rules, and readout procedures that determine how a latent virion–environment ensemble is conditioned and observed. Schematically, we write

$$\boxed{E = (E_{\text{mod}}, E_{\text{prep}}, E_{\text{field}}, E_{\text{surf}}, E_{\text{medium}}, E_{\text{time}}, E_{\text{sel}}, E_{\text{read}}).} \quad (2.1.1)$$

The entries of this tuple need not be statistically independent or sharply separable in a real experiment. The notation is an organizing device: it records the major protocol components through which experimental collapse can occur.

2.2 Latent and Observed State Spaces

Let

$$(\Psi, \Sigma_X)$$

be the measurable space of latent virion–environment states. A schematic single-particle latent state may be written as

$$X = (\mathbf{x}, \mathbf{v}, Q, \boldsymbol{\omega}, \mathbf{s}, \mathbf{c}, \mathbf{m}), \quad (2.2.1)$$

where \mathbf{x} and \mathbf{v} are position and velocity, Q is an orientation variable, $\boldsymbol{\omega}$ is angular velocity, \mathbf{s} denotes surface, spike, or conformational variables, \mathbf{c} denotes medium-contact, adhesion, receptor-binding, or environmental-contact variables, and \mathbf{m} denotes internal or collective mechanical mode amplitudes. The specific content of X depends on the modeling scale and on the experimental question. For example, Q may be irrelevant for an isotropic coarse-grained particle model, but essential for a spiked, anisotropic, field-responsive, or surface-bound virion model.

The reference latent ensemble is a time-dependent probability measure

$$P_{\text{ref},t}(dx) \quad \text{on} \quad (\Psi, \Sigma_X). \quad (2.2.2)$$

This measure represents the distribution of latent states in a specified biological or physical environment before the additional conditioning imposed by the measurement protocol. Thus $P_{\text{ref},t}$ may refer to virions in a particular extracellular fluid, mucus layer, aerosol droplet, buffer, surface microenvironment, temperature, ionic condition, or host-tissue context. It is not a universal free-particle ensemble.

An experiment generally does not report X itself. It reports an observed variable

$$Y_E \in \mathcal{Y}_E,$$

where $(\mathcal{Y}_E, \Sigma_{Y,E})$ is the protocol-specific non-null observation space. Depending on E , Y_E may be a reconstructed density map, an AFM height image, a force-indentation curve, a particle trajectory, an electrorotation spectrum, a fluorescence focus count, a plaque count, or an endpoint dilution readout. The observation space is therefore itself protocol-dependent.

To include non-detection, rejection, loss, failed infection, failed classification, or any other accepted absence of a reported datum, we enlarge the observation space by a null outcome:

$$\mathcal{Y}_E^\emptyset = \mathcal{Y}_E \cup \{\emptyset\}. \tag{2.2.3}$$

The null outcome \emptyset does not mean that nothing existed in the latent ensemble. It means that, under protocol E , the latent state did not enter the accepted non-null readout channel.

Remark 2.3 (Why measurable spaces are used). Measure notation is used because virological observables are not all ordinary Euclidean vectors. Some are continuous trajectories, some are discrete counts, some are reconstructed images, some are force curves, some are categorical classifications, and some are null outcomes. Writing ensembles as probability measures rather than only as densities allows the same formalism to cover imaging, tracking, mechanical readout, electrical forcing, and infectivity assays.

Remark 2.4 (Protocol dependence of the observation space). The notation \mathcal{Y}_E emphasizes that different experiments need not share the same observed state space. A cryo-EM reconstruction, an AFM force-indentation curve, a DEP trajectory, a single-particle tracking path, and a plaque count are not raw observations of the same mathematical type. They become comparable only after they are interpreted as outputs of protocol-specific observation maps acting on a common latent model.

2.3 Protocol Transformation Kernels

The first mathematical operation associated with a protocol is the transformation of the reference latent ensemble into a protocol-conditioned latent ensemble. This stage represents the part of the experiment that acts on the virion or virion-environment state before the final accepted readout is formed. We write this operation as a Markov kernel

$$\Pi_E^{\text{lat}}(dx_E \mid x), \tag{2.3.1}$$

from the reference latent space (Ψ, Σ_X) to a protocol-conditioned latent space $(\Psi_E, \Sigma_{X,E})$. The variable $x \in \Psi$ denotes the reference latent state, while $x_E \in \Psi_E$ denotes the state after conditioning by protocol E .

The protocol-conditioned state x_E may differ from x because the experiment can impose constraints, modify boundary conditions, induce deformation, add field-dependent degrees of freedom, alter medium-contact variables, remove unresolved coordinates, or define states that exist only under experimental conditions. For example, an adsorbed AFM state, a vitrified cryo-EM state, a field-polarized DEP

state, a mucus-bound tracking state, and an infection-pathway state in a plaque assay are not merely different readouts of the same object. They are different protocol-conditioned latent states.

The protocol-conditioned latent ensemble before survival, detection, or acceptance selection is

$$\tilde{P}_{E,t}^{\text{lat}}(A) = \int_{\Psi} \Pi_E^{\text{lat}}(A | x) P_{\text{ref},t}(dx), \quad A \in \Sigma_{X,E}. \quad (2.3.2)$$

Equivalently,

$$\tilde{P}_{E,t}^{\text{lat}} = P_{\text{ref},t} \Pi_E^{\text{lat}},$$

where the right-hand side denotes the action of the kernel on the reference measure. Equation (2.3.2) is the first formal stage of experimental collapse: the reference latent ensemble is carried into a protocol-conditioned latent ensemble by the physical, biological, and procedural action of the experiment.

Protocol action	Role in Π_E^{lat}
Surface adsorption	Maps freely suspended or weakly interacting particles into surface-associated states with altered orientation, adhesion, deformation, or accessible mechanical response.
Vitrification or fixation	Transforms a dynamic hydrated ensemble into a preserved structural ensemble conditioned by preparation, ice thickness, interface exposure, or chemical fixation.
Electric or mechanical forcing	Adds field-dependent polarization, trapping, torque, deformation, loading, or driven response variables to the conditioned state.
Structured medium exposure	Conditions the state by mucus, gel, extracellular matrix, overlay, buffer, ionic strength, confinement, adhesion, or local rheology.
Biological pathway conditioning	Represents states after adsorption to cells, entry attempts, replication competence, spread constraints, neutralization, or other assay-specific biological filters.

Table 5. Examples of protocol actions represented by the latent transformation kernel Π_E^{lat} . These actions occur before the final readout and may physically, chemically, mechanically, or biologically condition the latent ensemble.

Remark 2.5 (Why Π_E^{lat} is separated from the readout). The latent transformation kernel Π_E^{lat} describes what the protocol does to the virion state before final readout. This should be kept separate from the readout kernel, which describes how a surviving protocol-conditioned state is represented as data. Surface adsorption, vitrification, electric-field forcing, mechanical loading, incubation, and medium conditioning belong naturally to the latent transformation stage. Finite optical resolution, reconstruction, force-curve fitting, particle picking, thresholding, and counting belong to later selection or readout stages.

Remark 2.6 (Deterministic maps as a special case). If the protocol maps each reference latent

state deterministically to a conditioned state $T_E(x)$, then

$$\Pi_E^{\text{lat}}(dx_E | x) = \delta_{T_E(x)}(dx_E),$$

and the protocol-conditioned latent ensemble is the pushforward

$$\tilde{P}_{E,t}^{\text{lat}} = (T_E)_\# P_{\text{ref},t}.$$

The kernel formulation is more general because it also allows stochastic preparation, heterogeneous adsorption, variable vitrification outcomes, field-dependent fluctuations, stochastic cell entry, heterogeneous survival, and protocol-to-protocol variability.

2.4 Survival, Detection, and Null Observations

Not every protocol-conditioned latent state contributes to the final observed ensemble. Some particles are destroyed, excluded, immobilized outside the field of view, rejected during reconstruction, too dim to track, unable to infect the selected cell type, unable to form a visible plaque under the selected overlay condition, or otherwise absent from the accepted data channel. We therefore introduce a survival, detection, or acceptance weight

$$s_E : \Psi_E \rightarrow [0, 1], \quad (2.4.1)$$

where $s_E(x_E)$ is the probability that the protocol-conditioned latent state x_E survives the experimental pipeline and contributes to a non-null readout.

The total non-null detection probability is

$$\eta_E(t) = \int_{\Psi_E} s_E(x_E) \tilde{P}_{E,t}^{\text{lat}}(dx_E). \quad (2.4.2)$$

This quantity is the mass of the protocol-conditioned latent ensemble that passes into the accepted non-null channel. When $0 < \eta_E(t) \leq 1$, the detected protocol-conditioned latent ensemble is the conditional measure

$$\boxed{P_{E,t}^{\text{lat}}(A | \text{det}) = \frac{1}{\eta_E(t)} \int_A s_E(x_E) \tilde{P}_{E,t}^{\text{lat}}(dx_E), \quad A \in \Sigma_{X,E}.} \quad (2.4.3)$$

This equation separates transformation from selection. The kernel Π_E^{lat} describes how the protocol changes or conditions the latent state distribution. The weight s_E describes which conditioned states remain in the accepted data channel. The detected ensemble $P_{E,t}^{\text{lat}}(\cdot | \text{det})$ is therefore not generally the same object as the preselection ensemble $\tilde{P}_{E,t}^{\text{lat}}$. It is a reweighted and normalized subensemble.

If $\eta_E(t) = 0$, the protocol produces no accepted non-null observations at time t . In that case, the conditional detected ensemble is not defined, but the null-inclusive formulation remains meaningful because the full observed measure assigns all mass to the null channel.

Null observations are part of the protocol. Let \emptyset denote the null readout: no particle, no accepted track, no accepted reconstruction, no plaque, no focus, no detectable spectrum, no measurable response,

or no accepted classification. Then

$$\mathbb{P}_E(\emptyset) = 1 - \eta_E(t). \quad (2.4.4)$$

The null outcome does not necessarily mean that no virions were present in the reference ensemble. It means that, under protocol E , the relevant latent states did not pass into the accepted non-null readout channel.

Remark 2.7 (Why the null channel matters). The null channel prevents a common interpretive mistake: treating the reported ensemble as if it were the entire protocol-conditioned population. A protocol may return a clean observed distribution precisely because it has removed, rejected, destroyed, failed to amplify, or failed to detect many states. The missing probability mass is therefore part of the experiment. It records how strongly the protocol selects, filters, thresholds, rejects, or loses latent states.

Remark 2.8 (Selection is not the same as absence). A non-detected state is not automatically an absent state. In cryo-EM, a particle may be absent from the reconstruction because it was rejected during picking or classification. In tracking, a particle may be absent from the trajectory ensemble because it was below threshold, immobilized, or outside the observation window. In a plaque assay, a particle may be absent from the plaque count because it failed adsorption, entry, replication, spread, or visibility under the chosen protocol. In each case, the null channel records a protocol-conditioned failure to enter the accepted data stream, not necessarily the nonexistence of the latent object.

2.5 Readout Kernels and Observed Ensembles

Selection determines which protocol-conditioned latent states enter the accepted data channel, but it does not yet specify what is measured. The final non-null readout is represented by a Markov kernel

$$R_E(dy | x_E), \quad (2.5.1)$$

from the protocol-conditioned latent space $(\Psi_E, \Sigma_{X,E})$ to the non-null observation space $(\mathcal{Y}_E, \Sigma_{Y,E})$. The readout kernel describes how a surviving protocol-conditioned state is represented as data. Depending on the protocol, R_E may include projection, finite resolution, reconstruction, segmentation, thresholding, counting, fitting, classification, or measurement noise.

For a measurable non-null observation set $B \in \Sigma_{Y,E}$, the detected observed ensemble is

$$\boxed{P_{\text{obs},t}(B | E, \text{det}) = \int_{\Psi_E} R_E(B | x_E) P_{E,t}^{\text{lat}}(dx_E | \text{det})}. \quad (2.5.2)$$

Using the detected latent ensemble from Eq. (2.4.3), this can be written equivalently as

$$P_{\text{obs},t}(B | E, \text{det}) = \frac{1}{\eta_E(t)} \int_{\Psi_E} R_E(B | x_E) s_E(x_E) \tilde{P}_{E,t}^{\text{lat}}(dx_E), \quad (2.5.3)$$

provided $0 < \eta_E(t) \leq 1$. Thus the detected observed ensemble is obtained by three successive operations: latent protocol transformation, survival or detection weighting, and readout.

To retain non-detection explicitly, we enlarge the observation space by a null outcome:

$$\mathcal{Y}_E^\varnothing = \mathcal{Y}_E \cup \{\varnothing\}, \quad \Sigma_{Y,E}^\varnothing = \sigma(\Sigma_{Y,E} \cup \{\{\varnothing\}\}). \quad (2.5.4)$$

The full observed measure, including the null outcome, is then

$$\boxed{P_{\text{obs},t}^\varnothing(B | E) = \int_{\Psi_E} s_E(x_E) R_E(B \cap \mathcal{Y}_E | x_E) \tilde{P}_{E,t}^{\text{lat}}(dx_E) + (1 - \eta_E(t)) \delta_\varnothing(B), \quad B \in \Sigma_{Y,E}^\varnothing.} \quad (2.5.5)$$

Here δ_\varnothing is the point mass at the null outcome. This equation makes the probability accounting explicit. The first term is the probability mass assigned to accepted non-null observations. The second term is the probability mass assigned to states that fail to enter the accepted readout channel.

The null-inclusive observed measure reduces to the detected observed ensemble by conditioning on the non-null observation space:

$$P_{\text{obs},t}(B | E, \text{det}) = P_{\text{obs},t}^\varnothing(B | E, Y \in \mathcal{Y}_E) = \frac{P_{\text{obs},t}^\varnothing(B | E)}{P_{\text{obs},t}^\varnothing(\mathcal{Y}_E | E)}, \quad B \in \Sigma_{Y,E}, \quad (2.5.6)$$

whenever $P_{\text{obs},t}^\varnothing(\mathcal{Y}_E | E) = \eta_E(t) > 0$. This relation is useful because it separates two questions that are often conflated: what distribution is observed among accepted events, and how much latent probability mass was excluded, lost, rejected, or mapped to null.

Definition 2.9 (Full null-inclusive protocol kernel). The full null-inclusive protocol kernel is the Markov kernel

$$K_E^\varnothing(dy | x)$$

from the reference latent state space (Ψ, Σ_X) to the augmented observation space $(\mathcal{Y}_E^\varnothing, \Sigma_{Y,E}^\varnothing)$. It is obtained by composing the latent transformation kernel Π_E^{lat} , the survival or detection weight s_E , the readout kernel R_E , and the null channel. For $B \in \Sigma_{Y,E}^\varnothing$,

$$\boxed{K_E^\varnothing(B | x) = \int_{\Psi_E} s_E(x_E) R_E(B \cap \mathcal{Y}_E | x_E) \Pi_E^{\text{lat}}(dx_E | x) + \left[1 - \int_{\Psi_E} s_E(x_E) \Pi_E^{\text{lat}}(dx_E | x)\right] \delta_\varnothing(B).} \quad (2.5.7)$$

The first term in Eq. (2.5.7) describes all ways in which the original latent state x can be transformed into a protocol-conditioned state x_E , survive into the accepted readout channel, and generate an observed non-null datum. The second term assigns the remaining probability mass to \varnothing . Since $R_E(\mathcal{Y}_E | x_E) = 1$ and $0 \leq s_E(x_E) \leq 1$, the kernel is normalized:

$$K_E^\varnothing(\mathcal{Y}_E^\varnothing | x) = 1. \quad (2.5.8)$$

Definition 2.10 (Protocol observation operator). The *protocol observation operator* associated

with E is the map

$$\mathcal{M}_E^\varnothing : P_{\text{ref},t} \mapsto P_{\text{obs},t}^\varnothing(\cdot | E),$$

defined by

$$P_{\text{obs},t}^\varnothing(B | E) = (\mathcal{M}_E^\varnothing P_{\text{ref},t})(B) = \int_{\Psi} K_E^\varnothing(B | x) P_{\text{ref},t}(dx), \quad B \in \Sigma_{Y,E}^\varnothing. \quad (2.5.9)$$

It maps a reference latent ensemble to the full observed ensemble, including null observations.

Remark 2.11 (Linearity before conditioning). The null-inclusive operator $\mathcal{M}_E^\varnothing$ is linear in the input probability measure. If $P_{\text{ref},t} = \alpha P_1 + (1 - \alpha) P_2$, with $0 \leq \alpha \leq 1$, then

$$\mathcal{M}_E^\varnothing P_{\text{ref},t} = \alpha \mathcal{M}_E^\varnothing P_1 + (1 - \alpha) \mathcal{M}_E^\varnothing P_2.$$

The detected non-null ensemble $P_{\text{obs},t}(\cdot | E, \text{det})$ is obtained only after conditioning on \mathcal{Y}_E , and this conditioning introduces the normalization by $\eta_E(t)$. Thus the full probability accounting is linear before detection conditioning and generally nonlinear after conditioning on non-null observation.

Remark 2.12 (What the readout kernel adds). The readout kernel is not a duplicate of the latent transformation kernel. The latent transformation kernel describes how the protocol changes or conditions the state before observation. The readout kernel describes how an accepted conditioned state becomes data. For example, deformation under an AFM tip belongs to the conditioned latent state, whereas fitting a force-indentation curve to an elastic model belongs to readout. Particle orientation in vitrified ice belongs to the conditioned latent state, whereas classification and reconstruction belong to readout. Local infection and spread belong to the plaque-assay pathway, whereas staining, thresholding, and counting belong to readout.

2.6 Collapse Functionals

Experimental collapse is not a single universal number. It must be quantified relative to a specified observable, distribution, or inference target. A protocol may preserve one part of the latent ensemble while strongly transforming, selecting, or projecting another. For this reason, collapse functionals should state explicitly which feature of the latent system is being compared before and after protocol conditioning.

Let

$$g : \Psi \rightarrow \mathbb{R}, \quad g_E : \Psi_E \rightarrow \mathbb{R}$$

be comparable latent and protocol-conditioned quantities, such as radius, orientation, stiffness, mobility, infectious activity, angular response, adhesion state, or projected transport coefficient. Assume these quantities are integrable with respect to the relevant measures. A scalar collapse functional may be defined as

$$\mathcal{C}_E[g, g_E; t] = \left| \int_{\Psi_E} g_E(x_E) P_{E,t}^{\text{lat}}(dx_E | \text{det}) - \int_{\Psi} g(x) P_{\text{ref},t}(dx) \right|. \quad (2.6.1)$$

This quantity measures how strongly the detected protocol-conditioned ensemble displaces a chosen latent quantity from its reference expectation. It is useful when the target of interest is a scalar

feature, such as mean apparent radius, mean stiffness, mean mobility, mean infectious activity, or mean projected transport coefficient.

The same idea can be written without conditioning on detection by using the null-inclusive measure and a readout-level observable h on \mathcal{Y}_E^\emptyset :

$$\mathcal{C}_E^\emptyset[g, h; t] = \left| \int_{\mathcal{Y}_E^\emptyset} h(y) P_{\text{obs},t}^\emptyset(dy | E) - \int_{\Psi} g(x) P_{\text{ref},t}(dx) \right|. \quad (2.6.2)$$

This form is useful when the null channel itself is part of the quantity being studied, such as detection probability, infectivity failure, non-plaque-forming fraction, or rejection probability. The function h must specify how the null outcome is scored; for example, one may set $h(\emptyset) = 0$, or define a separate indicator $h(y) = \mathbf{1}_{\{y=\emptyset\}}$ to measure collapse into the null channel.

A distributional collapse functional may also be defined. Because Ψ , Ψ_E , and \mathcal{Y}_E need not be the same space, the distributions being compared must first be mapped to a common comparison space. Let

$$L_0 : \Psi \rightarrow \mathbb{W}, \quad L_E : \mathcal{Y}_E \rightarrow \mathbb{W}$$

be measurable maps into a common comparison space $(\mathbb{W}, \Sigma_{\mathbb{W}})$. Then

$$\mathfrak{c}_E^{\mathbb{W}}(t) = D_{\mathbb{W}}((L_0)_\# P_{\text{ref},t}, (L_E)_\# P_{\text{obs},t}(\cdot | E, \text{det})), \quad (2.6.3)$$

where $D_{\mathbb{W}}$ is a discrepancy on probability measures over \mathbb{W} . Depending on the geometry of the comparison target, $D_{\mathbb{W}}$ may be total variation distance, Wasserstein distance, maximum mean discrepancy, Jensen–Shannon divergence, Kullback–Leibler divergence when absolute continuity conditions are satisfied, or another problem-appropriate measure of distributional discrepancy.

Remark 2.13 (Why comparison spaces are needed). Writing a divergence directly between the latent ensemble and the observed ensemble is generally not meaningful unless they live on the same measurable space. A plaque count, a force–indentation curve, a cryo-EM reconstruction, an electrorotation spectrum, and a trajectory are different mathematical objects. The maps L_0 and L_E state exactly which quantity is being compared. They make explicit whether the comparison concerns size, orientation, stiffness, transport, infectious activity, detection probability, or some other derived feature.

Remark 2.14 (Collapse is observable only through chosen functionals). There is generally no single number called “the” collapse of a protocol. A protocol may strongly collapse orientation while preserving size, strongly select infectious competence while discarding structural heterogeneity, or preserve morphology while eliminating dynamic information. Collapse must therefore be reported relative to specified observables, distributions, or inference targets. The choice of collapse functional is part of the scientific question, not an afterthought.

Remark 2.15 (Collapse functionals versus inference). Collapse functionals quantify how a protocol changes, selects, projects, or reweights a chosen feature of the ensemble. They do not by themselves solve the inverse problem. Rather, they identify which aspects of the latent system are preserved, distorted, or erased by a protocol. This information can then be used to design complemen-

tary experiments, choose informative protocol variations, or determine which latent parameters are identifiable from the available observations.

2.7 Protocol Blindness and Fisher-Information Observability

The same operator formalism also identifies what a protocol cannot see. Once an observed ensemble is written as the image of a latent ensemble under a null-inclusive protocol operator, protocol blindness becomes a question about which changes in the latent model produce distinguishable changes in the observed law. Suppose the reference latent ensemble is parameterized by

$$P_{\text{ref},t} = P_{\theta,t}, \quad \theta \in \Theta, \quad (2.7.1)$$

where θ may encode stiffness, charge, spike-state heterogeneity, adhesive binding, rotational mobility, cell-entry competence, infectious activity, or other latent physical or biological features. Under protocol E , the null-inclusive observation operator induces an observed law

$$P_{\text{obs},t}^{\varnothing}(\cdot | E, \theta) = \mathcal{M}_E^{\varnothing} P_{\theta,t} \quad (2.7.2)$$

on the augmented observation space $(\mathcal{Y}_E^{\varnothing}, \Sigma_{Y,E}^{\varnothing})$.

When this observed law admits a density or mass function with respect to a common dominating measure ν_E^{\varnothing} , we write

$$p_E^{\varnothing}(y | \theta) = \frac{dP_{\text{obs},t}^{\varnothing}(\cdot | E, \theta)}{d\nu_E^{\varnothing}}(y), \quad y \in \mathcal{Y}_E^{\varnothing}. \quad (2.7.3)$$

The Fisher-information matrix for protocol E is then

$$\mathcal{I}_E(\theta) = \mathbb{E}_{Y \sim p_E^{\varnothing}(\cdot | \theta)} \left[\nabla_{\theta} \log p_E^{\varnothing}(Y | \theta) \nabla_{\theta} \log p_E^{\varnothing}(Y | \theta)^{\top} \right], \quad (2.7.4)$$

whenever the usual differentiability and integrability conditions are satisfied. Equivalently,

$$\mathcal{I}_E(\theta) = \int_{\mathcal{Y}_E^{\varnothing}} \nabla_{\theta} \log p_E^{\varnothing}(y | \theta) \nabla_{\theta} \log p_E^{\varnothing}(y | \theta)^{\top} p_E^{\varnothing}(y | \theta) \nu_E^{\varnothing}(dy).$$

A parameter direction $v \in T_{\theta}\Theta$ is locally unobservable under protocol E when

$$\boxed{v^{\top} \mathcal{I}_E(\theta) v = 0}. \quad (2.7.5)$$

The local blind subspace of the protocol is therefore

$$\mathcal{B}_E(\theta) = \ker \mathcal{I}_E(\theta) = \left\{ v \in T_{\theta}\Theta : v^{\top} \mathcal{I}_E(\theta) v = 0 \right\}. \quad (2.7.6)$$

Under standard regularity assumptions, this condition means that the directional score in direction v vanishes almost surely under the observed law. Thus, to first order, moving the latent model along v does not produce a statistically distinguishable change in the data generated by protocol E . Such a direction corresponds to an under-resolved latent sector: a change in the latent virion–environment ensemble that is not coupled to the protocol, is removed by selection, is averaged over by the readout,

is mapped into the null channel, or is confounded with another parameter direction. Fisher-information observability is therefore a local property of the protocol-conditioned forward map, not a context-free property of the latent variable itself.

A stronger, global form of protocol blindness occurs when two distinct parameter values induce the same observed law:

$$\boxed{P_{\text{obs},t}^{\varnothing}(\cdot | E, \theta_1) = P_{\text{obs},t}^{\varnothing}(\cdot | E, \theta_2), \quad \theta_1 \neq \theta_2.} \quad (2.7.7)$$

Equivalently, when densities exist,

$$p_E^{\varnothing}(\cdot | \theta_1) = p_E^{\varnothing}(\cdot | \theta_2) \quad \nu_E^{\varnothing}\text{-a.e.}$$

In that case, protocol E cannot distinguish the two latent hypotheses even in the infinite-data limit. Local Fisher degeneracy describes infinitesimal blindness near a parameter value; global observational equivalence describes exact non-identifiability of distinct latent hypotheses under the protocol.

Multiple protocols can reduce blindness when they probe different latent directions. If protocols E_1, \dots, E_M generate conditionally independent datasets given θ , and if nuisance parameters are fixed, calibrated, or appropriately handled, then their Fisher-information matrices add:

$$\boxed{\mathcal{I}_{\text{multi}}(\theta) = \sum_{j=1}^M \mathcal{I}_{E_j}(\theta).} \quad (2.7.8)$$

The corresponding local blind subspace is

$$\mathcal{B}_{\text{multi}}(\theta) = \ker \mathcal{I}_{\text{multi}}(\theta). \quad (2.7.9)$$

A latent sector that is invisible to one protocol may be partially visible to another. For example, a structural imaging protocol may strongly constrain morphology while remaining weakly sensitive to mechanical compliance or infectious activity; a mechanical protocol may constrain stiffness while discarding free-particle rotational dynamics; and a plaque assay may constrain protocol-conditioned infectivity while remaining blind to non-plaque-forming structural heterogeneity. This is the mathematical basis for multi-protocol consistency and complementarity: protocols are combined not because their raw observables are the same, but because their observation operators constrain different directions of a shared latent model.

Table 6. Schematic examples of protocol-conditioned observability. The table is conceptual: the relevant latent variables, observation kernels, and collapse functionals must be specified for each experimental system.

Protocol	Reported ensemble	Likely collapsed variables	Possible blind sectors
Cryo-EM/cryo-ET	Density maps, particle classes, reconstructed structures	Orientation distribution, conformation selection, interface survival, particle picking, reconstruction-dependent representation	Dynamics, rare states, preparation-sensitive conformations, fragile or transient configurations.
AFM	Height maps, force-indentation curves, rupture forces, apparent stiffness	Surface association, loading pathway, deformation state, hydration, tip-sample contact geometry	Free rotational dynamics, non-adhered populations, fragile states, unloaded mechanical modes.
DEP/electrorotation	Field-driven motion, trapping behavior, crossover frequencies, rotation spectra	Polarization state, medium-dependent dielectric response, hydrodynamic drag, field-induced orientation	Non-dielectric mechanical variables, field-fragile states, latent structural heterogeneity weakly coupled to polarization.
Mucus or gel tracking	Trajectories, diffusivities, confinement metrics, mobility classes	Accessible paths, adhesive binding, local rheology, time-windowed mobility, tracking thresholds	Non-trackable particles, short-lived binding states, structural variables not expressed through transport, infectivity.
Plaque/focus assay	PFU, FFU, endpoint infectious dose, visible lesions or foci	Cell-entry competence, replication, local spread, overlay survival, visibility threshold, counting rule	Noninfectious particles, structurally intact but non-plaque-forming virions, defective particles, neutralized or cell-line-incompatible states.

This completes the operator-level formulation needed for the more detailed development below. A measurement does not simply reveal a latent virion ensemble; it maps that ensemble through a protocol-conditioned transformation, selection, null channel, and readout. The resulting data are therefore interpretable only relative to the experimental map that produced them. The next sections develop the three ensemble levels—latent, protocol-conditioned, and observed—in greater detail and use them to analyze protocol blindness, inverse inference, multi-protocol consistency, and experimentally

collapsed infectivity.

3 Latent, Protocol-Conditioned, and Observed Ensembles

The preceding section defined the protocol observation operator. We now separate the ensemble levels on which that operator acts. The basic object in protocol-resolved virophysics is not a single observed virion, but a sequence of probability measures: a reference latent ensemble, a protocol-conditioned latent ensemble, and an observed ensemble. These measures need not live on the same state space, and they need not preserve the same physical distinctions.

The distinction may be summarized as

$$\boxed{P_{\text{ref},t} \xrightarrow{\Pi_E^{\text{lat}}} \tilde{P}_{E,t}^{\text{lat}} \xrightarrow{s_E, R_E, \emptyset} P_{\text{obs},t}^{\emptyset}(\cdot | E)}. \quad (3.1)$$

The reference latent ensemble describes the virion–environment system before the additional conditioning imposed by the measurement protocol. The protocol-conditioned latent ensemble describes the population after preparation, forcing, medium exposure, surface interaction, biological pathway conditioning, or other protocol-induced transformations, but before final accepted readout. The observed ensemble describes the reported data, including the possibility that some latent states are mapped to the null outcome.

The goal of this distinction is not to make experimental data appear less reliable. Rather, it is to state precisely what kind of ensemble a protocol reports. A protocol-conditioned observation may be highly reproducible, quantitative, and biologically meaningful while still being different from a direct sample of the reference latent population.

3.1 Reference Latent Ensembles

Definition 3.1 (Latent state space and reference latent ensemble). Let

$$(\Psi, \Sigma_X)$$

be the measurable space of latent virion–environment states appropriate to the level of description under study. The *reference latent ensemble* is a time-dependent probability measure

$$P_{\text{ref},t}(dx), \quad x \in \Psi, \quad (3.1.1)$$

describing the distribution of virion, virion–environment, or virion-assembly states in the biological or physical environment of interest before the additional conditioning imposed by the experimental protocol E .

The word *reference* should be read relative to a specified physical or biological setting. It does not mean that the ensemble is universal, equilibrium, unperturbed, or experimentally inaccessible in principle. Rather, it identifies the baseline ensemble whose transformation by the protocol is to be analyzed. Thus $P_{\text{ref},t}$ may describe virions in buffer, mucus, extracellular fluid, a gel, an aerosol droplet, a surface microenvironment, an overlay, or a host-tissue context.

When $P_{\text{ref},t}$ is absolutely continuous with respect to a reference measure μ_X , one may write

$$P_{\text{ref},t}(dx) = p_{\text{ref}}(x, t) \mu_X(dx), \quad (3.1.2)$$

where $p_{\text{ref}}(x, t)$ is a density. The measure notation is retained because many virological observables and latent descriptions are not naturally represented by ordinary Euclidean densities. They may include continuous mechanical coordinates, discrete conformational classes, particle counts, aggregates, damaged states, rejected states, and null outcomes.

Remark 3.2 (Interpretation of the reference ensemble). The reference ensemble is not required to be a free-particle ensemble. It may already include hydrodynamic forcing, electrolyte screening, thermal fluctuations, mucus confinement, extracellular matrix structure, receptor-rich surfaces, biologically relevant adhesion, or host-environment chemistry. These features belong to the physical system being modeled. Experimental collapse refers to the additional transformation, selection, reweighting, or projection introduced by the measurement protocol.

Remark 3.3 (Natural versus protocol-conditioned). In some contexts it is useful to call $P_{\text{ref},t}$ a natural latent ensemble. This terminology should always be understood relative to the chosen environment. A virion ensemble in mucus, in buffer, and in an aerosol droplet may all be natural relative to their respective physical settings. None is automatically the protocol-conditioned ensemble produced by cryo-EM, AFM, dielectrophoresis, tracking, or a plaque assay.

3.2 Protocol-Conditioned Latent Ensembles

Let E be a fixed experimental protocol. The protocol may include sample preparation, vitrification, staining, adsorption, field forcing, surface attachment, medium exchange, imaging cadence, cell type, overlay medium, particle-picking rules, thresholding, reconstruction, or any other operation that changes which virion states become experimentally accessible.

Definition 3.4 (Protocol-induced latent-state kernel). Let

$$(\Psi_E, \Sigma_{X,E})$$

be the protocol-conditioned latent state space. The *protocol-induced latent-state kernel* is a Markov kernel

$$\Pi_E^{\text{lat}}(dx_E | x), \quad x \in \Psi, \quad x_E \in \Psi_E, \quad (3.2.1)$$

giving the conditional distribution of protocol-conditioned latent states x_E generated from a reference latent state x before survival, selection, and readout.

For each fixed $x \in \Psi$, the kernel is normalized:

$$\Pi_E^{\text{lat}}(\Psi_E | x) = 1. \quad (3.2.2)$$

This normalization means that Π_E^{lat} accounts for how a reference state is transformed into some protocol-conditioned latent state. It does not by itself describe whether that state is ultimately detected, accepted, counted, reconstructed, or reported. Those effects are represented separately by the survival or detection weight and by the null channel.

The protocol-conditioned latent ensemble before survival or detection selection is the pushforward of

Example	Protocol-conditioned latent interpretation
Cryo-EM or cryo-ET	A hydrated, dynamic particle ensemble is transformed into a vitrified, grid-associated, orientation-conditioned structural ensemble before picking, classification, and reconstruction.
AFM	A free or weakly interacting particle ensemble is transformed into a surface-associated and mechanically loaded ensemble whose deformation path depends on tip geometry, loading rate, hydration, and adhesion.
DEP or electrorotation	A particle ensemble in medium is transformed into a field-conditioned ensemble with induced polarization, hydrodynamic response, torque, trapping, or frequency-dependent motion.
Mucus or gel tracking	A particle ensemble is conditioned by mesh structure, adhesion, local rheology, confinement, and the time window over which motion is sampled.
Plaque assay	A particle population is transformed into an assay-pathway ensemble conditioned by cell line, adsorption, entry, replication, overlay-limited spread, incubation, staining, and counting criteria.

Table 7. Examples of protocol-conditioned latent ensembles. The purpose of $\tilde{P}_{E,t}^{\text{lat}}$ is to represent the ensemble after protocol-induced physical, mechanical, chemical, or biological conditioning, but before the final accepted observed data are formed.

$P_{\text{ref},t}$ through the kernel Π_E^{lat} :

$$\tilde{P}_{E,t}^{\text{lat}}(A) = \int_{\Psi} \Pi_E^{\text{lat}}(A | x) P_{\text{ref},t}(dx), \quad A \in \Sigma_{X,E}. \quad (3.2.3)$$

This measure is the latent ensemble after protocol conditioning but before survival, detection, or acceptance selection. It is therefore distinct both from the reference ensemble $P_{\text{ref},t}$ and from the final observed ensemble $P_{\text{obs},t}^{\mathcal{O}}(\cdot | E)$.

If densities exist, and if Π_E^{lat} admits a transition density $\pi_E^{\text{lat}}(x_E | x)$ with respect to a reference measure $\mu_{X,E}$ on Ψ_E , then

$$\tilde{P}_{E,t}^{\text{lat}}(dx_E) = \tilde{p}_E^{\text{lat}}(x_E, t) \mu_{X,E}(dx_E), \quad (3.2.4)$$

where

$$\tilde{p}_E^{\text{lat}}(x_E, t) = \int_{\Psi} \pi_E^{\text{lat}}(x_E | x) p_{\text{ref}}(x, t) \mu_X(dx). \quad (3.2.5)$$

This density form is useful when the state spaces are continuous and dominated by convenient reference measures. The measure form in Eq. (3.2.3) remains the more general statement.

Remark 3.5 (Transformation versus selection). It is important not to force all protocol effects into a normalized transformation kernel. Some effects physically, chemically, mechanically, or biologically transform a virion state: field forcing, surface adsorption, vitrification, dehydration, tip loading, confinement, medium exposure, chemical treatment, cell attachment, or entry-pathway conditioning can change x into x_E . Other effects determine whether a state is reported at all: particles

may be lost during preparation, excluded during particle picking, immobilized outside the field of view, fail a signal-to-noise threshold, fail to infect the chosen cell type, fail to form a visible plaque, or move too quickly to be tracked. These are survival, selection, or detection effects. They require an additional weight and an explicit null-observation channel.

3.3 Survival, Detection, and Null Observations

The preselection ensemble $\tilde{P}_{E,t}^{\text{lat}}$ describes the population after protocol conditioning, but before the experiment determines which states enter the accepted data channel. The next step is therefore not readout itself, but survival, detection, acceptance, or biological success. These effects are represented by a protocol-dependent weight.

Definition 3.6 (Survival and detection weight). The *survival/detection weight* of protocol E is a measurable function

$$s_E : \Psi_E \rightarrow [0, 1], \quad (3.3.1)$$

where $s_E(x_E)$ is the probability that a protocol-conditioned latent state x_E survives the experimental pipeline and contributes to a non-null experimental record.

The total probability that a state drawn from $P_{\text{ref},t}$ produces a non-null record is

$$\eta_E(t) = \int_{\Psi_E} s_E(x_E) \tilde{P}_{E,t}^{\text{lat}}(dx_E). \quad (3.3.2)$$

We call $\eta_E(t)$ the *detection yield*. It measures the probability mass of the protocol-conditioned latent ensemble that reaches the accepted non-null data channel. When $0 < \eta_E(t) \leq 1$, the detected protocol-conditioned latent ensemble is the conditional measure

$$P_{E,t}^{\text{lat}}(A \mid \text{det}) = \frac{1}{\eta_E(t)} \int_A s_E(x_E) \tilde{P}_{E,t}^{\text{lat}}(dx_E), \quad A \in \Sigma_{X,E}. \quad (3.3.3)$$

Thus $P_{E,t}^{\text{lat}}(\cdot \mid \text{det})$ is not simply the protocol-conditioned latent ensemble. It is the protocol-conditioned ensemble after reweighting by survival, visibility, detectability, acceptance, or biological success, followed by normalization. If $\eta_E(t) = 0$, no detected non-null latent ensemble is defined, but the null-inclusive observed measure remains well defined and assigns all mass to the null channel.

Definition 3.7 (Augmented observation space). Let $(\mathcal{Y}_E, \Sigma_{Y,E})$ be the non-null observation space associated with protocol E . The augmented observation space is

$$\mathcal{Y}_E^\emptyset = \mathcal{Y}_E \cup \{\emptyset\}, \quad (3.3.4)$$

where \emptyset denotes non-detection, rejection, loss, failure to pass an acceptance threshold, failed amplification, or exclusion from the reported dataset. The corresponding augmented sigma-algebra is

$$\Sigma_{Y,E}^\emptyset = \sigma(\Sigma_{Y,E} \cup \{\{\emptyset\}\}). \quad (3.3.5)$$

Remark 3.8 (Why a null state is needed). The null state \emptyset keeps probability accounting explicit.

Without it, a protocol that reports only a selected subset of states can be mistaken for one that faithfully transforms every latent state into a measured state. In cryo-EM, for example, air–water interface exposure, ice thickness, support interaction, preferred orientation, particle picking, and reconstruction criteria may determine which particles contribute to the final density map [1, 2, 3, 4, 5]. In tracking experiments, particles that bind irreversibly, leave the focal volume, photobleach, or cannot be localized disappear from the reported trajectory ensemble. In plaque assays, particles that fail adsorption, entry, replication, local spread, visibility, or counting criteria disappear from the plaque count. The null channel represents this missing but experimentally meaningful part of the probability flow.

3.4 Readout Kernels and Observed Ensembles

Detection determines which protocol-conditioned latent states enter the accepted data channel. It does not yet specify what datum is recorded. The final readout step maps a detected protocol-conditioned latent state to an observed outcome.

Definition 3.9 (Readout kernel). The *readout kernel* of protocol E is a Markov kernel

$$R_E(dy \mid x_E), \quad x_E \in \Psi_E, \quad y \in \mathcal{Y}_E, \quad (3.4.1)$$

from $(\Psi_E, \Sigma_{X,E})$ to $(\mathcal{Y}_E, \Sigma_{Y,E})$, conditional on non-null detection. Hence

$$R_E(\mathcal{Y}_E \mid x_E) = 1 \quad \text{for each fixed } x_E \in \Psi_E. \quad (3.4.2)$$

The kernel R_E includes the final representation of a surviving state as data: projection, finite resolution, reconstruction, segmentation, thresholding, counting, fitting, classification, and measurement noise.

For a fixed reference latent state $x \in \Psi$, define the state-specific non-null passage probability

$$q_E(x) = \int_{\Psi_E} s_E(x_E) \Pi_E^{\text{lat}}(dx_E \mid x). \quad (3.4.3)$$

This is the probability that the latent state x , after protocol conditioning, reaches the accepted non-null readout channel. The full null-inclusive protocol observation kernel is then

$$\boxed{K_E^\varnothing(S \mid x) = \int_{\Psi_E} s_E(x_E) R_E(S \cap \mathcal{Y}_E \mid x_E) \Pi_E^{\text{lat}}(dx_E \mid x) + [1 - q_E(x)] \delta_\varnothing(S), \quad S \in \Sigma_{Y,E}^\varnothing.} \quad (3.4.4)$$

For each fixed x , this is a normalized probability measure on $\mathcal{Y}_E^\varnothing$:

$$K_E^\varnothing(\mathcal{Y}_E^\varnothing \mid x) = 1. \quad (3.4.5)$$

The normalization follows from the fact that $R_E(\mathcal{Y}_E \mid x_E) = 1$ and $0 \leq s_E(x_E) \leq 1$.

The full observed ensemble is the image of the reference latent ensemble under this augmented

protocol kernel:

$$P_{\text{obs},t}^{\varnothing}(S | E) = \int_{\Psi} K_E^{\varnothing}(S | x) P_{\text{ref},t}(dx), \quad S \in \Sigma_{Y,E}^{\varnothing}. \quad (3.4.6)$$

In particular, the probability of a null observation is

$$P_{\text{obs},t}^{\varnothing}(\{\varnothing\} | E) = 1 - \eta_E(t), \quad (3.4.7)$$

because

$$\eta_E(t) = \int_{\Psi} q_E(x) P_{\text{ref},t}(dx) = \int_{\Psi_E} s_E(x_E) \tilde{P}_{E,t}^{\text{lat}}(dx_E).$$

The reported non-null observed ensemble is obtained by conditioning the null-inclusive observed measure on the non-null observation space:

$$P_{\text{obs},t}(B | E, \text{det}) = \frac{P_{\text{obs},t}^{\varnothing}(B | E)}{\eta_E(t)}, \quad B \in \Sigma_{Y,E}, \quad 0 < \eta_E(t) \leq 1. \quad (3.4.8)$$

Equivalently,

$$P_{\text{obs},t}(B | E, \text{det}) = P_{\text{obs},t}^{\varnothing}(B | Y \in \mathcal{Y}_E, E). \quad (3.4.9)$$

This equation separates the reported shape of the non-null data distribution from the total amount of probability mass that survived into the reported data channel.

Remark 3.10 (Compact interpretation). The experimentally reported ensemble is not, in general, the reference latent ensemble itself. It is the detected, normalized image of the reference ensemble under a protocol-dependent composition of latent-state transformation, survival or selection, and readout:

$$P_{\text{ref},t} \xrightarrow{\Pi_E^{\text{lat}}} \tilde{P}_{E,t}^{\text{lat}} \xrightarrow{s_E} P_{E,t}^{\text{lat}}(\cdot | \text{det}) \xrightarrow{R_E} P_{\text{obs},t}(\cdot | E, \text{det}).$$

The null-inclusive ensemble $P_{\text{obs},t}^{\varnothing}(\cdot | E)$ retains the missing probability mass that is lost when one reports only detected observations.

Definition 3.11 (Protocol observation operator). The *protocol observation operator* associated with E is the map

$$\mathcal{M}_E^{\varnothing} : P_{\text{ref},t} \mapsto P_{\text{obs},t}^{\varnothing}(\cdot | E), \quad (3.4.10)$$

defined by

$$(\mathcal{M}_E^{\varnothing} P_{\text{ref},t})(S) = \int_{\Psi} K_E^{\varnothing}(S | x) P_{\text{ref},t}(dx), \quad S \in \Sigma_{Y,E}^{\varnothing}. \quad (3.4.11)$$

The non-null reported ensemble is obtained by conditioning $\mathcal{M}_E^{\varnothing} P_{\text{ref},t}$ on \mathcal{Y}_E .

Remark 3.12 (Why detection yield matters). The same normalized reported distribution $P_{\text{obs},t}(\cdot | E, \text{det})$ can arise from very different detection yields. A protocol that reports nearly every protocol-conditioned state and a protocol that reports only a small selected subset may produce superficially similar observed histograms after normalization. The detection yield $\eta_E(t)$ records the missing denominator. It is therefore part of experimental collapse, not merely a nuisance variable.

Remark 3.13 (Reported data versus probability flow). Reporting only the conditional non-null ensemble can hide important protocol effects. For example, two plaque assays may produce similar plaque size distributions among counted plaques while having very different plaque-forming probabilities. Two tracking experiments may produce similar mobility distributions among tracked particles while losing different fractions of immobilized or dim particles. Two reconstruction pipelines may produce similar particle classes after selection while rejecting different fractions of the original images. The null-inclusive formulation keeps both the reported distribution and the probability flow into the reported channel available for analysis.

3.5 Latent versus Observed Virion State

The distinction between latent and observed state is the practical center of experimental collapse. The *latent state* is the state on which the theory is formulated: it is the state whose evolution, interaction, deformation, transport, infectivity, or environmental coupling is described by equations of motion, transition rules, constitutive relations, and biological assumptions. The *observed state* is the state reported by an instrument, assay, reconstruction pipeline, tracking algorithm, classification rule, or counting procedure. In general, these two objects are not identical. They need not even belong to the same mathematical state space.

This distinction is especially important in virology because different experimental traditions report fundamentally different kinds of objects. A cryo-EM reconstruction reports preserved structural density. An AFM experiment reports surface-conditioned topography or force response. A single-virus tracking experiment reports localized positions or trajectories over a finite time window. A dielectrophoretic or electrorotation experiment reports field-conditioned motion or frequency response. A plaque assay reports visible infectious lesions. Each is a valid virological observable, but none should be identified automatically with the complete latent virion state.

$$\boxed{\text{latent state} \neq \text{observed state}, \quad X \in \Psi, \quad Y_E \in \mathcal{Y}_E.} \quad (3.5.1)$$

The point is not that the latent state is mysterious or metaphysical. A state is latent only relative to a specified protocol. It is the collection of variables that the model regards as mechanically, physically, chemically, or biologically relevant, whether or not a particular experiment records those variables in full. The observed state is the representation of that latent system after the protocol has transformed, selected, projected, reconstructed, classified, or counted it.

3.5.1 Latent state as the state of the model

Definition 3.14 (Latent virion state). A *latent virion state* is the mechanically, physically, chemically, or biologically relevant state variable entering the theory before protocol reduction. Depending on the scale of description, it may take one of the following schematic forms.

(i) **Single-virion level:**

$$X^{(1)} = (\mathbf{r}, \mathbf{v}, Q, \boldsymbol{\omega}, \mathbf{s}, \mathbf{c}, \theta_{\text{env}}, \theta_{\text{bio}}), \quad (3.5.1.1)$$

where \mathbf{r} and \mathbf{v} are position and velocity, Q is an orientation variable, $\boldsymbol{\omega}$ is angular velocity, \mathbf{s} denotes surface, spike, glycoprotein, conformational, or shell variables, \mathbf{c} denotes contact, adhesion, receptor-binding, or medium-contact state, θ_{env} denotes relevant local environmental parameters, and θ_{bio} denotes biological competence variables such as entry, replication, neutralization, or

plaque-forming capacity when those variables are part of the model.

(ii) **Pairwise interaction level:**

$$X^{(2)} = (\mathbf{r}_{ij}, \mathbf{v}_{ij}, Q_i, Q_j, \boldsymbol{\omega}_i, \boldsymbol{\omega}_j, \mathbf{c}_{ij}, \theta_{\text{env}}), \quad (3.5.1.2)$$

where \mathbf{r}_{ij} and \mathbf{v}_{ij} are relative position and relative velocity, Q_i, Q_j are orientations, $\boldsymbol{\omega}_i, \boldsymbol{\omega}_j$ are angular velocities, and \mathbf{c}_{ij} denotes contact, near-contact, receptor-mediated, electrostatic, hydrodynamic, steric, or orientation-dependent geometric data relevant to the interaction.

(iii) **Assembly or lattice level:**

$$X^{(\text{L})} = \{\mathbf{u}(\mathbf{R}), \boldsymbol{\eta}(\mathbf{R}), \dot{\mathbf{u}}(\mathbf{R}), \dot{\boldsymbol{\eta}}(\mathbf{R})\}_{\mathbf{R} \in \text{L}}, \quad (3.5.1.3)$$

together with shellwise constitutive parameters, boundary conditions, interaction coefficients, environmental variables, and any protocol-relevant constraints. Here $\mathbf{u}(\mathbf{R})$ may denote translational displacement at lattice site \mathbf{R} , while $\boldsymbol{\eta}(\mathbf{R})$ denotes rotational, orientational, spike, or internal mode variables, depending on the lattice model.

(iv) **Joint virion–environment level:**

$$X^{(\text{joint})} = (X_{\text{vir}}, X_{\text{env}}), \quad (3.5.1.4)$$

where X_{vir} contains virion-level variables and X_{env} contains local medium or assay variables such as viscosity, mesh size, mucin composition, antibody concentration, ionic strength, pH, conductivity, surface chemistry, receptor density, temperature, cell-line susceptibility, or overlay conditions.

These examples are not meant to impose a single universal state vector for all of virophysics. They show that the latent state is model-dependent. A structural model may emphasize geometry and conformation; a mechanical model may emphasize deformation, stiffness, and loading; a transport model may emphasize position, trajectory, adhesion, and medium structure; an infectivity model may emphasize entry, replication, spread, and assay compatibility. The latent state should therefore be chosen to close the theory at the scale of interest.

Remark 3.15 (What makes a state latent). A state is latent because it is not directly or completely reported by the protocol. It is not latent because it is unphysical. For example, a cryo-EM density map may preserve structural geometry while eliminating velocity, real-time force history, and the preparation pathway that led to the preserved state. An AFM image may report morphology and mechanical response after surface adsorption, but not the free pre-adsorption trajectory. A single-virus tracking experiment may record a projected path while leaving orientation, spike presentation, local adhesion state, fusion competence, or infectivity unresolved [2, 3, 4, 5, 8, 9, 41, 42, 43, 14, 15, 23].

Remark 3.16 (Why the latent state matters theoretically). The latent state is the state on which the theory closes. It is therefore the state in which equations of motion, collision rules, shell couplings, orientation dynamics, dielectric response, adhesion kinetics, infectivity transitions, and collective branch structure are naturally formulated. If a protocol compresses or transforms that state before readout, then the experimentally reported variables must be interpreted as functionals, projections, conditional distributions, or statistical images of the latent state rather than as the state

itself.

3.5.2 Observed state as the state of the protocol

Definition 3.17 (Observed virion state). For a fixed protocol E , the *observed virion state* is an element

$$Y_E \in \mathcal{Y}_E, \tag{3.5.2.1}$$

where $(\mathcal{Y}_E, \Sigma_{Y,E})$ is the protocol-dependent non-null observation space. Typical examples include:

- (i) reconstructed static geometry, density maps, subtomogram averages, particle-class averages, orientation distributions, or selected conformational classes in cryo-electron imaging;
- (ii) topography, height profiles, indentation curves, rupture events, adhesion estimates, force–distance curves, or stiffness estimates for surface-associated particles in AFM;
- (iii) trapping locations, field-driven trajectories, crossover frequencies, phase shifts, rotation rates, or response amplitudes in dielectrophoresis and electrorotation;
- (iv) tracked positions, mean-square displacements, residence times, anomalous-diffusion exponents, confined-transport statistics, pause states, directed-motion intervals, jump events, or drift events in single-virus tracking;
- (v) plaque counts, focus counts, endpoint dilution readouts, reporter signals, visible lesions, or inferred infectious units in infectivity assays.

The observed state is therefore not merely a noisy version of X . In many cases it is a different kind of mathematical object. A latent state may contain positions, velocities, orientations, spike states, environmental variables, and biological transition probabilities, while the corresponding observed state may be an image, curve, count, class label, trajectory, spectrum, or endpoint readout. This mismatch is precisely why the protocol kernel is needed.

Remark 3.18 (The observed state is protocol-specific). There is no universal observed virion state. A virion observed by cryo-EM is represented as a structural object. A virion observed by AFM is represented as a surface-associated mechanical object. A virion observed by single-particle tracking is represented as a time-indexed trajectory. A virion observed by DEP or electrorotation is represented through field response. A virion observed through a plaque assay is represented by its ability to generate a visible infectious lesion. These are not competing definitions of the virion. They are different protocol-conditioned representations of the same broader latent system.

Remark 3.19 (Observed does not mean complete). An observed state can be precise, reproducible, and experimentally valuable without being complete. A high-resolution structure may still omit dynamics, mechanical history, or infectivity. A clean trajectory may still omit orientation, surface chemistry, or biological competence. A plaque count may still omit particle number, defective-particle burden, aggregation state, and structural heterogeneity. Protocol-resolved virophysics does not demote these observables. It specifies what they are observations of.

3.5.3 From latent state to observed state

The latent and observed states are connected by the protocol. In the notation of the preceding sections, a reference latent state $x \in \Psi$ is first transformed into a protocol-conditioned latent state $x_E \in \Psi_E$. It

is then either mapped to a non-null observed datum $y_E \in \mathcal{Y}_E$ or sent to the null channel \emptyset :

$$\boxed{X \xrightarrow{\Pi_E^{\text{lat}}} X_E \xrightarrow{s_E, R_E} Y_E \quad \text{or} \quad \emptyset.} \quad (3.5.3.1)$$

The first arrow represents protocol-induced physical, chemical, biological, or mechanical conditioning. The second arrow represents survival, detection, projection, finite resolution, reconstruction, classification, counting, or null observation. Thus the observed state is not obtained from the latent state by a single universal measurement map. It is obtained through a protocol-dependent composition of conditioning, selection, and readout.

Definition 3.20 (Observation map with noise). When the readout can be represented in a vector-valued observation space, a useful reduced form is

$$Y_E = \mathcal{O}_E(X_E) + \nu_E, \quad (3.5.3.2)$$

where X_E is the protocol-conditioned latent state, \mathcal{O}_E is the protocol-dependent observation map, and ν_E is a measurement-noise term. This representation is less general than the kernel formulation, but it is useful when the readout is approximately additive or when the observed datum is a finite-dimensional vector. In this form, the distinction between latent and observed state is that \mathcal{O}_E is generally neither the identity map nor invertible.

The kernel formulation should be regarded as the primary statement. The noisy observation-map form in Eq. (3.5.3.2) is a convenient special case for familiar measurement models. It does not cover every kind of virological readout, since density maps, force curves, trajectories, categorical classes, plaque counts, and null outcomes need not be naturally represented as additive perturbations of a vector-valued latent state.

Definition 3.21 (Observation fiber). If a deterministic observation map

$$\mathcal{O}_E : \Psi_E \rightarrow \mathcal{Y}_E$$

is used, the *observation fiber* over an observed datum y_E is

$$\mathcal{F}_E(y_E) = \{x_E \in \Psi_E : \mathcal{O}_E(x_E) = y_E\}. \quad (3.5.3.3)$$

Remark 3.22 (Interpretation of the observation fiber). The fiber $\mathcal{F}_E(y_E)$ is the set of protocol-conditioned latent states that are indistinguishable to the observation map. If this set contains mechanically, structurally, dynamically, or biologically distinct states, then the protocol has collapsed those distinctions. For example, a plaque count may group many structurally different particles into the same infectious-unit readout; a trajectory may group different orientation states into the same projected path; and a reconstructed density may group different dynamical histories into the same preserved structural class.

Remark 3.23 (Fibers and stochastic readout). For stochastic readout kernels, exact fibers are replaced by conditional distributions over latent states compatible with an observation. In that case,

the relevant inverse object is not a set $\mathcal{F}_E(y_E)$, but a posterior or conditional law over Ψ_E given the observed datum. The deterministic fiber is therefore the geometric limit of a more general probabilistic inverse problem.

3.5.4 Common forms of latent-to-observed reduction

The same latent population may generate different observed ensembles under different protocols. The following reductions are especially common in virological work.

- (i) **State freezing.** A dynamic latent process is represented as a preserved structural snapshot. Cryo-EM and cryo-ET can provide extraordinary structural information, but the observed state is conditioned by preparation, vitrification, air–water interface exposure, particle selection, orientation statistics, and reconstruction [2, 3, 4, 5, 33].
- (ii) **Surface conditioning.** A freely suspended or weakly interacting particle is represented after adsorption, tethering, flattening, hydration change, or probe interaction. AFM therefore reports a surface-conditioned mechanical state rather than the unconstrained suspension-state dynamics of the same virion [6, 7, 8, 9].
- (iii) **Trajectory projection.** A high-dimensional virion–cell or virion–medium process is represented as a sequence of localized positions over a finite time window. Single-virus tracking can reveal entry, trafficking, confinement, directed motion, and transport regimes, but the observed trajectory depends on labeling, imaging cadence, localization, segmentation, and the variables chosen for analysis [41, 42, 43].
- (iv) **Medium filtering.** A virion moving through mucus, gel, extracellular matrix, or another structured medium is observed through the transport modes that survive the medium and the tracking window. In this case, the observed path is a joint virion–medium observable, not a property of the virion alone [14, 35, 15, 24, 23].
- (v) **Field-response projection.** A virion in dielectrophoresis or electrorotation is observed through its response to an imposed field. The observed state is therefore a field-conditioned response object involving virion polarizability, medium conductivity and permittivity, hydrodynamic drag, and frequency-dependent response [10, 11, 12, 13].
- (vi) **Biological amplification.** A latent particle population is represented by a functional biological output such as PFU, FFU, endpoint dilution, cytopathic effect, or reporter signal. These readouts are powerful precisely because they amplify selected biological events, but they do not report the total physical particle population [16, 17, 18, 37, 39].

Remark 3.24 (Examples of latent-to-observed reduction). In cryo-EM or cryo-ET, the observed state is dominated by preserved geometry after preparation, vitrification, particle selection, and reconstruction. In AFM, the observed state is conditioned by adsorption, local hydration, tip convolution, and mechanical loading. In dielectrophoresis, the observed state is a trajectory, trapping response, or spectrum in a field-biased medium. In mucus tracking, the observed state is a stochastic path shaped jointly by virion properties and the local microstructure, adhesivity, and rheology of the mucus network. In plaque assays, the observed state is a visible infectious event rather than a direct particle state.

3.5.5 Underrepresented dynamical and biological sectors

Remark 3.25 (Underrepresented dynamical sectors). A protocol may systematically underrepresent or eliminate entire classes of virion behavior. Static imaging may suppress dynamically transient states. Surface binding may suppress freely evolving orientations. Field-driven measurements may overweight electrically responsive subpopulations. Single-virus tracking may collapse orientation, local adhesion, deformation, or fusion competence into a projected trajectory. Preparation steps may favor configurations that survive the protocol well. Biological assays may collapse particle integrity, cell-entry competence, replication, local spread, and visibility into a single infectious-unit readout. The result is not that the experiment is “wrong,” but that the observed state space can be strictly smaller than the mechanically and biologically relevant latent state space.

Remark 3.26 (Virions as passive probes of environment). In many extracellular contexts, virions behave as passively responsive objects: their motion, survival, adhesion, deformation, or detectability can encode information about the medium in which they are embedded. The latent state X should therefore often be treated as a joint virion–environment state rather than as a particle state alone. Dielectric properties can be inferred from virus motion in nonuniform electric fields, while mucus microstructure, adhesivity, and barrier properties can be inferred from virion or particle tracking data [10, 11, 12, 13, 14, 35, 15, 23]. The theoretical significance of experimental collapse is that it makes such inverse environmental inference part of the formal structure rather than a purely informal interpretation.

Remark 3.27 (Protocol specificity is not a defect). The fact that observed states are protocol-specific should not be interpreted as a weakness of virological measurement. It is the reason different measurements are useful. A plaque assay intentionally discards most structural detail in order to report infectious activity. AFM intentionally applies force in order to measure mechanical response. Dielectrophoresis intentionally imposes a field in order to infer dielectric behavior. Single-virus tracking intentionally follows motion in order to identify transport regimes. The purpose of the latent–observed distinction is not to devalue these measurements, but to state precisely what each one makes visible.

Table 8. Examples of latent-to-observed reduction under common virological protocols. The table is schematic; a real protocol may combine several collapse channels.

Protocol	Latent variables affected	Typical observed variables	Dominant reduction
Cryo-EM / cryo-ET	Geometry, conformation, orientation, survivability in ice, particle-class membership	Density maps, subtomogram averages, class averages, orientation distributions	Preparation, selection, reconstruction
AFM	Surface attachment, height, deformation, stiffness, rupture pathway	Topography, force–distance curves, indentation stiffness	Surface conditioning, loading, readout
DEP / electrorotation	Polarization, charge response, orientation, hydrodynamic drag, field-induced motion	Trajectories, trapping, crossover frequencies, rotation rates	Field steering, dielectric selection
Single-virus tracking	Position, transport regime, confinement, directed motion, time-window persistence	Tracks, MSD, pause states, anomalous exponents, residence times	Trajectory projection, time-window filtering
Mucus / gel tracking	Position, confinement, adhesion, local mesh interaction, viscoelastic response	Tracks, MSD, confinement metrics, mobile/immobile fractions	Medium filtering, adhesive selection
Plaque / focus assay	Cell-entry competence, replication, spread, cytopathic effect, staining visibility	PFU, FFU, endpoint infectious dose	Biological selection, amplification, counting

Together, these examples motivate the protocol observation operator introduced below. Rather than treating observed states as direct copies of latent states, the operator formalism represents each experiment as a structured map from a reference latent ensemble to a protocol-specific observed ensemble, including selection, readout, and null outcomes.

3.6 Protocol Observation Operators

The previous sections constructed the full observed ensemble $P_{\text{obs},t}^{\emptyset}(\cdot | E)$ by composing latent-state transformation, survival or detection weighting, readout, and the null channel. It is useful to collect this construction into operator notation. In this form, an experimental protocol becomes a map from latent probability measures to observed probability measures.

Let

$$\text{Prob}(\Psi) := \text{Prob}(\Psi, \Sigma_X)$$

denote the set of probability measures on the reference latent state space, and let

$$\text{Prob}(\mathcal{Y}_E^\emptyset) := \text{Prob}(\mathcal{Y}_E^\emptyset, \Sigma_{Y,E}^\emptyset)$$

denote the set of probability measures on the augmented observation space

$$\mathcal{Y}_E^\emptyset = \mathcal{Y}_E \cup \{\emptyset\}.$$

The full protocol kernel K_E^\emptyset maps each latent state $x \in \Psi$ to a probability measure on \mathcal{Y}_E^\emptyset . Equivalently, by integration against an input latent ensemble, it defines an operator from latent ensembles to observed ensembles.

Definition 3.28 (Null-inclusive protocol observation operator). The *null-inclusive protocol observation operator* associated with protocol E is the map

$$\mathcal{M}_E^\emptyset : \text{Prob}(\Psi) \longrightarrow \text{Prob}(\mathcal{Y}_E^\emptyset) \quad (3.6.1)$$

defined by

$$\boxed{(\mathcal{M}_E^\emptyset P)(S) = \int_{\Psi} K_E^\emptyset(S | x) P(dx), \quad S \in \Sigma_{Y,E}^\emptyset.} \quad (3.6.2)$$

For the reference latent ensemble,

$$P_{\text{obs},t}^\emptyset(\cdot | E) = \mathcal{M}_E^\emptyset P_{\text{ref},t}. \quad (3.6.3)$$

The detection yield can now be written as a functional of the input latent measure:

$$\boxed{\eta_E[P] = (\mathcal{M}_E^\emptyset P)(\mathcal{Y}_E) = \int_{\Psi} q_E(x) P(dx),} \quad (3.6.4)$$

where

$$q_E(x) = K_E^\emptyset(\mathcal{Y}_E | x)$$

is the state-specific probability that latent state x produces a non-null observation under protocol E . For the reference ensemble,

$$\eta_E(t) = \eta_E[P_{\text{ref},t}] = P_{\text{obs},t}^\emptyset(\mathcal{Y}_E | E). \quad (3.6.5)$$

Definition 3.29 (Detected protocol observation operator). When $\eta_E[P] > 0$, the *detected protocol observation operator* is the conditional map

$$\mathcal{M}_E^{\text{det}} : \text{Prob}(\Psi) \longrightarrow \text{Prob}(\mathcal{Y}_E) \quad (3.6.6)$$

defined by

$$\boxed{(\mathcal{M}_E^{\text{det}} P)(B) = \frac{(\mathcal{M}_E^\emptyset P)(B)}{(\mathcal{M}_E^\emptyset P)(\mathcal{Y}_E)}, \quad B \in \Sigma_{Y,E}.} \quad (3.6.7)$$

Thus

$$P_{\text{obs},t}(\cdot | E, \text{det}) = \mathcal{M}_E^{\text{det}} P_{\text{ref},t}. \quad (3.6.8)$$

Equivalently, the detected operator is obtained by conditioning the null-inclusive output on the non-null observation space:

$$\mathcal{M}_E^{\text{det}} P = \mathcal{M}_E^\varnothing P(\cdot | \mathcal{Y}_E), \quad \eta_E[P] > 0. \quad (3.6.9)$$

This identity makes clear that the null-inclusive operator is the primary probability-preserving object, while the detected operator is a normalized conditional object.

Remark 3.30 (Linearity before conditioning, nonlinearity after conditioning). The null-inclusive operator $\mathcal{M}_E^\varnothing$ is linear in the input measure P . If

$$P = \alpha P_1 + (1 - \alpha) P_2, \quad 0 \leq \alpha \leq 1,$$

then

$$\mathcal{M}_E^\varnothing P = \alpha \mathcal{M}_E^\varnothing P_1 + (1 - \alpha) \mathcal{M}_E^\varnothing P_2.$$

The detected operator $\mathcal{M}_E^{\text{det}}$ is generally not linear, because it conditions on non-null detection by dividing by $\eta_E[P]$. This distinction matters experimentally. A normalized reported histogram can hide the fact that the protocol discarded, destroyed, failed to detect, or failed to amplify most of the original latent population.

Remark 3.31 (Core meaning of K_E^\varnothing). The kernel K_E^\varnothing is the mathematical object that contains the measurement-conditioned passage from latent virion behavior to experimental record. In a weakly perturbative experiment, it may be close to a noisy projection of the pre-existing latent state. In a strongly conditioning experiment, it can include substantial state transformation, survival selection, reweighting, biological amplification, and null observation before the final record is produced.

Remark 3.32 (Why the null-inclusive operator is primary). The null-inclusive operator preserves the full probability accounting of the experiment. It records both what is reported and what fails to enter the accepted data channel. The detected operator is often what appears in published histograms, reconstructed classes, tracked-particle summaries, or counted events, but it is a conditional distribution. For protocol-resolved inference, the missing probability mass can be as informative as the reported non-null distribution.

3.7 Protocol-Lifted Observables

Experimental observables are usually defined on the reported data space. The kernel formalism allows each such observable to be lifted back to the latent space, where it becomes an effective protocol-dependent observable. This is the mathematical reason a reported quantity such as an apparent stiffness, diffusion coefficient, field-response amplitude, plaque count, or class membership should not be interpreted as a protocol-free property unless the protocol dependence has been controlled, calibrated, or modeled.

Definition 3.33 (Observable expectations under a protocol). Let

$$h : \mathcal{Y}_E \rightarrow \mathbb{R}$$

be an experimentally reported observable, such as apparent radius, height, stiffness, diffusion coefficient, plaque count, focus count, rotation rate, capture probability, or class-membership indicator. Its detected protocol-conditioned expectation is

$$\langle h \rangle_E[P] = \int_{\mathcal{Y}_E} h(y) \left(\mathcal{M}_E^{\text{det}} P \right) (dy), \quad (3.7.1)$$

whenever $\eta_E[P] > 0$ and h is integrable with respect to $\mathcal{M}_E^{\text{det}} P$.

The expectation in Eq. (3.7.1) can be written as a ratio of two latent-space integrals:

$$\boxed{\langle h \rangle_E[P] = \frac{\int_{\Psi} \tilde{h}_E(x) P(dx)}{\int_{\Psi} \tilde{1}_E(x) P(dx)}, \quad \eta_E[P] > 0.} \quad (3.7.2)$$

Here

$$\tilde{h}_E(x) = \int_{\Psi_E} s_E(x_E) \left[\int_{\mathcal{Y}_E} h(y) R_E(dy | x_E) \right] \Pi_E^{\text{lat}}(dx_E | x) \quad (3.7.3)$$

is the *protocol-lifted observable* on the reference latent space, and

$$\tilde{1}_E(x) = \int_{\Psi_E} s_E(x_E) \Pi_E^{\text{lat}}(dx_E | x) = K_E^{\mathcal{Z}}(\mathcal{Y}_E | x) = q_E(x) \quad (3.7.4)$$

is the state-specific non-null detection probability. Thus the denominator in Eq. (3.7.2) is the detection yield $\eta_E[P]$.

Remark 3.34 (Interpretive meaning of lifted observables). Equation (3.7.2) states that every experimentally measured quantity can be interpreted as an effective observable on the latent state space. The protocol determines not only what is seen, but also which latent features are weighted, blurred, averaged, transformed, amplified, or ignored when a measurement is reported.

Remark 3.35 (Selection bias in lifted observables). The denominator in Eq. (3.7.2) is essential. The reported expectation is not the latent average of \tilde{h}_E alone; it is the latent average among states that enter the non-null data channel. Therefore, two protocols can have the same readout map but different reported averages if their detection functions $\tilde{1}_E$ weight the latent ensemble differently. This is the operator-level expression of selection bias, detectability bias, and protocol-conditioned enrichment.

Remark 3.36 (Plaque count as a lifted observable). In a plaque assay, the reported observable may be the number of plaques or the inferred plaque-forming units. In the lifted representation, this observable is not simply a count of physical virions. It is an effective latent-space observable that weights states by cell-entry competence, replication competence, local spread, overlay conditions, incubation time, staining visibility, and counting criteria. This makes plaque assays a natural worked example of experimental collapse.

Remark 3.37 (Vector-valued observables). The same construction applies componentwise to vector-valued observables

$$\mathbf{h} : \mathcal{Y}_E \rightarrow \mathbb{R}^m.$$

This is useful when a protocol reports several coupled summaries, such as particle size and orientation class, diffusion coefficient and confinement metric, force-curve stiffness and rupture threshold, or plaque count and plaque-size distribution.

Remark 3.38 (Null-inclusive observables). Some observables are naturally defined on the augmented observation space \mathcal{Y}_E^\emptyset , not only on the detected non-null space \mathcal{Y}_E . For example, the indicator

$$h_\emptyset(y) = \mathbf{1}_{\{y=\emptyset\}}$$

measures collapse into the null channel, while

$$h_{\text{det}}(y) = \mathbf{1}_{\{y \in \mathcal{Y}_E\}}$$

measures detection yield. Such observables should be evaluated using $\mathcal{M}_E^\emptyset P$, not the detected conditional operator $\mathcal{M}_E^{\text{det}} P$, because conditioning on detection removes the null probability by construction.

3.8 Mechanism-Resolved Collapse Channels

The kernel language is intentionally general. For experimental interpretation, however, it is useful to decompose a protocol into mechanism-specific stages. Different mechanisms reshape the latent ensemble in different ways: some physically transform the state, some select which states survive, some amplify particular biological pathways, and some compress a high-dimensional state into a lower-dimensional readout. A mechanism-resolved description identifies which part of the protocol is responsible for a given form of experimental collapse.

Definition 3.39 (Mechanism-resolved factorization of the latent-stage kernel). Let

$$(\Psi_{E,0}, \Sigma_{X,E,0}) = (\Psi, \Sigma_X), \quad (\Psi_{E,L}, \Sigma_{X,E,L}) = (\Psi_E, \Sigma_{X,E}),$$

and let

$$\Pi_{E,\ell}(dx_\ell | x_{\ell-1}), \quad \ell = 1, \dots, L,$$

be mechanism-specific Markov kernels between intermediate protocol state spaces. With the convention that the rightmost kernel acts first, the latent-stage kernel may be factorized as

$$\Pi_E^{\text{lat}} = \Pi_{E,L} \circ \Pi_{E,L-1} \circ \dots \circ \Pi_{E,1}. \quad (3.8.1)$$

Explicitly, for $G \in \Sigma_{X,E}$ and $x_0 = x$,

$$\boxed{\Pi_E^{\text{lat}}(G | x_0) = \int_{\Psi_{E,1}} \dots \int_{\Psi_{E,L}} \mathbf{1}_G(x_L) \Pi_{E,L}(dx_L | x_{L-1}) \dots \Pi_{E,1}(dx_1 | x_0).} \quad (3.8.2)$$

Typical latent-stage mechanisms may include

$$\Pi_E^{\text{prep}}, \quad \Pi_E^{\text{interface}}, \quad \Pi_E^{\text{surf}}, \quad \Pi_E^{\text{medium}}, \quad \Pi_E^{\text{field}}, \quad \Pi_E^{\text{load}}, \quad \Pi_E^{\text{time}}, \quad \Pi_E^{\text{bio}}.$$

The ordering is not universal. It must be chosen to match the physical, chemical, mechanical, biological,

and computational sequence of the experiment.

Remark 3.40 (Why mechanism order is protocol dependent). The factorization in Eq. (3.8.1) is a modeling choice, not a universal ordering of experimental reality. In one protocol, an electric field may steer particles before surface contact. In another, surface immobilization may occur before imaging or loading. In cryo-EM, preparation, thin-film behavior, air–water interface exposure, vitrification, particle orientation, particle picking, and reconstruction are tightly coupled [1, 2, 3, 4, 5]. In AFM, adsorption, hydration state, tip geometry, loading path, and deformation are coupled during measurement [6, 7, 8, 9]. The important point is not that every protocol must be decomposed in the same order, but that the protocol kernel can be resolved into mechanistically interpretable stages.

Definition 3.41 (Collapse channels). A *collapse channel* is a mechanism by which a protocol transforms, selects, reweights, amplifies, or compresses the latent ensemble before it becomes reported data. The main collapse channels considered in this paper include:

- (i) *geometric projection*, in which the protocol reports only a lower-dimensional representation, reconstruction, image, trajectory, curve, or summary of the latent geometry;
- (ii) *orientation selection*, in which certain orientations are preferentially preserved, detected, reconstructed, selected, or amplified;
- (iii) *surface immobilization*, in which adsorption or contact changes translational freedom, rotational freedom, contact geometry, adhesion state, or deformation pathway;
- (iv) *field steering*, in which external fields produce forces, torques, polarization, trapping, translation, rotation, sorting, or frequency-dependent response;
- (v) *mechanical loading*, in which the measurement applies force, indentation, compression, confinement, stretching, or deformation during preparation or readout;
- (vi) *time-window filtering*, in which only states that persist, move, bind, relax, amplify, or remain detectable on the instrumental or assay timescale contribute to the observed ensemble;
- (vii) *medium filtering*, in which the local medium admits, confines, slows, binds, immobilizes, transports, or excludes different virion states;
- (viii) *biological amplification and viability selection*, in which the protocol reports only states capable of completing a specified biological sequence, such as cell attachment, entry, replication, local spread, cytopathic effect, focus formation, reporter expression, or plaque formation;
- (ix) *survival or detectability selection*, in which only a subset of protocol-conditioned states enters the reported dataset at all.

These channels are not mutually exclusive. A single protocol may combine several of them. For example, a plaque assay combines biological amplification, time windowing, medium or overlay filtering, visibility thresholding, and counting. An AFM protocol may combine surface immobilization, hydration-dependent conditioning, mechanical loading, geometric projection, and force-curve readout. The channel language is therefore not a classification scheme for entire experiments, but a way to identify which mechanisms participate in the observed collapse.

Remark 3.42 (Latent transformation versus readout selection). Some selection effects physically alter the latent state, while others alter only the probability that a state is reported. The

former belong naturally in Π_E^{lat} . The latter belong in s_E , R_E , or the null channel \emptyset . The formalism allows either placement when a protocol model requires it, provided that the model states clearly where the effect enters and what probability mass is being transformed, selected, or nulled.

Remark 3.43 (Why collapse channels are useful). The channel language prevents a protocol from being described only as “biased” or “artifact-prone.” It asks a more precise question: which mechanism produced the observed conditioning? A preferred-orientation problem in cryo-EM, a surface-induced deformation in AFM, a field-induced drift in DEP, an adhesive immobilization event in mucus, and a plaque-forming selection step in an infectivity assay are different collapse mechanisms. They should therefore be modeled differently.

Table 9. Collapse channels and their mechanical interpretation. The listed mathematical locations are typical, not exclusive; a real protocol may distribute one physical effect across several kernels or weights.

Collapse channel	Typical mathematical location	Mechanical or experimental interpretation
Geometric projection	R_E or $\mathcal{O}_E : \Psi_E \rightarrow \mathcal{Y}_E$	Only selected coordinates, shapes, projections, reconstructions, curves, trajectories, or summaries are reported.
Orientation selection	$s_E(x_E)$, $R_E(dy x_E)$, or Π_E^{prep}	Some orientations are overrepresented because of preparation, interface effects, reconstruction, particle picking, or selection.
Surface immobilization	Π_E^{surf}	Adsorption or tethering constrains translation, rotation, deformation, contact geometry, and accessible mechanical response.
Field steering	Π_E^{field}	Electric, optical, magnetic, acoustic, or flow fields move, polarize, trap, orient, rotate, or sort virions.
Mechanical loading	Π_E^{load} or force-dependent R_E	Tip forces, indentation, confinement, compression, or stretching alter the measured state or the response inferred from it.
Time-window filtering	Π_E^{time} , s_E , or R_E	Transient, fast, rare, slow, delayed, or short-lived states are missed or underweighted.
Medium filtering	Π_E^{medium} or a joint virion–environment latent state	Mucus, gels, extracellular matrices, droplets, overlays, or buffers admit, bind, hinder, confine, immobilize, or exclude different virion states.
Biological amplification	Π_E^{bio} , s_E , R_E , or an assay-specific branching kernel	Only virions that complete a specified biological sequence generate plaques, foci, cytopathic effects, reporter signals, or endpoint signals.
Detection selection	$s_E(x_E)$ and \emptyset	Some states are absent from the reported ensemble because they are lost, destroyed, rejected, noninfectious under the assay, outside the observation window, or below threshold.

3.9 Quantifying Experimental Collapse

The word “collapse” is useful only if it can be quantified. The protocol kernel gives a constructive way to do this. Experimental collapse can be measured as a discrepancy between a reference latent

ensemble and a protocol-conditioned latent ensemble, between preselection and detected populations, between observed ensembles produced by different protocols, or between protocol-conditioned values of a chosen experimental observable.

A technical point is essential. The reference latent state space Ψ , the protocol-conditioned latent state space Ψ_E , and the observation space \mathcal{Y}_E need not be identical. A cryo-EM density map, an AFM force-indentation curve, a DEP trajectory, a mucus-tracking path, and a plaque count are different mathematical objects. Collapse functionals should therefore compare probability measures only after the relevant quantities have been placed on a common comparison space.

Definition 3.44 (Common comparison space). Let

$$(\mathbb{W}, \Sigma_{\mathbb{W}})$$

be a measurable comparison space. Let

$$L_0 : \Psi \rightarrow \mathbb{W}, \quad L_E : \Psi_E \rightarrow \mathbb{W}$$

be measurable maps that extract comparable quantities from the reference and protocol-conditioned latent states. Examples of L_0 and L_E include maps to radius, orientation, mobility, stiffness, infectivity class, adhesion state, deformation amplitude, field-response amplitude, normal-mode amplitude, branch participation weight, or another experimentally relevant summary.

Remark 3.45 (What the comparison space means experimentally). The comparison space \mathbb{W} encodes the scientific question. If the question concerns apparent size, then \mathbb{W} may be a radius or diameter space. If the question concerns orientation selection, \mathbb{W} may be an orientation space. If the question concerns infectivity, \mathbb{W} may be a binary or multistate competence space. If the question concerns transport, \mathbb{W} may contain diffusivities, residence times, confinement metrics, or anomalous exponents. Collapse is therefore always quantified relative to a chosen experimentally meaningful comparison.

Definition 3.46 (Latent distributional collapse functional). Let $D_{\mathbb{W}}(\cdot, \cdot)$ be a divergence, distance, or discrepancy between probability measures on $(\mathbb{W}, \Sigma_{\mathbb{W}})$. The preselection latent collapse magnitude is

$$\mathcal{C}_{\text{lat}}^{\mathbb{W}}(E; t) = D_{\mathbb{W}}\left((L_E)_{\#} \tilde{P}_{E,t}^{\text{lat}}, (L_0)_{\#} P_{\text{ref},t}\right). \quad (3.9.1)$$

If detection selection is important, the detected latent collapse is

$$\mathcal{C}_{\text{det}}^{\mathbb{W}}(E; t) = D_{\mathbb{W}}\left((L_E)_{\#} P_{E,t}^{\text{lat}}(\cdot \mid \text{det}), (L_0)_{\#} P_{\text{ref},t}\right), \quad 0 < \eta_E(t) \leq 1. \quad (3.9.2)$$

Remark 3.47 (Pre-detection versus detected collapse). The two functionals above answer different questions. $\mathcal{C}_{\text{lat}}^{\mathbb{W}}$ measures how much the protocol transforms the latent ensemble before survival or detection selection. $\mathcal{C}_{\text{det}}^{\mathbb{W}}$ measures the ensemble that actually remains visible after selection. Their difference is informative. If $\mathcal{C}_{\text{lat}}^{\mathbb{W}}$ is small but $\mathcal{C}_{\text{det}}^{\mathbb{W}}$ is large, the dominant collapse mechanism is selection rather than mechanical transformation. If both are large, the protocol may be both transforming and

selecting the latent ensemble.

Remark 3.48 (Why pushforwards are needed). Writing $D(P_{E,t}^{\text{lat}}, P_{\text{ref},t})$ is only meaningful when the two measures live on the same state space and share an appropriate reference structure. In many virological settings they do not. A protocol-conditioned latent state in AFM, a vitrified cryo-EM state, a field-conditioned DEP state, and a plaque-assay pathway state are not identical mathematical objects. The maps L_0 and L_E specify what is being compared.

Remark 3.49 (Choice of divergence). The choice of D_W depends on the application. A Kullback–Leibler divergence is natural when likelihood ratios are meaningful and absolute continuity conditions are satisfied. A Jensen–Shannon divergence is symmetric and finite in many cases where KL is inconvenient. A Wasserstein distance is useful when nearby states in \mathbb{W} should be treated as similar rather than categorically different. Maximum mean discrepancy and other integral-probability metrics are useful when distributions are compared through function classes or kernels [25, 26, 22, 27]. The theory does not require one universal metric. It requires that the chosen metric match the experimental question and the geometry of the data.

Definition 3.50 (Observed protocol-to-protocol collapse). Let E_1 and E_2 be two protocols. Let

$$H_{E_1} : \mathcal{Y}_{E_1} \rightarrow \mathbb{W}, \quad H_{E_2} : \mathcal{Y}_{E_2} \rightarrow \mathbb{W}$$

map their non-null observed outputs to a common comparison space. The observed protocol-to-protocol collapse is

$$\boxed{\mathcal{C}_{\text{obs}}^{\mathbb{W}}(E_1, E_2; t) = D_{\mathbb{W}}((H_{E_1})_{\#}P_{\text{obs},t}(\cdot | E_1, \text{det}), (H_{E_2})_{\#}P_{\text{obs},t}(\cdot | E_2, \text{det}))}. \quad (3.9.3)}$$

Remark 3.51 (What protocol-to-protocol collapse measures). Observed protocol-to-protocol collapse asks whether two protocols produce compatible observed summaries after both outputs are mapped to a common comparison space. A discrepancy need not mean that one experiment is wrong. It may indicate that the protocols observe different projections, select different subpopulations, perturb different latent sectors, or amplify different functional events. Conversely, a small discrepancy does not prove that the protocols see the full latent ensemble; it may mean that they share a blind direction or a common selection bias.

Definition 3.52 (Observable-level collapse). Let

$$\mathbf{h}_E : \mathcal{Y}_E \rightarrow \mathbb{R}^m, \quad \mathbf{h}_{E_0} : \mathcal{Y}_{E_0} \rightarrow \mathbb{R}^m$$

be comparable reported observables under protocols E and E_0 . Define

$$\boxed{\mathcal{C}_{\mathbf{h}}(E; E_0, t) = \|\langle \mathbf{h}_E \rangle_E(t) - \langle \mathbf{h}_{E_0} \rangle_{E_0}(t)\|, \quad (3.9.4)}$$

where the norm is chosen according to the scale, covariance structure, and scientific meaning of the

observable. A normalized scalar version is

$$\hat{\mathcal{C}}_{\mathbf{h}}(E; E_0, t) = \frac{\|\langle \mathbf{h}_E \rangle_E(t) - \langle \mathbf{h}_{E_0} \rangle_{E_0}(t)\|}{\|\langle \mathbf{h}_{E_0} \rangle_{E_0}(t)\| + \epsilon_h}, \quad (3.9.5)$$

with $\epsilon_h > 0$ included to regularize cases where the reference expectation is zero or near zero.

Remark 3.53 (What observable-level collapse measures). Observable-level collapse asks a practical question: how much does a reported quantity change when the protocol changes? The relevant observable could be an apparent radius, height, stiffness, diffusion coefficient, orientation distribution, branch speed, branch participation weight, trapping probability, rotation rate, plaque count, focus-forming count, endpoint titer, or another protocol-defined summary. This makes the abstract kernel framework experimentally testable.

Definition 3.54 (Detection-yield collapse). The detection-yield collapse between protocols E and E_0 is

$$\mathcal{C}_\eta(E; E_0, t) = |\eta_E(t) - \eta_{E_0}(t)|. \quad (3.9.6)$$

A logarithmic version,

$$\mathcal{C}_{\log \eta}(E; E_0, t) = \left| \log \frac{\eta_E(t) + \epsilon_\eta}{\eta_{E_0}(t) + \epsilon_\eta} \right|, \quad (3.9.7)$$

is useful when detection yields differ by orders of magnitude.

Remark 3.55 (Why detection-yield collapse is not optional). Two protocols may produce similar normalized observed distributions while having very different detection yields. A protocol that reports nearly every state and a protocol that reports only a small selected subset may appear similar after conditioning on detection. The yield $\eta_E(t)$ records the missing probability mass and is therefore part of experimental collapse itself. In practical terms, it is the denominator of the experiment.

Definition 3.56 (Selection-strength functional). When the survival/detection weight s_E is known or estimated, the strength of detection selection can be summarized by the variation of s_E over the preselection protocol-conditioned latent ensemble. One simple measure is

$$\mathcal{S}_E(t) = \text{Var}_{\tilde{P}_{E,t}^{\text{lat}}} [s_E(X_E)]. \quad (3.9.8)$$

Large $\mathcal{S}_E(t)$ indicates that survival or detection is strongly state dependent.

Remark 3.57 (Interpretation of selection strength). A small detection yield $\eta_E(t)$ and a large selection strength $\mathcal{S}_E(t)$ describe different aspects of collapse. The yield measures how much probability mass reaches the non-null record. The selection strength measures how unevenly that probability is distributed across protocol-conditioned latent states. A protocol can have low yield because every state is weakly detected, or because a small subpopulation is strongly detected while most states are nearly invisible. These cases have different experimental interpretations.

Remark 3.58 (Quantification is target-dependent). There is no protocol-independent scalar called “the collapse.” A protocol may weakly collapse size, strongly collapse orientation, selectively

preserve one mechanical mode, suppress another, and send a large fraction of the population into the null channel. Quantification must therefore specify the comparison space, the observable or distribution being compared, the role of detection conditioning, and the divergence or norm used. The next subsection applies this perspective to modal and dynamical collapse, where the relevant comparison targets are time-dependent degrees of freedom, mode amplitudes, and dynamical sectors of the latent state.

3.10 Modal and Dynamical Collapse

When the latent theory includes collective modes, branch amplitudes, orientation–translation coupling, or time-dependent state variables, a protocol can collapse not only static features but also dynamical sectors of the theory. This is especially relevant for assembly-level or lattice-level models in which displacement, orientation, spike presentation, contact variables, hydrodynamic response, or electrical response hybridize into collective branches.

The central point is that a protocol may preserve a structural snapshot while suppressing the dynamical pathway that produced it, or it may make a dynamical sector visible precisely by forcing, loading, tracking, or amplifying it. Static and dynamical observability are therefore distinct. A protocol can be highly informative about morphology while being nearly blind to relaxation, damping, rotation, adhesion kinetics, or branch participation.

Definition 3.59 (Modal collapse). Suppose a latent or protocol-conditioned model defines a branch diagnostic

$$B_{n,E}(\mathbf{k}),$$

such as a dispersion relation $\omega_{n,E}(\mathbf{k})$, a damping rate $\Gamma_{n,E}(\mathbf{k})$, a presentation or tilt weight $P_{\text{tilt},E}^{(n)}(\mathbf{k})$, a dielectric-response amplitude, an elastic participation factor, or a displacement–orientation participation ratio. The modal collapse of this branch diagnostic between protocols E and E_0 is

$$\mathcal{C}_{B_n}(E; E_0, \mathbf{k}) = \|B_{n,E}(\mathbf{k}) - B_{n,E_0}(\mathbf{k})\|. \quad (3.10.1)$$

The norm is chosen according to the nature of the branch diagnostic. For a scalar diagnostic it may be an absolute value; for a vector-valued or matrix-valued diagnostic it may be a Euclidean, spectral, Frobenius, or problem-specific norm.

For a comparison over a region Ω_k of wave-vector space, one may define an integrated modal-collapse functional:

$$\mathcal{C}_{B_n}^{\Omega_k}(E; E_0) = \left[\int_{\Omega_k} w_n(\mathbf{k}) \|B_{n,E}(\mathbf{k}) - B_{n,E_0}(\mathbf{k})\|^2 d\mathbf{k} \right]^{1/2}, \quad (3.10.2)$$

where $w_n(\mathbf{k}) \geq 0$ is a weighting function that encodes the experimentally relevant region of the branch, such as long-wavelength modes, high-participation modes, field-coupled modes, or modes within the detectable frequency band.

Remark 3.60 (Why modal collapse matters). A protocol may suppress, pin, reveal, or reweight different pieces of a latent dynamical branch structure. A branch that is hybrid in a weakly constrained ensemble may appear translational under a surface-bound protocol, while a field-biased protocol may

reveal an orientational or dielectric sector that is invisible in passive imaging. Modal collapse measures this protocol-dependent change directly.

Remark 3.61 (Connection to virological experiments). In many virological experiments, the relevant dynamical sectors are not measured as full normal modes. They appear indirectly through relaxation times in tracking data, indentation response in AFM, orientation statistics in structural imaging, frequency-dependent response in field-driven assays, or time-to-visibility in infectivity assays. The modal language is therefore most useful when it is tied to an explicit branch diagnostic that the protocol can actually constrain.

Definition 3.62 (Dynamical collapse). Let $X_{0:T}$ denote a latent trajectory over a time interval $[0, T]$, and let $Y_{0:T}^{(E)}$ denote the corresponding observed process under protocol E . Let

$$L_0^{\text{dyn}} : \{X_{0:T}\} \rightarrow \mathbf{Z}, \quad L_E^{\text{dyn}} : \{Y_{0:T}^{(E)}\} \rightarrow \mathbf{Z}$$

map latent and observed dynamical objects into a common dynamical comparison space $(\mathbf{Z}, \Sigma_{\mathbf{Z}})$, such as relaxation times, residence-time distributions, mean-square displacements, mode amplitudes, autocorrelation functions, transition rates, or branch participation weights. A dynamical collapse functional may be written as

$$\boxed{\mathcal{C}_{\text{dyn}}^{\mathbf{Z}}(E; t, T) = D_{\mathbf{Z}} \left((L_E^{\text{dyn}})_{\#} P_{\text{obs}, 0:T}(\cdot \mid E, \text{det}), (L_0^{\text{dyn}})_{\#} P_{\text{ref}, 0:T} \right)}. \quad (3.10.3)$$

This definition makes explicit that dynamical collapse is not simply the loss of a coordinate. It can be the loss of a time correlation, relaxation pathway, transition rate, branch amplitude, dwell-time distribution, or coupling between degrees of freedom. A protocol that preserves spatial position but destroys velocity information, or one that preserves average transport but removes short-lived adhesion states, can therefore be weakly collapsed in one variable and strongly collapsed in another.

3.11 Collapse Severity Classes

The preceding functionals measure collapse quantitatively. It is also useful to name broad qualitative regimes. These categories are not substitutes for the functionals above; they are interpretive labels that help explain which kind of protocol dependence dominates a given experiment.

Definition 3.63 (Collapse severity classes). A protocol may be classified by the size and mechanism of its collapse:

- (i) *weak readout collapse*, when $\tilde{P}_{E,t}^{\text{lat}} \approx P_{\text{ref}, t}$ in the relevant comparison space and the dominant effect is noise, finite resolution, reconstruction, classification, or projection in R_E ;
- (ii) *selection collapse*, when the latent transformation is weak but $P_{E,t}^{\text{lat}}(\cdot \mid \text{det})$ differs strongly from the reference ensemble because s_E is state dependent;
- (iii) *mechanical collapse*, when Π_E^{lat} physically changes the state distribution through fields, surfaces, loading, confinement, preparation, or medium interaction;
- (iv) *modal or dynamical collapse*, when the protocol suppresses, pins, averages, reweights, or reveals specific time-dependent sectors, normal-mode branches, relaxation pathways, or dynamical couplings;

- (v) *biological amplification collapse*, when a biological assay reports only states that pass through a protocol-specific viability, attachment, entry, infection, replication, spread, reporter, staining, or visibility pathway;
- (vi) *destructive or irreversible collapse*, when the protocol changes the accessible state space itself through deformation, rupture, aggregation, denaturation, irreversible adsorption, permanent inactivation, or loss of infectivity.

Remark 3.64 (Interpretation of severity classes). These classes are not judgments about experimental quality. They are interpretive labels. A highly perturbative protocol can be extremely valuable if its kernel is understood. AFM is valuable precisely because it applies force; dielectrophoresis and electrorotation are valuable precisely because they impose fields; cryo-EM is valuable precisely because it preserves structure; plaque assays are valuable precisely because they amplify infectious events into countable lesions. The point is to state what ensemble each protocol produces, rather than to treat all protocols as if they sampled the same latent distribution.

Table 10. Collapse severity classes and typical examples. The same protocol can occupy different regimes depending on the observable, comparison space, and latent sector being studied.

Severity class	Dominant mathematical signature	Typical interpretation
Weak readout collapse	R_E projects, blurs, classifies, or reconstructs, while Π_E^{lat} and s_E are weakly state dependent	The protocol mostly observes a pre-existing state with finite resolution or readout compression.
Selection collapse	$s_E(x_E)$ is strongly state dependent	The reported ensemble is a selected, enriched, or thresholded subset of the protocol-conditioned population.
Mechanical collapse	Π_E^{lat} substantially changes the latent distribution	Fields, surfaces, loading, confinement, preparation, or media reshape the particle state.
Modal or dynamical collapse	Branch diagnostics, relaxation statistics, or dynamical couplings change under E	The protocol suppresses, pins, averages, reveals, or reweights time-dependent sectors of the latent theory.
Biological amplification collapse	Observation requires successful passage through an assay-specific biological sequence	Infectious-unit assays report a selected and amplified functional subpopulation.
Destructive or irreversible collapse	The accessible state space changes, or the protocol cannot be reversed	Rupture, aggregation, denaturation, irreversible adsorption, or loss of infectivity removes states from later observation.

3.12 Experimental Collapse and Inverse Inference

The protocol kernel is not only a warning about measurement bias. It is also a tool for inference. If the protocol is known, estimated, calibrated, or parametrized, then the observed ensemble can be used to infer latent virion properties, environmental properties, and protocol-specific coupling parameters. In this sense, experimental collapse is not merely a loss of information. It is the forward map through which latent virion–environment mechanics becomes data.

The central inverse problem is therefore:

$$\boxed{\text{Observed protocol-conditioned data} \implies \left\{ \begin{array}{l} \text{Latent virion parameters} \\ \text{Environmental parameters} \\ \text{Protocol parameters} \end{array} \right\}.} \quad (3.12.1)$$

This arrow should not be read as a direct algebraic inversion. It denotes an inverse problem constrained by a forward model. A protocol-resolved analysis must specify how latent virion mechanics, environmental structure, and protocol operations jointly generate the observed ensemble [28, 29].

Definition 3.65 (Protocol-resolved parameter vector). Let

$$\theta = (\theta_{\text{vir}}, \theta_{\text{env}}, \theta_E) \in \Theta \quad (3.12.2)$$

denote a protocol-resolved parameter vector. Here θ_{vir} contains virion mechanical, structural, electrical, or biophysical parameters; θ_{env} contains environmental parameters; and θ_E contains protocol parameters.

Remark 3.66 (Examples of parameter blocks). The virion parameter block θ_{vir} may include radius distribution, effective charge, spike or surface-state parameters, polarizability, stiffness, compliance, adhesion strength, damping coefficients, orientation mobility, or infectivity-related latent variables. The environmental block θ_{env} may include viscosity, ionic strength, dielectric permittivity, conductivity, mucus mesh scale, mucin composition, antibody concentration, receptor density, pH, temperature, or cell-layer susceptibility. The protocol block θ_E may include field amplitude, field frequency, surface chemistry, grid type, imaging cadence, exposure time, force ramp rate, tip geometry, dilution factor, inoculum volume, adsorption time, overlay composition, incubation time, staining threshold, particle-picking rule, reconstruction parameters, or counting criterion.

Definition 3.67 (Protocol-resolved forward model). A *protocol-resolved forward model* is the map

$$\theta \longmapsto P_{\text{obs},t}^{\varnothing}(\cdot | E, \theta) = \mathcal{M}_E^{\varnothing}(\theta_E) P_{\text{ref},t}(\cdot | \theta_{\text{vir}}, \theta_{\text{env}}). \quad (3.12.3)$$

The non-null reported model is obtained by conditioning on detection:

$$P_{\text{obs},t}(\cdot | E, \theta, \text{det}) = \mathcal{M}_E^{\text{det}}(\theta_E) P_{\text{ref},t}(\cdot | \theta_{\text{vir}}, \theta_{\text{env}}), \quad (3.12.4)$$

provided the detection yield is nonzero.

Remark 3.68 (Meaning of the forward model). The forward model states that observed data are produced jointly by virion mechanics, environmental mechanics, and protocol mechanics. Thus

an apparent diffusion coefficient measured in mucus, an indentation stiffness measured by AFM, a dielectrophoretic crossover frequency, a cryo-EM orientation distribution, or a plaque count should not be interpreted as a property of the virion alone unless the environmental and protocol contributions have been controlled, marginalized, or modeled.

Remark 3.69 (Why collapse becomes useful for inference). A strongly conditioning protocol can be inferentially useful precisely because it changes the ensemble in a controlled or interpretable way. AFM loading can make mechanical compliance visible. Dielectrophoresis and electrorotation can make dielectric response visible. Mucus tracking can make adhesive confinement and transport heterogeneity visible. Plaque assays can make infectious activity visible. In each case, the protocol does not merely obscure the latent state; it asks a specific physical or biological question of that state.

This perspective prepares the likelihood-based formulation that follows. Once the forward model specifies $P_{\text{obs},t}^{\varnothing}(\cdot | E, \theta)$, one can write protocol-resolved likelihoods for observed data, separate virion parameters from environmental and protocol parameters, and analyze which directions in θ -space are identifiable under a given experimental design.

3.12.1 Protocol-Resolved Likelihoods

Once a protocol-resolved forward model has been specified, inference proceeds by writing the likelihood of the observed data under the protocol-conditioned observed law. The essential point is that the likelihood should be written for the data that the protocol actually reports, not for an idealized, protocol-free latent ensemble.

Definition 3.70 (Protocol-resolved dataset). Suppose protocol E produces observed data

$$\mathcal{D}_E = \{y_1, \dots, y_N\}, \quad y_i \in \mathcal{Y}_E^{\varnothing}. \quad (3.12.1.1)$$

The dataset may include both non-null outcomes $y_i \in \mathcal{Y}_E$ and null outcomes $y_i = \varnothing$, depending on whether the experiment records rejected, undetected, failed, or otherwise nonaccepted observations.

For a fixed parameter value θ , the protocol-resolved forward model defines the null-inclusive observed law

$$P_{\text{obs},t}^{\varnothing}(\cdot | E, \theta)$$

on $\mathcal{Y}_E^{\varnothing}$. When this law admits a density or mass function with respect to a dominating measure ν_E^{\varnothing} , we write

$$p_E^{\varnothing}(y | \theta) = \frac{dP_{\text{obs},t}^{\varnothing}(\cdot | E, \theta)}{d\nu_E^{\varnothing}}(y), \quad y \in \mathcal{Y}_E^{\varnothing}. \quad (3.12.1.2)$$

The dominating measure ν_E^{\varnothing} includes the appropriate continuous, discrete, or mixed structure of the non-null data, together with the atom at \varnothing .

Definition 3.71 (Null-inclusive protocol-resolved likelihood). If the observations are conditionally independent given θ , then the null-inclusive protocol-resolved likelihood is

$$\mathcal{L}_E^{\varnothing}(\theta; \mathcal{D}_E) = \prod_{i=1}^N p_E^{\varnothing}(y_i | \theta). \quad (3.12.1.3)$$

More generally, $\mathcal{L}_E^\varnothing$ denotes the probability or density of the complete dataset under the protocol-resolved observation model, including null outcomes whenever they are recorded.

Remark 3.72 (When the independent-observation likelihood is insufficient). The product likelihood in Eq. (3.12.1.3) is a clean first representation, but it is not universal. Time-correlated tracking data, spatially interacting plaques, shared cell-monolayer variability, particle aggregation, batch effects, field-induced correlations, and reconstruction pipelines can introduce dependence among observations. In such cases, the correct likelihood is not a product of single-observation factors, but a joint probability model for the entire dataset under the protocol-conditioned observation process.

Remark 3.73 (Why null-inclusive likelihoods matter). If null observations are discarded before modeling, inference may confuse selection with absence. For example, a protocol that produces few accepted particles, few trackable trajectories, few reconstructed classes, or few plaques may do so because the latent population is rare, because the relevant states fail the protocol, because the detection threshold is restrictive, or because the protocol maps many states into the null channel. A null-inclusive likelihood keeps these possibilities within the same probability model.

Definition 3.74 (Conditional non-null likelihood). If only non-null observations are retained, then the appropriate likelihood is conditional on detection. For a detected dataset

$$\mathcal{D}_E^{\text{det}} = \{y_1, \dots, y_{N_{\text{det}}}\}, \quad y_i \in \mathcal{Y}_E,$$

the conditional non-null likelihood is

$$\mathcal{L}_E^{\text{det}}(\theta; \mathcal{D}_E^{\text{det}}) = \prod_{i=1}^{N_{\text{det}}} p_E(y_i | \theta, \text{det}), \quad (3.12.1.4)$$

where

$$p_E(y | \theta, \text{det}) = \frac{p_E^\varnothing(y | \theta)}{\eta_E(\theta)}, \quad y \in \mathcal{Y}_E, \quad (3.12.1.5)$$

and

$$\eta_E(\theta) = P_{\text{obs},t}^\varnothing(\mathcal{Y}_E | E, \theta)$$

is the detection yield.

Remark 3.75 (Conditional likelihoods lose yield information). The conditional likelihood is useful when the dataset contains only accepted records, but it discards information about the detection yield $\eta_E(\theta)$. Therefore it cannot distinguish a protocol that observes nearly all states from one that observes only a small selected subset if the normalized non-null distributions are similar. Whenever null outcomes or denominators are experimentally available, the null-inclusive likelihood is more informative.

Remark 3.76 (Counts, denominators, and missing probability mass). In many virological assays, the denominator is scientifically meaningful. The number of particles rejected during image processing, the number of particles lost from a tracking field, the number of wells with no detectable infection, or the number of plaque-negative inoculations can all constrain the null channel. A reported non-null distribution describes what was observed after selection; the denominator helps determine

how much of the latent population entered that observed distribution in the first place.

3.12.2 Bayesian Inverse Formulation

Definition 3.77 (Bayesian inverse problem). Given a prior density or probability measure $q_0(\theta)$ and a protocol-resolved likelihood $\mathcal{L}_E^\varnothing(\theta; \mathcal{D}_E)$, the posterior distribution is

$$q(\theta \mid \mathcal{D}_E, E) = \frac{\mathcal{L}_E^\varnothing(\theta; \mathcal{D}_E) q_0(\theta)}{\int_{\Theta} \mathcal{L}_E^\varnothing(\vartheta; \mathcal{D}_E) q_0(\vartheta) d\vartheta}. \quad (3.12.2.1)$$

When only detected observations are modeled, the corresponding conditional posterior is obtained by replacing $\mathcal{L}_E^\varnothing$ with $\mathcal{L}_E^{\text{det}}$.

Remark 3.78 (Why q_0 is used for the prior). The symbol q_0 is used for the prior to avoid confusing the prior density with the latent transformation kernels Π_E^{lat} . This is a notation choice only; the posterior has the usual Bayesian form.

Remark 3.79 (Interpretation of the Bayesian form). The Bayesian form is natural for protocol-resolved virophysics because the unknowns are separated into virion parameters, environmental parameters, and protocol parameters. It also makes uncertainty explicit. Instead of producing a single fitted value of “virion stiffness,” “mucus mobility,” “dielectric response,” or “infectious titer,” the inference returns a posterior distribution whose width reflects experimental noise, nuisance-parameter uncertainty, finite sample size, protocol selection, and non-identifiability.

Remark 3.80 (Frequentist and Bayesian readings). The protocol-resolved framework is not tied to Bayesian inference. The same forward model can be used for maximum-likelihood estimation, profile likelihoods, confidence intervals, likelihood-ratio tests, posterior inference, posterior predictive checks, or model comparison. The central requirement is not a particular inferential philosophy. It is that the likelihood or objective function be written for the protocol-conditioned observed data rather than for an unconditioned latent ensemble.

3.13 Protocol Identifiability

Experimental collapse makes identifiability explicitly protocol dependent. A parameter may be real in the latent mechanics but invisible in a particular readout. Conversely, a strongly conditioning protocol may reveal a latent sector that a passive protocol cannot observe. Identifiability is therefore a property not only of the latent model, but of the latent model composed with the protocol observation operator.

Definition 3.81 (Target and nuisance parameters). Let the parameter vector be partitioned as

$$\theta = (\theta_a, \lambda), \quad (3.13.1)$$

where θ_a is the target parameter or parameter block, and λ contains nuisance parameters. Nuisance parameters may include environmental variables, protocol settings, calibration constants, selection thresholds, noise parameters, batch effects, reconstruction settings, or other quantities that are not the main target of inference but still affect the observed law.

Definition 3.82 (Protocol identifiability). The parameter block θ_a is *identifiable under protocol E* , relative to a specified model class and nuisance-parameter treatment, if distinct values of θ_a produce distinguishable null-inclusive observed laws after accounting for nuisance parameters.

In the fixed-nuisance case, this means

$$\boxed{P_{\text{obs},t}^{\varnothing}(\cdot | E, \theta_a, \lambda) = P_{\text{obs},t}^{\varnothing}(\cdot | E, \theta'_a, \lambda) \implies \theta_a = \theta'_a.} \quad (3.13.2)$$

In the profiled-nuisance case, θ_a is identifiable only if no distinct θ'_a can be compensated by an admissible nuisance value λ' :

$$\boxed{P_{\text{obs},t}^{\varnothing}(\cdot | E, \theta_a, \lambda) = P_{\text{obs},t}^{\varnothing}(\cdot | E, \theta'_a, \lambda') \implies \theta_a = \theta'_a.} \quad (3.13.3)$$

Remark 3.83 (Why nuisance parameters matter). Nuisance parameters are often where protocol collapse enters inference. An AFM stiffness estimate may be confounded by tip geometry, indentation depth, hydration, or surface adhesion. A DEP response may be confounded by medium conductivity, permittivity, viscosity, and field calibration. A mucus-tracking diffusivity may be confounded by local mesh heterogeneity, antibody binding, or adhesive trapping. A plaque count may be confounded by cell-line susceptibility, adsorption time, overlay composition, incubation time, staining threshold, and counting rule. If these quantities are ignored, a protocol-conditioned parameter can be mistaken for an intrinsic virion property.

Remark 3.84 (Structural versus practical identifiability). It is useful to distinguish two notions. *Structural identifiability* asks whether a parameter could be recovered in principle from ideal, unlimited data under the assumed protocol model. *Practical identifiability* asks whether the parameter can be estimated with useful precision from finite, noisy data. A latent sector may be structurally identifiable but practically weak if the likelihood is nearly flat, the Fisher information is small, the relevant observations are rare, the detection yield is low, or nuisance parameters are strongly correlated with the target parameter [30, 31, 32].

Definition 3.85 (Protocol equivalence class). For a fixed protocol E , define the observational equivalence class of θ by

$$[\theta]_E = \left\{ \theta' \in \Theta : P_{\text{obs},t}^{\varnothing}(\cdot | E, \theta') = P_{\text{obs},t}^{\varnothing}(\cdot | E, \theta) \right\}. \quad (3.13.4)$$

If $[\theta]_E$ contains more than one parameter point, then protocol E cannot distinguish those latent hypotheses, even in the infinite-data limit.

Remark 3.86 (Why identifiability is protocol dependent). A variable may be mechanically real but invisible under a given protocol. For example, a presentation-tilt sector may be present in the latent mechanical theory but unidentifiable in a static geometry-only readout. The same sector may become partially identifiable under a field-biased protocol, a surface-tilt assay, polarization-sensitive imaging, or another method that resolves orientation. Experimental collapse therefore explains why absence of evidence in one protocol is not necessarily evidence of absence in the latent mechanics.

Remark 3.87 (Experimental design consequence). The identifiability question suggests a design principle: choose protocol variations that change the observation kernel in directions that separate

the target parameter from nuisance parameters. Varying field frequency may help separate dielectric response from hydrodynamic drift. Varying surface chemistry or indentation depth may help separate stiffness from adhesion. Varying mucus composition or antibody concentration may help separate transport from binding. Varying cell line, adsorption time, overlay, or incubation time may help separate physical particle abundance from plaque-forming efficiency. Protocol variation is therefore not only a robustness check; it is a way to improve the rank and conditioning of the inverse problem.

The next subsection develops the local version of this identifiability problem using Fisher information. The global equivalence class $[\theta]_E$ describes exact non-identifiability of distinct parameter values; Fisher-information observability describes which infinitesimal directions in parameter space are locally visible or blind under a specified protocol.

3.14 Fisher-Information Observability

Identifiability can also be studied locally through Fisher information. The preceding definitions asked whether two parameter values can produce the same observed law. Fisher information asks the differential version of the same question: if the latent, environmental, or protocol parameters are changed slightly, does the protocol-conditioned likelihood change in a way that the experiment can detect?

In this sense, Fisher information measures the local sensitivity of the observed data distribution to parameter perturbations. A protocol has high Fisher information in a parameter direction if small changes in that direction produce distinguishable changes in the observed law. It has low Fisher information if those changes are weak relative to intrinsic noise, selection, projection, readout variability, or finite-sample limitations. It has zero Fisher information in a direction if the protocol is locally blind to that direction.

$$\boxed{\text{Fisher information} = \text{Local sensitivity of the protocol-conditioned likelihood.}} \quad (3.14.1)$$

For protocol-resolved virophysics, this is especially important because the likelihood is not a likelihood for the latent virion state alone. It is the likelihood of the observed state after latent-state transformation, survival or detection selection, readout, and possible null observation.

3.14.1 Score functions and protocol information

Assume that the null-inclusive observed law admits a density or mass function

$$p_E^\varnothing(y | \theta), \quad y \in \mathcal{Y}_E^\varnothing,$$

relative to an appropriate dominating measure ν_E^\varnothing . Here $\theta \in \Theta$ may include virion parameters, environmental parameters, and protocol parameters.

Definition 3.88 (Protocol score function). The *protocol score function* is

$$\boxed{\mathbf{u}_E(y; \theta) = \nabla_\theta \log p_E^\varnothing(y | \theta).} \quad (3.14.1.1)$$

It measures how sensitively the log-likelihood of an observed outcome y changes under infinitesimal changes in the parameter vector θ .

The word “observed” includes the null outcome when the likelihood is null-inclusive. Therefore, changes in θ may affect the score by changing the distribution of non-null data, the probability of entering the null channel, or both. In a plaque assay, for example, a parameter may change plaque sizes among visible plaques, the probability that a plaque forms at all, or both. In a tracking experiment, a parameter may change the distribution of recorded trajectories, the probability that a particle is trackable, or both.

Remark 3.89 (Interpretation of the score). If a parameter perturbation strongly changes the likelihood of the observed data, the score has a large component in that direction. If the perturbation barely changes the likelihood, the score has a small component. If the perturbation does not change the observed law at all, the score vanishes in that direction. Thus the score is the local derivative of the protocol-conditioned observation model.

Definition 3.90 (Protocol Fisher information). Assume the usual differentiability and integrability conditions hold. The *Fisher-information matrix* of protocol E is

$$\boxed{\mathcal{I}_E(\theta) = \mathbb{E}_{Y \sim p_E^\varnothing(\cdot|\theta)} \left[\mathbf{u}_E(Y; \theta) \mathbf{u}_E(Y; \theta)^\top \right]}. \quad (3.14.1.2)$$

Equivalently,

$$\mathcal{I}_E(\theta) = \int_{\mathcal{Y}_E^\varnothing} \nabla_\theta \log p_E^\varnothing(y | \theta) \nabla_\theta \log p_E^\varnothing(y | \theta)^\top p_E^\varnothing(y | \theta) \nu_E^\varnothing(dy). \quad (3.14.1.3)$$

Remark 3.91 (Fisher information as score covariance). Under standard regularity conditions, the expected score is zero:

$$\mathbb{E}_\theta [\nabla_\theta \log p_E^\varnothing(Y | \theta)] = 0.$$

Thus $\mathcal{I}_E(\theta)$ is the covariance matrix of the score. It measures how much the score fluctuates under repeated observations from the same protocol-conditioned model. Large score fluctuations indicate that the observed data are sensitive to the parameter; small score fluctuations indicate weak local sensitivity [44, 19, 20].

Remark 3.92 (Alternative curvature form). Under the usual regularity conditions, Fisher information can also be written as the negative expected Hessian of the log-likelihood:

$$\mathcal{I}_E(\theta) = -\mathbb{E}_{Y \sim p_E^\varnothing(\cdot|\theta)} \left[\nabla_\theta^2 \log p_E^\varnothing(Y | \theta) \right]. \quad (3.14.1.4)$$

This form gives the curvature interpretation. If the likelihood is sharply curved near the true parameter, the parameter is locally well constrained. If the likelihood is flat in some direction, that direction is weakly identifiable or blind under the protocol.

3.14.2 Directional information and local blindness

The full Fisher matrix summarizes information in all parameter directions. To ask whether a particular latent sector is visible, one evaluates the Fisher information in a chosen tangent direction.

Definition 3.93 (Directional Fisher information). Let $v \in T_\theta \Theta$ be a parameter direction. The

directional Fisher information of protocol E in direction v is

$$\boxed{\mathcal{I}_E(\theta; v) = v^\top \mathcal{I}_E(\theta) v.} \quad (3.14.2.1)$$

Equivalently,

$$\mathcal{I}_E(\theta; v) = \mathbb{E}_\theta \left[\left(v^\top \nabla_\theta \log p_E^\varnothing(Y | \theta) \right)^2 \right]. \quad (3.14.2.2)$$

Remark 3.94 (How to read directional Fisher information). The quantity $v^\top \mathcal{I}_E(\theta) v$ measures how strongly the observed law changes when the parameter vector is perturbed in direction v . For example, v could represent a change in virion stiffness, polarizability, spike-presentation heterogeneity, mucus-binding strength, cell-entry competence, adsorption probability, or a hidden orientation-sector parameter. If the directional information is large, the protocol is sensitive to that perturbation. If it is small, the protocol weakly resolves it.

Definition 3.95 (Locally blind parameter direction). A tangent direction $v \in T_\theta \Theta$ is *locally blind* under protocol E if

$$\boxed{v^\top \mathcal{I}_E(\theta) v = 0.} \quad (3.14.2.3)$$

It is *weakly observable* if this quantity is positive but small relative to the noise level, sample size, parameter scale, or experimental tolerance.

Definition 3.96 (Local protocol-blind subspace). The local protocol-blind subspace is

$$\boxed{\mathcal{B}_E(\theta) = \ker \mathcal{I}_E(\theta) = \left\{ v \in T_\theta \Theta : v^\top \mathcal{I}_E(\theta) v = 0 \right\}.} \quad (3.14.2.4)$$

Remark 3.97 (Protocol blindness as a null space). The null space of $\mathcal{I}_E(\theta)$ is the local protocol-blind sector. Perturbations of θ in this sector do not change the observed law to first order. In the language of experimental collapse, these are latent directions removed, averaged over, nulled, or compressed by the protocol observation operator.

Remark 3.98 (Why “local” matters). Fisher information is a local object. It describes the behavior of the likelihood near a specified parameter value θ . A direction may be blind near one parameter value but visible elsewhere, especially in nonlinear models. Thus Fisher-information observability should be interpreted as local identifiability, not as a universal statement about the entire parameter space.

3.14.3 Connection to estimation uncertainty

Fisher information is useful because it connects protocol sensitivity to estimation uncertainty. In regular parametric models, the Cramér–Rao inequality states that the covariance of any unbiased estimator is bounded below by the inverse Fisher information.

Definition 3.99 (Cramér–Rao interpretation). For an unbiased estimator $\hat{\theta}$ of θ , the Cramér–Rao bound has the schematic matrix form

$$\text{Cov}(\hat{\theta}) \succeq \mathcal{I}_E(\theta)^{-1}, \quad (3.14.3.1)$$

when $\mathcal{I}_E(\theta)$ is invertible and the regularity conditions for the bound hold.

Remark 3.100 (Protocol interpretation of the Cramér–Rao bound). Equation (3.14.3.1) says that a protocol with more Fisher information can, in principle, support more precise parameter estimates. If $\mathcal{I}_E(\theta)$ has a small eigenvalue, then uncertainty is large along the corresponding parameter direction. If $\mathcal{I}_E(\theta)$ is singular, then at least one direction is locally unidentifiable from that protocol alone [45, 46, 19, 20].

When the Fisher matrix is singular or nearly singular, the inverse should be interpreted cautiously. A Moore–Penrose pseudoinverse may describe uncertainty on the identifiable subspace, but it does not make blind directions identifiable. Those directions remain unconstrained by the protocol-conditioned likelihood unless additional structure, regularization, prior information, or protocol variation is introduced.

For N independent observations from the same protocol, the Fisher information adds:

$$\mathcal{I}_{E,N}(\theta) = N\mathcal{I}_E(\theta). \quad (3.14.3.2)$$

Thus additional data improve precision in directions that the protocol already sees. However, more data from the same protocol do not remove a structural blind direction.

Remark 3.101 (More data versus new protocol). If $v^\top \mathcal{I}_E(\theta)v = 0$, then

$$v^\top \mathcal{I}_{E,N}(\theta)v = 0$$

for every sample size N . More observations from the same protocol do not make a blind direction visible. To resolve that direction, one must change the observation kernel, add a complementary protocol, impose additional prior structure, or introduce controlled protocol variation.

3.14.4 Nuisance parameters and effective Fisher information

In protocol-resolved virophysics, the target parameter is often entangled with environmental or protocol parameters. This is why Fisher information should be interpreted after accounting for nuisance directions. Partition the parameter vector as

$$\theta = (\theta_a, \lambda),$$

where θ_a is the target parameter block and λ contains nuisance parameters. Write the Fisher matrix in block form:

$$\mathcal{I}_E(\theta) = \begin{pmatrix} \mathcal{I}_{aa} & \mathcal{I}_{a\lambda} \\ \mathcal{I}_{\lambda a} & \mathcal{I}_{\lambda\lambda} \end{pmatrix}. \quad (3.14.4.1)$$

Definition 3.102 (Effective Fisher information after nuisance profiling). When $\mathcal{I}_{\lambda\lambda}$ is invertible, the effective Fisher information for θ_a , after accounting for nuisance parameters, is the Schur complement

$$\boxed{\mathcal{I}_{a|\lambda} = \mathcal{I}_{aa} - \mathcal{I}_{a\lambda} \mathcal{I}_{\lambda\lambda}^{-1} \mathcal{I}_{\lambda a}}. \quad (3.14.4.2)$$

Remark 3.103 (Interpretation of nuisance-corrected information). The matrix $\mathcal{I}_{a|\lambda}$ measures

how much information about the target parameter remains after nuisance parameters are allowed to adjust. If $\mathcal{I}_{a|\lambda}$ is small, then the protocol may appear sensitive to θ_a when nuisance parameters are fixed, but weakly informative once realistic uncertainty in protocol or environmental parameters is included. This is common in virological settings: apparent stiffness can be confounded with surface adhesion or indentation depth, field response with medium conductivity and viscosity, mucus transport with binding heterogeneity, and plaque count with cell-line or overlay conditions.

Remark 3.104 (When the nuisance block is singular). If $\mathcal{I}_{\lambda\lambda}$ is singular, then some nuisance directions are themselves locally unidentifiable under the protocol. In that case, the Schur complement must be replaced by an appropriate generalized inverse, reparameterization, regularized information matrix, or explicit prior model. The singularity is not merely a technical inconvenience; it indicates that the experiment may not separate target and nuisance effects without additional protocol variation or external calibration.

This completes the local observability analysis for a single protocol. Fisher information identifies which infinitesimal parameter directions are visible, weakly resolved, nuisance-confounded, or locally blind under the protocol-conditioned likelihood. The next step is to ask how this structure changes when additional protocols are introduced.

3.14.5 Information gain from additional protocols

Fisher-information observability gives a direct experimental-design principle: a new protocol is most useful when it adds information in parameter directions that are blind, weakly resolved, or nuisance-confounded under the existing protocol set. In protocol-resolved virophysics, the goal is therefore not merely to repeat an observation, but to change the observation kernel in a way that probes the latent virion–environment system from a new direction.

Definition 3.105 (Information gain from an additional protocol). Let E_1 be an existing protocol and E_2 a proposed additional protocol. For a parameter direction $v \in T_\theta\Theta$, the directional information gain supplied by E_2 , relative to E_1 , is

$$\Delta\mathcal{I}_{E_2|E_1}(\theta; v) = v^\top \mathcal{I}_{E_2}(\theta)v. \quad (3.14.5.1)$$

If the datasets generated by E_1 and E_2 are conditionally independent given θ , then the combined information is

$$\boxed{\mathcal{I}_{E_1, E_2}(\theta) = \mathcal{I}_{E_1}(\theta) + \mathcal{I}_{E_2}(\theta)}. \quad (3.14.5.2)$$

More generally, for conditionally independent protocols E_1, \dots, E_M ,

$$\mathcal{I}_{\text{multi}}(\theta) = \sum_{j=1}^M \mathcal{I}_{E_j}(\theta). \quad (3.14.5.3)$$

Equation (3.14.5.1) is most important when v lies in, or near, the blind subspace of the existing protocol. If

$$v \in \mathcal{B}_{E_1}(\theta) = \ker \mathcal{I}_{E_1}(\theta),$$

then E_1 supplies no local information in direction v . The proposed protocol E_2 reduces that blindness

precisely when

$$v^\top \mathcal{I}_{E_2}(\theta)v > 0.$$

Thus the value of an additional protocol is not determined only by how much total information it adds, but by whether it adds information in the directions that are missing from the current experimental design.

Definition 3.106 (Blind-subspace information gain). Let $\mathcal{B}_{E_1}(\theta) = \ker \mathcal{I}_{E_1}(\theta)$ be the local blind subspace of protocol E_1 . The blind-subspace information gain of an additional protocol E_2 may be summarized by the restriction

$$\mathcal{I}_{E_2}^{\mathcal{B}}(\theta) = \mathcal{I}_{E_2}(\theta)|_{\mathcal{B}_{E_1}(\theta)}. \quad (3.14.5.4)$$

If this restricted form is nonzero, then E_2 probes at least one direction that was locally blind under E_1 .

Remark 3.107 (Experimental design interpretation). Equation (3.14.5.3) gives an experimental design principle. A new protocol is most valuable when it adds information in directions that are blind or weakly constrained under the existing protocol. Thus the best complementary experiment is not necessarily the one that most closely reproduces the first experiment. It is often the one whose observation kernel projects, perturbs, selects, or amplifies the latent mechanics differently.

Remark 3.108 (Examples of complementary Fisher information). A cryo-EM or cryo-ET protocol may provide strong information about geometry, symmetry, morphology, and selected conformational classes, but weak information about free dynamics, compliance, or infectious activity. AFM may add information about surface-conditioned stiffness, deformation, rupture, or adhesion. Dielectrophoresis and electrorotation may add information about dielectric response, polarizability, charge asymmetry, hydrodynamic drag, and frequency-dependent field coupling. Mucus or gel tracking may add information about adhesion, residence time, confinement, mobile and immobile fractions, and transport heterogeneity. A plaque or focus assay may add information about assay-conditioned infectious competence. Each protocol adds Fisher information in the directions to which its observation kernel is sensitive.

Remark 3.109 (When Fisher information does not simply add). The additive formula in Eq. (3.14.5.3) assumes conditional independence of the datasets given the parameters. If protocols share batch effects, preparation artifacts, calibration errors, cell-culture variability, environmental drift, or correlated sample history, then the joint likelihood must include those dependencies explicitly. In that case, the multi-protocol Fisher information is obtained from the joint likelihood, not by naively summing single-protocol matrices.

3.15 Multi-Protocol Consistency

Multi-protocol comparison is often described as checking whether different experiments agree. In protocol-resolved virophysics, the more precise question is whether different observed ensembles can be explained by a common latent model passed through different protocol kernels. Agreement is therefore not required at the level of raw observables. A density map, an indentation curve, a field-response spectrum, a trajectory ensemble, and a plaque count need not look alike, because they are not the same kind of object. The relevant question is whether their differences are compatible with a shared

latent virion–environment model plus protocol-specific transformations, selections, readouts, and null channels.

Definition 3.110 (Multi-protocol consistency). Let E_1, \dots, E_M be experimental protocols with datasets

$$\mathcal{D}_1, \dots, \mathcal{D}_M.$$

A latent model $P_{\text{ref},t}(\cdot | \theta)$ is *multi-protocol consistent* if there exists a common latent parameter set θ , together with admissible protocol-specific nuisance parameters $\lambda_1, \dots, \lambda_M$, such that

$$P_{\text{obs},t}^{(j),\varnothing}(\cdot | E_j, \theta, \lambda_j) = \mathcal{M}_{E_j}^{\varnothing}(\lambda_j)P_{\text{ref},t}(\cdot | \theta), \quad j = 1, \dots, M, \quad (3.15.1)$$

adequately explains the observed data for all protocols.

Here θ represents the shared latent virion–environment parameters, while λ_j represents protocol-local quantities such as calibration constants, surface chemistry, imaging thresholds, cell-line conditions, field settings, overlay composition, reconstruction choices, or counting rules. The distinction between θ and λ_j is important: multi-protocol consistency does not require all protocols to have the same nuisance parameters. It requires that their protocol-specific differences be compatible with a shared latent explanation.

Equivalently, when the datasets are conditionally independent given the shared latent parameters and protocol-specific nuisance parameters, the joint multi-protocol likelihood is

$$\mathcal{L}_{\text{multi}}(\theta, \lambda_1, \dots, \lambda_M) = \prod_{j=1}^M \mathcal{L}_{E_j}^{\varnothing}(\theta, \lambda_j; \mathcal{D}_j). \quad (3.15.2)$$

When only detected non-null observations are available for some protocols, the corresponding conditional likelihoods $\mathcal{L}_{E_j}^{\text{det}}$ may be used, with the understanding that yield information has then been discarded or must be modeled separately.

Remark 3.111 (Why multi-protocol comparison is powerful). Experimental collapse makes multi-protocol comparison more valuable, not less. If cryo-ET, AFM, dielectrophoresis, plaque assays, and mucus tracking are interpreted as different kernels acting on related latent mechanics, then disagreement between their observations can become informative. It may indicate that one protocol pins orientation, another selects geometry, another probes dielectric response, another amplifies infectivity, and another reports medium-filtered transport. The goal is not to force all protocols to agree at the observation level. The goal is to ask whether they can be explained by a coherent latent model plus distinct protocol kernels.

Definition 3.112 (Protocol inconsistency). A set of protocols E_1, \dots, E_M is *protocol-inconsistent* relative to a latent model class \mathcal{P} if no admissible $P_{\text{ref},t}(\cdot | \theta) \in \mathcal{P}$ and no admissible protocol-specific nuisance parameters $\lambda_1, \dots, \lambda_M$ can jointly account for the observed datasets under the specified protocol kernels.

Remark 3.113 (Interpretation of inconsistency). Protocol inconsistency is not automatically experimental failure. It may indicate that the latent model is missing a relevant state variable,

that a protocol kernel is misspecified, that an environmental variable was uncontrolled, that the virion population changed between experiments, or that a biological assay is selecting a functional subpopulation not represented in the mechanical model. The inconsistency is therefore diagnostic. It tells the modeler where the assumed latent state, environmental description, or protocol kernel may be incomplete.

Remark 3.114 (Agreement can also be misleading). Just as disagreement is not automatically failure, agreement is not automatically full validation. Two protocols can agree because they share the same blind direction, select the same subpopulation, or collapse different latent states into the same reported summary. Multi-protocol consistency is strongest when the protocols are complementary, not merely redundant.

Remark 3.115 (Section-level interpretation). Fisher-information observability gives a quantitative language for experimental collapse. It asks not only whether a protocol produces data, but which latent directions those data can constrain. In this framework, a protocol is not simply “informative” or “uninformative.” It is informative in particular parameter directions, weak in others, and blind in others. Multi-protocol design is the process of choosing complementary kernels whose information directions jointly resolve the latent virion–environment model.

3.16 Inverse Environmental Inference

In many virological settings, the environment is not merely background. Mucus, extracellular matrix, aerosols, droplets, buffers, ionic conditions, surfaces, overlays, and cellular monolayers can determine which virion states are accessible, mobile, adhesive, mechanically responsive, infectious, detectable, or countable. The protocol-resolved formalism therefore supports not only inference about virions, but also inverse inference about the environments through which virions move, bind, deform, polarize, or amplify.

This point is important because many virological observables are naturally joint virion–environment observables. A trajectory in mucus reflects both the virion and the mucus network. A dielectrophoretic response reflects both the particle and the electrical properties of the suspending medium. An AFM indentation curve reflects both particle mechanics and surface-contact conditions. A plaque assay reflects both virion infectious competence and the susceptibility, spatial restriction, and amplification properties of the cellular assay environment. Thus the inverse problem is often not

observed data \longrightarrow virion parameters alone,

but rather

$$\boxed{\text{observed protocol-conditioned data} \longrightarrow \left\{ \begin{array}{l} \text{virion parameters} \\ \text{environmental parameters} \\ \text{protocol parameters} \end{array} \right\}.} \quad (3.16.1)$$

Definition 3.116 (Joint virion–environment latent state). A joint virion–environment latent state has the schematic form

$$X = (X_{\text{vir}}, X_{\text{env}}), \quad (3.16.2)$$

where X_{vir} contains virion-level variables and X_{env} contains local environmental variables. Examples include viscosity, viscoelastic relaxation time, mesh size, mucin composition, binding-site density, antibody concentration, ionic strength, dielectric permittivity, conductivity, flow field, surface chemistry, receptor density, cell-layer susceptibility, pH, and temperature.

Remark 3.117 (Environment as a latent variable). The environmental component X_{env} may vary from particle to particle and from location to location. In mucus or extracellular matrix, two virions in the same nominal sample may experience different local mesh sizes, adhesive states, or viscoelastic environments. In a plaque assay, different regions of the monolayer may differ in cell density, susceptibility, or local spread conditions. In a field-driven experiment, the effective medium parameters may depend on ionic strength, conductivity, temperature, and field frequency. Thus the environment should often be modeled as part of the latent state rather than as a fixed background constant.

Definition 3.118 (Environmental parameter block). Let

$$\theta = (\theta_{\text{vir}}, \theta_{\text{env}}, \theta_E)$$

be the protocol-resolved parameter vector. The environmental parameter block θ_{env} contains parameters governing the distribution or dynamics of X_{env} . Examples include mucus mesh scale, adhesive binding rate, effective viscosity, viscoelastic relaxation time, dielectric permittivity, conductivity, surface-binding strength, receptor density, cell-layer susceptibility, local spread efficiency, antibody concentration, ionic strength, pH, and temperature.

Remark 3.119 (Virions as passive probes). Because extracellular virions are passively responsive physical objects, their observed motion, survival, adhesion, deformation, or field response can encode information about the environment. A particle trajectory in mucus may contain information about confinement, adhesion, local viscoelastic structure, or mobile and immobile subpopulations [14, 35, 15, 23]. A dielectrophoretic or electrorotational response may contain information about dielectric contrast, medium conductivity, hydrodynamic drag, and field-frequency-dependent response [10, 11, 12, 13]. A plaque assay may contain information not only about virion infectivity but also about cell susceptibility, overlay restrictions, local spread, incubation time, and visibility threshold [16, 17, 18].

Definition 3.120 (Environmental inverse problem). Given protocol-conditioned data \mathcal{D}_E , the environmental inverse problem is to infer θ_{env} , possibly jointly with θ_{vir} and θ_E , from the protocol-resolved likelihood

$$\mathcal{L}_E^\varnothing(\theta_{\text{vir}}, \theta_{\text{env}}, \theta_E; \mathcal{D}_E). \quad (3.16.3)$$

In Bayesian form, the marginal posterior for the environmental parameters is

$$\boxed{q(\theta_{\text{env}} \mid \mathcal{D}_E, E) = \int q(\theta_{\text{vir}}, \theta_{\text{env}}, \theta_E \mid \mathcal{D}_E, E) d\theta_{\text{vir}} d\theta_E.} \quad (3.16.4)$$

Remark 3.121 (Virion–environment confounding). Environmental inference is useful but can be confounded. A slow trajectory in mucus may reflect a strongly adhesive virion, a dense local mucus mesh, antibody cross-linking, low local water content, or a combination of these effects. A weak plaque count may reflect low infectious competence, poor cell susceptibility, restrictive overlay conditions,

insufficient incubation time, or a stringent staining threshold. A weak field response may reflect particle polarizability, medium conductivity, viscosity, or hydrodynamic drag. Environmental inference is therefore strongest when protocol variation or complementary measurements separate virion parameters from environmental parameters.

Definition 3.122 (Environmental identifiability under a protocol). An environmental parameter block θ_{env} is identifiable under protocol E , relative to a chosen model class and nuisance-parameter treatment, if distinct values of θ_{env} produce distinguishable null-inclusive observed laws after accounting for virion and protocol nuisance parameters. In the profiled- nuisance case, this requires

$$\boxed{P_{\text{obs},t}^{\varnothing}(\cdot \mid E, \theta_{\text{env}}, \lambda) = P_{\text{obs},t}^{\varnothing}(\cdot \mid E, \theta'_{\text{env}}, \lambda') \implies \theta_{\text{env}} = \theta'_{\text{env}},} \quad (3.16.5)$$

where λ, λ' contain virion and protocol nuisance parameters.

Remark 3.123 (Why inverse environmental inference belongs in virophysics). Inverse environmental inference is not separate from virophysics. Virions do not move, bind, polarize, deform, or infect in an abstract vacuum. They do so in media, on surfaces, in droplets, in gels, in mucus, on cell layers, and under specific experimental constraints. A protocol-resolved theory should therefore allow the experiment to teach us about the environment as well as about the virion.

Remark 3.124 (Design implication for environmental inference). Environmental parameters are most identifiable when the experimental design changes the environment in controlled ways while also monitoring virion response. Examples include varying mucus composition or antibody concentration in tracking assays, varying ionic strength or conductivity in DEP and electrorotation, varying surface chemistry in AFM, or varying cell line, overlay, and incubation time in plaque assays. Such variations change the protocol-conditioned observation kernel and can separate environmental effects from intrinsic virion properties.

The worked-example template below translates these ideas into a practical comparison procedure. Rather than asking whether two protocols produce identical raw outputs, it asks whether their protocol-conditioned observations can be mapped to a common comparison target and interpreted as complementary views of a shared latent virion–environment system.

3.17 Worked Example Template: Comparing Protocols

The formalism can be applied to a pair or family of protocols by following a standard sequence. The purpose of the template is to prevent protocol comparison from becoming a direct comparison of raw observables that may not live in the same state space. Instead, each observed ensemble is interpreted through its own protocol kernel and then compared through a shared latent model, a common comparison space, or a specified inference target.

The guiding question is therefore not simply

Do the experiments give the same result?

but rather

$$\boxed{\text{Can one latent virion–environment model explain all protocol-conditioned observations?}} \quad (3.17.1)$$

This framing is essential in virophysics because different protocols often probe different physical, mechanical, electrical, transport, or biological sectors of the same underlying system.

- (i) **Choose the latent model.** Specify the latent state X , the latent state space (Ψ, Σ_X) , the reference ensemble $P_{\text{ref},t}(dx \mid \theta)$, and the parameter blocks of interest:

$$\theta = (\theta_{\text{vir}}, \theta_{\text{env}}, \theta_E).$$

Here θ_{vir} may describe virion mechanics, structure, charge, spike presentation, polarizability, adhesion, or infectivity; θ_{env} may describe medium, surface, field, mucus, overlay, or cell-layer properties; and θ_E describes protocol-specific settings and nuisance parameters.

- (ii) **Specify each protocol.** For every protocol E_j , identify the protocol-conditioned latent space $(\Psi_{E_j}, \Sigma_{X,E_j})$, the latent transformation kernel $\Pi_{E_j}^{\text{at}}$, the survival or detection weight s_{E_j} , the readout kernel R_{E_j} , and the null channel \emptyset . This step states how the protocol transforms, selects, projects, amplifies, or rejects latent states before they become reported data.
- (iii) **Define observed quantities.** Specify the non-null observation spaces

$$(\mathcal{Y}_{E_j}, \Sigma_{Y,E_j})$$

and the reported observables

$$\mathbf{h}_{E_j} : \mathcal{Y}_{E_j} \rightarrow \mathbb{R}^{m_j}.$$

Examples include density-map summaries, force-curve parameters, trajectory statistics, field-response amplitudes, plaque counts, focus counts, endpoint titers, orientation classes, or inferred stiffness and mobility parameters.

- (iv) **Map to a common comparison space when needed.** If the protocols report different kinds of data, introduce measurable maps

$$H_{E_j} : \mathcal{Y}_{E_j} \rightarrow W$$

into a common comparison space (W, Σ_W) . This step states exactly what is being compared: size, stiffness, mobility, infectivity, orientation, dielectric response, environmental transport parameters,

mechanical compliance, plaque-forming efficiency, or another shared summary.

- (v) **Compute collapse functionals.** Evaluate distributional, observable-level, yield-level, modal, dynamical, or Fisher-information collapse measures. Examples include

$$\mathcal{C}_{\text{lat}}^{\text{W}}(E_j; t), \quad \mathcal{C}_{\text{obs}}^{\text{W}}(E_i, E_j; t), \quad \mathcal{C}_\eta(E_i; E_j, t), \quad \mathcal{I}_{E_j}(\theta).$$

These quantities determine whether the relevant difference is mainly latent transformation, detection selection, readout compression, dynamical-sector loss, nuisance confounding, or protocol-to-protocol discrepancy.

- (vi) **Test multi-protocol consistency.** Ask whether a common latent parameter set θ , together with protocol-specific nuisance parameters $\lambda_1, \dots, \lambda_M$, can explain all observed datasets:

$$P_{\text{obs},t}^{(j),\varnothing}(\cdot | E_j, \theta, \lambda_j) = \mathcal{M}_{E_j}^{\varnothing}(\lambda_j) P_{\text{ref},t}^{\varnothing}(\cdot | \theta), \quad j = 1, \dots, M. \quad (3.17.2)$$

This step asks whether apparent differences between protocols can be explained as distinct protocol-conditioned views of the same latent virion–environment system.

- (vii) **Identify blind or weakly resolved sectors.** Use sensitivity matrices, Fisher information, yield differences, protocol-to-protocol discrepancies, or posterior uncertainty to identify latent directions that are invisible, weakly constrained, or confounded with nuisance parameters. In Fisher-information language, this means examining

$$\mathcal{B}_{E_j}(\theta) = \ker \mathcal{I}_{E_j}(\theta), \quad \mathcal{B}_{\text{multi}}(\theta) = \ker \mathcal{I}_{\text{multi}}(\theta).$$

A useful complementary protocol is one that reduces the blind subspace or improves the conditioning of the inverse problem.

- (viii) **Revise the model or protocol kernels if consistency fails.** Inconsistency may signal a missing latent variable, an incorrect protocol kernel, an unmodeled environmental effect, uncontrolled nuisance variation, population heterogeneity, batch dependence, or genuine biological differences between experimental conditions. The inconsistency is therefore diagnostic, not merely negative.

Remark 3.125 (How to read protocol disagreement). If two protocols disagree at the level of raw observed data, the disagreement is not automatically an error. It may indicate that the protocols project different latent sectors, apply different selection weights, impose different mechanical or biological conditions, or amplify different functional subpopulations. The template above asks whether such disagreement can be explained by a shared latent model plus distinct protocol kernels.

3.18 Section Reference: Core Objects and Equations

Table 11. Core objects, equations, and interpretations introduced in the protocol-resolved ensemble and inference framework. This table is a compact reference for the notation used in later sections.

Object or equation	Mathematical form	Interpretation
Reference latent ensemble	$P_{\text{ref},t}(dx)$ on (Ψ, Σ_X)	Baseline distribution of latent virion–environment states before measurement-protocol conditioning.
Protocol parameter vector	$\theta = (\theta_{\text{vir}}, \theta_{\text{env}}, \theta_E)$	Parameter vector separating virion properties, environmental properties, and protocol-specific quantities.
Protocol-conditioned latent ensemble	$\tilde{P}_{E,t}^{\text{lat}} = P_{\text{ref},t} \Pi_E^{\text{lat}}$	Latent ensemble after preparation, forcing, medium exposure, surface contact, biological pathway conditioning, or another protocol-induced transformation.
Latent transformation kernel	$\Pi_E^{\text{lat}}(dx_E x)$	Maps a reference latent state $x \in \Psi$ to a protocol-conditioned latent state $x_E \in \Psi_E$.
Survival/detection weight	$s_E : \Psi_E \rightarrow [0, 1]$	Probability that a protocol-conditioned latent state enters the accepted non-null data channel.
Detection yield	$\eta_E(t) = \int_{\Psi_E} s_E(x_E) \tilde{P}_{E,t}^{\text{lat}}(dx_E)$	Total probability mass that survives, is detected, is accepted, or successfully amplifies into a non-null record.
Detected latent ensemble	$P_{E,t}^{\text{lat}}(A \text{det}) = \frac{\int_A s_E(x_E) \tilde{P}_{E,t}^{\text{lat}}(dx_E)}{\eta_E(t)}$	Protocol-conditioned latent ensemble after selection, detection, visibility, or biological success, normalized over non-null outcomes.
Non-null observation space	$(\mathcal{Y}_E, \Sigma_{\mathcal{Y},E})$	Protocol-specific space of reported non-null data: images, curves, trajectories, spectra, counts, classes, or endpoint readouts.
Null-augmented observation space	$\mathcal{Y}_E^{\emptyset} = \mathcal{Y}_E \cup \{\emptyset\}$	Observation space enlarged by the null outcome representing non-detection, rejection, failed amplification, loss, or failure to enter the accepted record.
Null channel	\emptyset	Outcome assigned to latent states that fail to produce accepted, visible, countable, trackable, reconstructable, or otherwise recorded data under the protocol.

Continued on next page.

Table 11. Core objects, equations, and interpretations introduced in the protocol-resolved ensemble and inference framework. *Continued from previous page.*

Object or equation	Mathematical form	Interpretation
Readout kernel	$R_E(dy x_E)$	Maps a detected protocol-conditioned latent state to reported data, including finite resolution, fitting, reconstruction, thresholding, classification, counting, and measurement noise.
State-specific detection probability	$q_E(x) = K_E^\varnothing(\mathcal{Y}_E x)$ $= \int_{\Psi_E} s_E(x_E) \Pi_E^{\text{lat}}(dx_E x)$	Probability that latent state x generates a non-null observation under protocol E .
Null-inclusive protocol kernel	$K_E^\varnothing(S x) = \int_{\Psi_E} s_E(x_E) R_E(S \cap \mathcal{Y}_E x_E) \Pi_E^{\text{lat}}(dx_E x)$ $+ [1 - q_E(x)] \delta_\varnothing(S)$	Full state-to-observation kernel including latent transformation, selection, readout, and probability flow into the null channel.
Null-inclusive observation operator	$(\mathcal{M}_E^\varnothing P)(S) = \int_{\Psi} K_E^\varnothing(S x) P(dx)$	Linear operator mapping a latent ensemble to the full observed ensemble, including null outcomes.
Null-inclusive observed ensemble	$P_{\text{obs},t}^\varnothing(\cdot E) = \mathcal{M}_E^\varnothing P_{\text{ref},t}$	Observed ensemble generated by applying the protocol observation operator to the reference latent ensemble.
Detected observation operator	$(\mathcal{M}_E^{\text{det}} P)(B) = \frac{(\mathcal{M}_E^\varnothing P)(B)}{(\mathcal{M}_E^\varnothing P)(\mathcal{Y}_E)}$	Conditional operator giving the reported non-null observed ensemble after normalization by detection yield.
Protocol-resolved observed density	$p_E^\varnothing(y \theta) = \frac{dP_{\text{obs},t}^\varnothing(\cdot E, \theta)}{d\nu_E^\varnothing}(y)$	Density or mass function of the null-inclusive observed law with respect to an appropriate dominating measure.
Protocol-lifted observable	$\tilde{h}_E(x) = \int_{\Psi_E} s_E(x_E) \left[\int_{\mathcal{Y}_E} h(y) R_E(dy x_E) \right]$ $\times \Pi_E^{\text{lat}}(dx_E x)$	Turns a reported observable h into an effective protocol-dependent observable on the latent state space.
Observed expectation under a protocol	$\langle h \rangle_E[P] = \frac{\int_{\Psi} \tilde{h}_E(x) P(dx)}{\int_{\Psi} q_E(x) P(dx)}$	Expected reported value among detected observations; the denominator explicitly accounts for protocol-dependent selection.
Common comparison space	$L_0 : \Psi \rightarrow W, \quad L_E : \Psi_E \rightarrow W$	Places latent and protocol-conditioned objects into a shared space before computing collapse magnitudes or protocol-to-protocol discrepancies.
Latent distributional collapse	$\mathcal{C}_{\text{lat}}^W(E; t) = D_W((L_E)_\# \tilde{P}_{E,t}^{\text{lat}}, (L_0)_\# P_{\text{ref},t})$	Measures how strongly the protocol transforms the latent ensemble before detection selection.

Continued on next page.

Table 11. Core objects, equations, and interpretations introduced in the protocol-resolved ensemble and inference framework. *Continued from previous page.*

Object or equation	Mathematical form	Interpretation
Detected latent collapse	$C_{\text{det}}^W(E; t) = D_W((L_E)_{\#} P_{E,t}^{\text{lat}}(\cdot \text{det}), (L_0)_{\#} P_{\text{ref},t})$	Measures the collapse of the latent subpopulation that actually reaches the detected channel.
Detection-yield collapse	$C_{\eta}(E; E_0, t) = \eta_E(t) - \eta_{E_0}(t) $	Compares how much probability mass reaches the non-null data channel under two protocols.
Null-inclusive likelihood	$\mathcal{L}_E^{\otimes}(\theta; \mathcal{D}_E) = \prod_i p_E^{\otimes}(y_i \theta)$	Likelihood of the complete null-inclusive dataset under the protocol-conditioned observed law.
Conditional detected likelihood	$\mathcal{L}_E^{\text{det}}(\theta; \mathcal{D}_E^{\text{det}}) = \prod_i p_E(y_i \theta, \text{det})$	Likelihood for datasets in which only non-null accepted observations are retained.
Bayesian inverse formulation	$q(\theta \mathcal{D}_E, E) = \frac{\mathcal{L}_E^{\otimes}(\theta; \mathcal{D}_E) q_0(\theta)}{\int_{\Theta} \mathcal{L}_E^{\otimes}(\vartheta; \mathcal{D}_E) q_0(\vartheta) d\vartheta}$	Posterior distribution over latent, environmental, and protocol parameters after observing protocol-conditioned data.
Target/nuisance partition	$\theta = (\theta_a, \lambda)$	Separates the target parameter block θ_a from nuisance parameters λ , such as environmental variables, protocol settings, calibration constants, thresholds, or noise parameters.
Protocol identifiability	$P_{\text{obs},t}^{\otimes}(\cdot E, \theta_a, \lambda)$ $= P_{\text{obs},t}^{\otimes}(\cdot E, \theta'_a, \lambda') \Rightarrow \theta_a = \theta'_a$	Target parameter block remains identifiable after accounting for admissible nuisance-parameter variation.
Protocol equivalence class	$[\theta]_E = \{\theta' \in \Theta : P_{\text{obs},t}^{\otimes}(\cdot E, \theta') = P_{\text{obs},t}^{\otimes}(\cdot E, \theta)\}$	Set of parameter values that a protocol cannot distinguish, even in the ideal infinite-data limit.
Protocol score function	$\mathbf{u}_E(y; \theta) = \nabla_{\theta} \log p_E^{\otimes}(y \theta)$	Local derivative of the protocol-conditioned log-likelihood with respect to the parameter vector.
Fisher information	$\mathcal{I}_E(\theta) = \mathbb{E}_{\theta}[\mathbf{u}_E(Y; \theta) \mathbf{u}_E(Y; \theta)^{\top}]$	Local sensitivity of the protocol-conditioned likelihood to parameter perturbations.
Directional Fisher information	$\mathcal{I}_E(\theta; v) = v^{\top} \mathcal{I}_E(\theta) v$	Amount of local information supplied by protocol E in parameter direction v .
Local blind subspace	$\mathcal{B}_E(\theta) = \ker \mathcal{I}_E(\theta)$	Infinitesimal parameter directions that the protocol cannot locally resolve.
Effective Fisher information	$\mathcal{I}_{a \lambda} = \mathcal{I}_{aa} - \mathcal{I}_{a\lambda} \mathcal{I}_{\lambda\lambda}^{-1} \mathcal{I}_{\lambda a}$	Information about the target block θ_a after nuisance parameters are allowed to adjust.

Continued on next page.

Table 11. Core objects, equations, and interpretations introduced in the protocol-resolved ensemble and inference framework. *Continued from previous page.*

Object or equation	Mathematical form	Interpretation
Multi-protocol information	$\mathcal{I}_{\text{multi}}(\theta) = \sum_{j=1}^M \mathcal{I}_{E_j}(\theta)$	Combined Fisher information for conditionally independent protocols. Complementary protocols can reduce blind directions.
Multi-protocol consistency	$P_{\text{obs},t}^{(j),\varnothing} = \mathcal{M}_{E_j}^{\varnothing}(\lambda_j) P_{\text{ref},t}(\cdot \theta)$	Asks whether different protocol-conditioned datasets can be explained by a shared latent virion-environment model with protocol-specific nuisance parameters.

4 Mechanisms of Experimental Collapse

The preceding sections introduced experimental collapse as a protocol-conditioned map from a reference latent ensemble to an observed ensemble. We now resolve that map into mechanism-specific collapse channels. This decomposition is not merely taxonomic. It identifies which part of an experiment transforms the latent state, which part selects or rejects states, which part conditions survival or detectability, and which part projects surviving states into the reported data space.]

The central laboratory question is:

$$\boxed{\text{What happened to the latent virion–environment ensemble before it became reported data?}} \quad (4.1)$$

This question is practical rather than philosophical. A cryo-EM reconstruction, an AFM force curve, a dielectrophoretic trajectory, a mucus-tracking path, and a plaque count are all real observations. The point is that each is produced by a specific sequence of preparation, conditioning, selection, survival, detection, and readout operations.

Furthermore, a protocol is rarely one operation. It is usually a sequence of physical, chemical, biological, computational, and instrumental steps. Each step may preserve some latent variables while transforming, filtering, amplifying, compressing, or erasing others. Before writing the full kernel composition, it is useful to state the pipeline in its most compact form:

$$\boxed{\text{Latent State} \longrightarrow \text{Conditioned State} \longrightarrow \text{Selected State} \longrightarrow \text{Reported Datum.}} \quad (4.2)$$

Here “conditioned” means that the virion has been placed into the physical, chemical, biological, and procedural environment of the experiment. A cryo-EM specimen is conditioned by grid preparation, thin-film formation, air–water interface exposure, vitrification, particle selection, and reconstruction. An AFM specimen is conditioned by surface attachment, hydration, probe geometry, indentation, and loading rate. A DEP or electrorotation specimen is conditioned by the imposed field, suspending medium, conductivity, permittivity, and hydrodynamic drag. A mucus-tracking experiment is conditioned by the structured medium, adhesion landscape, imaging cadence, and tracking window. A plaque assay is conditioned by the cell line, adsorption time, overlay, incubation time, staining method, visibility threshold, and counting rule.

A slightly more detailed schematic is

$$\boxed{X \longrightarrow X_{\text{prep}} \longrightarrow X_{\text{constr}} \longrightarrow X_{\text{det}} \longrightarrow Y_E \text{ or } \emptyset.} \quad (4.3)$$

The first arrow represents preparation or handling. The second represents surface, field, medium, loading, confinement, or biological constraints. The third represents survival, selection, detectability, or acceptance. The final arrow represents readout or null observation. The variables in Eq. (4.3) are schematic rather than universal. Their purpose is to help identify where each mechanism acts in a real experiment.

Remark 4.1 (How to use this section). For any protocol, the mechanism-resolved analysis proceeds in stages. First, list the experimental steps. Second, decide whether each step transforms the

latent state, changes the probability of detection, or changes the final readout. Third, assign that step to a kernel, weight, readout map, or null channel.

4.1 Mechanism-Resolved Factorization

Let E be a fixed protocol. Instead of treating the latent-stage kernel Π_E^{lat} as an indivisible object, we may factor it into mechanism-specific kernels. The simplest symbolic statement is

$$\boxed{\Pi_E^{\text{lat}} = \Pi_E^{\text{last}} \circ \cdots \circ \Pi_E^{\text{first}}.} \quad (4.1.1)$$

This equation states that the protocol-conditioned latent state is produced by applying several experimentally meaningful stages in sequence. The rightmost kernel acts first.

More explicitly, let

$$(\Psi_{E,0}, \Sigma_{X,E,0}) = (\Psi, \Sigma_X), \quad (\Psi_{E,L}, \Sigma_{X,E,L}) = (\Psi_E, \Sigma_{X,E}),$$

and let

$$\Pi_{E,\ell}(dx_\ell \mid x_{\ell-1}), \quad \ell = 1, \dots, L,$$

be Markov kernels between intermediate protocol-conditioned state spaces.

Definition 4.2 (Mechanism-resolved protocol factorization). A *mechanism-resolved factorization* of the latent-stage protocol kernel is a composition

$$\Pi_E^{\text{lat}} = \Pi_{E,L} \circ \Pi_{E,L-1} \circ \cdots \circ \Pi_{E,1}, \quad (4.1.2)$$

where each factor represents a physically, chemically, biologically, or procedurally interpretable protocol stage. For $G \in \Sigma_{X,E}$,

$$\boxed{\Pi_E^{\text{lat}}(G \mid x_0) = \int_{\Psi_{E,1}} \cdots \int_{\Psi_{E,L}} \mathbf{1}_G(x_L) \Pi_{E,L}(dx_L \mid x_{L-1}) \cdots \Pi_{E,1}(dx_1 \mid x_0).} \quad (4.1.3)$$

This expression is the unfolded version of Eq. (4.1.1). A state begins as x_0 , passes through intermediate protocol states

$$x_1, \dots, x_L,$$

and ends in the final protocol-conditioned latent state $x_L \in \Psi_E$. The indicator $\mathbf{1}_G(x_L)$ asks whether the final conditioned state lies in the set G . The multiple integral sums over all possible intermediate protocol histories.

Typical mechanism-specific factors include

$$\Pi_E^{\text{prep}}, \quad \Pi_E^{\text{interface}}, \quad \Pi_E^{\text{surf}}, \quad \Pi_E^{\text{field}}, \quad \Pi_E^{\text{load}}, \quad \Pi_E^{\text{medium}}, \quad \Pi_E^{\text{time}}, \quad \Pi_E^{\text{bio}}. \quad (4.1.4)$$

The order of these factors is protocol dependent. A cryo-EM pipeline, an AFM indentation experiment, a dielectrophoretic trapping experiment, a mucus tracking experiment, and a plaque assay do not apply the same sequence of operations.

Remark 4.3 (Mechanism order is part of the model). The factorization in Eq. (4.1.2) is not a universal ordering of experimental reality. It is a model of a particular protocol. In cryo-EM, sample application, thin-film formation, air–water interface exposure, vitrification, particle orientation, particle picking, and reconstruction are coupled stages of one preparation-and-readout pipeline [3, 4, 5, 33, 34, 47]. In AFM, adsorption, hydration, probe geometry, indentation depth, loading rate, and deformation pathway are coupled during measurement [6, 7, 8, 9]. The correct factorization is therefore the one that matches the experimental sequence being modeled.

Remark 4.4 (Transformation, selection, and readout should not be conflated). A mechanism may enter the model in three different ways. It may transform the latent state, which belongs in Π_E^{lat} . It may alter whether a state produces a usable record, which belongs in s_E or the null channel \emptyset . Or it may alter how a surviving state is represented, which belongs in R_E . For example, surface contact may physically deform a virion, making it a latent transformation, while particle picking may reject low-contrast particles without changing them, making it a selection effect.

Table 12. Practical placement of common collapse mechanisms in the protocol formalism. The entries are schematic; a real protocol may distribute one mechanism across several mathematical objects.

Experimental question	Mathematical location	Interpretation
Did the protocol physically, chemically, mechanically, or biologically change the state?	Π_E^{lat}	Preparation, surface binding, field forcing, loading, confinement, medium interaction, cell contact, or assay-pathway conditioning changes the latent ensemble before readout.
Did the state survive or become detectable?	s_E, η_E, \emptyset	Only some protocol-conditioned states produce usable, visible, countable, trackable, reconstructable, or amplified records.
How is a surviving state represented as data?	R_E, \mathcal{O}_E	The readout projects, reconstructs, thresholds, localizes, classifies, counts, fits, or otherwise summarizes the surviving state.
What is lost by reporting only the data object?	Observation fibers or quotient classes	Many mechanically or biologically distinct states may map to the same observed image, track, spectrum, class, plaque count, or endpoint readout.

4.2 Preparation and Interface Collapse

Preparation collapse occurs when the sample-handling pipeline changes the population before the instrument or assay reports it. In structural virology, especially cryo-EM and cryo-ET, this may include dilution, buffer exchange, blotting, thin-film formation, air–water interface exposure, support-film interaction, vitrification, ice-thickness variation, beam sensitivity, particle picking, classification, and reconstruction. The preparation stage is therefore not a neutral prelude to measurement. It is part of the measurement map.

The simplest representation is

$$\boxed{X \xrightarrow{\Pi_E^{\text{prep}}} X_{\text{prep}}.} \quad (4.2.1)$$

The prepared state X_{prep} need not have the same distribution as the reference latent state X . It may be enriched for certain orientations, depleted of fragile states, altered by surfaces or interfaces, restricted to states that survive preparation, or reweighted by the criteria used for particle selection and reconstruction.

Definition 4.5 (Preparation/interface collapse). *Preparation/interface collapse* is the protocol-induced transformation or selection of latent states during sample preparation, surface or interface exposure, preservation, fixation, vitrification, staining, buffer exchange, or other pre-instrumental conditioning. It may be represented by a combination of

$$\Pi_E^{\text{prep}}, \quad \Pi_E^{\text{interface}}, \quad s_E, \quad R_E.$$

The precise placement depends on whether the mechanism transforms the state, selects which states survive, or changes how surviving states are represented.

In cryo-EM, a useful schematic factorization is

$$\Pi_E^{\text{prep}} = \Pi_E^{\text{vit}} \circ \Pi_E^{\text{AWI}} \circ \Pi_E^{\text{thinfilm}} \circ \Pi_E^{\text{grid}}, \quad (4.2.2)$$

where Π_E^{grid} represents interaction with the grid or support, Π_E^{thinfilm} represents formation of the thin aqueous layer, Π_E^{AWI} represents air–water interface exposure, and Π_E^{vit} represents vitrification. The order is schematic; in a real preparation, grid chemistry, thin-film formation, interface exposure, and vitrification are coupled.

Remark 4.6 (Cryo-EM as a concrete example). Cryo-EM is often discussed as a structure-preserving method, and in many cases it is extraordinarily successful. However, the ensemble that enters a reconstruction can be strongly conditioned by preparation. Air–water interface interactions can produce particle adsorption, denaturation, dissociation, preferred orientation, or uneven particle distribution; ice thickness can determine whether particles are visible; grid and support interactions can alter where particles localize; and particle picking can transmit only the subset satisfying contrast, shape, and reconstruction criteria [1, 3, 4, 5, 33, 34, 47]. In the language of experimental collapse, cryo-EM does not merely project a pre-existing ensemble into images. It can also create a preparation-conditioned structural ensemble before readout.

Remark 4.7 (Preparation collapse as an experimental variable). Preparation collapse is not only a nuisance. It can become an experimental variable. Changing grid type, support chemistry, blotting conditions, dispense-to-plunge time, surfactant, buffer composition, vitrification strategy, or particle-picking criteria changes the preparation kernel. If the observed ensemble changes under these variations, the change is evidence that the preparation stage is selecting or transforming latent states. This is why grid-preparation metadata should be treated as part of the protocol, not as peripheral documentation.

A simple orientation-selection model illustrates the point. Let $Q \in SO(3)$ denote particle orientation,

and let $w_E(Q) \geq 0$ be the preparation-and-selection weight for orientation Q . The compact idea is

Detected orientation density \propto Selection weight \times Reference orientation density.

In normalized form,

$$\boxed{p_{E,\text{det}}(Q) = \frac{w_E(Q) p_{\text{ref}}(Q)}{\int_{SO(3)} w_E(Q') p_{\text{ref}}(Q') dQ'}}. \quad (4.2.3)$$

If $w_E(Q)$ is nearly constant, the protocol approximately preserves the reference orientation distribution. If $w_E(Q)$ is sharply peaked, the protocol creates an orientation-collapsed ensemble. Preferred-orientation problems in single-particle cryo-EM are a concrete instance of this logic, and tilted data collection is one strategy for increasing the range of sampled views [48, 47].

Remark 4.8 (How to read the orientation-selection model). Equation (4.2.3) is not meant to capture all of cryo-EM preparation. It isolates one mechanism: state-dependent survival or representation of orientations. The same mathematical structure applies to other selection processes. A tracking protocol may overweight mobile particles. An AFM protocol may overweight particles that adhere stably to a surface. A plaque assay may overweight states that amplify efficiently in the chosen cell line. In each case, the observed distribution is a normalized, protocol-weighted version of a larger latent distribution.

Remark 4.9 (Laboratory interpretation). The practical implication is that preparation variables are model variables. If changing the grid, support film, plunge conditions, buffer, incubation time, surface chemistry, or selection threshold changes the reported ensemble, then the protocol has revealed a preparation-sensitive latent sector. The correct response is not simply to discard the observation as an artifact, but to ask which mechanism in the preparation kernel changed and what latent feature it was selecting, suppressing, or transforming.

4.3 Geometric Projection and Reconstruction Collapse

Geometric projection occurs when the reported object is a lower-dimensional, processed, reconstructed, or summarized representation of the latent state. This collapse channel is present whenever a three-dimensional, time-dependent, deformable, orientation-dependent, or internally heterogeneous state is reported as an image, density map, class average, trajectory, scalar coefficient, spectrum, endpoint readout, or count.

The simplest deterministic representation is

$$\boxed{Y_E = \mathcal{O}_E(X_E)}, \quad (4.3.1)$$

where $X_E \in \Psi_E$ is the protocol-conditioned latent state, $Y_E \in \mathcal{Y}_E$ is the reported non-null object, and $\mathcal{O}_E : \Psi_E \rightarrow \mathcal{Y}_E$ is the protocol-dependent observation map. The important point is that \mathcal{O}_E is usually not invertible. Many different protocol-conditioned latent states can produce the same observed datum.

Definition 4.10 (Geometric projection collapse). *Geometric projection collapse* occurs when the

readout map

$$\mathcal{O}_E : \Psi_E \rightarrow \mathcal{Y}_E$$

is non-injective, so that distinct protocol-conditioned latent states $x_E, x'_E \in \Psi_E$ satisfy

$$\mathcal{O}_E(x_E) = \mathcal{O}_E(x'_E)$$

and are therefore indistinguishable at the level of the reported datum. In kernel form, this non-invertible readout is represented by $R_E(dy | x_E)$, which may include noise, reconstruction, projection, classification, thresholding, or summarization.

The latent information compressed by a deterministic readout can be described by the observation fiber

$$\mathcal{F}_E(y_E) = \{x_E \in \Psi_E : \mathcal{O}_E(x_E) = y_E\}. \quad (4.3.2)$$

If $\mathcal{F}_E(y_E)$ contains mechanically, dynamically, structurally, or biologically distinct states, then the observation is under-resolved with respect to those latent directions.

Remark 4.11 (How to read the observation fiber). The fiber $\mathcal{F}_E(y_E)$ is the set of protocol-conditioned latent states that become indistinguishable after readout. If y_E is a two-dimensional projected track, the fiber may contain many unobserved three-dimensional paths, orientations, and binding histories. If y_E is a density map, the fiber may contain different preparation histories, conformational pathways, or dynamical trajectories that led to the same preserved structure. If y_E is a plaque count, the fiber contains many possible infection, replication, spread, and staining histories that produce the same counted outcome. The fiber is therefore the geometric version of protocol blindness.

Remark 4.12 (Stochastic reconstruction and posterior fibers). When the readout is stochastic, the exact fiber $\mathcal{F}_E(y_E)$ should be replaced by a conditional distribution over protocol-conditioned latent states given the observation. In that case, the relevant inverse object is

$$P_E(dx_E | y_E, \text{det}),$$

or an approximation to it. This posterior fiber describes which latent states remain compatible with the reported datum after accounting for the protocol kernel, readout noise, reconstruction algorithm, and selection rules.

Remark 4.13 (Reconstruction as a protocol-dependent inverse problem). Reconstruction does not simply return the latent state. It estimates a structured object from noisy, incomplete, selected, and processed data. In single-particle cryo-EM, the observed micrographs are noisy projections of particles with unknown orientations, and reconstruction depends on alignment, classification, orientation coverage, particle selection, and post-processing. In cryo-ET, a limited tilt range can produce missing-wedge effects and anisotropic resolution, so the reconstructed tomogram is not a complete sampling of all Fourier directions [48, 49]. In protocol-resolved language, reconstruction belongs to the readout kernel R_E , and its limitations are part of the experimental collapse rather than a separate afterthought.

Remark 4.14 (Laboratory use: diagnosing reconstruction-limited conclusions). The practical question is not only whether a reconstruction is high resolution, but which latent distinctions

the reconstruction can and cannot support. A density map may strongly constrain morphology while remaining weakly sensitive to transient dynamics, preparation history, rare conformational states, or orientation-dependent mechanical response. A protocol-resolved analysis asks whether an apparent structural absence reflects true absence in the latent ensemble, insufficient sampling of the relevant views, rejection during classification, or compression by the reconstruction pipeline.

Remark 4.15 (Examples of geometric projection). A cryo-EM class average may preserve characteristic views while suppressing particle-to-particle variability. A reconstructed density may preserve geometry while removing velocity, force history, preparation pathway, and short-lived conformational transitions. A single-particle tracking experiment may report two-dimensional projected positions while discarding body orientation, spike configuration, local binding state, deformation, and unresolved pauses. A plaque assay may compress an entire infection, replication, spread, and staining history into a single counted lesion. These are not failures of the methods. They are examples of protocol-specific projection.

Table 13. Examples of geometric projection and reconstruction collapse. The table identifies the observed object, the latent content it often preserves, and the latent content it commonly compresses or erases.

Protocol	Observed object	Often preserved	Often compressed
Cryo-EM / cryo-ET	Density map, class average, subtomogram average	Structural geometry, selected conformations, particle classes	Dynamics, force history, preparation pathway, rare states, missing orientations, anisotropic resolution
Single-virus tracking	Projected trajectory, MSD, transport-state classification	Position history, transport regimes, residence times	Orientation, deformation, spike state, local binding state, unresolved short events
AFM	Topography or force-indentation curve	Height, deformation response, rupture or stiffness signature	Free-suspension state, pre-contact trajectory, full unloaded 3D shape, orientation before adsorption
DEP / electrorotation	Field-driven trajectory, crossover frequency, rotation rate	Polarization response, trapping behavior, frequency dependence	Field-free Brownian dynamics, non-electrical latent variables, uncoupled mechanical sectors
Plaque assay	Plaque count or plaque-size distribution	Visible infectious amplification	Physical particle count, morphology, noninfectious states, failed infection histories, cell-line-incompatible particles

Remark 4.16 (Open-problem perspective). Several recurring experimental difficulties can be phrased as geometric projection problems. Preferred orientation in cryo-EM asks which orientations are absent or downweighted before reconstruction. Missing-wedge artifacts in cryo-ET ask which Fourier directions are under-sampled. Trajectory projection in tracking asks which three-dimensional, orientational, or binding-state variables are compressed into a two-dimensional path. Plaque counting asks which infection histories have been compressed into the same lesion count. In each case, the protocol-resolved remedy is similar: identify the fiber, estimate which latent variables vary within it, and add protocol variations that split the fiber into experimentally distinguishable subsets.

4.4 Medium Filtering and Adhesive Collapse

Many virological measurements occur in structured media rather than simple dilute buffers. Mucus, gels, droplets, extracellular matrix, tissue fluids, airway surface liquid, overlays, and cell-surface glycocalyxes can filter virions by size, shape, surface chemistry, adhesion, charge, receptor mimicry, enzymatic activity, antibody binding, and local rheology. In such cases, the medium is not merely background. It is part of the latent state and part of the protocol-conditioned observation map.

The simplest schematic is

$$\boxed{X \longrightarrow X_{\text{medium}}(\theta_{\text{env}})}, \quad (4.4.1)$$

where X is the reference latent state and X_{medium} is the state after interaction with a structured medium. The environmental parameter block θ_{env} may include mesh size, viscosity, viscoelastic relaxation time, mucin composition, binding-site density, antibody concentration, ionic strength, pH, local flow, hydration, or local biochemical composition.

Definition 4.17 (Medium-filtering collapse). *Medium-filtering collapse* is the state-dependent slowing, trapping, binding, exclusion, channeling, immobilization, or mobility-state switching of virions by a structured medium. It may be represented by a medium-dependent kernel

$$\Pi_E^{\text{medium}}(dx_{\text{medium}} \mid x; \theta_{\text{env}}),$$

where $x \in \Psi$ is the pre-medium latent state, $x_{\text{medium}} \in \Psi_{E,\text{medium}}$ is the medium-conditioned state, and θ_{env} parameterizes the local medium.

Remark 4.18 (The medium as a selector). A structured medium can act as a mechanical filter, an adhesive filter, and a biochemical filter at the same time. A particle may be mobile because it is small relative to the mesh, because its surface chemistry avoids adhesive binding, because enzymatic activity clears receptor-like obstacles, or because local rheology permits motion on the observation timescale. Conversely, a particle may be immobilized because it is sterically hindered, adhesively bound, cross-linked, trapped in a dense region, or too slow to be tracked within the chosen time window.

For a trajectory-level model, one may write the unfolded medium-conditioned motion schematically as

$$d\mathbf{r}_t = \mathbf{b}_E(\mathbf{r}_t, Q_t, M_t, \theta_{\text{env}}) dt + \sqrt{2} \mathbf{B}_E(\mathbf{r}_t, Q_t, M_t, \theta_{\text{env}}) d\mathbf{W}_t + d\mathbf{J}_t, \quad (4.4.2)$$

with

$$D_E(\mathbf{r}_t, Q_t, M_t, \theta_{\text{env}}) = \mathbf{B}_E \mathbf{B}_E^T. \quad (4.4.3)$$

Here \mathbf{b}_E is a drift field, D_E is an effective diffusion tensor, Q_t is orientation, M_t is a hidden mobility or binding state, and \mathbf{J}_t represents jumps, sticking events, release events, or transitions between mobility regimes.

Remark 4.19 (How to read the medium-filtered trajectory model). Equation (4.4.2) is not meant to impose one universal model of mucus or gel transport. It identifies where different mechanisms enter. Drift may represent flow, chemophysical bias, or directed transport. The tensor D_E represents local anisotropic or heterogeneous mobility. The hidden state M_t represents mobile, confined, adhesive, bound, or immobile modes. The jump term \mathbf{J}_t allows intermittent release, sticking, hopping, or sudden

changes in local environment. Thus a measured trajectory is a joint virion–medium process, not merely free diffusion with noise added.

Definition 4.20 (Mobility-state decomposition). A medium-filtered trajectory may be decomposed into latent mobility states

$$M_t \in \{\text{mobile, confined, adhesive, immobile, released}\}.$$

The observed trajectory is then a projection of the joint process

$$X_t = (\mathbf{r}_t, Q_t, M_t, X_{\text{env},t}) \quad (4.4.4)$$

onto reported positions, tracks, or trajectory summaries.

Remark 4.21 (Why hidden mobility states matter). A single reported diffusivity can hide multiple latent mobility states. A trajectory with intermittent pauses may be fit by an effective diffusion coefficient, but the pauses may correspond to adhesive binding, steric confinement, transient receptor-like interactions, antibody cross-linking, or local mesh heterogeneity. The medium-filtering formalism encourages reporting not only an effective diffusivity, but also the protocol assumptions that determine which mobility states can be distinguished.

Definition 4.22 (Medium-filtered observables). Typical medium-filtered observables include

$$h_{\text{med}}(Y_E) \in \{D_{\text{eff}}, \alpha_{\text{MSD}}, \tau_{\text{res}}, f_{\text{mobile}}, f_{\text{immobile}}, \ell_{\text{conf}}, k_{\text{bind}}, k_{\text{release}}\},$$

where D_{eff} is an effective diffusivity, α_{MSD} is an anomalous-transport exponent, τ_{res} is a residence time, f_{mobile} and f_{immobile} are mobile and immobile fractions, ℓ_{conf} is a confinement scale, and $k_{\text{bind}}, k_{\text{release}}$ are effective binding and release rates.

Remark 4.23 (Mucus tracking as a concrete example). Single-particle tracking in mucus reports a joint virion–medium process. Observed trajectories depend on virion size and surface chemistry, but also on mucus mesh structure, mucin binding, antibodies, adhesivity, hydration, and local rheology. HIV virion motion in cervical mucus and influenza motion in airway mucus illustrate this point: the trajectory ensemble is not simply a free-diffusion ensemble with noise added, but a medium-filtered ensemble whose immobilized, confined, and mobile subpopulations may carry biological meaning [14, 35, 15, 24, 23].

Remark 4.24 (Medium filtering as inverse environmental inference). Medium-filtered collapse can be useful precisely because the medium changes the trajectory. If the protocol kernel is modeled, trajectory data can be used to infer environmental quantities such as effective mesh scale, adhesive binding, local viscoelasticity, antibody-mediated immobilization, hydration, or flow. The risk is confounding: a slow trajectory may reflect a sticky virion, a dense medium, a local antibody interaction, low frame rate, poor localization, or a tracking threshold. Therefore medium inference is strongest when particle properties, medium properties, and protocol settings are varied or independently constrained.

Remark 4.25 (Laboratory use: separating virion and medium effects). Medium-filtering collapse gives a practical way to design more informative tracking experiments. One can vary virion surface chemistry, antibody concentration, mucin composition, ionic strength, hydration, or imaging cadence and ask which fitted quantities change: D_{eff} , α_{MSD} , f_{immobile} , residence times, or binding/release rates. If the same virion preparation changes behavior across media, the protocol has identified an environmental sector. If different virion preparations behave differently in the same medium, the protocol has identified a virion-surface or binding sector. If both change together, a joint virion–environment model is required.

Table 14. Medium-filtering mechanisms and their interpretation. A structured medium may transform the latent state, select the observed population, and alter the reported trajectory statistics simultaneously.

Medium mechanism	Possible mathematical location	Experimental interpretation
Steric hindrance	$\Pi_E^{\text{medium}}, D_E(\cdot)$	Mesh geometry slows or excludes particles depending on size, shape, orientation, and local density.
Adhesive binding	$\Pi_E^{\text{medium}}, \text{hidden state } M_t, s_E$	Particles switch between mobile, bound, confined, immobile, and released states.
Antibody or mucin immobilization	$\Pi_E^{\text{medium}}, s_E$	Binding or cross-linking can shift particles into confined or immobile subpopulations.
Local rheology	$D_E(\cdot), \mathbf{b}_E(\cdot), \text{memory terms}$	Viscosity and viscoelasticity determine effective diffusivity, residence time, confinement, and anomalous transport.
Flow or mucociliary clearance	$\mathbf{b}_E(\cdot), s_E$	Advection can bias trajectories and alter the probability that particles remain in the observation window.
Tracking threshold	R_E, s_E, \emptyset	Particles that are too slow, too dim, too fast, too intermittent, or too poorly localized may be excluded from the reported trajectory ensemble.

Remark 4.26 (Transition to time-window collapse). Medium filtering is closely linked to time-window collapse. A particle may be mobile on long timescales but appear immobile during a short observation, or it may undergo rare release events that are missed by the tracking window. Thus, the next collapse mechanism concerns persistence: which states last long enough, recur often enough, or amplify quickly enough to enter the reported dataset.

4.5 Time-Window and Persistence Collapse

Every protocol observes over a finite time window. Short-lived states may vanish before measurement begins. Rare transitions may not occur during acquisition. Slow relaxation may be mistaken for a

static state. Fast motion may blur, evade localization, or be excluded during analysis. Long incubation assays may amplify small initial differences into countable outcomes. Thus time is not merely the axis along which data are collected. It is a filtering mechanism.

The simplest schematic is

$$\boxed{\text{Latent time process} \longrightarrow \text{Sampled, averaged, or time-integrated record.}} \quad (4.5.1)$$

A time-dependent latent process may therefore appear static, averaged, missing, or amplified depending on the observation window, sampling cadence, exposure time, preparation delay, incubation time, and analysis rule.

Definition 4.27 (Time-window collapse). *Time-window collapse* is the state-dependent filtering produced by the observation interval, sampling cadence, exposure time, preparation delay, incubation time, or analysis window of the protocol. It is represented by a time-window kernel

$$\Pi_E^{\text{time}}(dx_{\text{time}} \mid x; t_0, t_1, \Delta t_{\text{samp}}, \tau_{\text{exp}}),$$

where t_0 and t_1 define the observation window, Δt_{samp} is the sampling interval when the record is discrete in time, and τ_{exp} is the exposure or integration time when individual measurements average over finite temporal intervals.

Let X_t be a latent stochastic process. A discrete-time observation model may be written as

$$Y_m = \mathcal{O}_E(X_{t_m}) + \nu_m, \quad t_m = t_0 + m\Delta t_{\text{samp}}, \quad m = 1, \dots, M. \quad (4.5.2)$$

When exposure or integration over a finite frame matters, a more realistic form is

$$Y_m = \frac{1}{\tau_{\text{exp}}} \int_{t_m}^{t_m + \tau_{\text{exp}}} \mathcal{O}_E(X_t) dt + \nu_m. \quad (4.5.3)$$

Equation (4.5.3) makes explicit that fast motion, short pauses, transient binding, and rapid conformational changes may be blurred or averaged within a single recorded datum.

If the relevant state persists for a lifetime τ_{state} , the degree of time-window visibility depends on dimensionless ratios such as

$$\boxed{\Pi_{\text{samp}} = \frac{\tau_{\text{state}}}{\Delta t_{\text{samp}}}, \quad \Pi_{\text{win}} = \frac{\tau_{\text{state}}}{t_1 - t_0}, \quad \Pi_{\text{exp}} = \frac{\tau_{\text{state}}}{\tau_{\text{exp}}}.} \quad (4.5.4)$$

When $\Pi_{\text{samp}} \ll 1$, the state is typically shorter-lived than the sampling interval and is likely to be missed or averaged over. When $\Pi_{\text{samp}} \gg 1$, the state persists across many samples and is more directly visible. When $\Pi_{\text{win}} \ll 1$, the state occupies only a small part of the observation window. When $\Pi_{\text{win}} \gg 1$, it may appear static over the experiment. When $\Pi_{\text{exp}} \ll 1$, the state is short compared with the exposure time and may be motion-blurred or integrated away.

Remark 4.28 (Sampling does not merely discretize time). Sampling changes what is inferable. A fast binding–release process may appear as a reduced effective diffusion coefficient. A short-lived

conformational state may disappear before vitrification. A rare transition may not occur during the recorded movie. A slow relaxation may be mistaken for a stable state. Thus sampling cadence, exposure time, and observation duration are protocol parameters, not only technical metadata.

Definition 4.29 (Persistence-biased detection). Let $A \subseteq \Psi$ be a latent state class, such as a bound state, mobile state, deformation state, conformational state, fusion intermediate, or infection stage. Define the persistence time

$$\tau_A = \text{Leb} \{t \in [t_0, t_1] : X_t \in A\},$$

the total time spent in A during the observation window. A protocol with minimum resolvable persistence τ_{\min} detects this state class with a weight of the schematic form

$$s_E^{\text{time}}(A) = \Pr(\tau_A \geq \tau_{\min} \mid E). \quad (4.5.5)$$

Remark 4.30 (Interpretation of persistence-biased detection). Persistence-biased detection means that long-lived states are easier to observe than short-lived states, even if the short-lived states are mechanistically important. This is relevant for transient binding, fusion intermediates, short pauses in tracking data, fragile structural states during preparation, rare orientation states, and early infection events that do not persist long enough to become visible under the chosen assay.

Definition 4.31 (Time-integrated readout). Some protocols report a time-integrated functional rather than a sequence of instantaneous observations. A general form is

$$Y_E = \int_{t_0}^{t_1} h_E(X_t) dt + \nu_E, \quad (4.5.6)$$

where h_E is a protocol-dependent contribution function and ν_E is measurement noise. Plaque counts, fluorescence accumulation, reporter signals, cytopathic-effect readouts, and endpoint assays often have this time-integrated character.

Remark 4.32 (Incubation time as a collapse mechanism). In biological amplification assays, incubation time determines which infection events become visible. A short incubation may miss slow-growing or weakly amplifying events. A long incubation may merge plaques, saturate a reporter signal, obscure early kinetic differences, or amplify initially small differences into large observed differences. Thus incubation time is part of the protocol kernel, not merely a scheduling choice.

Remark 4.33 (Cryo-EM preparation time as a concrete example). In cryo-EM preparation, the time between sample application and vitrification sets the interval during which particles can interact with the grid, support film, thin aqueous layer, and air–water interface. Studies varying grid-making or dispense-to-plunge times show that macromolecules can respond to the thin-film environment on experimentally relevant timescales, and that reducing this time can alter particle behavior but is not a universal solution for all specimens [34, 52, 47]. In the present language, preparation time changes the time-window kernel.

Remark 4.34 (Laboratory use: choosing the observation window). Time-window collapse

suggests a practical design rule: choose the sampling cadence and observation duration to match the latent event being tested. If the target is transient binding in mucus, the frame interval must be short enough to resolve pauses and release events. If the target is viscoelastic relaxation under AFM loading, the loading rate and dwell time must be treated as part of the mechanical protocol. If the target is slow plaque-forming competence, incubation time and readout threshold must be varied rather than assumed fixed. In each case, timing parameters can be used deliberately to separate fast, slow, persistent, and rare latent sectors.

Remark 4.35 (Examples of time-window collapse). In tracking experiments, fast binding–unbinding events may be averaged into an effective diffusion coefficient. In cryo-EM preparation, the interval between sample deposition and vitrification determines how long particles can interact with the air–water interface or support. In AFM, loading rate and dwell time determine whether a response appears elastic, viscoelastic, plastic, or destructive. In DEP and electrorotation, pulse duration, field frequency, and observation time determine which polarization and trapping responses are visible. In plaque assays, adsorption time, incubation time, and readout time determine which infectious events become visible plaques. Thus time is not only an acquisition coordinate. It is a selection mechanism.

Table 15. Time-window and persistence collapse in common virological protocols. Timing parameters determine which latent events are visible, averaged, amplified, saturated, or missed.

Protocol	Timing parameter	Latent events affected	Risk if ignored
Single-virus tracking	Frame interval, exposure time, trajectory length	Short pauses, binding–release events, directed intervals, confinement states	Fast states are collapsed into effective diffusion or missed entirely.
Cryo-EM / cryo-ET	Application-to-vitrification time, blotting time, plunge speed	Interface contact, orientation selection, dissociation, denaturation, thin-film response	The prepared ensemble is mistaken for the preparation ensemble.
AFM	Loading rate, dwell time, recovery time	Viscoelastic relaxation, rupture, plastic deformation, recovery	Rate-dependent response is treated as static stiffness.
DEP / electrorotation	Field frequency, pulse duration, observation time	Polarization relaxation, trapping, aggregation, field-induced loss	Driven response is mistaken for equilibrium or field-free behavior.
Plaque / focus assay	Adsorption time, incubation time, staining/readout time	Entry, replication, local spread, plaque visibility, plaque merging	Visible count is treated as protocol-independent infectivity.

Remark 4.36 (Transition to biological amplification). Time-window collapse leads naturally to biological amplification collapse. In plaque, focus-forming, endpoint dilution, cytopathic-effect, and reporter assays, the observed datum is not a direct microscopic state. It is the outcome of a time-extended biological pathway. The next subsection treats that pathway as a collapse mechanism in its own right.

4.5.1 Plaque, Focus, and Endpoint Assays as Biological Kernels

Plaque, focus-forming, endpoint dilution, reporter-cell, cytopathic-effect, and neutralization assays are biological observation kernels. They do not report the latent virion population directly. Instead, they place that population into a specified biological environment and report the subset of states that can pass through an assay-dependent sequence of delivery, attachment, entry, replication, spread, signal generation, visibility, and counting.

For a plaque assay, a schematic latent sequence is

$$\boxed{x \longrightarrow \text{Cell attachment} \longrightarrow \text{Entry} \longrightarrow \text{Replication} \longrightarrow \text{Local spread} \longrightarrow \text{Visible plaque} \longrightarrow \text{Count}.}$$
(4.5.1.1)

A physical virion that fails any required step contributes to the null channel for that assay, even if it is structurally intact. Thus the assay readout is not a direct particle census; it is a protocol-conditioned biological success measure.

Definition 4.37 (Plaque-forming probability). For a latent state x , define the plaque-forming probability

$$\boxed{\pi_{\text{PFU}}(x; E_{\text{PFU}}) = \Pr\left(\begin{array}{l} x \text{ generates a visible, countable plaque} \\ \text{under plaque-assay protocol } E_{\text{PFU}} \end{array}\right).}$$
(4.5.1.2)

This probability is a protocol-conditioned biological weight. It includes delivery, adsorption, entry, replication, local spread, plaque visibility, and counting under the specified plaque-assay protocol.

Remark 4.38 (Plaque assay as a concrete example). Plaque assays are often reported in plaque-forming units, but a plaque-forming unit is not the same object as a physical virion. It is a protocol-conditioned infectious event made visible by a cell monolayer, inoculation conditions, adsorption time, overlay medium, incubation time, staining procedure, and counting rule [16, 17, 18]. This makes the plaque assay one of the clearest examples of experimental collapse: the observed count is a selected and amplified functional projection of a larger latent population.

In the null-inclusive kernel language, the plaque assay may be written as a binary biological observation kernel:

$$K_{E_{\text{PFU}}}^{\emptyset}(\{\text{plaque}\} \mid x) = \pi_{\text{PFU}}(x; E_{\text{PFU}}), \quad K_{E_{\text{PFU}}}^{\emptyset}(\{\emptyset\} \mid x) = 1 - \pi_{\text{PFU}}(x; E_{\text{PFU}}).$$
(4.5.1.3)

The null outcome includes physical particles that fail delivery, fail attachment, fail entry, fail replication, fail local spread, fail visibility, or fail the counting rule. These null states are biologically different, but they are observationally identical unless additional protocol variation or auxiliary measurements separate them.

Focus-forming assays have a closely related structure, but the final visible event is typically an immunostained or reporter-detected focus rather than a macroscopic plaque. Endpoint dilution assays collapse the readout even further: instead of counting localized plaques or foci, they report whether infection, cytopathic effect, antigen expression, or reporter signal is detected at each dilution. An endpoint quantity such as TCID_{50} is then estimated from a binary infection/noninfection pattern across dilutions and replicate wells [53, 55].

Definition 4.39 (Biological readout spaces). Different biological amplification assays correspond to different observation spaces:

$$\mathcal{Y}_{\text{PFU}} = \{0, 1, 2, \dots\}, \quad \text{Plaque count}, \quad (4.5.1.4)$$

$$\mathcal{Y}_{\text{FFU}} = \{0, 1, 2, \dots\}, \quad \text{Focus count}, \quad (4.5.1.5)$$

$$\mathcal{Y}_{\text{ED}} = \{0, 1\}^{J \times R}, \quad \text{Endpoint-dilution infection/noninfection pattern}, \quad (4.5.1.6)$$

$$\mathcal{Y}_{\text{rep}} \subseteq \mathbb{R}, \quad \text{Reporter intensity or accumulated signal}. \quad (4.5.1.7)$$

Here J denotes the number of dilutions and R the number of replicate wells per dilution.

Remark 4.40 (Different biological assays report different projections). PFU, FFU, TCID₅₀, cytopathic-effect endpoints, and reporter signals are not interchangeable direct counts of physical virions. They are different protocol-conditioned projections of infectious activity. A virus that forms clear plaques under one overlay and cell line may produce foci, reporter signals, or endpoint responses under another. The appropriate comparison is not whether the raw assay numbers are identical, but whether they can be explained by a shared latent infectivity model passed through different biological kernels.

A compact way to compare biological kernels is to write an assay-specific success probability:

$$\pi_{\text{bio}}^{(a)}(x; E_a) = \Pr(\text{latent state } x \text{ produces assay signal } a \mid E_a), \quad (4.5.1.8)$$

where $a \in \{\text{PFU}, \text{FFU}, \text{ED}, \text{rep}, \text{CPE}\}$ labels the assay type. The same latent state x may have different success probabilities under different biological kernels:

$$\pi_{\text{PFU}}(x; E_{\text{PFU}}) \neq \pi_{\text{FFU}}(x; E_{\text{FFU}}) \neq \pi_{\text{ED}}(x; E_{\text{ED}}).$$

This is not inconsistency. It means that each assay asks a different biological question of the latent population.

Remark 4.41 (Laboratory interpretation). A discrepancy between PFU, FFU, reporter signal, and endpoint dilution need not mean that one assay is wrong. It may indicate that the assays are sensitive to different biological stages. A focus assay may detect infected cells before macroscopic plaques form. A reporter assay may detect intracellular expression without requiring the same spatial spread. An endpoint dilution assay may report whether infection occurred in a well without resolving how many local infection events occurred. Treating each assay as a biological kernel makes the disagreement interpretable rather than merely inconvenient.

4.5.2 Amplification, Thresholds, and Saturation

Biological amplification assays often include thresholds. A local infection may exist but remain below the staining threshold. A reporter signal may be produced but remain below detection. A plaque may form but be too small, too diffuse, or merged with another plaque to be counted. Conversely, strong amplification can drive a signal into saturation, making different high-infectivity histories appear similar. Thus biological amplification is coupled to detection selection.

Definition 4.42 (Biological visibility threshold). Let

$$A_E(x_{\text{bio}})$$

be a biological amplification signal, such as infected-cell number, local antigen amount, reporter intensity, cytopathic-effect score, plaque area, or focus area. A simple visibility rule is

$$s_E^{\text{bio}}(x_{\text{bio}}) = \mathbf{1}\{A_E(x_{\text{bio}}) \geq a_E^*\}, \quad (4.5.2.1)$$

where a_E^* is the assay-specific visibility or counting threshold. A soft threshold may instead use a smooth detection function

$$s_E^{\text{bio}}(x_{\text{bio}}) = \rho_E(A_E(x_{\text{bio}})), \quad 0 \leq \rho_E \leq 1. \quad (4.5.2.2)$$

Remark 4.43 (Thresholds are part of the protocol). Visibility thresholds are not minor analysis details. They determine which biological events enter the reported dataset. A focus-forming assay may detect infection earlier than a plaque assay because it does not require the same macroscopic lesion. A cytopathic-effect endpoint may ignore subvisible infection that does not cross the scoring threshold. A reporter assay may saturate at high signal. These threshold effects belong in s_E , R_E , or both.

Definition 4.44 (Amplification gain). Let $A_E(x_{\text{bio}}, t)$ be a biological signal generated by a latent state under protocol E . A schematic amplification gain over an incubation window $[t_0, t_1]$ is

$$G_E(x) = \frac{A_E(x_{\text{bio}}, t_1) + \epsilon_A}{A_E(x_{\text{bio}}, t_0) + \epsilon_A}, \quad \epsilon_A > 0. \quad (4.5.2.3)$$

Large G_E indicates that a small initial latent difference has been expanded into a large observable difference by replication, spread, reporter expression, antigen accumulation, or cytopathic amplification.

Remark 4.45 (Amplification can both reveal and hide). Amplification reveals rare biologically competent events by making them countable. At the same time, it hides many microscopic distinctions among events that cross the same threshold. Two infection histories may differ substantially in entry time, replication speed, local spread, plaque morphology, or reporter kinetics and still produce the same final count. Conversely, two initially similar states may produce very different observations after nonlinear amplification.

A useful schematic model is to treat the biological signal as a growing, saturating quantity:

$$\frac{dA_E}{dt} = g_E(A_E, x_{\text{bio}}, \theta_{\text{env}}, \theta_E), \quad Y_E = \rho_E(A_E(t_1)) + \nu_E. \quad (4.5.2.4)$$

Here g_E represents replication, spread, reporter production, antigen accumulation, or cytopathic progression, while ρ_E represents visibility, thresholding, or saturation. The same final signal can arise from different growth histories, and the same growth history can be reported differently under different thresholds.

Remark 4.46 (Laboratory use: separating growth from readout). When possible, measuring

multiple readout times can help separate growth from thresholding. A single endpoint signal may confound slow replication, delayed entry, low initial infectious competence, reporter threshold, and saturation. Time-course reporter data, multiple staining times, or plaque-size distributions can partially separate these effects by adding temporal or morphological structure to the biological kernel.

4.6 Detection, Rejection, and Null-Channel Collapse

Detection collapse occurs whenever the reported dataset includes only accepted, visible, reconstructable, localizable, countable, or biologically amplified states. It is represented by the survival/detection weight s_E , the detection yield $\eta_E(t)$, and the null observation \emptyset .

The simplest schematic is

$$\boxed{X_E \longrightarrow Y_E \text{ with probability } s_E(X_E), \quad X_E \longrightarrow \emptyset \text{ with probability } 1 - s_E(X_E).} \quad (4.6.1)$$

The null channel is the mathematical place where missing probability mass is kept.

Definition 4.47 (Detection-selection collapse). *Detection-selection collapse* is the state-dependent loss of probability mass from the non-null observed ensemble. It is quantified by

$$\boxed{s_E(x_E) \in [0, 1], \quad \eta_E(t) = \int_{\Psi_E} s_E(x_E) \tilde{P}_{E,t}^{\text{lat}}(dx_E).} \quad (4.6.2)$$

The missing probability $1 - \eta_E(t)$ is assigned to the null channel \emptyset .

Remark 4.48 (Why the null channel is mechanistic). The null channel is not merely a bookkeeping device. It is mechanistic. A particle may be null because it was destroyed during preparation, adsorbed in an unusable orientation, too dim to localize, too fast to track, too deformed to reconstruct, unable to infect the chosen cell type, unable to activate a reporter, unable to form a visible plaque, or rejected by a computational criterion. These are different physical and biological mechanisms, even if they produce the same observed outcome: no reported datum.

Definition 4.49 (Null-channel decomposition). When mechanisms can be distinguished, the null probability may be decomposed schematically as

$$1 - \eta_E(t) = p_{\text{loss}} + p_{\text{damage}} + p_{\text{reject}} + p_{\text{below}} + p_{\text{biofail}} + p_{\text{other}}, \quad (4.6.3)$$

where the terms represent loss during preparation, damage or inactivation, computational or instrumental rejection, below-threshold signal, biological failure, and other null mechanisms. In a rigorous model these terms should be defined as probabilities of disjoint null categories or replaced by a categorical null variable.

A more explicit version introduces a categorical null label

$$Z_{\emptyset} \in \{\text{loss, damage, reject, below, biofail, other}\}.$$

Then

$$P_{\text{obs},t}^{\emptyset}(\{\emptyset, Z_{\emptyset} = z\} | E) = \int_{\Psi_E} p_E(z | x_E, \emptyset) [1 - s_E(x_E)] \tilde{P}_{E,t}^{\text{lat}}(dx_E), \quad (4.6.4)$$

whenever the experiment or model can justify assigning null outcomes to mechanistic categories.

Remark 4.50 (Null categories should not be invented without evidence). The decomposition in Eq. (4.6.3) is useful only when the experiment can distinguish null mechanisms or when a justified model is being used. Otherwise, the safe statement is that probability mass entered the null channel. Assigning that mass to damage, rejection, failed infection, or below-threshold signal requires additional evidence.

Remark 4.51 (Why normalized datasets can mislead). A dataset conditioned on detection can look clean even when most of the latent population was lost. For example, a cryo-EM reconstruction may be high quality after extensive particle rejection; a tracking analysis may report smooth trajectories after excluding short or dim tracks; a plaque assay may produce countable plaques while ignoring non-plaque-forming particles. The normalized observed distribution is therefore incomplete without the detection yield and, when possible, the null-channel structure.

Remark 4.52 (Laboratory use: recording denominators). The practical recommendation is to record denominators whenever possible: particles imaged versus particles picked, picked particles versus particles retained after classification, attempted tracks versus accepted tracks, wells inoculated versus wells positive, plaques counted versus wells excluded, and reporter-positive versus reporter-negative events. These denominators estimate parts of the null channel. Without them, the experiment reports only the conditional distribution of successful observations.

4.6.1 Stage-Resolved Biological Amplification as a Protocol Design Tool

The biological-kernel formulation suggests a practical way to use amplification assays more diagnostically. Instead of treating a plaque count, focus count, endpoint readout, or reporter signal as a single scalar measure of “infectivity,” one can vary controlled components of the assay and ask which stage of the biological pathway is most responsible for the observed change. In this sense, biological amplification assays can be used not only to quantify infectious activity, but also to probe where the latent population is being filtered by the assay.

Let the biological pathway be written as

$$A_0, A_1, \dots, A_K,$$

where the stages may represent delivery to the assay environment, adsorption, cell attachment, entry, genome release, replication, local spread, reporter activation, staining, visibility, and counting. The assay-success probability has the conditional factorization

$$\pi_{\text{bio}}(x; E) = \Pr(A_0 | x, E) \prod_{k=1}^K \Pr(A_k | A_0, \dots, A_{k-1}, x, E). \quad (4.6.1.1)$$

The protocol E determines every factor in this product. Changing the cell line, adsorption time, inoculum volume, overlay, incubation time, staining method, reporter threshold, or counting rule

changes the biological kernel and therefore changes which latent states enter the visible assay channel.

Definition 4.53 (Stage-resolved biological protocol family). A *stage-resolved biological protocol family* is a collection of related assay protocols

$$\mathcal{E}_{\text{bio}} = \{E^{(1)}, E^{(2)}, \dots, E^{(M)}\},$$

constructed by varying one or more biological-assay parameters while holding the remaining conditions fixed when possible. Examples include variation of cell line, receptor availability, adsorption time, neutralization condition, overlay composition, incubation time, staining threshold, reporter readout, or counting criterion.

For each protocol $E^{(m)}$, the biological kernel induces a success probability

$$\pi_{\text{bio}}(x; E^{(m)}).$$

The corresponding effective biological signal is

$$\Lambda_{\text{bio}}(E^{(m)}) = \int_{\Psi} \pi_{\text{bio}}(x; E^{(m)}) n_{\text{ref}}(x) dx, \quad (4.6.1.2)$$

where $n_{\text{ref}}(x)$ is the latent number-density distribution over virion or virion–assay-relevant states. For plaque assays, Λ_{bio} reduces to an effective plaque-forming concentration; for focus assays it becomes an effective focus-forming concentration; for endpoint assays it controls the dilution-dependent probability of detecting infection.

Remark 4.54 (Assay variation as kernel perturbation). Controlled assay variation should be interpreted as a perturbation of the biological observation kernel. Varying adsorption time primarily perturbs delivery, attachment, and entry factors. Varying cell line perturbs receptor availability, entry compatibility, intracellular permissiveness, and local spread. Varying overlay composition perturbs diffusion, cell-to-cell spread, lesion morphology, and plaque coalescence. Varying incubation time perturbs replication, spread, visibility, and saturation. Varying staining or reporter threshold perturbs the final readout. Thus, each assay variation asks a different question of the same latent virion population.

Definition 4.55 (Stage-sensitivity index). Let ξ_r be a controllable assay parameter, such as adsorption time, overlay viscosity, antibody concentration, incubation time, reporter threshold, or cell-line condition. The local stage-sensitivity of the effective biological signal to ξ_r may be defined as

$$S_r(E) = \frac{\partial}{\partial \xi_r} \log [\Lambda_{\text{bio}}(E; \xi_r) + \epsilon_{\Lambda}], \quad \epsilon_{\Lambda} > 0. \quad (4.6.1.3)$$

Large $|S_r(E)|$ indicates that the reported biological signal is sensitive to the assay stage controlled by ξ_r .

Remark 4.56 (Interpretation of stage sensitivity). The stage-sensitivity index is not meant to replace detailed mechanistic modeling. It is a compact diagnostic. If the signal changes strongly with

adsorption time, the assay may be limited by delivery, attachment, entry, or early cell interaction. If it changes strongly with overlay conditions, local spread or plaque morphology may be limiting. If it changes strongly with incubation time, growth rate, delayed replication, visibility, or saturation may dominate. If it changes strongly with staining threshold, the final readout rather than the biological infection process may be the limiting factor.

Definition 4.57 (Biological bottleneck decomposition). A biological amplification assay is *bottlenecked* at stage A_k if the conditional factor

$$\Pr(A_k \mid A_0, \dots, A_{k-1}, x, E)$$

is small, highly variable across latent states, or strongly sensitive to a protocol parameter. A schematic bottleneck score for stage A_k is

$$\mathcal{B}_k(E) = 1 - \int_{\Psi} \Pr(A_k \mid A_0, \dots, A_{k-1}, x, E) P_{\text{ref},t}(dx), \quad (4.6.1.4)$$

with larger values indicating stronger average loss at that stage.

Remark 4.58 (Bottlenecks and latent heterogeneity). A high bottleneck score may reflect a genuine biological limitation, a protocol limitation, or both. For example, weak plaque formation may reflect low infectious competence in the latent virion population, poor compatibility with the chosen cell line, overly restrictive overlay conditions, insufficient incubation time, or a stringent visibility threshold. The bottleneck decomposition therefore helps convert a low PFU, FFU, or endpoint readout into a structured hypothesis about where the assay is filtering the latent population.

Table 16. Stage-resolved perturbations of biological amplification assays. Each protocol variation changes a different component of the biological kernel and can therefore help identify which assay stage limits the observed signal.

Protocol variation	Biological stage primarily probed	Interpretation in the collapse framework
Adsorption time	Delivery, attachment, entry initiation	Tests whether the assay is limited by early contact with the cell layer or by insufficient time for productive adsorption.
Cell line or receptor condition	Receptor binding, entry compatibility, intracellular permissiveness	Separates intrinsic virion competence from host-cell compatibility and cell-line-specific amplification.
Neutralization or antibody condition	Attachment, entry, aggregation, immobilization, immune blocking	Determines whether the latent population is being shifted into a non-amplifying or null biological channel.
Overlay composition	Local spread, lesion morphology, plaque separation	Tests whether visible plaque formation is limited by diffusion, cell-to-cell spread, medium restriction, or plaque coalescence.
Incubation time	Replication, spread, signal growth, visibility	Distinguishes early failure from delayed amplification, slow growth, plaque merging, reporter saturation, or late visibility.
Staining or reporter threshold	Visibility, classification, counting	Tests whether events occur biologically but fail to cross the accepted readout threshold.
Dilution series and replicate wells	Count statistics, endpoint probability, dynamic range	Improves precision and reveals saturation, overlap, zero-inflation, or dilution-dependent deviations from the assumed count model.

Remark 4.59 (Application to difficult assay interpretation). The stage-resolved view is useful in common ambiguous cases. A high particle count with low PFU may indicate many defective particles, but it may also indicate poor cell-line compatibility, neutralization, aggregation, loss during adsorption, restrictive overlay conditions, or an overly stringent readout. A low focus count may reflect weak entry, weak antigen expression, or thresholding. A positive endpoint dilution pattern with few visible plaques may indicate infection without efficient local spread. These distinctions are lost if the assay is summarized only as a single infectious titer.

Definition 4.60 (Cross-assay biological consistency). Let E_{PFU} , E_{FFU} , and E_{ED} denote plaque, focus-forming, and endpoint-dilution protocols. A latent infectivity model is *cross-assay biologically*

consistent if there exists a common latent distribution $P_{\text{ref},t}(\cdot | \theta)$ and assay-specific biological kernels such that

$$P_{\text{obs}}^{\varnothing}(\cdot | E_j, \theta, \lambda_j) = \mathcal{M}_{E_j}^{\text{bio},\varnothing}(\lambda_j)P_{\text{ref},t}(\cdot | \theta), \quad E_j \in \{E_{\text{PFU}}, E_{\text{FFU}}, E_{\text{ED}}\}. \quad (4.6.1.5)$$

Remark 4.61 (Why cross-assay consistency matters). PFU, FFU, endpoint dilution, reporter intensity, and cytopathic-effect readouts may disagree numerically while still being compatible with a shared latent infectivity model. Conversely, apparent agreement can be misleading if the assays share the same blind sector or threshold. Cross-assay consistency therefore asks a stronger and more useful question than whether titers match: it asks whether distinct biological kernels can explain the observed assay outputs from the same latent population.

4.6.2 Count Statistics, Spatial Interaction, and Assay-Level Nonidealities

The biological-kernel framework also clarifies why infectious-unit assays often deviate from ideal count models. In the dilute, well-mixed, independent-event limit, plaque and focus counts are often modeled as Poisson random variables. However, this limit is itself a protocol regime. Aggregation, local cell-layer heterogeneity, clustered infection, variable adsorption efficiency, uneven overlay conditions, plaque merging, and well-to-well variation can all move the assay away from Poisson behavior.

The simplest ideal count model is

$$\boxed{N_d | \Lambda_{\text{bio}} \sim \text{Poisson}(V_{\text{inoc}} f_d \Lambda_{\text{bio}}(E))}, \quad (4.6.2.1)$$

where N_d is the observed plaque or focus count at dilution fraction f_d , V_{inoc} is the inoculum volume, and $\Lambda_{\text{bio}}(E)$ is the effective protocol-conditioned biological signal concentration. For a plaque assay, Λ_{bio} may be identified with an effective plaque-forming concentration; for a focus assay, it may be identified with an effective focus-forming concentration.

Remark 4.62 (The Poisson model is a protocol regime). The Poisson model assumes that visible biological events arise independently, that the inoculum is well mixed, that plaques or foci do not strongly overlap, that local cell susceptibility is approximately homogeneous, and that each counted event is generated by an independent assay-success pathway. These are not merely statistical assumptions. They are statements about the biological and spatial regime of the assay.

Overdispersion. Observed plaque or focus counts may have variance larger than the Poisson mean. This overdispersion can arise from virion aggregation, spatial clustering, heterogeneous cell susceptibility, variation in local overlay thickness, well-to-well differences, batch effects, or stochastic differences in adsorption and spread. A common phenomenological replacement is the negative-binomial model:

$$\boxed{N_d \sim \text{NegBin}(\mu_d, \kappa), \quad \mu_d = V_{\text{inoc}} f_d \Lambda_{\text{bio}}(E)}, \quad (4.6.2.2)$$

with variance

$$\text{Var}(N_d) = \mu_d + \frac{\mu_d^2}{\kappa}. \quad (4.6.2.3)$$

Here $\kappa > 0$ is an overdispersion parameter. In the limit $\kappa \rightarrow \infty$, the model approaches the Poisson variance $\text{Var}(N_d) = \mu_d$.

Remark 4.63 (Interpretation of overdispersion). Overdispersion is not merely a statistical inconvenience. It is evidence that the assay may contain unmodeled heterogeneity. For example, a high variance across wells may indicate variable delivery to the monolayer, local differences in cell susceptibility, clustered infection due to aggregates, or heterogeneous amplification after entry. In the protocol-kernel language, overdispersion suggests that $\Lambda_{\text{bio}}(E)$ is not fixed across replicates, but varies with latent well-level, local environmental, or protocol-specific factors.

A hierarchical way to express this is

$$N_{dr} \mid \Lambda_r \sim \text{Poisson}(V_{\text{inoc}} f_d \Lambda_r), \quad \Lambda_r \sim G_E, \quad (4.6.2.4)$$

where r indexes replicate wells and G_E describes replicate-to-replicate variation in the effective biological signal. A gamma choice for G_E yields a negative-binomial marginal distribution. Other choices may be appropriate when the dominant heterogeneity is aggregation, spatial clustering, or cell-layer structure.

Zero inflation and null-enriched assays. Some datasets contain more zero-count wells than expected under a Poisson or negative-binomial model. This may occur when a fraction of wells receive no effective infectious units, when delivery fails, when adsorption is inefficient, when neutralization is strong, when the cell layer is locally nonpermissive, or when the biological signal remains below threshold. A zero-inflated model writes

$$N_d \sim \begin{cases} 0, & \text{with probability } \zeta_E, \\ \text{Poisson}(\mu_d), & \text{with probability } 1 - \zeta_E, \end{cases} \quad (4.6.2.5)$$

or, more explicitly,

$$\Pr(N_d = 0) = \zeta_E + (1 - \zeta_E)e^{-\mu_d}, \quad \Pr(N_d = n) = (1 - \zeta_E)e^{-\mu_d} \frac{\mu_d^n}{n!}, \quad n \geq 1. \quad (4.6.2.6)$$

The parameter ζ_E represents a protocol-conditioned structural-zero probability: the probability that a well, field, or assay unit is effectively unable to produce a visible biological signal.

Remark 4.64 (Zero inflation as null-channel enrichment). Zero inflation is the count-level expression of null-channel enrichment. A zero plaque count may mean that no infectious units were present, but it may also mean that the relevant latent states failed delivery, attachment, entry, replication, spread, visibility, or counting. The zero-inflated parameter ζ_E should therefore be interpreted as a protocol-conditioned null probability, not automatically as absence of virions.

Spatial interaction and plaque merging. Plaque and focus assays also have a spatial component. At low density and short enough incubation, visible lesions may be approximately independent. At higher inoculum, longer incubation, or weaker overlay restriction, lesions may overlap, merge, compete for susceptible cells, or become difficult to segment. The “countable range” is therefore a spatial

protocol regime, not only a convenient laboratory rule.

Let

$$\Phi_E = \{z_1, \dots, z_N\} \subset \Omega_{\text{well}}$$

denote the spatial point pattern of visible plaques or foci in the well or imaging region Ω_{well} . A first idealization is an inhomogeneous Poisson point process with intensity

$$\lambda_E(z) = \lambda_E(z \mid \theta_{\text{vir}}, \theta_{\text{env}}, \theta_E),$$

so that

$$\mathbb{E}[N] = \int_{\Omega_{\text{well}}} \lambda_E(z) dz. \quad (4.6.2.7)$$

Spatial heterogeneity in $\lambda_E(z)$ can represent nonuniform cell susceptibility, uneven inoculum distribution, local overlay variation, edge effects, or spatial variation in staining or imaging.

Plaque merging can be represented by a detection or segmentation map

$$\mathcal{S}_E : \Phi_E^{\text{true}} \longrightarrow \Phi_E^{\text{obs}},$$

where Φ_E^{true} is the latent pattern of biological lesions and Φ_E^{obs} is the observed pattern after overlap, merging, thresholding, and segmentation. In count form,

$$N_{\text{obs}} = \# \mathcal{S}_E(\Phi_E^{\text{true}}) \leq \# \Phi_E^{\text{true}}, \quad (4.6.2.8)$$

when merging or segmentation failure combines multiple biological events into a single visible lesion.

Remark 4.65 (Countable range as a protocol condition). The usual countable range for plaques or foci can be interpreted as the regime in which \mathcal{S}_E is close to one-to-one and the spatial process is approximately noninteracting. Outside this regime, the observed count is not only a noisy version of the latent lesion number. It is a spatially collapsed readout affected by lesion growth, overlap, local depletion of susceptible cells, staining threshold, and segmentation.

Endpoint dilution as censored biological observation. Endpoint dilution assays, including TCID₅₀-type readouts, do not directly count individual infectious lesions. They report binary or categorical outcomes across dilutions and replicate wells. The observation at dilution j and replicate r may be written as

$$Z_{jr} \in \{0, 1\},$$

where $Z_{jr} = 1$ indicates detectable infection, cytopathic effect, reporter signal, or another endpoint criterion.

A simple endpoint model is

$$\Pr(Z_{jr} = 1 \mid \theta, E) = 1 - \exp[-V_{\text{inoc}} f_j \Lambda_{\text{ED}}(E, \theta)], \quad (4.6.2.9)$$

where Λ_{ED} is the effective concentration of units capable of producing a positive endpoint under the endpoint-dilution protocol. This is not a plaque count. It is a thresholded detection probability.

More generally, if A_{jr} is a latent biological signal in well jr , then

$$Z_{jr} = \mathbf{1}\{A_{jr} \geq a_E^*\}, \quad (4.6.2.10)$$

where a_E^* is the endpoint scoring threshold. The observed dilution pattern

$$\mathcal{D}_{\text{ED}} = \{Z_{jr} : j = 1, \dots, J, r = 1, \dots, R\}$$

is therefore a censored or thresholded representation of a latent biological amplification process.

Remark 4.66 (Endpoint assays as censored kernels). Endpoint dilution assays collapse quantitative biological histories into binary or categorical outcomes. A well scored positive may contain very different amounts of replication, cytopathic effect, or reporter signal; a well scored negative may contain no infection, failed infection, or subthreshold infection. Endpoint assays are therefore naturally represented as censored biological kernels rather than as direct counts of infectious particles.

Neutralization as biological-kernel deformation. Neutralization assays can be described as deformations of the biological kernel. Antibodies, inhibitors, serum components, or other neutralizing agents may reduce the probability of attachment, entry, fusion, replication, local spread, or readout visibility. If c denotes neutralizing-agent concentration, then the stage-resolved success probability becomes

$$\pi_{\text{bio}}(x; E, c) = \Pr(A_0 \mid x, E, c) \prod_{k=1}^K \Pr(A_k \mid A_0, \dots, A_{k-1}, x, E, c). \quad (4.6.2.11)$$

The neutralizing condition shifts latent states toward the null biological channel by reducing one or more stage probabilities.

A compact neutralization curve can be written as

$$F_{\text{neutral}}(c) = 1 - \frac{\Lambda_{\text{bio}}(E, c)}{\Lambda_{\text{bio}}(E, 0) + \epsilon_\Lambda}, \quad \epsilon_\Lambda > 0, \quad (4.6.2.12)$$

where

$$\Lambda_{\text{bio}}(E, c) = \int_{\Psi} \pi_{\text{bio}}(x; E, c) n_{\text{ref}}(x) dx.$$

This form emphasizes that neutralization is not merely a change in the observed count. It is a protocol-conditioned deformation of the biological pathway.

Remark 4.67 (Interpreting neutralization mechanisms). A reduction in PFU, FFU, endpoint positivity, or reporter signal can arise from different neutralization mechanisms. The agent may prevent attachment, block fusion or entry, aggregate particles, promote immobilization, reduce replication, alter spread, or change readout visibility. These mechanisms can produce similar dose–response curves at the level of final signal. A stage-resolved kernel helps identify which biological step is being deformed.

Plaque morphology as additional information. A plaque assay need not be reduced to a scalar count. Plaque size, shape, opacity, boundary sharpness, time-to-visibility, and growth rate can carry information about replication kinetics, local spread, cell-layer susceptibility, overlay restriction,

cytopathic effect, and immune or inhibitor-mediated restriction. Let

$$M_i = (A_i, R_i, S_i, T_i, \chi_i, \dots)$$

denote a morphology vector for plaque i , where A_i is area, R_i is an effective radius, S_i is a shape or circularity descriptor, T_i is time-to-visibility, and χ_i represents intensity, opacity, or edge structure. The enriched plaque readout is then

$$Y_{\text{PFU}}^{\text{morph}} = (N, M_1, \dots, M_N), \quad (4.6.2.13)$$

rather than $Y_{\text{PFU}} = N$ alone.

Remark 4.68 (Why plaque morphology matters). Plaque morphology can partially split the fiber associated with a scalar PFU count. Two wells with the same plaque count may have different plaque-size distributions, growth rates, edge structures, or time-to-visibility. These differences can contain information about local spread, replication kinetics, cell susceptibility, overlay restriction, or inhibitory effects. Thus plaque morphology can turn a scalar biological amplification readout into a richer protocol-conditioned observation.

Definition 4.69 (Morphology-augmented biological kernel). A morphology-augmented biological kernel maps a latent state x not only to a binary success or null outcome, but to a distribution over lesion morphologies:

$$K_E^{\text{morph}, \emptyset}(dN, dM_1, \dots, dM_N \mid x). \quad (4.6.2.14)$$

This kernel contains more information than the count-only projection whenever morphology depends on latent replication, spread, cell-layer, overlay, or inhibitor parameters.

Remark 4.70 (Summary of statistical nonidealities). The ideal PFU or FFU model is useful because it provides a clean baseline. The protocol-resolved framework does not discard that baseline; it states its assumptions. Overdispersion, zero inflation, spatial interaction, endpoint censoring, neutralization, and morphology are not merely complications. They are additional protocol-conditioned signals that can reveal aggregation, heterogeneous cell susceptibility, environmental restriction, biological bottlenecks, or latent subpopulations when modeled explicitly.

4.7 Mechanism-Level Identifiability and Fisher-Information Observability

The collapse mechanisms described above are not only qualitative descriptions of experimental bias. They determine which latent parameters are identifiable under a protocol. A parameter may be real in the latent virion–environment model and still be invisible under a particular readout. Conversely, a parameter may become identifiable only when the protocol intentionally drives, pins, selects, amplifies, perturbs, or otherwise couples to the relevant latent sector.

Thus identifiability is not a property of a latent parameter alone. It is a property of the latent model after composition with the protocol observation operator:

$$\boxed{\text{Identifiability under } E \text{ is a property of } \mathcal{M}_E^{\emptyset} P_{\text{ref},t}(\cdot \mid \theta)}. \quad (4.7.1)$$

Equivalently, the relevant object is not the latent ensemble by itself, but the protocol-conditioned observed law

$$P_{\text{obs},t}^{\varnothing}(\cdot | E, \theta) = \mathcal{M}_E^{\varnothing} P_{\text{ref},t}(\cdot | \theta).$$

This is the law that determines which parameter directions can be estimated, which are weakly constrained, and which are collapsed into protocol-blind directions.

This distinction matters because the same latent parameter can be strongly visible in one protocol and nearly invisible in another. A static geometry-only readout may be insensitive to a hidden orientational, dynamical, or presentation-state sector. A surface-bound AFM protocol may be sensitive to surface-conditioned stiffness but weakly sensitive to free rotational diffusion. A dielectrophoretic or electrorotation protocol may be sensitive to polarizability, charge asymmetry, and hydrodynamic drag, but not to the same morphological statistics that dominate cryo-EM. A mucus-tracking protocol may be sensitive to adhesive transport, confinement, residence time, and mobile versus immobile fractions, while remaining blind to full body orientation or spike presentation. A plaque assay may be sensitive to assay-conditioned infectious activity while remaining largely blind to noninfectious physical particles [3, 4, 8, 9, 11, 12, 14, 15, 18].

4.7.1 Identifiability after mechanism-resolved collapse

Let

$$\theta = (\theta_{\text{vir}}, \theta_{\text{env}}, \theta_E) \in \Theta$$

be the protocol-resolved parameter vector. Here θ_{vir} contains virion parameters, θ_{env} contains environmental parameters, and θ_E contains protocol parameters. A mechanism-resolved protocol may make one block more visible while confounding or suppressing another. For this reason, identifiability should always be stated relative to the protocol kernel, the nuisance-parameter treatment, and the experimental regime.

Let

$$\theta = (\theta_a, \lambda),$$

where θ_a is the target parameter block and λ contains nuisance parameters. The nuisance block may include environmental variables, protocol settings, calibration constants, selection thresholds, noise parameters, batch effects, reconstruction settings, staining thresholds, cell-line conditions, or other quantities that affect the observed law but are not the main target of inference.

A compact statement of protocol identifiability is:

$$\boxed{P_{\text{obs},t}^{\varnothing}(\cdot | E, \theta_a, \lambda) = P_{\text{obs},t}^{\varnothing}(\cdot | E, \theta'_a, \lambda') \implies \theta_a = \theta'_a} \quad (4.7.1.1)$$

for all admissible nuisance values λ, λ' . This is the profiled nuisance version: it asks whether a change in the target parameter can be mimicked by changing environmental, protocol, calibration, or readout parameters.

Remark 4.71 (Why the nuisance treatment must be stated). A parameter can appear identifiable when nuisance variables are artificially fixed, but become non-identifiable when those nuisance variables are allowed to vary. An AFM stiffness estimate may be confounded by tip geometry, indentation depth, surface adhesion, or hydration state. A DEP response may be confounded by

medium conductivity, permittivity, viscosity, and field calibration. A mucus-transport parameter may be confounded by local mesh heterogeneity, adhesive binding, antibody cross-linking, or tracking threshold. A plaque count may be confounded by cell-line susceptibility, adsorption time, overlay composition, incubation time, staining threshold, and counting rule. Protocol identifiability is therefore always a statement about a target parameter together with a nuisance-parameter model.

Remark 4.72 (Structural versus practical identifiability). Structural identifiability asks whether a parameter could be recovered in principle from ideal, unlimited data generated by the specified protocol model. Practical identifiability asks whether it can be estimated with useful precision from finite, noisy data under realistic conditions [30, 31, 32]. This distinction is especially important in virophysics because rare conformations, weakly populated orientations, transient binding events, low-yield infectious events, and small mechanically active subpopulations may be structurally present while remaining practically difficult to estimate.

Definition 4.73 (Mechanism-level protocol equivalence class). For a fixed protocol E , define the observational equivalence class of θ by

$$[\theta]_E = \left\{ \theta' \in \Theta : P_{\text{obs},t}^\varnothing(\cdot | E, \theta') = P_{\text{obs},t}^\varnothing(\cdot | E, \theta) \right\}. \quad (4.7.1.2)$$

If $[\theta]_E$ contains more than one parameter point, then protocol E cannot distinguish those latent hypotheses, even in the infinite-data limit.

Remark 4.74 (Protocol blindness as equivalence). The equivalence class $[\theta]_E$ is the parameter-space version of protocol blindness. Distinct latent explanations may be observationally equivalent because the protocol projects away the relevant distinction, because selection weights erase it, because a nuisance parameter compensates for it, or because the readout does not couple to that sector. Failure to observe a latent feature under one protocol should therefore be interpreted as protocol-limited visibility, not automatically as mechanical or biological absence.

4.7.2 Observable sensitivity as a mechanism diagnostic

Before using the full likelihood, it is often useful to inspect the sensitivity of reported observables to model parameters. This is a lower-dimensional, observable-level diagnostic. It is not a substitute for the likelihood, but it helps identify which experimental summaries respond to which latent sectors.

Let

$$\mathbf{h}_E : \mathcal{Y}_E \rightarrow \mathbb{R}^M$$

be a vector of reported observables, such as apparent radius, height, orientation-class frequency, indentation stiffness, rupture force, effective diffusivity, residence time, trapping probability, rotation rate, plaque count, focus count, plaque area, or time-to-visibility. Define the protocol-conditioned expectation vector

$$\mathbf{H}_E(\theta) = \mathbb{E}_{\theta,E} [\mathbf{h}_E(Y_E) | \det]. \quad (4.7.2.1)$$

Definition 4.75 (Protocol sensitivity matrix). The *protocol sensitivity matrix* is

$$\mathbf{S}_E(\theta) = \frac{\partial \mathbf{H}_E}{\partial \theta} = \left[\frac{\partial H_{E,\mu}}{\partial \theta_a} \right]_{\mu a}. \quad (4.7.2.2)$$

Remark 4.76 (Reading the sensitivity matrix). The column indexed by θ_a indicates which reported observables respond to that parameter. A nearly zero column means that the parameter is weakly visible under the chosen protocol and observable set. Strongly correlated columns indicate degeneracy: two different latent mechanisms produce similar changes in the reported summaries. For example, a decrease in observed mucus mobility may be produced by stronger virion adhesion, denser local mucus mesh, antibody cross-linking, or a tracking threshold. A sensitivity matrix helps decide whether these mechanisms can be separated by the available observables.

Remark 4.77 (Why sensitivity is not the whole story). Sensitivity matrices measure how chosen summaries change. They may miss information contained in distributional shape, higher moments, null frequency, time correlations, rare events, spatial structure, or morphology. Fisher information extends the same principle to the full protocol-conditioned likelihood.

4.7.3 Fisher-information observability

Fisher information gives the likelihood-level version of protocol observability. It asks how sharply the protocol-conditioned likelihood changes when the parameter vector is perturbed. Equivalently, it measures local distinguishability of nearby parameter values under the composed map

$$\theta \mapsto P_{\text{obs},t}^{\varnothing}(\cdot \mid E, \theta).$$

$$\boxed{\text{Large Fisher information} \iff \text{Nearby parameter values are easier to distinguish under protocol } E.} \quad (4.7.3.1)$$

Small Fisher information indicates weak observability, while zero Fisher information indicates local protocol blindness.

Assume that the null-inclusive observed law admits a density or probability mass function

$$p_E^{\varnothing}(y \mid \theta), \quad y \in \mathcal{Y}_E^{\varnothing},$$

and that the usual differentiability and integrability conditions hold. The protocol score function is

$$\mathbf{u}_E(y; \theta) = \nabla_{\theta} \log p_E^{\varnothing}(y \mid \theta), \quad (4.7.3.2)$$

and the Fisher-information matrix is

$$\boxed{\mathcal{I}_E(\theta) = \mathbb{E}_{Y \sim p_E^{\varnothing}(\cdot \mid \theta)} \left[\mathbf{u}_E(Y; \theta) \mathbf{u}_E(Y; \theta)^{\top} \right].} \quad (4.7.3.3)$$

Under standard regularity conditions, this is also the negative expected Hessian of the log-likelihood,

$$\mathcal{I}_E(\theta) = -\mathbb{E}_{Y \sim p_E^\varnothing(\cdot|\theta)} \left[\nabla_\theta^2 \log p_E^\varnothing(Y | \theta) \right]. \quad (4.7.3.4)$$

This gives the curvature interpretation: sharply curved likelihoods constrain parameters strongly, while flat directions are weakly resolved or blind [44, 45, 46, 19, 20].

For a tangent direction $v \in T_\theta\Theta$, the directional Fisher information is

$$\mathcal{I}_E(\theta; v) = v^\top \mathcal{I}_E(\theta) v = \mathbb{E}_{\theta, E} \left[\left(v^\top \nabla_\theta \log p_E^\varnothing(Y | \theta) \right)^2 \right]. \quad (4.7.3.5)$$

The direction v may represent a change in stiffness, polarizability, adhesion strength, mucus-binding rate, field-response coefficient, plaque-forming probability, cell-entry competence, neutralization sensitivity, or a hidden orientation-sector parameter. If $v^\top \mathcal{I}_E v$ is large, the protocol is locally sensitive to that perturbation. If it is small, the perturbation is weakly resolved. If it is zero, the protocol is locally blind.

The local blind subspace is therefore

$$\mathcal{B}_E(\theta) = \ker \mathcal{I}_E(\theta) = \left\{ v \in T_\theta\Theta : v^\top \mathcal{I}_E(\theta) v = 0 \right\}. \quad (4.7.3.6)$$

Remark 4.78 (More data versus a different protocol). For N independent observations from the same protocol,

$$\mathcal{I}_{E,N}(\theta) = N\mathcal{I}_E(\theta).$$

Thus more data improve precision in directions the protocol already sees. However, if $v^\top \mathcal{I}_E(\theta) v = 0$, then $v^\top \mathcal{I}_{E,N}(\theta) v = 0$ for every N . More data from the same protocol do not make a structurally blind direction visible. Resolving that direction requires a different observation kernel, controlled protocol variation, additional prior structure, or a complementary measurement.

4.7.4 Practical identifiability rank

Because Fisher matrices carry units and can mix parameters with different scales, the matrix should be nondimensionalized before comparing eigenvalues. Let D_θ be a diagonal matrix of characteristic parameter scales. The scaled Fisher-information matrix is

$$\widehat{\mathcal{I}}_E(\theta) = D_\theta \mathcal{I}_E(\theta) D_\theta. \quad (4.7.4.1)$$

Equivalently, $\widehat{\mathcal{I}}_E$ is the Fisher matrix expressed in dimensionless local coordinates.

For a tolerance $\delta_{\text{id}} > 0$, define the practical identifiability rank by

$$r_E(\delta_{\text{id}}) = \# \left\{ \lambda_j(\widehat{\mathcal{I}}_E) : \lambda_j(\widehat{\mathcal{I}}_E) > \delta_{\text{id}} \right\}. \quad (4.7.4.2)$$

This rank estimates the number of independent parameter combinations that are practically visible under protocol E at the chosen tolerance.

Remark 4.79 (Interpretation of identifiability rank). The rank $r_E(\delta_{\text{id}})$ is not an absolute

property of the virion. It depends on the protocol, parameter scaling, noise level, sample size, model class, and chosen threshold. A protocol with small rank may still be scientifically valuable if it measures one important sector cleanly. For example, a plaque assay may have limited structural identifiability while strongly constraining assay-conditioned infectious activity; AFM may have limited information about free dynamics while strongly constraining surface-conditioned mechanics.

4.7.5 Nuisance parameters and effective information

Many protocol-resolved inverse problems contain nuisance parameters that can absorb or mimic changes in latent virion parameters. Partition the parameter vector as

$$\theta = (\theta_a, \lambda),$$

where θ_a is the target parameter block and λ contains nuisance parameters. Write the Fisher matrix in block form:

$$\mathcal{I}_E(\theta) = \begin{pmatrix} \mathcal{I}_{aa} & \mathcal{I}_{a\lambda} \\ \mathcal{I}_{\lambda a} & \mathcal{I}_{\lambda\lambda} \end{pmatrix}. \quad (4.7.5.1)$$

When $\mathcal{I}_{\lambda\lambda}$ is invertible, the effective Fisher information for θ_a , after accounting for nuisance directions, is the Schur complement

$$\boxed{\mathcal{I}_{a|\lambda} = \mathcal{I}_{aa} - \mathcal{I}_{a\lambda}\mathcal{I}_{\lambda\lambda}^{-1}\mathcal{I}_{\lambda a}}. \quad (4.7.5.2)$$

Remark 4.80 (Interpretation of nuisance-corrected information). The matrix $\mathcal{I}_{a|\lambda}$ measures how much information remains about the target parameter after nuisance parameters are allowed to adjust. If $\mathcal{I}_{a|\lambda}$ is small, then the protocol may appear sensitive to θ_a when nuisance parameters are fixed, but weakly informative once realistic uncertainty in protocol or environmental parameters is included. This is a common route by which experimental collapse becomes practical non-identifiability.

Remark 4.81 (If the nuisance block is singular). If $\mathcal{I}_{\lambda\lambda}$ is singular or ill-conditioned, the nuisance parameters are themselves weakly identifiable. In that case, the Schur complement may be replaced by a regularized or generalized-inverse version, or the model may require stronger priors, additional calibration data, controlled protocol variation, or a reduced parameterization. A singular nuisance block is not just a technical inconvenience; it is evidence that the protocol does not separate target and nuisance directions well.

Remark 4.82 (Mechanism-level design implication). The identifiability tools in this subsection show how mechanism-resolved collapse can guide experimental design. If a preparation mechanism collapses orientation, vary preparation or acquisition geometry. If a medium-filtering mechanism confounds virion adhesion with mucus structure, vary particle surface chemistry or medium composition. If a biological amplification kernel confounds virion competence with cell-line susceptibility, vary cell line, adsorption time, overlay, or incubation. If a Fisher eigenvalue remains small, the remedy is not simply more data from the same protocol, but a protocol change that rotates the sensitivity direction.

4.8 Multi-Protocol Inference after Mechanism-Resolved Collapse

The mechanism-resolved view of experimental collapse changes how protocol disagreement should be interpreted. Disagreement across protocols need not be a direct contradiction, because different

protocols may report different conditioned projections of the same latent virion–environment system. A cryo-EM reconstruction, an AFM force curve, a dielectrophoretic trajectory, a mucus-tracking ensemble, and a plaque count are not competing measurements of the same mathematical object. They are different protocol-conditioned outputs.

The appropriate multi-protocol question is therefore not whether all protocols produce the same observed distribution. They generally should not. The question is whether a common latent model can explain all protocol-conditioned datasets after each protocol kernel, nuisance structure, readout map, and null channel has been applied:

$$\boxed{\text{one latent virion–environment model} \xrightarrow{\text{distinct protocol kernels}} \text{multiple observed ensembles.}} \quad (4.8.1)$$

This is the constructive counterpart of protocol blindness. A single protocol may collapse, select, or project away one latent sector, while another protocol may probe, perturb, or amplify that same sector. Multi-protocol inference uses these differences as information rather than treating them only as disagreement.

Remark 4.83 (Why raw agreement is the wrong criterion). Raw agreement is usually the wrong criterion for comparing protocols. Cryo-EM may report selected structural classes; AFM may report surface-conditioned mechanical response; DEP or electrorotation may report field-conditioned dielectric response; mucus tracking may report medium-filtered transport; and plaque assays may report assay-conditioned infectious activity. Agreement should be tested after each protocol kernel has acted, not before.

4.8.1 Shared latent parameters and protocol-local parameters

Multi-protocol inference begins by separating parameters that are intended to be common across protocols from parameters that belong to individual protocol kernels. This separation is essential because mechanism-resolved collapse often enters through protocol-local quantities.

Definition 4.84 (Multi-protocol parameter structure). Let

$$\theta = (\theta_{\text{vir}}, \theta_{\text{env}})$$

denote the shared latent parameter vector, containing virion and environmental parameters intended to describe the same underlying system across protocols. For protocols E_1, \dots, E_M , let

$$\lambda_j = \lambda_{E_j}, \quad j = 1, \dots, M,$$

denote protocol-local nuisance or calibration parameters. The full multi-protocol parameter set is

$$\Theta_{\text{multi}} = (\theta, \lambda_1, \dots, \lambda_M). \quad (4.8.1.1)$$

The shared parameter vector θ contains quantities intended to persist across protocols: radius distribution, spike-length scale, effective charge range, polarizability anisotropy, compliance, orientational stiffness, damping scale, adhesion scale, or latent infectivity structure. The protocol-local parameters λ_j contain quantities such as field amplitude, field frequency, medium conductivity, surface chemistry,

tip geometry, imaging noise, frame rate, grid-preparation variables, particle-selection thresholds, overlay composition, incubation time, staining threshold, or reconstruction filters.

Remark 4.85 (Why this separation is essential). Without the shared/protocol-local separation, multi-protocol comparison can become misleading. If an AFM-derived stiffness differs from a stiffness-like quantity inferred from another assay, the discrepancy may reflect surface adhesion, indentation depth, hydration, or tip geometry rather than a true change in the virion. If plaque titers differ across cell lines, the discrepancy may reflect cell susceptibility or overlay conditions rather than a different physical particle concentration. If tracking statistics differ across mucus samples, the difference may reflect the medium rather than the virion alone. The decomposition $(\theta, \lambda_1, \dots, \lambda_M)$ is the statistical expression of this distinction.

4.8.2 Protocol-specific forward models and likelihoods

Let

$$\mathcal{D} = \{\mathcal{D}_{E_1}, \dots, \mathcal{D}_{E_M}\}$$

be datasets collected under protocols E_1, \dots, E_M . Each protocol has its own augmented observation space

$$\mathcal{Y}_{E_j}^\emptyset = \mathcal{Y}_{E_j} \cup \{\emptyset\},$$

its own null-inclusive observation operator

$$\mathcal{M}_{E_j}^\emptyset(\lambda_j),$$

and its own protocol-local nuisance parameters λ_j .

For each protocol,

$$\boxed{P_{\text{obs},t}^{(j),\emptyset}(\cdot \mid \theta, \lambda_j) = \mathcal{M}_{E_j}^\emptyset(\lambda_j) P_{\text{ref},t}(\cdot \mid \theta).} \quad (4.8.2.1)$$

Thus each dataset is interpreted as a distinct protocol-conditioned image of the same shared latent model.

Definition 4.86 (Multi-protocol likelihood). Suppose that the datasets are conditionally independent given the shared latent parameter vector θ and protocol-local nuisance parameters $\lambda_1, \dots, \lambda_M$. The multi-protocol likelihood is

$$\boxed{\mathcal{L}_{\text{multi}}(\theta, \lambda_1, \dots, \lambda_M) = \prod_{j=1}^M \mathcal{L}_{E_j}^\emptyset(\theta, \lambda_j; \mathcal{D}_{E_j}).} \quad (4.8.2.2)$$

Equivalently,

$$\log \mathcal{L}_{\text{multi}} = \sum_{j=1}^M \log \mathcal{L}_{E_j}^\emptyset(\theta, \lambda_j; \mathcal{D}_{E_j}). \quad (4.8.2.3)$$

Remark 4.87 (Conditional independence is a modeling assumption). The factorized likelihood assumes conditional independence of the datasets given the shared and protocol-local parameters. This is a useful first model, but it is not automatic. Shared batches, common sample preparation,

common calibration errors, correlated cell-culture conditions, repeated measurements of the same stock, or shared field-of-view effects can introduce dependence between datasets. In such cases, the joint likelihood should include shared nuisance variables or an explicit dependence structure.

Definition 4.88 (Bayesian multi-protocol posterior). Given a prior

$$q_0(\theta, \lambda_1, \dots, \lambda_M),$$

the multi-protocol posterior is

$$q(\theta, \lambda_1, \dots, \lambda_M | \mathcal{D}) = \frac{\mathcal{L}_{\text{multi}}(\theta, \lambda_1, \dots, \lambda_M) q_0(\theta, \lambda_1, \dots, \lambda_M)}{\int \mathcal{L}_{\text{multi}}(\vartheta, \ell_1, \dots, \ell_M) q_0(\vartheta, \ell_1, \dots, \ell_M) d\vartheta d\ell_1 \cdots d\ell_M}. \quad (4.8.2.4)$$

The marginal posterior for the shared latent parameters is obtained by integrating over protocol-local nuisance parameters:

$$q(\theta | \mathcal{D}) = \int q(\theta, \lambda_1, \dots, \lambda_M | \mathcal{D}) d\lambda_1 \cdots d\lambda_M. \quad (4.8.2.5)$$

Remark 4.89 (Why marginalization matters). The marginal posterior $q(\theta | \mathcal{D})$ represents what all protocols jointly imply about the shared latent model after protocol-level uncertainty has been accounted for. Point estimates that ignore the λ_j can overstate agreement or create artificial disagreement by treating protocol-specific effects as intrinsic latent properties.

4.8.3 Multi-protocol consistency as shared latent explanation

Multi-protocol consistency is not equality of raw datasets. It is the existence of a shared latent explanation after the appropriate protocol kernels have acted.

Definition 4.90 (Multi-protocol consistency). A latent model

$$P_{\text{ref},t}(dx | \theta)$$

is *multi-protocol consistent* with observed datasets $\mathcal{D}_{E_1}, \dots, \mathcal{D}_{E_M}$ if there exists a shared parameter θ and admissible protocol-local nuisance parameters $\lambda_1, \dots, \lambda_M$ such that

$$P_{\text{obs},t}^{(j),\varnothing}(\cdot) \approx \mathcal{M}_{E_j}^{\varnothing}(\lambda_j) P_{\text{ref},t}(\cdot | \theta), \quad j = 1, \dots, M. \quad (4.8.3.1)$$

The approximation symbol represents statistical agreement under a specified likelihood, discrepancy, posterior predictive check, calibration criterion, or model-comparison rule.

Remark 4.91 (What consistency means). Consistency means that the same latent model can generate each observed dataset after the corresponding protocol kernel has acted. In this sense, apparent disagreement can be diagnostic. It may reveal which states survive preparation, which orientations are pinned by surfaces, which particles respond electrically, which trajectories are filtered by mucus microstructure, or which states are infectious under a given biological assay.

Definition 4.92 (Protocol inconsistency). A collection of protocols is *protocol-inconsistent* relative

to a model class \mathcal{P} if no admissible latent model $P_{\text{ref},t}(\cdot | \theta) \in \mathcal{P}$, together with admissible protocol-local nuisance parameters, can explain all observed datasets under the specified protocol kernels.

Remark 4.93 (Interpreting protocol inconsistency). Protocol inconsistency is not automatically experimental failure. It may mean that the latent model is missing a relevant state variable, that a protocol kernel is misspecified, that a nuisance parameter was uncontrolled, that the sample changed between protocols, that a biological assay selected a functional subpopulation absent from the mechanical model, or that a hidden environmental variable is driving the discrepancy. Inconsistency is therefore a guide to model revision.

4.8.4 Complementary Fisher information

Multi-protocol inference improves identifiability when protocols provide information in different parameter directions. The local version of this statement is Fisher-information additivity.

Proposition 4.94 (Complementary protocols improve local identifiability). *Let $\mathcal{I}_{E_j}(\theta)$ be the Fisher-information matrix associated with protocol E_j . If the datasets are conditionally independent given θ and nuisance parameters are fixed, calibrated, marginalized, or appropriately profiled, then the Fisher information for the shared parameter has the additive form*

$$\boxed{\mathcal{I}_{\text{multi}}(\theta) = \sum_{j=1}^M \mathcal{I}_{E_j}(\theta).} \quad (4.8.4.1)$$

Consequently, protocols with different sensitivity directions can jointly identify parameter combinations that none of them identify alone.

Proof. For conditionally independent datasets, the joint likelihood factorizes:

$$\mathcal{L}_{\text{multi}}(\theta) = \prod_{j=1}^M \mathcal{L}_{E_j}(\theta).$$

Therefore,

$$\log \mathcal{L}_{\text{multi}}(\theta) = \sum_{j=1}^M \log \mathcal{L}_{E_j}(\theta).$$

The score is the gradient of the log-likelihood, so the total score is the sum of the protocol-specific scores. Under the usual regularity conditions, Fisher information is the expected outer product of the score, or equivalently the negative expected Hessian of the log-likelihood. Conditional independence implies that the protocol-specific score cross terms vanish in expectation, so the Fisher-information matrices add. \square

Remark 4.95 (How complementary information works). A geometry-rich protocol may identify size and morphology but not dielectric response. A field-driven protocol may identify polarizability but not native morphology. An AFM protocol may identify surface-conditioned stiffness but not free rotational mobility. A mucus-tracking protocol may identify transport and binding parameters but not internal branch structure. A plaque assay may identify infectious activity but not total physical

particle number. Together, these protocols can constrain a latent model more tightly than any single protocol can.

Definition 4.96 (Incremental directional information gain). Let \mathcal{E}_{old} denote an existing protocol set and E_{new} a proposed additional protocol. For a target direction $v \in T_{\theta}\Theta$, define the incremental directional information gain by

$$\Delta\mathcal{I}(E_{\text{new}}; v) = v^{\top}\mathcal{I}_{E_{\text{new}}}(\theta)v. \quad (4.8.4.2)$$

If v is weakly observed by the existing protocol set but strongly observed by E_{new} , then E_{new} is complementary for that parameter direction.

Remark 4.97 (Design principle). The best complementary protocol is not necessarily the one that resembles the existing protocol most closely. It is the protocol whose kernel exposes a previously blind or nuisance-confounded direction. In experimental-design terms, one should choose protocol variations that rotate, enlarge, or sharpen the Fisher-information ellipsoid in the target parameter space.

4.8.5 Cross-Protocol Prediction

A useful test of a shared latent model is cross-protocol prediction. One fits, constrains, or updates the latent model using one protocol and then asks whether the same latent model predicts the outcome of a second protocol after the second protocol kernel is applied. This is stronger than asking whether the first protocol is internally well fit. It asks whether the inferred latent virion–environment model transfers across a different observation mechanism.

Definition 4.98 (Cross-protocol prediction). Suppose protocol E_a has produced data \mathcal{D}_{E_a} . Let $q(\theta | \mathcal{D}_{E_a})$ denote the posterior or fitted uncertainty distribution for the shared latent parameters after accounting for E_a -specific nuisance parameters. The predicted null-inclusive observed law under a second protocol E_b is

$$\boxed{P_{\text{pred}}^{(b),\varnothing}(S | \mathcal{D}_{E_a}) = \int P_{\text{obs},t}^{(b),\varnothing}(S | E_b, \theta, \lambda_b) \times q(\theta, \lambda_b | \mathcal{D}_{E_a}) d\theta d\lambda_b, \quad S \in \Sigma_{Y,E_b}^{\varnothing}.} \quad (4.8.5.1)$$

Here λ_b denotes nuisance or calibration parameters for the predicted protocol E_b .

Remark 4.99 (Why cross-protocol prediction is useful). Cross-protocol prediction tests whether a latent model inferred from one projection predicts another projection. A structural model inferred from cryo-EM may be asked to predict an AFM deformation response, an electrorotation spectrum, a mucus-transport distribution, or an infectivity readout only after the corresponding protocol kernel is applied. Failure of this prediction may indicate a missing latent variable, a misspecified protocol kernel, an uncontrolled nuisance parameter, or a functional subpopulation not captured by the original model.

Remark 4.100 (Prediction should include protocol uncertainty). Cross-protocol prediction should propagate uncertainty in the predicted protocol’s nuisance parameters λ_b . A prediction that conditions on a single fixed overlay composition, surface adhesion value, field calibration, reconstruction threshold, or staining criterion may appear overly precise. Protocol uncertainty is part of the predictive distribution, not an external correction.

Remark 4.101 (Predictive failure as information). A failed cross-protocol prediction is not automatically a negative result. It can identify where the latent model or protocol kernel is incomplete. For example, a cryo-EM-derived structural model that fails to predict AFM response may be missing hydration, surface adhesion, or deformation variables. A tracking-derived transport model that fails to predict plaque formation may be missing infectivity, entry, or replication competence. A plaque-derived infectivity model that fails to predict particle-count or genome-count data may be collapsing defective, damaged, neutralized, or non-plaque-forming sectors into a single functional readout.

4.8.6 Practical Workflow for Multi-Protocol Inference

A practical multi-protocol analysis can be organized as a sequence of modeling decisions. The purpose is not to force all assays into the same observed space, but to specify how each protocol samples, transforms, selects, amplifies, and reports the shared latent system.

- (i) **Define the shared latent target.** Specify which parameters are intended to be common across protocols: morphology, charge, compliance, polarizability, adhesion, infectivity competence, environmental transport parameters, or collective branch structure.
- (ii) **Define protocol-specific kernels.** For each protocol, specify

$$\Pi_{E_j}^{\text{lat}}, \quad s_{E_j}, \quad R_{E_j}, \quad \emptyset.$$

State which components are known, calibrated, estimated, approximated, or left as nuisance structure.

- (iii) **Separate shared parameters from protocol-local parameters.** Decide which parameters belong to the shared latent vector θ and which belong to the protocol-local nuisance vectors λ_j . This prevents preparation, readout, surface, medium, field, cell-line, or threshold effects from being absorbed into intrinsic virion parameters.
- (iv) **Write protocol-specific likelihoods.** Use null-inclusive likelihoods when null outcomes, rejection rates, failed tracks, missing plaques, endpoint-negative wells, below-threshold signals, or detection yields are available.
- (v) **Fit jointly or test cross-protocol prediction.** Either estimate all protocols jointly through $\mathcal{L}_{\text{multi}}$, or fit one protocol and test the predicted output of another protocol through $P_{\text{pred}}^{(b),\emptyset}$.
- (vi) **Inspect identifiability.** Use sensitivity matrices, Fisher information, profile likelihoods, posterior correlations, posterior predictive checks, or discrepancy functionals to identify blind, weakly constrained, or nuisance-confounded directions.
- (vii) **Revise the latent model or protocol kernels.** If consistency fails, determine whether the failure is best explained by a missing latent sector, a misspecified kernel, uncontrolled nuisance variation, sample heterogeneity, batch effects, or a genuine biological difference.

Table 17. Examples of protocol-specific inferential strengths. The entries are schematic: real studies may combine several sectors, and each entry depends on the detailed protocol kernel.

Protocol	Strongly visible sectors	Typical latent quantities inferred
Cryo-EM / cryo-ET	Geometry, conformation, spike distribution, particle classes, selected orientations	Shape distributions, preserved conformational classes, orientation-selection profiles, structural heterogeneity.
AFM	Surface-conditioned morphology, indentation response, rupture or deformation pathways	Effective stiffness, compliance, adhesion, surface-conditioned height, mechanical fragility.
DEP / electrorotation	Field response, trapping, crossover behavior, signed rotation, polarization-dependent motion	Effective polarizability, dielectric relaxation scale, charge response, rotational drag under forcing.
Mucus or gel tracking	Transport, confinement, residence time, anomalous diffusion, adhesive trapping	Effective diffusivity, binding strength, mesh interaction, viscoelastic or heterogeneous transport parameters.
Plaque / focus / endpoint assay	Infectious amplification, local spread, cytopathic effect, staining or reporter visibility	Infectious-unit concentration, cell-entry competence, assay-conditioned replication or spread efficiency.

4.8.7 Branch-Level Inverse Inference

If the latent theory contains collective branches, then experimental collapse also determines which branches are visible. A branch may exist mechanically but remain experimentally hidden if the protocol does not couple to the sector in which that branch primarily lives. Conversely, an active protocol can reveal a branch by coupling to a variable that passive imaging, center tracking, or scalar counting would not resolve.

This point is the dynamical analogue of protocol-conditioned observation. Many mechanically interesting degrees of freedom are not reported as complete normal modes. They may appear indirectly through relaxation rates, force-indentation response, field-driven rotation, fluctuation spectra, orientation statistics, transport-state switching, or biological response. Branch-level inference is therefore an inverse problem:

$$\boxed{\text{branch-sensitive data} \implies \text{latent branch parameters through a protocol-specific visibility map.}} \quad (4.8.7.1)$$

Definition 4.102 (Latent branch parameter vector). For a collective branch n , define a reduced latent branch parameter vector

$$\theta_{\mathbf{B}_n} = \left(\omega_n(\mathbf{k}), \Gamma_n(\mathbf{k}), P_{\text{tilt}}^{(n)}(\mathbf{k}), \Pi_{\text{hyb}}^{(n)}(\mathbf{k}), \Pi_{\text{dir}}^{(n)}(\mathbf{k}), \Pi_{\text{stab}}^{(n)}(\mathbf{k}) \right)_{\mathbf{k} \in \mathbf{K}}. \quad (4.8.7.2)$$

Here ω_n is a branch frequency, Γ_n is a damping or decay rate, $P_{\text{tilt}}^{(n)}$ is a tilt or presentation participation weight, $\Pi_{\text{hyb}}^{(n)}$ measures hybridization between sectors, $\Pi_{\text{dir}}^{(n)}$ measures directional anisotropy, and $\Pi_{\text{stab}}^{(n)}$

measures stability or persistence. The set \mathbf{K} denotes the wavevectors, spatial scales, finite-size modes, or experimentally accessible fluctuation modes probed by the protocol or simulation.

Remark 4.103 (Interpretation of branch parameters). The vector $\theta_{\mathbf{B}_n}$ is a reduced summary of a branch, not a claim that all branch information is directly measurable. In simulation, these quantities may be extracted from a dynamical matrix, covariance spectrum, normal-mode decomposition, or response calculation. In experiments, they may be inferred only through protocol-sensitive observables. This is why branch visibility must be tied to a specific readout and protocol kernel [57, 58, 59].

Definition 4.104 (Branch-readout kernel). A *branch-readout kernel* is a protocol-dependent map

$$R_E^{\text{br}}(dy_{\text{br}} \mid \theta_{\mathbf{B}_n}) \quad (4.8.7.3)$$

that describes how latent branch information is projected into an observed branch-sensitive datum y_{br} . Examples include a relaxation rate, fluctuation amplitude, deformation pattern, alignment statistic, finite-frequency response peak, field-driven rotation signal, or orientation-sensitive response amplitude.

Remark 4.105 (Why R_E^{br} is reduced notation). The notation R_E^{br} denotes a reduced branch-sensitive readout model, not the full null-inclusive protocol kernel K_E^\emptyset . The full kernel still contains latent transformation, survival or selection, readout, and null observation. The branch-readout kernel isolates the component of the readout that is informative about branch-level structure.

Definition 4.106 (Branch-sensitive observable). Let

$$h_{\text{br}} : \mathcal{Y}_E \rightarrow \mathbb{R}^m$$

be a branch-sensitive observable under protocol E . Examples include a spectral peak, a relaxation time, a response amplitude, an indentation-mode coefficient, a field-driven rotation rate, an orientation-class statistic, or a projection of a trajectory onto a mode-like basis. Its protocol-conditioned expectation is

$$\mathbf{H}_{\text{br},E}(\theta_{\mathbf{B}_n}) = \mathbb{E}_E [h_{\text{br}}(Y) \mid \theta_{\mathbf{B}_n}, \text{det}]. \quad (4.8.7.4)$$

Definition 4.107 (Branch observability score). The branch observability score for branch n at wavevector or scale \mathbf{k} is

$$\mathcal{V}_n(E, \mathbf{k}) = \frac{\|D_{\theta_{\mathbf{B}_n}(\mathbf{k})} \mathbf{H}_{\text{br},E}\|}{V_0 + \|D_{\theta_{\mathbf{B}_n}(\mathbf{k})} \mathbf{H}_{\text{br},E}\|}, \quad V_0 > 0. \quad (4.8.7.5)$$

Here $D_{\theta_{\mathbf{B}_n}(\mathbf{k})} \mathbf{H}_{\text{br},E}$ denotes the local sensitivity of the branch-sensitive observable to the branch parameters at \mathbf{k} . The constant V_0 sets the scale at which the score transitions from weak to strong visibility.

Remark 4.108 (Interpretation of branch observability). Values near zero indicate that the branch is effectively hidden under the protocol and chosen branch readout. Values near one indicate that the protocol is sensitive to that branch. The score is not an intrinsic property of the branch alone.

It depends on the protocol, readout, noise level, scale normalization, and nuisance parameters.

Definition 4.109 (Fisher branch observability). If the branch-sensitive observed law admits a density or mass function

$$p_E^{\text{br}}(y_{\text{br}} \mid \theta_{\mathbf{B}_n}),$$

then the branch-level Fisher information is

$$\mathcal{I}_E^{\text{br}}(\theta_{\mathbf{B}_n}) = \mathbb{E} \left[\nabla_{\theta_{\mathbf{B}_n}} \log p_E^{\text{br}}(Y_{\text{br}} \mid \theta_{\mathbf{B}_n}) \nabla_{\theta_{\mathbf{B}_n}} \log p_E^{\text{br}}(Y_{\text{br}} \mid \theta_{\mathbf{B}_n})^\top \right]. \quad (4.8.7.6)$$

A branch direction v_{br} is locally invisible under protocol E if

$$v_{\text{br}}^\top \mathcal{I}_E^{\text{br}}(\theta_{\mathbf{B}_n}) v_{\text{br}} = 0. \quad (4.8.7.7)$$

Proposition 4.110 (Orientation-sensitive protocols can reveal tilt branches). *Suppose branch n has nonzero tilt or presentation participation,*

$$P_{\text{tilt}}^{(n)}(\mathbf{k}) > 0.$$

If protocol E includes a branch-sensitive observable whose expectation depends nontrivially on the tilt or presentation sector through field coupling, surface alignment, orientation-sensitive contrast, or torque-sensitive response, then

$$\mathcal{V}_n(E, \mathbf{k}) > 0$$

for the corresponding branch readout, even if passive center-tracking observability is negligible.

Proof. By assumption, the branch readout depends nontrivially on the tilt or presentation sector. Thus, for at least one component of the branch parameter vector,

$$\frac{\partial \mathbf{H}_{\text{br},E}}{\partial P_{\text{tilt}}^{(n)}(\mathbf{k})} \neq 0.$$

Therefore

$$\left\| D_{\theta_{\mathbf{B}_n}(\mathbf{k})} \mathbf{H}_{\text{br},E} \right\| > 0,$$

and Eq. (4.8.7.5) gives $\mathcal{V}_n(E, \mathbf{k}) > 0$. In a passive center-tracking protocol, the corresponding derivative may vanish or be small because the readout projects primarily onto translational coordinates rather than orientation or presentation variables. \square

Remark 4.111 (Biological interpretation of branch-level inference). For spike-bearing virions, branch-level inference asks whether collective motion involves only center displacement or also organized changes in spike-bearing presentation. This is relevant to surface-bound layers, field-conditioned clusters, dense aggregates, mucus-constrained assemblies, and orientation-biased preparation. A branch that appears as simple translational relaxation in one protocol may contain hidden presentation dynamics that become visible when orientation-sensitive forcing or readout is added.

Remark 4.112 (Branch-level inference as experimental design). The practical design question is: which protocol should be added to make a branch visible? If the branch is predicted to live mostly in

translation, tracking or fluctuation analysis may be sufficient. If it lives in orientation, presentation, or torque response, field coupling, polarization-sensitive readout, surface alignment, or orientation-sensitive imaging may be required. If it lives in deformation, mechanical loading may be the useful perturbation. Branch-level inverse inference therefore turns latent branch structure into an experimental design problem.

4.8.8 Design Principles for Protocol-Resolved Inference

The formalism above suggests practical design principles. These principles are not additional assumptions. They follow from treating experiments as protocol kernels: each experimental setting transforms, selects, amplifies, detects, and reads out the latent virion–environment ensemble in a specific way.

The guiding design question is:

Which latent sectors does this protocol make visible, and Which sectors does it collapse?

(4.8.8.1)

(i) **Report protocol variables as model parameters.**

Field frequency, ionic strength, conductivity, surface chemistry, frame rate, exposure time, tip geometry, force ramp rate, particle-selection thresholds, cell line, overlay composition, incubation time, staining rule, counting criterion, grid chemistry, vitrification route, and preparation timing are not peripheral metadata. They are parameters of \mathcal{M}_E^\emptyset .

(ii) **Preserve the null channel when possible.**

Rejected particles, nonlocalized trajectories, failed reconstructions, particles lost from the field of view, absent plaques, missing foci, below-threshold reporter signals, and excluded tracks carry information about s_E , η_E , and the null channel \emptyset . Removing these outcomes too early can erase the denominator of the experiment.

(iii) **Use controlled protocol variation.**

A single protocol may leave important parameter directions unidentifiable. Controlled variation changes the observation kernel and can expose different latent sectors. The purpose of protocol variation is not merely to check robustness; it is to change the kernel in a known direction.

(iv) **Separate intrinsic parameters from protocol-conditioned parameters.**

A stiffness measured by AFM is surface- and loading-conditioned unless modeled otherwise. A diffusion coefficient in mucus is medium-conditioned. A DEP crossover frequency is field- and medium-conditioned. A cryo-EM orientation distribution is preparation- and reconstruction-conditioned. A plaque count is cell-line-, overlay-, incubation-, staining-, and threshold-conditioned.

(v) **Compare protocols through a shared latent model.**

Cryo-EM, AFM, DEP/electrorotation, plaque assays, and tracking need not agree at the observation level. The appropriate consistency test is whether one latent model can reproduce each dataset after the corresponding protocol kernel is applied:

$$P_{\text{obs},t}^{(j),\emptyset}(\cdot) \approx \mathcal{M}_{E_j}^\emptyset(\lambda_j)P_{\text{ref},t}(\cdot | \theta). \quad (4.8.8.2)$$

(vi) **Design complementary protocols around blind directions.**

A protocol should be paired with another protocol when its Fisher information has weak or zero

directions that matter for the scientific question. In Fisher-information language, the aim is to choose E_{new} such that

$$v^\top \mathcal{I}_{E_{\text{new}}}(\theta)v > 0 \tag{4.8.8.3}$$

for a direction v that is weakly resolved or blind under the existing protocol set.

(vii) **Do not confuse invisibility with absence.**

A hidden branch, orientation sector, force–torque coupling, adhesive state, defective-particle sector, or infectious subpopulation may be real but unobservable under a particular readout. The stronger claim that such a sector is absent requires a protocol sensitive to that sector, a multi-protocol argument that rules it out, or a mechanistic model showing that the sector cannot be populated under the relevant conditions.

(viii) **Treat protocol design as part of model design.**

Choosing a protocol is choosing which projection of the latent system will be measured. Choosing protocol variations is choosing which degeneracies may be broken. Choosing what to record as null, rejected, or below threshold is choosing whether the detection denominator will be available for inference.

Table 18. Design principles for protocol-resolved inference. Each principle corresponds to a specific part of the observation model.

Design principle	Mathematical object	Practical implication
Report protocol variables	$\theta_E, \lambda_E, \mathcal{M}_E^\emptyset$	Treat field settings, grids, surfaces, overlays, timing, thresholds, and instrument settings as model variables.
Preserve null outcomes	s_E, η_E, \emptyset	Record rejected, failed, missing, nonlocalized, below-threshold, or non-plaque-forming outcomes when possible.
Vary protocols deliberately	$\Pi_E^{\text{lat}}, s_E, R_E$	Change the kernel to expose sectors that are weakly visible under one protocol.
Separate intrinsic and effective quantities	$\theta_{\text{vir}}, \theta_{\text{env}}, \theta_E$	Do not interpret protocol-conditioned stiffness, diffusivity, dielectric response, or PFU as protocol-free properties.
Compare through shared latent model	$a P_{\text{ref},t}(\cdot \theta), \mathcal{M}_{E_j}^\emptyset$	Test whether one latent model can generate all observed datasets after protocol-specific kernels act.
Design around blind directions	$\mathcal{I}_E(\theta), \ker \mathcal{I}_E(\theta)$	Add protocols that contribute information in weakly resolved parameter directions.

Remark 4.113 (Section-level summary). Experimental collapse converts the interpretation of experiments from a direct readout problem into a protocol-resolved inverse problem. The observed data are not simply the latent mechanics. They are the latent mechanics after transformation, selection,

amplification, detection, and readout by a specified protocol. Once this is accepted, the same framework becomes constructive: controlled protocol variation can reveal mechanical, environmental, or biological parameters that are otherwise hidden.

In this sense, experimental collapse is not only a warning. It is an inference principle. A protocol asks a question of the virion–environment system, and the observed ensemble is the answer to that question.

4.8.9 Observation Equivalence and Quotient Latent Spaces

Protocol blindness can also be expressed globally. Fisher-information blindness describes local statistical indistinguishability: it identifies parameter directions in which the likelihood fails to change to first order. A stronger question is whether two distinct latent states produce exactly the same observed law under the entire protocol. This leads naturally to an observation-equivalence relation.

Definition 4.114 (Protocol observation equivalence). Two latent states $x_1, x_2 \in \Psi$ are *observation-equivalent* under protocol E , written

$$x_1 \sim_E x_2,$$

if they induce the same null-inclusive observed law:

$$\boxed{K_E^\emptyset(\cdot | x_1) = K_E^\emptyset(\cdot | x_2) \text{ as probability measures on } \mathcal{Y}_E^\emptyset.} \quad (4.8.9.1)$$

Proposition 4.115 (Observation equivalence is an equivalence relation). *The relation \sim_E is an equivalence relation on Ψ .*

Proof. For any $x \in \Psi$,

$$K_E^\emptyset(\cdot | x) = K_E^\emptyset(\cdot | x),$$

so the relation is reflexive. If $x_1 \sim_E x_2$, then equality of probability measures gives $x_2 \sim_E x_1$, so the relation is symmetric. Finally, if $x_1 \sim_E x_2$ and $x_2 \sim_E x_3$, then

$$K_E^\emptyset(\cdot | x_1) = K_E^\emptyset(\cdot | x_2) = K_E^\emptyset(\cdot | x_3),$$

so $x_1 \sim_E x_3$. Thus the relation is transitive. □

Remark 4.116 (Interpretation of observation equivalence). If $x_1 \sim_E x_2$, then no amount of repeated observation under protocol E alone can distinguish x_1 from x_2 , unless additional assumptions or additional protocols are introduced. The two states may be mechanically or biologically different, but they are identical from the perspective of the protocol. Protocol blindness can therefore be structural, not merely a consequence of noise or finite sample size.

Definition 4.117 (Protocol quotient space). The *protocol quotient space* is the set of observation-equivalence classes

$$\Psi / \sim_E = \{[x]_E : x \in \Psi\}, \quad (4.8.9.2)$$

where

$$[x]_E = \{x' \in \Psi : x' \sim_E x\}. \quad (4.8.9.3)$$

Remark 4.118 (Observed data as a quotient of latent mechanics). The quotient space Ψ/\sim_E is the part of latent state space that remains distinguishable after protocol collapse. Latent distinctions that lie within the same equivalence class are mechanically or biologically present in the model but observationally compressed. Thus a protocol does not merely add noise to the latent state. It may identify distinct latent states as experimentally equivalent.

Remark 4.119 (Measurability of the quotient). The quotient notation is used here primarily to express the partition of latent state space induced by the protocol. In applications requiring integration over Ψ/\sim_E , one must specify an appropriate quotient σ -algebra or work with finite-dimensional summaries of the equivalence classes. For the present theory, the essential point is the induced observational partition: different latent states may belong to the same protocol-defined observational class.

Definition 4.120 (Approximate protocol equivalence). Exact equality of observed laws is often too strict for finite-resolution experiments. Let D_E be a distance or divergence between probability measures on $\mathcal{Y}_E^\varnothing$. For a tolerance $\varepsilon > 0$, two latent states are ε -equivalent under protocol E if

$$D_E(K_E^\varnothing(\cdot | x_1), K_E^\varnothing(\cdot | x_2)) \leq \varepsilon. \quad (4.8.9.4)$$

Remark 4.121 (Approximate equivalence and practical blindness). Approximate equivalence is the global counterpart of practical under-resolution. Two latent states may not induce exactly the same observed law, but if their observed laws are closer than the experimental noise, finite-sample uncertainty, nuisance-parameter uncertainty, or chosen resolution threshold, then the protocol cannot reliably distinguish them in practice.

Proposition 4.122 (Deterministic blindness as the local tangent form of equivalence). Suppose the protocol is summarized locally by a differentiable deterministic forward map

$$\mathcal{F}_E : \Psi \rightarrow \mathbb{R}^m.$$

Let $x(\epsilon)$ be a smooth curve in Ψ with $x(0) = x_0$. If

$$\mathcal{F}_E(x(\epsilon)) = \mathcal{F}_E(x_0) + O(\epsilon^2), \quad (4.8.9.5)$$

then its tangent vector

$$v = \left. \frac{dx}{d\epsilon} \right|_{\epsilon=0}$$

lies in the deterministic protocol-blind subspace:

$$v \in \ker D\mathcal{F}_E(x_0). \quad (4.8.9.6)$$

Proof. Differentiating Eq. (4.8.9.5) at $\epsilon = 0$ gives

$$D\mathcal{F}_E(x_0) \left. \frac{dx}{d\epsilon} \right|_{\epsilon=0} = 0.$$

Therefore $v \in \ker D\mathcal{F}_E(x_0)$. □

Remark 4.123 (Local versus global blindness). The quotient relation \sim_E is global: it compares the full observed laws generated by two latent states. The deterministic blind subspace $\ker D\mathcal{F}_E$ is local: it describes tangent directions along which a chosen observable summary fails to change to first order. Fisher blindness is also local, but likelihood-based rather than deterministic. These three notions are related but not identical. Together, they describe protocol blindness at three levels: global equivalence, deterministic sensitivity, and statistical distinguishability.

Proposition 4.124 (Multi-protocol quotient refinement). *Let E_1, \dots, E_M be protocols. Define*

$$x_1 \sim_{\text{multi}} x_2$$

if

$$K_{E_j}^\emptyset(\cdot | x_1) = K_{E_j}^\emptyset(\cdot | x_2) \quad \text{for every } j = 1, \dots, M. \quad (4.8.9.7)$$

Then

$$x_1 \sim_{\text{multi}} x_2 \iff x_1 \sim_{E_j} x_2 \text{ for all } j = 1, \dots, M. \quad (4.8.9.8)$$

Thus multi-protocol observation refines the latent quotient by intersecting the equivalence relations induced by the individual protocols.

Proof. By definition, $x_1 \sim_{\text{multi}} x_2$ holds exactly when the two latent states induce the same observed law under every protocol E_j . This is precisely the condition $x_1 \sim_{E_j} x_2$ for all $j = 1, \dots, M$. □

Remark 4.125 (Interpretation of quotient refinement). Each protocol partitions latent state space into observational equivalence classes. Adding a complementary protocol can split some of those classes into smaller classes, thereby making previously collapsed distinctions visible. This is the global analogue of the local statement that multi-protocol sensitivity reduces the blind subspace.

Remark 4.126 (Why the quotient viewpoint is useful). The quotient viewpoint separates mechanical existence from experimental distinguishability. A sector may be present in the latent mechanics but collapsed into the same observational equivalence class as another sector. In that case, failure to observe the sector is not evidence of mechanical absence. It is evidence that the chosen protocol quotient has removed the distinction.

The next section applies this logic to a concrete virological protocol. The plaque assay is especially instructive because its observed state space is not a microscopic mechanical state space. It is a count, morphology, or endpoint pattern generated by visible infectious lesions. Mechanically and structurally distinct virion states may therefore be collapsed into the same observational categories: plaque-forming, focus-forming, endpoint-positive, non-plaque-forming, or unobserved. This makes the plaque assay a useful worked example of protocol blindness, biological amplification, null observation, and protocol-resolved inverse inference.

4.9 Section Reference: Mechanisms, Inference, and Protocol Design

Table 19. Core mechanisms, equations, and diagnostic concepts introduced in the mechanism-resolved experimental-collapse framework. The table summarizes how laboratory protocols transform, select, amplify, project, and report latent virion–environment states.

Concept or object	Mathematical form	Interpretation
Mechanism-resolved protocol pipeline	$X \rightarrow X_{\text{prep}} \rightarrow X_{\text{constr}} \rightarrow X_{\text{det}} \rightarrow Y_E \text{ or } \emptyset$	Schematic laboratory sequence: preparation, experimental conditioning, selection or detection, readout, and null observation.
Mechanism-resolved kernel factorization	$\Pi_E^{\text{lat}} = \Pi_{E,L} \circ \dots \circ \Pi_{E,1}$	Represents the latent-stage protocol kernel as a sequence of physically, chemically, mechanically, biologically, or procedurally interpretable stages.
Mechanism-specific kernels	$\Pi_E^{\text{prep}}, \Pi_E^{\text{interface}}, \Pi_E^{\text{surf}}, \Pi_E^{\text{field}}, \Pi_E^{\text{medium}}, \Pi_E^{\text{bio}}$	Representative factors isolating preparation, interface exposure, surface interaction, field forcing, medium filtering, and biological amplification.
Preparation/interface collapse	$X \xrightarrow{\Pi_E^{\text{prep}}} X_{\text{prep}}$	Collapse induced by sample handling, staining, buffer exchange, vitrification, fixation, grid interaction, air–water interface exposure, or other pre-readout conditioning.
Cryo-EM preparation factorization	$\Pi_E^{\text{prep}} = \Pi_E^{\text{vit}} \circ \Pi_E^{\text{AWI}} \circ \Pi_E^{\text{thinfil}} \circ \Pi_E^{\text{grid}}$	Schematic decomposition of cryo-EM preparation into grid or support interaction, thin-film behavior, air–water interface exposure, and vitrification.
Orientation-selection model	$p_{E,\text{det}}(Q) = \frac{w_E(Q)p_{\text{ref}}(Q)}{\int_{SO(3)} w_E(Q')p_{\text{ref}}(Q') dQ'}$	Shows how preparation or selection weights transform a reference orientation distribution into a detected, protocol-conditioned orientation distribution.
Surface/contact collapse	$X \xrightarrow{\Pi_E^{\text{surf}}} X_{\text{surf}}$	Collapse caused by adsorption, immobilization, receptor contact, substrate interaction, cell-surface coupling, or surface-induced deformation.
Mechanical loading collapse	$X_{\text{surf}} \xrightarrow{\Pi_E^{\text{load}}} X_{\text{load}}$	Protocol-induced deformation, rupture, indentation response, or rate-dependent mechanical conditioning caused by applied force.

Continued on next page.

Table 19. Core mechanisms, equations, and diagnostic concepts introduced in the mechanism-resolved experimental-collapse framework. *Continued from previous page.*

Concept or object	Mathematical form	Interpretation
Field/electrical collapse	$X \xrightarrow{\Pi_E^{\text{field}}(\theta_{\text{env}}, \theta_E)} X_{\text{field}}$	State transformation or selection induced by electric fields, dielectric contrast, conductivity, polarization, trapping, torque, or field-sensitive loss.
Geometric projection collapse	$Y_E = \mathcal{O}_E(X_E)$	Occurs when a high-dimensional latent state is reported as a projection, image, reconstruction, trajectory, curve, count, class, spectrum, or summary statistic.
Observation fiber	$\mathcal{F}_E(y_E) = \{x_E \in \Psi_E : \mathcal{O}_E(x_E) = y_E\}$	Set of protocol-conditioned latent states that map to the same observed datum. Large fibers indicate collapsed latent distinctions.
Posterior fiber	$P_E(dx_E y_E, \text{det})$	Probabilistic analogue of the observation fiber for stochastic readout, reconstruction uncertainty, thresholding, noise, or model-based inversion.
Medium-filtering collapse	$\Pi_E^{\text{medium}}(dx_{\text{medium}} x; \theta_{\text{env}})$	State-dependent slowing, trapping, exclusion, confinement, immobilization, or mobility switching caused by mucus, gels, extracellular matrix, droplets, overlays, or other structured media.
Medium-filtered trajectory model	$dx_t = \mathbf{b}_E dt + \sqrt{2}\mathbf{B}_E d\mathbf{W}_t + d\mathbf{J}_t,$ $D_E = \mathbf{B}_E \mathbf{B}_E^T$	Represents drift, anisotropic or heterogeneous diffusion, and jump, sticking, release, or state-switching events in structured media.
Hidden mobility state	$M_t \in \{\text{mobile, confined, adhesive, immobile, released}\}$	Latent transport mode that may be only partially visible through the reported trajectory.
Joint medium-filtered latent process	$X_t = (\mathbf{r}_t, Q_t, M_t, X_{\text{env}, t})$	Coupled process containing position, orientation, hidden mobility state, and local environmental state.
Time-window collapse	$\Pi_E^{\text{time}}(dx_{\text{time}} x; t_0, t_1, \Delta t_{\text{samp}}, \tau_{\text{exp}})$	Collapse caused by finite observation duration, frame interval, exposure time, preparation delay, incubation time, or analysis window.
Finite-exposure observation	$Y_m = \frac{1}{\tau_{\text{exp}}} \int_{t_m}^{t_m + \tau_{\text{exp}}} \mathcal{O}_E(X_t) dt + \nu_m$	Makes explicit that fast latent motion, transient binding, or short-lived states can be blurred or averaged within one recorded frame.

Continued on next page.

Table 19. Core mechanisms, equations, and diagnostic concepts introduced in the mechanism-resolved experimental-collapse framework. *Continued from previous page.*

Concept or object	Mathematical form	Interpretation
Time-window ratios	$\Pi_{\text{samp}} = \frac{\tau_{\text{state}}}{\Delta t_{\text{samp}}}, \quad \Pi_{\text{win}} = \frac{\tau_{\text{state}}}{t_1 - t_0}, \quad \Pi_{\text{exp}} = \frac{\tau_{\text{state}}}{\tau_{\text{exp}}}$	Dimensionless measures of whether a latent state is sampled, persistent, averaged, motion-blurred, or missed under the protocol timing.
Persistence-biased detection	$s_E^{\text{time}}(A) = \Pr(\tau_A \geq \tau_{\text{min}} E)$	States that persist long enough are more likely to enter the observed ensemble than short-lived, rare, or rapidly switching states.
Time-integrated readout	$Y_E = \int_{t_0}^{t_1} h_E(X_t) dt + \nu_E$	Readout formed by accumulated biological, optical, reporter, cytopathic, or mechanical signal over an incubation or acquisition window.
Biological amplification collapse	$X \rightarrow X_{\text{bio}} \rightarrow Y_{\text{bio}} \text{ or } \emptyset$	Assay reports only latent states that complete a biological pathway sufficient to generate a plaque, focus, reporter signal, endpoint response, or cytopathic effect.
Biological pathway probability	$\pi_{\text{bio}}(x; E) = \Pr(A_0 x, E) \prod_{k=1}^K \Pr(A_k A_0, \dots, A_{k-1}, x, E)$	Stage-resolved probability that a latent state passes through the required biological assay events.
Binary biological observation kernel	$K_E^{\text{bio}, \emptyset}(\{\text{signal}\} x) = \pi_{\text{bio}}(x; E),$ $K_E^{\text{bio}, \emptyset}(\{\emptyset\} x) = 1 - \pi_{\text{bio}}(x; E)$	Maps latent states into a biological signal channel or the biological null channel.
Plaque-forming probability	$\pi_{\text{PFU}}(x; E_{\text{PFU}}) = \Pr(x \text{gen} E_{\text{PFU}})$	Protocol-conditioned probability that a latent virion, aggregate, or infectious unit generates a countable plaque.
Biological readout spaces	$\mathcal{Y}_{\text{PFU}} = \{0, 1, 2, \dots\}, \quad \mathcal{Y}_{\text{ED}} = \{0, 1\}^{J \times R}$	Plaque and focus assays report counts; endpoint dilution assays report binary or categorical infection patterns across dilutions and replicate wells.
Biological visibility threshold	$s_E^{\text{bio}}(x_{\text{bio}}) = \mathbf{1}\{A_E(x_{\text{bio}}) \geq a_E^*\}$	Assay event becomes visible, countable, or scoreable only after crossing a protocol-specific threshold.
Amplification gain	$G_E(x) = \frac{A_E(x_{\text{bio}}, t_1) + \epsilon_A}{A_E(x_{\text{bio}}, t_0) + \epsilon_A}$	Quantifies how a biological process expands a small latent difference into a visible assay signal.
Stage-resolved protocol family	$\mathcal{E}_{\text{bio}} = \{E^{(1)}, E^{(2)}, \dots, E^{(M)}\}$	Collection of related biological assays formed by varying cell line, adsorption time, overlay, incubation, reporter threshold, neutralization, or another controlled stage parameter.

Continued on next page.

Table 19. Core mechanisms, equations, and diagnostic concepts introduced in the mechanism-resolved experimental-collapse framework. *Continued from previous page.*

Concept or object	Mathematical form	Interpretation
Stage-sensitivity index	$S_r(E) = \frac{\partial}{\partial \xi_r} \log[\Lambda_{\text{bio}}(E; \xi_r) + \epsilon_\Lambda]$	Measures how strongly the biological signal changes when a controlled assay-stage parameter ξ_r is varied.
Biological bottleneck score	$\mathcal{B}_k(E) = 1 - \int_{\Psi} \Pr(A_k A_0, \dots, A_{k-1}, x, E) P_{\text{ref},t}(dx)$	Identifies assay stages that strongly filter the latent population.
Ideal Poisson count model	$N_d \Lambda_{\text{bio}} \sim \text{Poisson}(V_{\text{inoc}} f_d \Lambda_{\text{bio}}(E))$	Baseline model for independent biological events in the dilute, well-mixed, non-overlapping, countable regime.
Negative-binomial count model	$N_d \sim \text{NegBin}(\mu_d, \kappa),$ $\text{Var}(N_d) = \mu_d + \frac{\mu_d^2}{\kappa}$	Models overdispersed plaque or focus counts caused by aggregation, heterogeneous cell susceptibility, well-to-well variation, clustered input, or other replicate-level heterogeneity.
Zero-inflated count model	$\Pr(N_d = 0) = \zeta_E + (1 - \zeta_E)e^{-\mu_d}$	Models excess zero counts caused by structural null outcomes, failed delivery, failed amplification, non-permissive wells, or subthreshold signal.
Censored/countability model	$N_{\text{obs}} = \begin{cases} N, & N_{\min} \leq N \leq N_{\max}, \\ \text{censored}, & \text{otherwise.} \end{cases}$	Represents wells that are too dense, too sparse, merged, or otherwise outside the exact-count regime.
Spatial plaque process	$\Phi_E = \{z_1, \dots, z_N\} \subset \Omega_{\text{well}}, \quad \mathbb{E}[N] = \int_{\Omega_{\text{well}}} \lambda_E(z) dz$	Represents plaques or foci as spatial events rather than independent scalar counts.
Plaque-merging map	$\mathcal{S}_E : \Phi_E^{\text{true}} \rightarrow \Phi_E^{\text{obs}}, \quad N_{\text{obs}} = \#\mathcal{S}_E(\Phi_E^{\text{true}})$	Models overlap, merging, segmentation failure, or loss of countability at high inoculum, weak overlay restriction, or long incubation.
Endpoint dilution model	$\Pr(Z_{jr} = 1 \theta, E) = 1 - \exp[-V_{\text{inoc}} f_j \Lambda_{\text{ED}}(E, \theta)]$	Represents TCID ₅₀ -type assays as binary or categorical censored readouts across dilution and replicate wells.
Endpoint threshold model	$Z_{jr} = \mathbf{1}\{A_{jr} \geq a_E^*\}$	Represents endpoint positivity as a thresholded observation of a latent biological signal.
Neutralization as kernel deformation	$\pi_{\text{bio}}(x; E, c) = \Pr(A_0 x, E, c)$ $\times \prod_{k=1}^K \Pr(A_k A_0, \dots, A_{k-1}, x, E, c)$	Neutralizing agents deform the biological kernel by altering one or more stage probabilities and shifting latent states toward null biological channels.

Continued on next page.

Table 19. Core mechanisms, equations, and diagnostic concepts introduced in the mechanism-resolved experimental-collapse framework. *Continued from previous page.*

Concept or object	Mathematical form	Interpretation
Neutralization signal loss	$F_{\text{neutral}}(c) = 1 - \frac{\Lambda_{\text{bio}}(E, c)}{\Lambda_{\text{bio}}(E, 0) + \epsilon_{\Lambda}}$	Summarizes the concentration-dependent loss of biological signal under a neutralizing or inhibitory condition.
Morphology-augmented plaque readout	$Y_{\text{PFU}}^{\text{morph}} = (N, M_1, \dots, M_N)$	Extends PFU beyond scalar count by including plaque size, shape, opacity, time-to-visibility, boundary structure, or growth features.
Morphology-augmented biological kernel	$K_E^{\text{morph}, \emptyset}(dN, dM_1, \dots, dM_N x)$	Maps latent states to count and morphology distributions, retaining more information than a count-only plaque readout.

5 Worked Example: The Plaque Assay as Experimental Collapse

The plaque assay provides a simple and instructive example of experimental collapse. In a standard plaque assay, a virus-containing sample is serially diluted, applied to a susceptible cell monolayer, allowed to adsorb, covered with a semi-solid or otherwise spatially restrictive overlay, incubated until localized infection events become visible, and then stained or otherwise read out as a number of plaques. The final observable is a count. The latent process that produces that count is much richer [16, 36, 17, 18, 60].

This makes the plaque assay an especially useful worked example for protocol-resolved virophysics. It is familiar, experimentally concrete, and quantitative, but it is also a strong example of protocol-conditioned projection. A plaque assay does not directly report virion position, orientation, spike presentation, angular velocity, contact geometry, local force history, deformation pathway, or collective branch structure. It also does not directly report total physical particles, total genomes, or total antigen. Instead, it reports a biologically defined functional projection of the latent population: the number of infectious units that successfully generate visible, countable lesions under a specified cell-line, adsorption, overlay, incubation, staining, and counting protocol.

At the most compact level, the plaque assay performs the reduction

$$\begin{array}{c} \text{Latent Virion or Infectious-Unit Population} \\ \Downarrow \\ \text{Protocol-Conditioned Infectious Events} \\ \Downarrow \\ \text{Visible Plaque Count} \end{array} \quad (5.1)$$

Thus, a plaque count is not a direct count of total virions. It is a count of visible infectious lesions generated under particular assay conditions.

Remark 5.1 (Plaque count versus physical particle count). The distinction between physical particles and plaque-forming units is essential. A physical particle may be structurally intact but noninfectious, damaged, neutralized, genome-defective, aggregation-associated, unable to attach to the chosen cells, unable to enter, unable to replicate productively, unable to spread under the overlay, or unable to generate a visible lesion above the counting threshold. Conversely, in the dilute and countable regime, a counted plaque is often interpreted as arising from one infectious unit. That infectious unit need not be identical to one isolated physical virion in every case, especially when aggregation, co-delivery, or collective infectivity are present [37, 39, 38].

Remark 5.2 (Why the plaque assay is a useful worked example). The plaque assay compresses a high-dimensional latent population into a one-dimensional count. This makes the collapse structure unusually clear. Physical particles that differ in morphology, genome integrity, receptor-binding competence, aggregation state, medium history, neutralization state, or cell-entry probability may all

be mapped to the same observed category: plaque-forming or non-plaque-forming under the chosen protocol. The assay is therefore valuable precisely because it reports an experimentally defined functional projection of the population.

Remark 5.3 (Why this is not a criticism of plaque assays). The point is not that plaque assays are unreliable. The point is that they are specific. A plaque assay is powerful because it asks a biologically meaningful question: how much of this sample can produce visible infectious lesions under these conditions? Protocol-resolved notation makes that question explicit rather than treating PFU as a protocol-free particle count.

5.1 Plaque-Assay Protocol as a Collapse Map

The plaque assay is not defined only by the act of counting plaques. It is defined by the full biological and procedural pathway through which a latent particle population is converted into visible lesions. In the notation of the general framework, the plaque assay is a biological observation protocol with a null channel: many latent states enter the assay, but only some generate countable plaques.

Definition 5.4 (Plaque-assay protocol). Let E_{PFU} denote a plaque-assay protocol specified by

$$E_{\text{PFU}} = \left(\begin{array}{l} \text{virus preparation, cell line, cell density or monolayer state, dilution series, } V_{\text{inoc}}, t_{\text{ads}}, \\ \text{wash or medium exchange, overlay composition and thickness, } t_{\text{inc}}, \text{ temperature,} \\ \text{fixation or staining method, plaque-detection threshold, counting rule} \end{array} \right).$$

(5.1.1)

Here V_{inoc} is the plated inoculum volume, t_{ads} is the adsorption time, and t_{inc} is the incubation time before plaque visualization.

Remark 5.5 (What the plaque protocol fixes). The protocol E_{PFU} fixes more than the counting procedure. It fixes the biological environment in which the virus is tested, including the susceptible cell type, receptor and entry context, adsorption window, washing or medium exchange, spatial restriction imposed by the overlay, duration allowed for local amplification, and criterion by which an infection focus becomes a visible plaque. Changing any of these choices can change the plaque-forming probability of the same physical virion population [18, 60].

Remark 5.6 (Overlay as a physical and biological constraint). The overlay is a useful example of protocol mechanics. Its purpose is not merely to make the assay convenient. It restricts long-range spread so that local infection events remain spatially localized and can develop into countable plaques. Overlay composition, viscosity, thickness, and compatibility with the virus–cell system can therefore affect plaque size, shape, visibility, and countability [18, 60].

Definition 5.7 (Latent virion state for the plaque assay). Let $X \in \Psi$ denote the latent state of a virion, particle, aggregate, or infectious unit immediately before the plaque-assay protocol is applied.

For this worked example, X may include

$$X = \left(\begin{array}{l} \text{Particle integrity,} \\ \text{Genome integrity and replication competence,} \\ \text{Spike or receptor-binding competence,} \\ \text{Surface charge and transport state,} \\ \text{Orientation or presentation variables,} \\ \text{Aggregation or co-delivery state,} \\ \text{Neutralization or damage state,} \\ \text{Local medium and handling history} \end{array} \right). \quad (5.1.2)$$

The assay does not report these components separately. It reports whether the latent state contributes to a visible plaque-forming event.

Remark 5.8 (Why the latent object may be an infectious unit). In the simplest dilute interpretation, the latent object is an individual virion. More generally, the plaque-relevant latent object may be an infectious unit: an isolated virion, an aggregate, a co-delivered packet, or another experimentally inseparable unit that behaves as one plaque-producing event under dilution. This wording avoids over-interpreting PFU as a literal count of individual physical virions.

Remark 5.9 (Why plaque competence is composite). A virion does not become plaque-forming merely by existing as a physical particle. It must remain structurally and genetically competent, encounter a susceptible cell, adsorb productively, enter, initiate productive replication, spread locally under the overlay, and generate a visible lesion under the readout conditions. For many viruses, particle number and infectious-unit number can differ substantially; high particle-to-PFU ratios may reflect inert particles, structural defects, incomplete or defective genomes, lethal mutations, aggregation, assay incompatibility, neutralization, decay, or failure to complete one of the required assay steps [37, 39, 40, 38].

5.2 Plaque-Forming Probability as a Protocol Weight

The central protocol-resolved quantity is the probability that a latent state becomes a visible plaque under the specified plaque-assay protocol. For a virologist, this is the state-dependent probability that a particle or infectious unit is plaque-forming in the chosen assay. For the mathematical framework, it is a protocol-dependent biological amplification and detection weight.

Definition 5.10 (Plaque-forming probability of a latent state). Define

$$\pi_{\text{PFU}}(x; E_{\text{PFU}}) = \Pr \left(\begin{array}{l} \text{latent state } x \text{ generates a visible, countable plaque} \\ \text{under the plaque-assay protocol } E_{\text{PFU}} \end{array} \right). \quad (5.2.1)$$

This probability is the plaque-assay analogue of a protocol survival, amplification, and detection weight. It maps a latent state to its probability of producing a visible plaque under a specified assay.

The simplest conceptual statement is

$$\text{Plaque-Forming Probability} = \text{Probability of Passing the Plaque-Assay Pathway.}$$

A more explicit protocol-chain representation is

$$\boxed{\pi_{\text{PFU}}(x; E_{\text{PFU}}) = p_{\text{surv}}(x; E_{\text{PFU}})p_{\text{deliv}}(x; E_{\text{PFU}})p_{\text{ads}}(x; E_{\text{PFU}}) \\ \times p_{\text{entry}}(x; E_{\text{PFU}})p_{\text{rep}}(x; E_{\text{PFU}})p_{\text{spread}}(x; E_{\text{PFU}})p_{\text{vis}}(x; E_{\text{PFU}}).} \quad (5.2.2)$$

The factors represent survival through handling, delivery to the monolayer, productive adsorption, entry, productive replication, local spread under the overlay, and visibility under the final readout criterion.

Remark 5.11 (How to interpret the factorization). Equation (5.2.2) is a reduced protocol-chain model, not a claim that the stages are microscopically independent. More formally, the factors should be read as conditional probabilities along the assay pathway. For example,

$$p_{\text{entry}} = \Pr(\text{entry} \mid \text{survival, delivery, adsorption}, x, E_{\text{PFU}}),$$

and similarly for later factors. The important point is that plaque formation requires the virion or infectious unit to pass through several biological and physical filters. A particle may be physically present but fail to survive handling, fail to reach the cell layer, fail to adsorb, fail to enter, fail to replicate productively, fail to spread locally, or fail to generate a visible plaque above threshold.

Remark 5.12 (Why this probability is protocol-conditioned). The probability $\pi_{\text{PFU}}(x; E_{\text{PFU}})$ belongs to the state–protocol pair. It is not a context-free property of the particle alone. A particle that fails to form a plaque in one cell line, overlay, or incubation condition may be plaque-forming under another protocol. Likewise, a particle that is physically intact may be non-plaque-forming under a protocol that does not support its entry, replication, local spread, or visibility.

Definition 5.13 (Effective plaque-forming concentration). Let $n_{\text{ref}}(x)$ denote the latent number-density distribution of physical particles or infectious units per unit sample volume over the state space Ψ . The *effective plaque-forming concentration* under protocol E_{PFU} is

$$\boxed{\Lambda_{\text{PFU}}(E_{\text{PFU}}) = \int_{\Psi} \pi_{\text{PFU}}(x; E_{\text{PFU}})n_{\text{ref}}(x) dx.} \quad (5.2.3)$$

More generally, if the latent population is represented by a measure rather than a density, the same expression is written as an integral with respect to that measure. The quantity Λ_{PFU} has units of visible plaque-forming events per unit sample volume.

Remark 5.14 (PFU is a protocol-conditioned projection). The concentration Λ_{PFU} is a protocol-conditioned infectious projection of the latent ensemble. It is not the same as the total physical particle concentration

$$C_{\text{part}} = \int_{\Psi} n_{\text{ref}}(x) dx. \quad (5.2.4)$$

The two quantities are related only through the state-dependent plaque-forming probability π_{PFU} . This is why two samples with similar particle counts can have different plaque titers, and why two samples with different latent state distributions can produce similar plaque counts if their protocol-weighted plaque-forming concentrations agree.

Definition 5.15 (Particle-to-PFU ratio). When an independent particle-counting, genome-counting, or antigen-counting measurement is available and $\Lambda_{\text{PFU}} > 0$, define the particle-to-PFU ratio by

$$\mathcal{R}_{\text{part/PFU}} = \frac{C_{\text{part}}}{\Lambda_{\text{PFU}}}. \quad (5.2.5)$$

This ratio summarizes how strongly the physical particle ensemble is compressed by the plaque-forming projection.

Remark 5.16 (Interpretation of the particle-to-PFU ratio). A large $\mathcal{R}_{\text{part/PFU}}$ does not by itself identify a single cause. It may reflect noninfectious particles, damaged particles, incomplete or defective genomes, lethal mutations, unfavorable adsorption, low entry efficiency, aggregation, protocol mismatch, host-cell incompatibility, neutralization, or readout limitations. In the present framework, all of these possibilities correspond to different mechanisms by which the latent ensemble is filtered before becoming a visible plaque count [37, 39, 40].

Remark 5.17 (Why independent particle measurements matter). A plaque assay by itself estimates a protocol-weighted infectious concentration. It does not determine the total particle concentration or the fraction of particles that are structurally intact, genome-containing, antigen-positive, entry-competent, or replication-competent. Independent measurements such as particle counting, genome quantification, antigen measurement, or structural imaging can therefore be combined with PFU data to separate physical abundance from plaque-forming efficiency. In the language of this paper, such measurements add additional protocol kernels that constrain different latent sectors.

5.3 Plaque-Count Statistics in the Dilute Regime

Once the effective plaque-forming concentration Λ_{PFU} has been defined, the standard plaque-count statistics arise as a dilute-regime closure of the biological kernel. This is the regime in which plaque-forming events are sufficiently rare to be spatially separable, sufficiently independent to be treated as isolated infectious events, and sufficiently numerous in the selected dilution range to support quantitative counting.

The simplest statistical statement is

$$\begin{aligned} \text{Expected plaque count} &= \text{Plated volume} \\ &\quad \times \text{Dilution fraction} \\ &\quad \times \text{Effective plaque-forming} \\ &\quad \quad \text{concentration} \end{aligned} \quad (5.3.1)$$

The effective plaque-forming concentration is not the total physical particle concentration. It is the protocol-weighted concentration Λ_{PFU} produced by the state-dependent plaque-forming probability

$\pi_{\text{PFU}}(x; E_{\text{PFU}})$.

Proposition 5.18 (Poisson plaque-count model in the dilute limit). *Let $f_d \in (0, 1]$ denote the dilution fraction plated in a given well, and let V_{inoc} be the plated inoculum volume. In the dilute, independent, non-overlapping-plaque regime, the observed plaque count N_d may be modeled as*

$$\boxed{N_d \sim \text{POISSON}(V_{\text{inoc}} f_d \Lambda_{\text{PFU}}(E_{\text{PFU}}))}. \quad (5.3.2)$$

Consequently, a basic single-dilution estimator of the effective plaque-forming concentration is

$$\hat{\Lambda}_{\text{PFU},d} = \frac{N_d}{V_{\text{inoc}} f_d}. \quad (5.3.3)$$

Proof. The expected number of plated latent units with state in dx is

$$V_{\text{inoc}} f_d n_{\text{ref}}(x) dx.$$

Each such latent unit contributes a visible plaque with probability $\pi_{\text{PFU}}(x; E_{\text{PFU}})$. Under dilute independent thinning, the plaque-forming events form an approximately Poisson process with intensity

$$V_{\text{inoc}} f_d \pi_{\text{PFU}}(x; E_{\text{PFU}}) n_{\text{ref}}(x) dx.$$

Integrating over the latent state space gives the mean

$$V_{\text{inoc}} f_d \int_{\Psi} \pi_{\text{PFU}}(x; E_{\text{PFU}}) n_{\text{ref}}(x) dx = V_{\text{inoc}} f_d \Lambda_{\text{PFU}}(E_{\text{PFU}}).$$

Thus N_d is Poisson with the stated mean in the dilute independent-event limit. \square

Remark 5.19 (What the Poisson model assumes biologically). The Poisson approximation assumes that plaque-forming events are rare, independent, spatially separable, and countable after dilution. It also assumes that each counted plaque corresponds to one effective plaque-forming event in the selected dilution range. These assumptions are useful for standard plaque-titer estimation, but they are protocol-regime assumptions rather than universal features of plaque assays. Aggregation, plaque merging, cell-layer heterogeneity, uneven adsorption, localized spread effects, and counting thresholds can all produce departures from the Poisson ideal.

Remark 5.20 (Connection to the usual titer formula). If the dilution is reported as a dilution factor $D_d = 1/f_d$, then Eq. (5.3.3) becomes the usual plaque-titer form

$$\hat{\Lambda}_{\text{PFU},d} = \frac{N_d D_d}{V_{\text{inoc}}}. \quad (5.3.4)$$

Thus the standard PFU per unit volume calculation is recovered as the simplest estimator of the protocol-weighted concentration Λ_{PFU} , usually after selecting a dilution whose plaques are countable and sufficiently separated.

Definition 5.21 (Dilution-series likelihood). Suppose plaque counts are collected across dilution

fractions f_1, \dots, f_J , with replicate wells indexed by $r = 1, \dots, R_j$. Let N_{jr} be the plaque count in replicate r at dilution f_j . Under the dilute-regime Poisson model,

$$N_{jr} \sim \text{Poisson}(V_{\text{inoc}} f_j \Lambda_{\text{PFU}}). \quad (5.3.5)$$

The corresponding likelihood is

$$\mathcal{L}_{\text{PFU}}(\Lambda_{\text{PFU}}) = \prod_{j=1}^J \prod_{r=1}^{R_j} \frac{(V_{\text{inoc}} f_j \Lambda_{\text{PFU}})^{N_{jr}} e^{-V_{\text{inoc}} f_j \Lambda_{\text{PFU}}}}{N_{jr}!}. \quad (5.3.6)$$

Proposition 5.22 (Maximum-likelihood estimator for a dilution series). *Under the likelihood in Eq. (5.3.6), using only wells treated as exact count observations, the maximum-likelihood estimator is*

$$\hat{\Lambda}_{\text{PFU}}^{\text{MLE}} = \frac{\sum_{j=1}^J \sum_{r=1}^{R_j} N_{jr}}{V_{\text{inoc}} \sum_{j=1}^J R_j f_j}. \quad (5.3.7)$$

Proof. The log-likelihood is

$$\log \mathcal{L}_{\text{PFU}} = \sum_{j,r} [N_{jr} \log(V_{\text{inoc}} f_j \Lambda_{\text{PFU}}) - V_{\text{inoc}} f_j \Lambda_{\text{PFU}} - \log(N_{jr}!)].$$

Differentiating with respect to Λ_{PFU} gives

$$\frac{\partial}{\partial \Lambda_{\text{PFU}}} \log \mathcal{L}_{\text{PFU}} = \frac{1}{\Lambda_{\text{PFU}}} \sum_{j,r} N_{jr} - V_{\text{inoc}} \sum_j R_j f_j.$$

Setting this derivative equal to zero gives Eq. (5.3.7). □

Remark 5.23 (Why the dilution-series likelihood is useful). The usual plaque-titer calculation often uses a countable dilution range and a simple dilution correction. The likelihood form makes the statistical assumptions explicit and allows replicate wells, multiple dilutions, uncertainty intervals, and model extensions to be handled in a unified way. It also makes clear that the inferred quantity is Λ_{PFU} , the protocol-weighted plaque-forming concentration, not the total physical particle concentration.

Remark 5.24 (Countable dilution ranges and censored wells). In laboratory practice, very dense wells may be recorded as too numerous to count, while very sparse wells may provide little information beyond a zero or near-zero count. A more complete likelihood can treat such wells as censored or thresholded observations rather than as exact counts. This does not change the definition of Λ_{PFU} . It changes the statistical readout model R_E for how plaque-forming events become recorded data.

Remark 5.25 (Scope of the Poisson approximation). The Poisson model is the natural first closure when plaque-forming events are rare, independent, and spatially non-overlapping. At high

concentrations, plaques can overlap, merge, compete for susceptible cells, or become difficult to count. At very low concentrations, sampling noise dominates. Across replicate wells, additional variability may arise from plating heterogeneity, cell-monolayer variation, pipetting error, aggregation, local differences in adsorption and spread, overlay thickness, incubation conditions, staining contrast, or counting thresholds. These effects can be represented by overdispersed, zero-inflated, spatial, or censored count models when needed.

Definition 5.26 (Overdispersed plaque-count model). When replicate counts exhibit variance larger than the Poisson mean, an overdispersed count model may be used. One convenient representation is

$$N_{jr} \sim \text{NegBin}(\mu_{jr}, \kappa), \quad \mu_{jr} = V_{\text{inoc}} f_j \Lambda_{\text{PFU}}, \quad (5.3.8)$$

with variance, for one common parameterization,

$$\text{Var}(N_{jr}) = \mu_{jr} + \frac{\mu_{jr}^2}{\kappa}. \quad (5.3.9)$$

The parameter $\kappa > 0$ controls overdispersion; the Poisson limit is recovered as $\kappa \rightarrow \infty$. This changes the statistical model for count fluctuations, not the definition of Λ_{PFU} .

Remark 5.27 (Aggregation and non-independent infectious units). The dilute Poisson model treats plaque-forming events as independent. Viral aggregation, co-delivery, cell-to-cell heterogeneity, local clustering, collective infection, or spatially correlated susceptibility can violate this assumption. In the experimental-collapse framework, such effects do not invalidate the plaque assay. They indicate that the latent object being counted may not be a single isolated physical virion, but an assay-conditioned infectious unit, aggregate, or co-delivered packet. This is one reason Λ_{PFU} should be interpreted as an effective plaque-forming concentration rather than as a direct concentration of individual physical virions.

5.4 Single-Unit Readout Kernel and Null Channel

The preceding count model describes the aggregate number of visible plaques. It is also useful to write the corresponding single-unit readout, because this makes the null channel explicit. In this subsection, a “unit” means whatever latent assay unit behaves as one independent plaque-forming opportunity under the dilution model: often a single virion, but potentially an aggregate, co-delivered packet, or other experimentally inseparable infectious unit.

Definition 5.28 (Single-unit plaque-assay readout kernel). For a single latent state x , define the binary plaque-event variable

$$B \in \{0, 1\},$$

with the interpretation

$$B = \begin{cases} 1, & x \text{ produces a visible, countable plaque under } E_{\text{PFU}}, \\ 0, & x \text{ does not produce a visible, countable plaque.} \end{cases} \quad (5.4.1)$$

The protocol-conditioned plaque-forming probability is

$$\Pr(B = 1 \mid x, E_{\text{PFU}}) = \pi_{\text{PFU}}(x; E_{\text{PFU}}). \quad (5.4.2)$$

Equivalently, the single-unit readout is described by the Bernoulli kernel

$$\boxed{K_{\text{PFU}}^{\emptyset}(B \mid x) = [\pi_{\text{PFU}}(x; E_{\text{PFU}})]^B [1 - \pi_{\text{PFU}}(x; E_{\text{PFU}})]^{1-B},} \quad (5.4.3)$$

$$B \in \{0, 1\}.$$

Thus, $K_{\text{PFU}}^{\emptyset}$ assigns probability $\pi_{\text{PFU}}(x; E_{\text{PFU}})$ to the plaque-producing outcome and probability $1 - \pi_{\text{PFU}}(x; E_{\text{PFU}})$ to the non-plaque outcome. The macroscopic plaque count N_d is then obtained by summing these binary plaque events over the diluted plated population, under the additional assumptions of dilution, independence, and non-overlap.

Remark 5.29 (Why “single-unit” is used). The phrase “single-unit” is used instead of “single-virion” because the plaque-producing unit may not always be one isolated physical virion. In many standard dilute applications, the single-virion approximation is appropriate. However, aggregation, co-delivery, or collective infection can make the plaque-relevant unit larger than one physical particle. The Bernoulli readout kernel applies to whatever latent unit the assay treats as one independent plaque-forming opportunity.

Remark 5.30 (Null observation in the plaque assay). For a plaque assay, the null channel includes all latent states that fail to produce a visible counted plaque. The null state is therefore not a single biological mechanism. It includes units that are absent from the plated inoculum, fail to survive handling, do not reach a susceptible cell, fail to adsorb or enter, enter but do not replicate productively, spread too weakly to remain visible under the overlay, merge with neighboring lesions, or remain below the detection or counting threshold.

Remark 5.31 (What collapses in the plaque assay). The plaque assay collapses many latent distinctions into one binary event: plaque or no plaque. A virion that is structurally intact but noninfectious, a virion that is infectious in principle but fails to adsorb during t_{ads} , a virion that enters but does not replicate productively in the chosen cell line, a virion whose local spread is suppressed by the overlay or incubation conditions, and a virion whose plaque is obscured, merged, or below threshold may all be absent from the final count. The observed plaque number therefore compresses structural, mechanical, environmental, and biological variation into a protocol-conditioned visible-infection event.

Table 20. Experimental-collapse mechanisms in the plaque assay. A standard virological protocol implements the abstract collapse structure through transport, contact, replication, spread, visibility, and counting stages.

Collapse mechanism	Plaque-assay realization	Observed consequence
Transport conditioning	Dilution, mixing, inoculum volume, and local transport toward the cell layer	Only units delivered to susceptible cells within the adsorption window can contribute.
Surface or contact conditioning	Adsorption to the cell monolayer, receptor engagement, and local membrane contact	States with poor adsorption, receptor binding, or entry competence are suppressed.
Preparation or handling conditioning	Storage, freeze–thaw history, buffer exchange, dilution, washing, and overlay addition	Units that lose infectious competence before readout do not contribute.
Replication filtering	Cell-line compatibility, entry, genome release, replication, and production of infectious progeny	Units that enter but fail to amplify locally are not counted as PFU.
Spread and overlay filtering	Semi-solid overlay, local diffusion limits, cell-to-cell spread, and incubation time	Only infection events that grow into visible local lesions are counted.
Geometry or visibility selection	Plaque size, plaque separation, staining contrast, thresholding, and countability	Foci that are merged, too small, too diffuse, or below threshold may be undercounted.

5.5 Plaque-Assay Protocol Blindness

The plaque assay is highly sensitive to one composite direction in latent state space: the direction that changes visible plaque formation under the chosen protocol. It is comparatively blind to latent distinctions that do not alter the state-dependent plaque-forming probability

$$\pi_{\text{PFU}}(x; E_{\text{PFU}})$$

under those conditions. Thus, plaque-count data are informative about assay-conditioned infectious activity, but they are not an injective observation of the full physical, structural, mechanical, or genomic virion ensemble.

Remark 5.32 (Protocol blindness in the plaque assay). Two latent virion subpopulations may differ strongly in orientation distribution, spike presentation mechanics, rotational diffusion, collision history, aggregation pathway, charge state, genome integrity, morphology, or preparation history. If those differences do not change π_{PFU} under E_{PFU} , then they are invisible to the plaque count at leading order. Conversely, a small physical or biochemical difference that strongly affects adsorption, entry, replication, local spread, or visibility may have a large effect on PFU.

Proposition 5.33 (Many latent ensembles can yield the same expected plaque count). *Let*

$n_1(x)$ and $n_2(x)$ be two latent number-density distributions over Ψ . If

$$\int_{\Psi} \pi_{\text{PFU}}(x; E_{\text{PFU}}) n_1(x) dx = \int_{\Psi} \pi_{\text{PFU}}(x; E_{\text{PFU}}) n_2(x) dx, \quad (5.5.1)$$

then the two ensembles have the same expected plaque count at every dilution in the dilute Poisson regime, even if n_1 and n_2 differ substantially as latent mechanical, structural, genomic, or biochemical ensembles.

Proof. Under the dilute Poisson plaque-count model,

$$\mathbb{E}[N_d] = V_{\text{inoc}} f_d \int_{\Psi} \pi_{\text{PFU}}(x; E_{\text{PFU}}) n(x) dx.$$

If the protocol-weighted integrals agree for n_1 and n_2 , then

$$\mathbb{E}_{n_1}[N_d] = \mathbb{E}_{n_2}[N_d]$$

for every dilution fraction f_d . Therefore plaque counts alone cannot distinguish these two latent ensembles in the dilute regime. \square

Remark 5.34 (Interpretation of the non-identifiability result). This proposition is the plaque-assay version of protocol blindness. The assay is extremely valuable for measuring infectious titer under specified conditions, but it is not an injective map from latent virion mechanics to observed data. It reports a biologically important projection of the ensemble, not the ensemble itself.

Definition 5.35 (Plaque-assay observation equivalence). Two latent number-density distributions n_1 and n_2 are *PFU-equivalent* under protocol E_{PFU} , written

$$n_1 \sim_{\text{PFU}} n_2,$$

if they induce the same effective plaque-forming concentration:

$$\boxed{\int_{\Psi} \pi_{\text{PFU}}(x; E_{\text{PFU}}) n_1(x) dx = \int_{\Psi} \pi_{\text{PFU}}(x; E_{\text{PFU}}) n_2(x) dx.} \quad (5.5.2)$$

Remark 5.36 (Plaque assay as a quotient of latent ensemble space). The relation in Eq. (5.5.2) is the plaque-assay version of the quotient viewpoint introduced earlier. Many distinct latent ensembles are collapsed into the same PFU-equivalence class. The observed plaque count distinguishes those classes only through the scalar Λ_{PFU} , unless additional measurements, richer plaque morphology, endpoint structure, or protocol variations are introduced.

Remark 5.37 (What PFU-equivalence does and does not imply). PFU-equivalence does not imply that two samples have the same number of physical particles, the same genome content, the same structural integrity, or the same distribution of latent states. It means only that the plaque protocol assigns them the same weighted plaque-forming concentration. This distinction is central to interpreting particle-to-PFU ratios and to combining PFU assays with particle counting, genome quantification, antigen measurement, structural imaging, or single-particle measurements.

Remark 5.38 (Transition to the two-subpopulation reduction). The next step is to reduce the latent ensemble to two sectors: a plaque-competent sector and a plaque-incompetent, weakly competent, or assay-incompatible sector. This reduction is intentionally simple, but it exposes the essential inverse problem. A plaque count estimates a weighted sum over latent subpopulations; it does not, by itself, reveal how much of the sample belongs to each sector.

5.6 Two-Subpopulation Reduction

The general plaque-assay collapse integral

$$\Lambda_{\text{PFU}}(E_{\text{PFU}}) = \int_{\Psi} \pi_{\text{PFU}}(x; E_{\text{PFU}}) n_{\text{ref}}(x) dx$$

is the essential mathematical statement of the worked example. The plaque assay does not report the full latent ensemble. It reports a protocol-weighted infectious projection of that ensemble. To make the resulting inverse problem explicit, it is useful to reduce the latent population to two subpopulations.

This reduction should be read as protocol-aware. The two sectors are not necessarily “infectious” and “noninfectious” in an absolute biological sense. They are plaque-competent and plaque-incompetent, weakly competent, or assay-incompatible relative to the specified protocol E_{PFU} . A particle that is non-plaque-forming in one cell line, overlay, incubation time, or staining condition may be more competent under another protocol.

Definition 5.39 (Two-subpopulation plaque reduction). Suppose the latent number-density distribution decomposes as

$$n_{\text{ref}}(x) = n_{\text{C}}(x) + n_{\text{I}}(x), \quad (5.6.1)$$

where n_{C} denotes plaque-competent states and n_{I} denotes plaque-incompetent, weakly competent, damaged, defective, neutralized, aggregated, or assay-incompatible states. Define the corresponding physical concentrations

$$C_{\text{C}} = \int_{\Psi} n_{\text{C}}(x) dx, \quad C_{\text{I}} = \int_{\Psi} n_{\text{I}}(x) dx, \quad C_{\text{part}} = C_{\text{C}} + C_{\text{I}}. \quad (5.6.2)$$

When $C_{\text{C}} > 0$ and $C_{\text{I}} > 0$, define the subpopulation-averaged plaque-forming probabilities

$$\bar{p}_{\text{C}}(E_{\text{PFU}}) = \frac{\int_{\Psi} \pi_{\text{PFU}}(x; E_{\text{PFU}}) n_{\text{C}}(x) dx}{C_{\text{C}}}, \quad \bar{p}_{\text{I}}(E_{\text{PFU}}) = \frac{\int_{\Psi} \pi_{\text{PFU}}(x; E_{\text{PFU}}) n_{\text{I}}(x) dx}{C_{\text{I}}}. \quad (5.6.3)$$

Then the effective plaque-forming concentration is exactly

$$\boxed{\Lambda_{\text{PFU}} = \bar{p}_{\text{C}} C_{\text{C}} + \bar{p}_{\text{I}} C_{\text{I}}.} \quad (5.6.4)$$

Proof. Using $n_{\text{ref}} = n_{\text{C}} + n_{\text{I}}$,

$$\Lambda_{\text{PFU}} = \int_{\Psi} \pi_{\text{PFU}}(x; E_{\text{PFU}}) n_{\text{C}}(x) dx + \int_{\Psi} \pi_{\text{PFU}}(x; E_{\text{PFU}}) n_{\text{I}}(x) dx.$$

By the definitions of \bar{p}_C and \bar{p}_I , these two terms are

$$\bar{p}_C C_C \quad \text{and} \quad \bar{p}_I C_I,$$

respectively. Hence

$$\Lambda_{\text{PFU}} = \bar{p}_C C_C + \bar{p}_I C_I.$$

□

Remark 5.40 (Why the averaged probabilities are preferable). The averaged quantities \bar{p}_C and \bar{p}_I are more rigorous than assigning a single microscopic probability to every member of a subpopulation. They allow each sector to remain internally heterogeneous. A plaque-competent sector may contain particles with different adsorption probabilities, entry probabilities, replication efficiencies, and local-spread efficiencies. A plaque-incompetent sector may contain particles that are completely non-plaque-forming together with particles that are weakly competent under some assay conditions. Thus the two-subpopulation model reduces the latent ensemble without assuming that either sector is microscopically uniform.

Remark 5.41 (Protocol dependence of the two sectors). The labels C and I should be interpreted relative to the protocol. A state may belong effectively to the plaque-competent sector for one cell line or overlay condition and to a weakly competent or assay-incompatible sector for another. This is not a contradiction. It reflects the fact that plaque competence is a property of the latent state together with the assay environment.

Corollary 5.42 (Constant-probability approximation). *If the plaque-forming probability is approximately constant within each subpopulation,*

$$\begin{aligned} \pi_{\text{PFU}}(x; E_{\text{PFU}}) &\approx p_C, \quad x \in \Psi_C, \\ \pi_{\text{PFU}}(x; E_{\text{PFU}}) &\approx p_I, \quad x \in \Psi_I. \end{aligned} \tag{5.6.5}$$

where Ψ_C denotes the plaque-competent sector and Ψ_I denotes the plaque-incompetent or weakly competent sector. Then,

$$\boxed{\Lambda_{\text{PFU}} \approx p_C C_C + p_I C_I.} \tag{5.6.6}$$

Remark 5.43 (What the two-subpopulation reduction demonstrates). If $p_I \approx 0$, the plaque assay is effectively blind to the plaque-incompetent subpopulation, even if that subpopulation dominates the physical particle count. Conversely, changes in p_C caused by cell line, adsorption time, buffer conditions, overlay composition, incubation time, temperature, or readout threshold can change Λ_{PFU} without changing the total number of physical particles. This is the simplest mathematical demonstration of why PFU is a protocol-conditioned infectious projection rather than a direct physical particle count.

5.6.1 Competent Fraction and Particle-to-PFU Compression

The two-subpopulation model becomes especially transparent when written in terms of the plaque-competent fraction of the physical particle population. This form separates three quantities that are

often compressed into a single PFU measurement: total physical abundance, the fraction of particles in a plaque-competent sector, and the protocol-dependent efficiency with which each sector produces visible plaques.

Definition 5.44 (Plaque-competent fraction). Define the plaque-competent fraction by

$$\varphi_C = \frac{C_C}{C_{\text{part}}}, \quad 1 - \varphi_C = \frac{C_I}{C_{\text{part}}}, \quad (5.6.1.1)$$

where

$$C_{\text{part}} = C_C + C_I.$$

Under the constant-probability approximation, the effective plaque-forming concentration can be written as

$$\Lambda_{\text{PFU}} = C_{\text{part}} [p_I + (p_C - p_I)\varphi_C]. \quad (5.6.1.2)$$

Proof. From the two-subpopulation approximation,

$$\Lambda_{\text{PFU}} = p_C C_C + p_I C_I.$$

Using

$$C_C = \varphi_C C_{\text{part}}, \quad C_I = (1 - \varphi_C) C_{\text{part}},$$

gives

$$\Lambda_{\text{PFU}} = C_{\text{part}} [p_C \varphi_C + p_I (1 - \varphi_C)] = C_{\text{part}} [p_I + (p_C - p_I)\varphi_C].$$

□

Remark 5.45 (What a plaque assay can and cannot infer). Equation (5.6.1.2) shows that a plaque assay alone identifies the combination

$$C_{\text{part}} [p_I + (p_C - p_I)\varphi_C],$$

not C_{part} , p_C , p_I , and φ_C separately. Additional information is required to separate physical particle concentration from plaque competence and protocol-dependent plaque-forming efficiency. This is the two-subpopulation version of protocol non-identifiability.

Definition 5.46 (Two-subpopulation particle-to-PFU ratio). Assume $\Lambda_{\text{PFU}} > 0$. Under the constant-probability two-subpopulation approximation, the particle-to-PFU ratio is

$$\mathcal{R}_{\text{part}/\text{PFU}} = \frac{C_{\text{part}}}{\Lambda_{\text{PFU}}} = \frac{1}{p_I + (p_C - p_I)\varphi_C}. \quad (5.6.1.3)$$

Remark 5.47 (Interpretation of the two-subpopulation ratio). A large particle-to-PFU ratio can arise for several distinct reasons: φ_C may be small; p_C may be small under the chosen protocol; p_I may be effectively zero; or the assay conditions may suppress one or more stages of plaque formation. The ratio is therefore not a single mechanistic explanation. It is a compressed summary of latent composition and protocol efficiency [37, 39, 40, 38].

Remark 5.48 (Compression interpretation). The factor

$$p_I + (p_C - p_I)\varphi_C$$

is the average plaque-forming probability of a randomly selected physical particle or assay unit under the protocol. The particle-to-PFU ratio is the reciprocal of this average probability. Thus particle-to-PFU compression quantifies how strongly the physical particle ensemble is reduced when viewed through the plaque-forming projection.

5.6.2 Special Cases

The two-subpopulation formula is useful because several familiar virological situations appear as simple limiting cases.

Remark 5.49 (Nearly ideal competent sector). If $p_C \approx 1$ and $p_I \approx 0$, then

$$\Lambda_{\text{PFU}} \approx C_C, \quad \mathcal{R}_{\text{part/PFU}} \approx \frac{1}{\varphi_C}.$$

In this idealized limit, the particle-to-PFU ratio approximately reports the inverse of the competent fraction. This interpretation fails if competent particles have $p_C < 1$, if weakly competent particles have $p_I > 0$, or if aggregation, co-delivery, or collective infection changes the effective plaque-forming unit.

Remark 5.50 (Assay suppression of otherwise competent particles). If $p_C \ll 1$ under a given protocol, then even a sample with a large competent physical subpopulation may produce a low PFU titer. Biologically, this may occur because the chosen cell line is poorly susceptible, adsorption time is short, the overlay suppresses local spread, incubation time is insufficient, temperature or medium conditions are unfavorable, or the readout threshold is high. In this case, low PFU does not necessarily imply absence of physically competent particles; it may indicate poor assay coupling to the competent sector.

Remark 5.51 (Weakly competent or conditionally competent sector). If $p_I > 0$, the nominally incompetent sector is not truly invisible. It may contain weakly competent, partially damaged, semi-infectious, cell-line-dependent, or conditionally competent states. Such states contribute weakly to Λ_{PFU} and may become more visible under protocol variation. This is one reason that the labels C and I should be treated as reduced modeling sectors rather than absolute biological categories.

Remark 5.52 (Protocol change can move states between effective sectors). The same physical state may be effectively plaque-incompetent under one protocol and weakly or strongly plaque-competent under another. Changing the cell line, adsorption time, overlay composition, incubation time, temperature, neutralization condition, or staining threshold changes the biological kernel and can therefore change the effective values of p_C , p_I , and even the sector assignment implicit in φ_C . This prepares the protocol-variation argument in the next subsection.

5.6.3 Non-Identifiability from PFU Alone

Proposition 5.53 (Non-identifiability from PFU alone). *Suppose the plaque count identifies only*

$$\Lambda_{\text{PFU}} = p_C C_C + p_I C_I.$$

Then C_C , C_I , p_C , and p_I are not jointly identifiable from plaque counts alone.

Proof. A plaque count in the dilute Poisson regime depends on the subpopulation parameters only through the scalar

$$\Lambda_{\text{PFU}} = p_C C_C + p_I C_I.$$

There are infinitely many parameter quadruples

$$(C_C, C_I, p_C, p_I)$$

that yield the same scalar value. For example, if $p_I = 0$, then

$$\Lambda_{\text{PFU}} = p_C C_C.$$

Multiplying p_C by a factor $a > 0$ and dividing C_C by the same factor leaves Λ_{PFU} unchanged whenever the transformed probability remains in the admissible range $0 \leq ap_C \leq 1$. Therefore the individual subpopulation sizes and plaque-forming probabilities are not identifiable from PFU data alone. \square

Remark 5.54 (Interpretation of the non-identifiability). This proposition does not weaken the plaque assay. It clarifies its target. The assay is designed to estimate an effective infectious concentration under a specified protocol. It is not designed, by itself, to decompose that concentration into physical particle abundance, competent fraction, adsorption probability, entry probability, replication competence, local spread, and visibility threshold. Those decompositions require additional measurements, controlled protocol variation, or prior biological assumptions.

Remark 5.55 (A single PFU value is a weighted sum, not a composition). A PFU estimate reports the weighted sum

$$p_C C_C + p_I C_I.$$

It does not report the mixture composition (C_C, C_I) , nor does it report the stage-specific probabilities that determine p_C and p_I . This is why samples with different latent compositions can yield the same PFU titer, and why identical physical particle counts can yield different PFU titers.

5.6.4 Using Additional Measurements to Resolve the Two Populations

The two-subpopulation model also shows how complementary protocols can reduce plaque-assay blindness. Suppose an independent particle-counting, genome-counting, antigen-counting, or structural measurement provides information about C_{part} or about the composition of the physical particle population. Then the plaque assay and the auxiliary measurement together can begin to separate physical abundance from plaque-forming efficiency.

Proposition 5.56 (Competent fraction from particle count and PFU count). *Assume the constant-probability two-subpopulation model, with $p_C \neq p_I$, and suppose both C_{part} and Λ_{PFU} are known.*

Then

$$\varphi_C = \frac{\Lambda_{\text{PFU}}/C_{\text{part}} - p_I}{p_C - p_I}. \quad (5.6.4.1)$$

Proof. Starting from Eq. (5.6.1.2),

$$\frac{\Lambda_{\text{PFU}}}{C_{\text{part}}} = p_I + (p_C - p_I)\varphi_C.$$

Solving for φ_C gives Eq. (5.6.4.1). □

Remark 5.57 (Why calibration matters). Equation (5.6.4.1) is useful only if p_C and p_I are known, estimated, or constrained by additional experiments. If these probabilities are unknown, then adding a particle count separates total physical abundance from the infectious projection, but it still does not uniquely determine which biological stage limits plaque formation.

Remark 5.58 (What auxiliary measurements contribute). Different auxiliary measurements constrain different latent sectors. A particle count constrains physical abundance. A genome count constrains genome-containing material. An antigen measurement constrains protein-bearing material. Structural imaging constrains morphology and particle integrity. A neutralization or receptor-binding assay constrains entry-related competence. None of these measurements is identical to PFU, but that is precisely why they are useful: each adds a different protocol-conditioned projection of the latent population.

Remark 5.59 (Transition to protocol variation). Auxiliary measurements constrain the latent composition from outside the plaque assay. Protocol variation provides a complementary strategy from within the biological assay itself. By changing cell line, adsorption time, overlay, incubation time, neutralization condition, or readout threshold, one changes the effective values of p_C and p_I . The next subsection uses this idea to treat protocol variation as a two-subpopulation design problem.

5.6.5 Protocol Variation as a Two-Subpopulation Design

Controlled plaque-assay variation can reduce the non-identifiability exposed by the two-subpopulation model. The goal is not to vary assay conditions arbitrarily, but to vary them in ways that change the plaque-forming probabilities of the two latent sectors differently. In this sense, protocol variation is a design tool: it changes the biological observation kernel so that previously confounded subpopulations may become distinguishable.

Definition 5.60 (Protocol variation as a two-subpopulation design). Let E_1, \dots, E_M be plaque-assay protocols that differ in cell line, adsorption time, overlay composition, incubation time, temperature, readout threshold, neutralization condition, receptor availability, or another controlled protocol variable. Under the constant-probability two-subpopulation approximation, each protocol produces an effective plaque-forming concentration

$$\Lambda_m = p_C^{(m)}C_C + p_I^{(m)}C_I, \quad m = 1, \dots, M, \quad (5.6.5.1)$$

where $p_C^{(m)}$ and $p_I^{(m)}$ are the protocol-conditioned plaque-forming probabilities of the competent and

incompetent or weakly competent sectors under E_m . In matrix form,

$$\Lambda = \mathbf{P}\mathbf{C}, \quad \mathbf{P} = \begin{pmatrix} p_C^{(1)} & p_I^{(1)} \\ \vdots & \vdots \\ p_C^{(M)} & p_I^{(M)} \end{pmatrix}, \quad \mathbf{C} = \begin{pmatrix} C_C \\ C_I \end{pmatrix}. \quad (5.6.5.2)$$

Proposition 5.61 (Rank condition for resolving two subpopulations). *In the ideal noiseless setting, the concentrations (C_C, C_I) are identifiable from Λ only if*

$$\boxed{\text{rank}(\mathbf{P}) = 2.} \quad (5.6.5.3)$$

Proof. The system

$$\Lambda = \mathbf{P}\mathbf{C}$$

has a unique solution for the two-dimensional vector \mathbf{C} only if the two columns of \mathbf{P} are linearly independent. This is exactly the condition

$$\text{rank}(\mathbf{P}) = 2.$$

If the rank is one or zero, then at least one nonzero direction in (C_C, C_I) -space lies in the null space of \mathbf{P} , so different subpopulation concentrations produce the same vector of effective plaque-forming concentrations. \square

Remark 5.62 (Interpretation of the rank condition). Varying a protocol is useful only if it changes the plaque-forming probabilities of the two subpopulations differently. If every protocol merely scales p_C and p_I by the same factor, then the columns of \mathbf{P} remain effectively collinear and the two sectors remain confounded. A useful protocol variation is one that changes the observation kernel in a direction that separates latent sectors.

Remark 5.63 (Examples of useful plaque-assay variations). Changing cell line can alter receptor usage, entry, replication, or local spread. Changing adsorption time can alter the probability that particles reach and bind susceptible cells. Changing overlay composition can alter local spread, plaque morphology, and countability. Changing incubation time can alter whether weak, slow, or delayed infection events become visible. Changing staining or reporter threshold can alter final visibility. Adding a neutralization or receptor-blocking condition can preferentially suppress some latent sectors. Each variation changes the biological protocol kernel and can, in principle, expose a different mixture of latent subpopulations.

Remark 5.64 (Calibration versus identification). The rank condition assumes that the protocol probability matrix \mathbf{P} is known, calibrated, estimated, or otherwise constrained. If the entries $p_C^{(m)}$ and $p_I^{(m)}$ are unknown, then protocol variation alone does not automatically identify (C_C, C_I) . In that case, the experiment identifies a combined inverse problem involving both subpopulation concentrations and protocol-specific plaque-forming probabilities. Additional calibration, prior biological information, auxiliary measurements, or stronger model structure is then required.

5.6.6 Fisher Information in the Two-Subpopulation Plaque Model

The same identifiability issue can be expressed locally through Fisher information. For a single dilution fraction f_d , the Poisson mean is

$$\mu_d = V_{\text{inoc}} f_d (p_C C_C + p_I C_I).$$

Let

$$\theta = (C_C, C_I)^\top, \quad \mathbf{p} = (p_C, p_I)^\top.$$

Then

$$\mu_d = V_{\text{inoc}} f_d \mathbf{p}^\top \theta.$$

Proposition 5.65 (Rank-one Fisher information for a single plaque protocol). *For a single plaque-assay protocol in the two-subpopulation Poisson model, the Fisher information for*

$$\theta = (C_C, C_I)^\top$$

is

$$\mathcal{I}_E(\theta) = \frac{(V_{\text{inoc}} f_d)^2}{\mu_d} \mathbf{p} \mathbf{p}^\top. \quad (5.6.6.1)$$

Therefore, if $\mathbf{p} \neq 0$, the Fisher matrix has rank one and only the concentration combination

$$p_C C_C + p_I C_I$$

is locally identifiable from that protocol alone.

Proof. For a Poisson random variable with mean $\mu_d(\theta)$, the Fisher information is

$$\mathcal{I}_E(\theta) = \frac{1}{\mu_d} \nabla_\theta \mu_d \nabla_\theta \mu_d^\top.$$

Since

$$\nabla_\theta \mu_d = V_{\text{inoc}} f_d \mathbf{p},$$

we obtain Eq. (5.6.6.1). The matrix $\mathbf{p} \mathbf{p}^\top$ has rank one when $\mathbf{p} \neq 0$, so the protocol identifies only one linear combination of the two concentrations. \square

Remark 5.66 (Multiple dilutions under one protocol). Multiple dilutions and replicate wells improve precision for the scalar Λ_{PFU} , but they do not by themselves separate C_C from C_I if all wells share the same probability vector

$$\mathbf{p} = (p_C, p_I)^\top.$$

Dilution changes the scale of the Poisson mean; it does not rotate the sensitivity direction in subpopulation space.

Remark 5.67 (Fisher form of plaque-assay blindness). The rank-one Fisher matrix is the local information-theoretic version of plaque-assay protocol blindness. A single plaque protocol is sensitive to the direction (p_C, p_I) in subpopulation space and blind to directions orthogonal to it. Multi-protocol

variation can increase the Fisher rank only when different protocols have non-collinear probability vectors

$$(p_C^{(m)}, p_I^{(m)}).$$

Proposition 5.68 (Fisher information under protocol variation). *For independent plaque-count data from protocols E_1, \dots, E_M , with Poisson means*

$$\mu_m = V_m f_m (p_C^{(m)} C_C + p_I^{(m)} C_I),$$

the Fisher information for

$$\theta = (C_C, C_I)^\top$$

is

$$\mathcal{I}_{\text{multi}}(\theta) = \sum_{m=1}^M \frac{(V_m f_m)^2}{\mu_m} \mathbf{p}_m \mathbf{p}_m^\top, \quad \mathbf{p}_m = \begin{pmatrix} p_C^{(m)} \\ p_I^{(m)} \end{pmatrix}. \quad (5.6.6.2)$$

The Fisher rank can be two only if at least two protocol probability vectors are not collinear.

Proof. Each independent Poisson count contributes Fisher information

$$\frac{1}{\mu_m} \nabla_{\theta} \mu_m \nabla_{\theta} \mu_m^\top.$$

Since

$$\nabla_{\theta} \mu_m = V_m f_m \mathbf{p}_m,$$

summing independent protocol contributions gives Eq. (5.6.6.2). The resulting Fisher matrix can span the two-dimensional parameter space only if the vectors \mathbf{p}_m span that space. \square

Remark 5.69 (Design interpretation of the Fisher sum). Equation (5.6.6.2) gives the local design principle for plaque-assay variation. Additional wells, replicates, and dilutions increase information along the sensitivity directions already present. Additional protocol conditions can add new sensitivity directions. Thus a second protocol is most useful when its probability vector \mathbf{p}_m is not merely a rescaled version of the first.

Remark 5.70 (Uncertainty in protocol probabilities). In real applications, the protocol probabilities $p_C^{(m)}$ and $p_I^{(m)}$ may themselves be estimated or uncertain. This adds nuisance parameters to the inverse problem and can reduce the effective information about (C_C, C_I) . A full analysis may therefore require profiling, marginalizing, or experimentally calibrating the probability vectors \mathbf{p}_m . This is the plaque-assay version of the general nuisance-parameter problem described earlier.

Table 21. Protocol variations in the two-subpopulation plaque model. A useful variation changes the probability vector $\mathbf{p}_m = (p_C^{(m)}, p_I^{(m)})^\top$ in a direction that helps separate latent sectors.

Protocol variation	Likely effect on probability vector	Interpretive use
Cell line or receptor condition	Changes entry, intracellular permissiveness, or local spread	Helps distinguish physically present particles from cell-line-compatible plaque-forming units.
Adsorption time	Changes delivery, attachment, and early cell-contact probability	Tests whether low PFU reflects poor adsorption rather than absence of competent particles.
Overlay composition or viscosity	Changes local spread, lesion expansion, and plaque countability	Separates entry/replication competence from spread-limited visibility.
Incubation time	Changes whether slow or weak events become visible	Tests delayed amplification, slow replication, or threshold-limited plaque detection.
Neutralization or receptor-blocking condition	Changes attachment, entry, aggregation, or null-channel probability	Identifies sectors sensitive to antibody, inhibitor, or receptor-mediated blocking.
Staining or reporter threshold	Changes final visibility and counting probability	Separates biological amplification from readout-threshold collapse.

5.6.7 Illustrative Worked Numerical Reading

The two-subpopulation model can be read numerically. The purpose of the example is not to assign universal values to plaque competence, but to show how the same equations distinguish physical particle abundance from protocol-conditioned plaque-forming concentration.

Suppose a plaque assay is described by the constant-probability approximation

$$\Lambda_{\text{PFU}} = C_{\text{part}} [p_I + (p_C - p_I)\varphi_C],$$

where C_{part} is the total physical particle concentration, φ_C is the plaque-competent fraction, p_C is the plaque-forming probability of the competent sector, and p_I is the plaque-forming probability of the weakly competent or assay-incompatible sector.

Remark 5.71 (Same particle concentration, different PFU projection). Let two samples have the same physical particle concentration

$$C_{\text{part}} = 10^8 \text{ particles per mL},$$

and suppose the plaque-assay protocol has

$$p_C = 0.80, \quad p_I = 10^{-3}.$$

If sample A has

$$\varphi_C = 0.10,$$

then

$$\Lambda_{\text{PFU}}^{(A)} = 10^8 \left[10^{-3} + (0.80 - 10^{-3})(0.10) \right] \approx 8.09 \times 10^6 \text{ PFU/mL}. \quad (5.6.7.1)$$

If sample B has

$$\varphi_C = 0.01,$$

then

$$\Lambda_{\text{PFU}}^{(B)} = 10^8 \left[10^{-3} + (0.80 - 10^{-3})(0.01) \right] \approx 8.99 \times 10^5 \text{ PFU/mL}. \quad (5.6.7.2)$$

The two samples have the same total physical particle concentration, but the PFU projections differ by almost an order of magnitude because the protocol-weighted plaque-competent fraction differs.

For a plated inoculum volume

$$V_{\text{inoc}} = 0.1 \text{ mL}$$

and dilution fraction

$$f_d = 10^{-4},$$

the expected plaque counts are

$$\mathbb{E}[N_d^{(A)}] = 0.1 \times 10^{-4} \times 8.09 \times 10^6 \approx 80.9, \quad (5.6.7.3)$$

and

$$\mathbb{E}[N_d^{(B)}] = 0.1 \times 10^{-4} \times 8.99 \times 10^5 \approx 9.0. \quad (5.6.7.4)$$

Thus, under the same plating and dilution conditions, two samples with identical particle concentration may yield very different count regimes.

Remark 5.72 (Particle-to-PFU compression in the numerical example). The particle-to-PFU ratios in the two samples are

$$\mathcal{R}_{\text{part/PFU}}^{(A)} = \frac{10^8}{8.09 \times 10^6} \approx 12.4, \quad \mathcal{R}_{\text{part/PFU}}^{(B)} = \frac{10^8}{8.99 \times 10^5} \approx 111.2. \quad (5.6.7.5)$$

The ratio is therefore not an intrinsic constant of the virus preparation alone. It reflects the latent composition of the sample and the plaque-forming probabilities imposed by the assay protocol.

Remark 5.73 (Same PFU projection, different latent composition). The inverse ambiguity can also be seen directly. Suppose one plaque protocol has

$$p_C = 0.80, \quad p_I = 0.05,$$

and suppose the observed effective plaque-forming concentration is

$$\Lambda_{\text{PFU}} = 8.0 \times 10^6 \text{ PFU/mL}.$$

Then all pairs (C_C, C_I) satisfying

$$0.80 C_C + 0.05 C_I = 8.0 \times 10^6 \quad (5.6.7.6)$$

have the same expected plaque count under this protocol. For example,

$$(C_C, C_I) = (1.0 \times 10^7, 0)$$

and

$$(C_C, C_I) = (5.0 \times 10^6, 8.0 \times 10^7)$$

both yield

$$\Lambda_{\text{PFU}} = 8.0 \times 10^6 \text{ PFU/mL.}$$

The first sample is dominated by plaque-competent units, while the second has a much larger weakly competent or assay-incompatible sector. A single plaque protocol cannot distinguish these latent compositions if they lie on the same PFU-equivalence line.

Remark 5.74 (Numerical protocol variation). Now suppose two plaque protocols produce different probability vectors:

$$\mathbf{p}_1 = \begin{pmatrix} 0.80 \\ 0.05 \end{pmatrix}, \quad \mathbf{p}_2 = \begin{pmatrix} 0.20 \\ 0.15 \end{pmatrix}.$$

These vectors are not collinear. If the true subpopulation concentrations are

$$\mathbf{C} = \begin{pmatrix} C_C \\ C_I \end{pmatrix} = \begin{pmatrix} 1.0 \times 10^7 \\ 8.0 \times 10^7 \end{pmatrix} \text{ mL}^{-1},$$

then the two effective plaque-forming concentrations are

$$\Lambda_1 = 0.80(1.0 \times 10^7) + 0.05(8.0 \times 10^7) = 1.2 \times 10^7 \text{ PFU/mL}, \quad (5.6.7.7)$$

and

$$\Lambda_2 = 0.20(1.0 \times 10^7) + 0.15(8.0 \times 10^7) = 1.4 \times 10^7 \text{ PFU/mL}. \quad (5.6.7.8)$$

The corresponding design matrix is

$$\mathbf{P} = \begin{pmatrix} 0.80 & 0.05 \\ 0.20 & 0.15 \end{pmatrix},$$

with determinant

$$\det \mathbf{P} = 0.80(0.15) - 0.05(0.20) = 0.11 \neq 0. \quad (5.6.7.9)$$

In the ideal noiseless and calibrated setting, the two protocols therefore provide enough independent directions to resolve the two concentrations.

Table 22. Numerical illustration of particle-to-PFU compression and protocol variation in the two-subpopulation plaque model. The numbers are illustrative and are chosen only to show the structure of the inverse problem.

Scenario	Latent composition	Protocol weights	Observed implication
Same particle count, different competence	$C_{\text{part}} = 10^8$, with $\varphi_C = 0.10$ versus 0.01	$p_C = 0.80, p_I = 10^{-3}$	Same particle concentration gives $\Lambda_{\text{PFU}} \approx 8.09 \times 10^6$ versus 8.99×10^5 PFU/mL.
Same PFU, different composition	$(C_C, C_I) = (10^7, 0)$ or $(5 \times 10^6, 8 \times 10^7)$	$p_C = 0.80, p_I = 0.05$	Both lie on the same PFU-equivalence line and give $\Lambda_{\text{PFU}} = 8.0 \times 10^6$ PFU/mL.
Two non-collinear protocols	$(C_C, C_I) = (10^7, 8 \times 10^7)$	$\mathbf{p}_1 = (0.80, 0.05)^\top, \mathbf{p}_2 = (0.20, 0.15)^\top$	The design matrix has nonzero determinant, so the two protocols add independent sensitivity directions in the ideal calibrated case.

5.6.8 Closing Interpretation of the Plaque-Assay Worked Example

Remark 5.75 (Why the plaque assay closes the worked example). The plaque assay closes the worked example well because it makes the abstract framework immediately concrete. Experimental collapse is not an exotic phenomenon reserved for advanced imaging, electrorotation, or nanomechanical manipulation. It is already present in one of the most basic measurements in virology. A plaque count is powerful precisely because it compresses a complex biological process into a simple observable. The theory developed in this paper does not weaken that observable. It clarifies what the observable means, what it measures, and what latent sectors it necessarily leaves unresolved.

Remark 5.76 (Main lesson of the worked example). The plaque assay estimates a protocol-conditioned infectious concentration,

$$\Lambda_{\text{PFU}},$$

not the full physical virion population. In the dilute regime, this concentration enters the familiar Poisson counting model and gives the standard PFU titer formula. In the latent-state view, however,

$$\Lambda_{\text{PFU}} = \int_{\Psi} \pi_{\text{PFU}}(x; E_{\text{PFU}}) n_{\text{ref}}(x) dx,$$

so the titer is a weighted projection of particle abundance, plaque-forming competence, assay environment, and readout threshold. This is exactly what makes PFU biologically meaningful, but it is also what makes it protocol-conditioned.

Section Reference: Plaque Assay as Experimental Collapse

Table 23. Core objects, equations, and interpretations introduced in the plaque-assay worked example. The table summarizes how a plaque assay maps a latent virion or infectious-unit ensemble into a protocol-conditioned infectious readout.

Concept or object	Mathematical form	Interpretation
Plaque-assay collapse map	$\begin{array}{c} \text{latent virion or infectious-unit population} \\ \downarrow \\ \text{protocol-conditioned infectious events} \\ \downarrow \\ \text{visible plaque count} \end{array}$	Compact statement that a plaque assay reports a visible infectious-lesion count, not a direct census of total virions, genomes, antigens, or latent mechanical states.
Plaque-assay protocol	$E_{\text{PFU}} = \left(\begin{array}{l} \text{virus preparation, cell line, monolayer state} \\ \text{dilution series, } V_{\text{inoc}}, t_{\text{ads}} \\ \text{overlay, } t_{\text{inc}}, \text{ temperature} \\ \text{staining, threshold, counting rule} \end{array} \right)$	Specifies the biological and procedural conditions that define the plaque assay, beyond the final act of counting plaques.
Latent plaque-assay state	$X \in \Psi$	Latent virion, particle, aggregate, or infectious-unit state before the plaque protocol acts. It may include integrity, genome competence, receptor binding, aggregation, neutralization, orientation, charge, and handling history.
Plaque-forming probability	$\pi_{\text{PFU}}(x; E_{\text{PFU}}) = \Pr \left(\begin{array}{l} x \text{ generates a visible,} \\ \text{countable plaque under } E_{\text{PFU}} \end{array} \right)$	State- and protocol-dependent probability that a latent unit passes the plaque-assay pathway and produces a visible countable plaque.
Staged plaque-pathway factorization	$\begin{aligned} \pi_{\text{PFU}}(x; E_{\text{PFU}}) = & p_{\text{surv}} p_{\text{deliv}} p_{\text{ads}} p_{\text{entry}} \\ & \times p_{\text{rep}} p_{\text{spread}} p_{\text{vis}} \end{aligned}$	Reduced representation of plaque formation as a staged biological pathway: survival, delivery, adsorption, entry, replication, local spread, and visibility. The factors should be interpreted as conditional pathway probabilities.
Effective plaque-forming concentration	$\Lambda_{\text{PFU}}(E_{\text{PFU}}) = \int_{\Psi} \pi_{\text{PFU}}(x; E_{\text{PFU}}) n_{\text{ref}}(x) dx$	Central collapse equation for the plaque assay: the protocol-weighted concentration of latent units that generate visible plaque-forming events.
Physical particle concentration	$C_{\text{part}} = \int_{\Psi} n_{\text{ref}}(x) dx$	Total physical particle or assay-unit concentration before plaque-forming weighting. In general, this is not equal to Λ_{PFU} .
Particle-to-PFU ratio	$\mathcal{R}_{\text{part}/\text{PFU}} = \frac{C_{\text{part}}}{\Lambda_{\text{PFU}}}$	Summarizes how strongly the physical particle ensemble is compressed by the plaque-forming projection.
Dilute-regime expected count	$\mathbb{E}[N_d] = V_{\text{inoc}} f_d \Lambda_{\text{PFU}}$	Expected plaque count equals plated volume times dilution fraction times the effective plaque-forming concentration.

Continued on next page.

Table 23. Core objects, equations, and interpretations introduced in the plaque-assay worked example. *Continued from previous page.*

Concept or object	Mathematical form	Interpretation
Dilute Poisson plaque-count model	$N_d \sim \text{Poisson}(\mu_d),$ $\mu_d = V_{\text{inoc}} f_d \Lambda_{\text{PFU}}(E_{\text{PFU}})$	Baseline count model when plaque-forming events are dilute, independent, spatially separated, and countable.
Single-dilution PFU estimator	$\widehat{\Lambda}_{\text{PFU},d} = \frac{N_d}{V_{\text{inoc}} f_d}$	Basic estimator of the effective plaque-forming concentration from one countable dilution.
Usual PFU titer formula	$\widehat{\Lambda}_{\text{PFU},d} = \frac{N_d D_d}{V_{\text{inoc}}}, \quad D_d = \frac{1}{f_d}$	Standard titer formula expressed as an estimator of Λ_{PFU} , the protocol-conditioned infectious concentration.
Dilution-series likelihood	$\mathcal{L}_{\text{PFU}}(\Lambda_{\text{PFU}}) = \prod_{j=1}^J \prod_{r=1}^{R_j} \frac{\mu_{jr}^{N_{jr}} e^{-\mu_{jr}}}{N_{jr}!},$ $\mu_{jr} = V_{\text{inoc}} f_j \Lambda_{\text{PFU}}$	Likelihood for replicate plaque counts across dilution fractions under the dilute Poisson model.
Dilution-series MLE	$\widehat{\Lambda}_{\text{PFU}}^{\text{MLE}} = \frac{\sum_{j=1}^J \sum_{r=1}^{R_j} N_{jr}}{V_{\text{inoc}} \sum_{j=1}^J R_j f_j}$	Maximum-likelihood estimator for Λ_{PFU} using exact count observations in a dilution series.
Overdispersed plaque-count model	$N_{jr} \sim \text{NegBin}(\mu_{jr}, \kappa),$ $\mu_{jr} = V_{\text{inoc}} f_j \Lambda_{\text{PFU}},$ $\text{Var}(N_{jr}) = \mu_{jr} + \frac{\mu_{jr}^2}{\kappa}$	Optional extension when replicate counts vary more than expected under the Poisson model, due to aggregation, cell-layer heterogeneity, plating variation, or other nonidealities.
Single-unit plaque event	$B \in \{0, 1\},$ $\Pr(B = 1 \mid x, E_{\text{PFU}}) = \pi_{\text{PFU}}(x; E_{\text{PFU}})$	Binary event describing whether one latent assay unit produces a visible countable plaque.
Single-unit readout kernel	$K_{\text{PFU}}^{\mathcal{B}}(B \mid x) = [\pi_{\text{PFU}}(x; E_{\text{PFU}})]^B \times [1 - \pi_{\text{PFU}}(x; E_{\text{PFU}})]^{1-B}$	Bernoulli null-inclusive readout kernel for an individual latent plaque-forming opportunity.
Plaque-assay null channel	$B = 0$	Null outcome containing all latent states that fail to produce a visible counted plaque because of loss, failed adsorption, failed entry, failed replication, weak spread, merging, or subthreshold visibility.
PFU-equivalence of latent distributions	$n_1 \sim_{\text{PFU}} n_2 \iff \int_{\Psi} \pi_{\text{PFU}}(x; E_{\text{PFU}}) n_1(x) dx = \int_{\Psi} \pi_{\text{PFU}}(x; E_{\text{PFU}}) n_2(x) dx$	Two latent ensembles are indistinguishable by plaque counts under the same protocol when they have the same effective plaque-forming concentration.
Two-subpopulation decomposition	$n_{\text{ref}}(x) = n_{\text{C}}(x) + n_{\text{I}}(x)$	Reduces the latent ensemble into plaque-competent and plaque-incompetent, weakly competent, damaged, neutralized, or assay-incompatible sectors.

Continued on next page.

Table 23. Core objects, equations, and interpretations introduced in the plaque-assay worked example. *Continued from previous page.*

Concept or object	Mathematical form	Interpretation
Subpopulation concentrations	$C_C = \int_{\Psi} n_C(x) dx,$ $C_I = \int_{\Psi} n_I(x) dx,$ $C_{\text{part}} = C_C + C_I$	Physical concentrations of the two reduced latent sectors and their total.
Subpopulation-averaged plaque probabilities	$\bar{p}_C = \frac{\int_{\Psi} \pi_{\text{PFU}}(x; E_{\text{PFU}}) n_C(x) dx}{C_C},$ $\bar{p}_I = \frac{\int_{\Psi} \pi_{\text{PFU}}(x; E_{\text{PFU}}) n_I(x) dx}{C_I}$	Averaged plaque-forming probabilities that allow each sector to remain internally heterogeneous.
Exact two-subpopulation PFU projection	$\Lambda_{\text{PFU}} = \bar{p}_C C_C + \bar{p}_I C_I$	Exact weighted-sum representation after decomposing the latent ensemble into two sectors.
Constant-probability approximation	$\Lambda_{\text{PFU}} \approx p_C C_C + p_I C_I$	Simplified two-sector model when the plaque-forming probability is approximately constant within each sector.
Plaque-competent fraction	$\varphi_C = \frac{C_C}{C_{\text{part}}},$ $1 - \varphi_C = \frac{C_I}{C_{\text{part}}}$	Fraction of the physical particle or assay-unit population belonging to the plaque-competent sector.
Competent-fraction form	$\Lambda_{\text{PFU}} = C_{\text{part}} [p_I + (p_C - p_I)\varphi_C]$	Separates physical abundance, latent competent fraction, and protocol-dependent plaque-forming probabilities.
Two-subpopulation particle-to-PFU ratio	$\mathcal{R}_{\text{part}/\text{PFU}} = \frac{1}{p_I + (p_C - p_I)\varphi_C}$	Particle-to-PFU compression is the reciprocal of the average plaque-forming probability of a randomly selected physical particle or assay unit.
Nearly ideal competent-sector limit	$p_C \approx 1, \quad p_I \approx 0,$ $\Lambda_{\text{PFU}} \approx C_C, \quad \mathcal{R}_{\text{part}/\text{PFU}} \approx \frac{1}{\varphi_C}$	Idealized case in which PFU approximately reports the competent-sector concentration and the particle-to-PFU ratio approximates the inverse competent fraction.
Non-identifiability from PFU alone	$\Lambda_{\text{PFU}} = p_C C_C + p_I C_I$	A single PFU readout identifies only one weighted sum, not C_C , C_I , p_C , and p_I separately.
Competent fraction from auxiliary particle count	$\varphi_C = \frac{\Lambda_{\text{PFU}}/C_{\text{part}} - p_I}{p_C - p_I}$	If C_{part} , Λ_{PFU} , and the two protocol probabilities are known or calibrated, the competent fraction can be inferred.
Protocol-variation linear system	$\Lambda_m = p_C^{(m)} C_C + p_I^{(m)} C_I, \quad m = 1, \dots, M$	Multiple plaque protocols define multiple weighted projections of the same two-sector latent composition.

Continued on next page.

Table 23. Core objects, equations, and interpretations introduced in the plaque-assay worked example. *Continued from previous page.*

Concept or object	Mathematical form	Interpretation
Two-subpopulation design matrix	$\mathbf{A} = \mathbf{P}\mathbf{C},$ $\mathbf{P} = \begin{pmatrix} p_C^{(1)} & p_I^{(1)} \\ \vdots & \vdots \\ p_C^{(M)} & p_I^{(M)} \end{pmatrix}, \quad \mathbf{C} = \begin{pmatrix} C_C \\ C_I \end{pmatrix}$	Matrix form of protocol variation as a two-subpopulation inverse problem.
Rank condition for two-sector resolution	$\text{rank}(\mathbf{P}) = 2$	In the ideal noiseless and calibrated case, the two subpopulation concentrations are identifiable only if the protocol probability vectors are not collinear.
Single-protocol Fisher information	$\mathcal{I}_E(\theta) = \frac{(V_{\text{inoc}} f_d)^2}{\mu_d} \mathbf{p}\mathbf{p}^\top,$ $\theta = (C_C, C_I)^\top$	A single plaque protocol contributes rank-one information and identifies only one concentration combination.
Multi-protocol Fisher information	$\mathcal{I}_{\text{multi}}(\theta) = \sum_{m=1}^M \frac{(V_m f_m)^2}{\mu_m} \mathbf{p}_m \mathbf{p}_m^\top,$ $\mathbf{p}_m = \begin{pmatrix} p_C^{(m)} \\ p_I^{(m)} \end{pmatrix}$	Independent protocol contributions add. The Fisher rank can increase only when the protocol probability vectors span more than one direction.
Protocol-variation design principle	$\mathbf{p}_m \not\parallel \mathbf{p}_{m'}$	A useful plaque-assay variation changes the biological observation kernel in a direction that separates latent sectors rather than merely rescaling the same PFU projection.

6 Conclusion

This paper has developed a protocol-resolved formulation of experimental collapse in virophysics. The central claim is that a virological measurement does not, in general, report the full latent virion state or the full latent virion–environment ensemble. It reports a protocol-conditioned observed ensemble shaped by preparation, forcing, medium interaction, selection, survival, detection, amplification, and readout. The observed ensemble is therefore not always the same mathematical object as the reference latent ensemble. It is the ensemble produced by a specified experimental map.

The paper began by distinguishing reference latent ensembles, protocol-conditioned latent ensembles, and observed ensembles. This distinction was expressed through protocol kernels, survival or detection weights, readout kernels, and null observations. In this language, an experiment is not only a passive window onto a virion population. It is a map

$$P_{\text{ref},t} \longmapsto P_{\text{obs},t}^\mathcal{E}(\cdot | E),$$

whose structure determines which latent states are preserved, transformed, selected, discarded, amplified, or made visible. The concept of experimental collapse was then decomposed into concrete mechanisms. Preparation and interface effects can reshape the ensemble before measurement. Surfaces can immobilize

or deform particles. Fields can steer, polarize, trap, or rotate virions. Structured media such as mucus can filter transport by adhesion, confinement, and local rheology. Biological assays can amplify only those states that complete a required sequence of attachment, entry, replication, spread, and visibility. Detection thresholds and rejection criteria can assign large parts of the population to the null channel. These mechanisms do not make experiments invalid. They define what each experiment actually measures.

The framework also clarifies protocol blindness. A protocol may be insensitive to mechanically or biologically real latent sectors, either locally through a deterministic blind subspace, statistically through Fisher-blind directions, or globally through observational equivalence classes. The quotient-space viewpoint makes this especially clear: a protocol partitions latent state space into classes of states that are indistinguishable under that protocol. Multi-protocol experiments refine this partition. They can make previously collapsed distinctions visible by probing the latent ensemble through different kernels.

This perspective converts experimental collapse from a warning into an inference principle. If the protocol kernel is known, estimated, calibrated, or parametrized, then the observed data can be used to infer latent virion parameters, environmental parameters, and protocol-specific coupling parameters. A strongly conditioning protocol can be scientifically powerful precisely because it generates signal: AFM loading reveals mechanical response, dielectrophoresis and electrorotation reveal dielectric response, mucus tracking reveals medium-filtered transport, cryo-EM reveals preparation-conditioned structural ensembles, and plaque assays reveal assay-conditioned infectious activity.

The plaque-assay worked example illustrated the value of the framework in one of virology’s most familiar measurements. A plaque count is not a count of total physical virions, total genomes, total particles, or total mechanically admissible states. It is a count of visible infectious lesions under a specified cell-line, adsorption, overlay, incubation, staining, and counting protocol. In the notation of this paper, the assay estimates an effective plaque-forming concentration

$$\Lambda_{\text{PFU}} = \int_{\Psi} \pi_{\text{PFU}}(x; E_{\text{PFU}}) n_{\text{ref}}(x) dx,$$

a protocol-weighted projection of the latent ensemble. The two-subpopulation reduction showed that a single plaque protocol identifies only a weighted combination of plaque-competent and plaque-incompetent, weakly competent, or assay-incompatible sectors. Additional measurements or controlled protocol variation are required to resolve the underlying latent composition.

The broader conclusion is methodological. Virological observables are most powerful when interpreted together with the protocols that produce them. Particle counts, plaque counts, force curves, density maps, field-driven trajectories, and mucus-tracking statistics need not be treated as competing direct reports of the same object. They can instead be understood as different protocol-conditioned projections of a shared latent virion–environment system. Disagreement between protocols is therefore not automatically a problem. It may be evidence that the protocols are resolving different sectors of the same latent mechanics.

The final message of the paper is:

Latent virion–environment mechanics + Protocol mechanics = Experimentally visible virophysics.

(6.1)

A rigorous virophysical interpretation should specify both sides. It should describe the latent state being modeled, and it should state how the experimental protocol transforms that state into data. Experimental collapse is the formal bridge between these two levels.

References

- [1] Y. Cheng, “Single-particle cryo-EM at crystallographic resolution,” *Cell*, vol. 161, no. 3, pp. 450–457, 2015. doi: [10.1016/j.cell.2015.03.049](https://doi.org/10.1016/j.cell.2015.03.049).
- [2] R. F. Thompson, M. Walker, C. A. Siebert, S. P. Muench, and N. A. Ranson, “An introduction to sample preparation and imaging by cryo-electron microscopy for structural biology,” *Methods*, vol. 100, pp. 3–15, 2016. doi: [10.1016/j.ymeth.2016.02.017](https://doi.org/10.1016/j.ymeth.2016.02.017).
- [3] A. J. Noble, H. Wei, V. P. Dandey, Z. Zhang, Y. Z. Tan, C. S. Potter, and B. Carragher, “Reducing effects of particle adsorption to the air–water interface in cryo-EM,” *Nature Methods*, vol. 15, pp. 793–795, 2018. doi: [10.1038/s41592-018-0139-3](https://doi.org/10.1038/s41592-018-0139-3).
- [4] J. Chen, A. J. Noble, J. Y. Kang, and S. A. Darst, “Eliminating effects of particle adsorption to the air/water interface in single-particle cryo-electron microscopy: Bacterial RNA polymerase and CHAPSO,” *Journal of Structural Biology: X*, vol. 1, p. 100005, 2019. doi: [10.1016/j.yjsbx.2019.100005](https://doi.org/10.1016/j.yjsbx.2019.100005).
- [5] N. Liu and H.-W. Wang, “Better cryo-EM specimen preparation: How to deal with the air–water interface?” *Journal of Molecular Biology*, vol. 435, no. 9, p. 167926, 2023. doi: [10.1016/j.jmb.2022.167926](https://doi.org/10.1016/j.jmb.2022.167926).
- [6] M. G. Mateu, “Mechanical properties of viruses analyzed by atomic force microscopy: A virological perspective,” *Virus Research*, vol. 168, no. 1–2, pp. 1–22, 2012. doi: [10.1016/j.virusres.2012.06.008](https://doi.org/10.1016/j.virusres.2012.06.008).
- [7] M. Marchetti, G. J. L. Wuite, and W. H. Roos, “Atomic force microscopy observation and characterization of single virions and virus-like particles by nano-indentation,” *Current Opinion in Virology*, vol. 18, pp. 82–88, 2016. doi: [10.1016/j.coviro.2016.05.002](https://doi.org/10.1016/j.coviro.2016.05.002).
- [8] B. Kiss, Z. Kis, B. Pályi, and M. S. Z. Kellermayer, “Topography, spike dynamics, and nanomechanics of individual native SARS-CoV-2 virions,” *Nano Letters*, vol. 21, no. 6, pp. 2675–2680, 2021. doi: [10.1021/acs.nanolett.0c04465](https://doi.org/10.1021/acs.nanolett.0c04465).
- [9] S. Lyonais, M. Hénaut, A. Neyret, P. Merida, C. Cazevielle, N. Gros, C. Chable-Bessia, and D. Muriaux, “Atomic force microscopy analysis of native infectious and inactivated SARS-CoV-2 virions,” *Scientific Reports*, vol. 11, article 11885, 2021. doi: [10.1038/s41598-021-91371-4](https://doi.org/10.1038/s41598-021-91371-4).

- [10] M. P. Hughes, H. Morgan, F. J. Rixon, J. P. H. Burt, and R. Pethig, “Manipulation of herpes simplex virus type 1 by dielectrophoresis,” *Biochimica et Biophysica Acta: General Subjects*, vol. 1425, no. 1, pp. 119–126, 1998. doi: [10.1016/S0304-4165\(98\)00058-0](https://doi.org/10.1016/S0304-4165(98)00058-0).
- [11] M. P. Hughes, H. Morgan, and F. J. Rixon, “Measuring the dielectric properties of herpes simplex virus type 1 virions with dielectrophoresis,” *Biochimica et Biophysica Acta: General Subjects*, vol. 1571, no. 1, pp. 1–8, 2002. doi: [10.1016/S0304-4165\(02\)00161-7](https://doi.org/10.1016/S0304-4165(02)00161-7).
- [12] R. Pethig, “Review article—Dielectrophoresis: Status of the theory, technology, and applications,” *Biomeicrofluidics*, vol. 4, no. 2, p. 022811, 2010. doi: [10.1063/1.3456626](https://doi.org/10.1063/1.3456626).
- [13] D. Kim, M. Sonker, and A. Ros, “Dielectrophoresis: From molecular to micrometer-scale analytes,” *Analytical Chemistry*, vol. 91, no. 1, pp. 277–295, 2019. doi: [10.1021/acs.analchem.8b05454](https://doi.org/10.1021/acs.analchem.8b05454).
- [14] H. Boukari, B. Brichacek, P. Stratton, S. F. Mahoney, J. D. Lifson, L. Margolis, and R. Nossal, “Movements of HIV-virions in human cervical mucus,” *Biomacromolecules*, vol. 10, no. 9, pp. 2482–2488, 2009. doi: [10.1021/bm900344q](https://doi.org/10.1021/bm900344q).
- [15] L. Kaler, E. Iverson, S. Bader, D. Song, M. A. Scull, and G. A. Duncan, “Influenza A virus diffusion through mucus gel networks,” *Communications Biology*, vol. 5, article 249, 2022. doi: [10.1038/s42003-022-03204-3](https://doi.org/10.1038/s42003-022-03204-3).
- [16] R. Dulbecco, “Production of plaques in monolayer tissue cultures by single particles of an animal virus,” *Proceedings of the National Academy of Sciences of the United States of America*, vol. 38, no. 8, pp. 747–752, 1952. doi: [10.1073/pnas.38.8.747](https://doi.org/10.1073/pnas.38.8.747).
- [17] P. D. Cooper, “The plaque assay of animal viruses,” *Advances in Virus Research*, vol. 8, pp. 319–378, 1961. doi: [10.1016/S0065-3527\(08\)60689-2](https://doi.org/10.1016/S0065-3527(08)60689-2).
- [18] A. Baer and K. Kehn-Hall, “Viral concentration determination through plaque assays: Using traditional and novel overlay systems,” *Journal of Visualized Experiments*, no. 93, e52065, 2014. doi: [10.3791/52065](https://doi.org/10.3791/52065).
- [19] S. M. Kay, *Fundamentals of Statistical Signal Processing, Volume I: Estimation Theory*. Upper Saddle River, NJ: Prentice Hall PTR, 1993.
- [20] A. W. van der Vaart, *Asymptotic Statistics*. Cambridge: Cambridge University Press, 1998. doi: [10.1017/CBO9780511802256](https://doi.org/10.1017/CBO9780511802256).
- [21] T. M. Cover and J. A. Thomas, *Elements of Information Theory*, 2nd ed. Hoboken, NJ: Wiley-Interscience, 2006. doi: [10.1002/047174882X](https://doi.org/10.1002/047174882X).
- [22] C. Villani, *Optimal Transport: Old and New*. Berlin: Springer, 2009. doi: [10.1007/978-3-540-71050-9](https://doi.org/10.1007/978-3-540-71050-9).

- [23] M. Abrami, A. Biasin, F. Tescione, D. Tierno, B. Dapas, A. Carbone, G. Grassi, M. Conese, S. Di Gioia, D. Larobina, and M. Grassi, “Mucus structure, viscoelastic properties, and composition in chronic respiratory diseases,” *International Journal of Molecular Sciences*, vol. 25, no. 3, article 1933, 2024. doi: [10.3390/ijms25031933](https://doi.org/10.3390/ijms25031933).
- [24] M. D. Vahey and D. A. Fletcher, “Influenza A virus surface proteins are organized to help penetrate host mucus,” *eLife*, vol. 8, e43764, 2019. doi: [10.7554/eLife.43764](https://doi.org/10.7554/eLife.43764).
- [25] S. Kullback and R. A. Leibler, “On information and sufficiency,” *The Annals of Mathematical Statistics*, vol. 22, no. 1, pp. 79–86, 1951. doi: [10.1214/aoms/1177729694](https://doi.org/10.1214/aoms/1177729694).
- [26] J. Lin, “Divergence measures based on the Shannon entropy,” *IEEE Transactions on Information Theory*, vol. 37, no. 1, pp. 145–151, 1991. doi: [10.1109/18.61115](https://doi.org/10.1109/18.61115).
- [27] A. Gretton, K. M. Borgwardt, M. J. Rasch, B. Schölkopf, and A. Smola, “A kernel two-sample test,” *Journal of Machine Learning Research*, vol. 13, no. 25, pp. 723–773, 2012.
- [28] A. Tarantola, *Inverse Problem Theory and Methods for Model Parameter Estimation*. Philadelphia, PA: Society for Industrial and Applied Mathematics, 2005. doi: [10.1137/1.9780898717921](https://doi.org/10.1137/1.9780898717921).
- [29] J. Kaipio and E. Somersalo, *Statistical and Computational Inverse Problems*. New York: Springer, 2005. doi: [10.1007/b138659](https://doi.org/10.1007/b138659).
- [30] R. Bellman and K. J. Åström, “On structural identifiability,” *Mathematical Biosciences*, vol. 7, no. 3–4, pp. 329–339, 1970. doi: [10.1016/0025-5564\(70\)90132-X](https://doi.org/10.1016/0025-5564(70)90132-X).
- [31] E. Walter and L. Pronzato, *Identification of Parametric Models from Experimental Data*. London: Springer, 1997. doi: [10.1007/978-3-642-58923-3](https://doi.org/10.1007/978-3-642-58923-3).
- [32] A. Raue, C. Kreutz, T. Maiwald, J. Bachmann, M. Schilling, U. Klingmüller, and J. Timmer, “Structural and practical identifiability analysis of partially observed dynamical models by exploiting the profile likelihood,” *Bioinformatics*, vol. 25, no. 15, pp. 1923–1929, 2009. doi: [10.1093/bioinformatics/btp358](https://doi.org/10.1093/bioinformatics/btp358).
- [33] E. D’Imprima, D. Floris, M. Joppe, R. Sánchez, M. Grininger, and W. Kühlbrandt, “Protein denaturation at the air–water interface and how to prevent it,” *eLife*, vol. 8, e42747, 2019. doi: [10.7554/eLife.42747](https://doi.org/10.7554/eLife.42747).
- [34] T. S. Levitz, E. J. Brignole, I. Fong, M. C. Darrow, and C. L. Drennan, “Effects of chameleon dispense-to-plunge speed on particle concentration, complex formation, and final resolution: A case study using the *Neisseria gonorrhoeae* ribonucleotide reductase inactive complex,” *Journal of Structural Biology*, vol. 214, no. 1, p. 107825, 2022. doi: [10.1016/j.jsb.2021.107825](https://doi.org/10.1016/j.jsb.2021.107825).
- [35] Y.-Y. Wang, D. Harit, D. B. Subramani, H. Arora, P. A. Kumar, and S. K. Lai, “Influenza-binding antibodies immobilise influenza viruses in fresh human airway mucus,” *European Respiratory Journal*, vol. 49, no. 1, p. 1601709, 2017. doi: [10.1183/13993003.01709-2016](https://doi.org/10.1183/13993003.01709-2016).

- [36] R. Dulbecco and M. Vogt, “Plaque formation and isolation of pure lines with poliomyelitis viruses,” *Journal of Experimental Medicine*, vol. 99, no. 2, pp. 167–182, 1954. doi: [10.1084/jem.99.2.167](https://doi.org/10.1084/jem.99.2.167).
- [37] P. J. Klasse, “Molecular determinants of the ratio of inert to infectious virus particles,” *Progress in Molecular Biology and Translational Science*, vol. 129, pp. 285–326, 2015. doi: [10.1016/bs.pmbts.2014.10.012](https://doi.org/10.1016/bs.pmbts.2014.10.012).
- [38] C. B. Brooke, “Biological activities of ‘noninfectious’ influenza A virus particles,” *Future Virology*, vol. 9, no. 1, pp. 41–51, 2014. doi: [10.2217/fvl.13.118](https://doi.org/10.2217/fvl.13.118).
- [39] R. Sanjuán, “Collective properties of viral infectivity,” *Current Opinion in Virology*, vol. 33, pp. 1–6, 2018. doi: [10.1016/j.coviro.2018.06.001](https://doi.org/10.1016/j.coviro.2018.06.001).
- [40] W. McCormick and L. A. Mermel, “The basic reproductive number and particle-to-plaque ratio: Comparison of these two parameters of viral infectivity,” *Virology Journal*, vol. 18, article 92, 2021. doi: [10.1186/s12985-021-01566-4](https://doi.org/10.1186/s12985-021-01566-4).
- [41] S.-L. Liu, Z.-G. Wang, H.-Y. Xie, A. A. Liu, D. C. Lamb, and D.-W. Pang, “Single-virus tracking: From imaging methodologies to virological applications,” *Chemical Reviews*, vol. 120, no. 3, pp. 1936–1979, 2020. doi: [10.1021/acs.chemrev.9b00692](https://doi.org/10.1021/acs.chemrev.9b00692).
- [42] I.-H. Wang, C. J. Burckhardt, A. Yakimovich, and U. F. Greber, “Imaging, tracking and computational analyses of virus entry and egress with the cytoskeleton,” *Viruses*, vol. 10, no. 4, article 166, 2018. doi: [10.3390/v10040166](https://doi.org/10.3390/v10040166).
- [43] L. Nathan and S. Daniel, “Single virion tracking microscopy for the study of virus entry processes in live cells and biomimetic platforms,” in *Physical Virology: Virus Structure and Mechanics*, U. F. Greber, ed., *Advances in Experimental Medicine and Biology*, vol. 1215, pp. 13–43, Cham: Springer, 2019. doi: [10.1007/978-3-030-14741-9_2](https://doi.org/10.1007/978-3-030-14741-9_2).
- [44] R. A. Fisher, “On the mathematical foundations of theoretical statistics,” *Philosophical Transactions of the Royal Society of London. Series A*, vol. 222, pp. 309–368, 1922. doi: [10.1098/rsta.1922.0009](https://doi.org/10.1098/rsta.1922.0009).
- [45] C. R. Rao, “Information and the accuracy attainable in the estimation of statistical parameters,” *Bulletin of the Calcutta Mathematical Society*, vol. 37, no. 3, pp. 81–91, 1945.
- [46] H. Cramér, *Mathematical Methods of Statistics*. Princeton, NJ: Princeton University Press, 1946.
- [47] I. J. Hirst, W. J. R. Thomas, R. A. Davies, and S. P. Muench, “CryoEM grid preparation: A closer look at advancements and impact of preparation mode and new approaches,” *Biochemical Society Transactions*, vol. 52, no. 3, pp. 1529–1537, 2024. doi: [10.1042/BST20231553](https://doi.org/10.1042/BST20231553).
- [48] Y. Z. Tan, P. R. Baldwin, J. H. Davis, J. R. Williamson, C. S. Potter, B. Carragher, and D. Lyumkis, “Addressing preferred specimen orientation in single-particle cryo-EM through tilting,” *Nature Methods*, vol. 14, pp. 793–796, 2017. doi: [10.1038/nmeth.4347](https://doi.org/10.1038/nmeth.4347).

- [49] S. Wiedemann and R. Heckel, “A deep learning method for simultaneous denoising and missing wedge reconstruction in cryogenic electron tomography,” *Nature Communications*, vol. 15, article 8255, 2024. doi: [10.1038/s41467-024-51438-y](https://doi.org/10.1038/s41467-024-51438-y).
- [50] M. Baclayon, G. J. L. Wuite, and W. H. Roos, “Imaging and manipulation of single viruses by atomic force microscopy,” *Soft Matter*, vol. 6, no. 21, pp. 5273–5285, 2010. doi: [10.1039/B923992H](https://doi.org/10.1039/B923992H).
- [51] H. A. Pohl, “The motion and precipitation of suspensoids in divergent electric fields,” *Journal of Applied Physics*, vol. 22, no. 7, pp. 869–871, 1951. doi: [10.1063/1.1700065](https://doi.org/10.1063/1.1700065).
- [52] D. P. Klebl, M. S. C. Gravett, D. Kontziampasis, D. J. Wright, R. S. Bon, D. C. F. Monteiro, M. Trebbin, F. Sobott, H. D. White, M. C. Darrow, R. F. Thompson, and S. P. Muench, “Need for speed: Examining protein behavior during cryoEM grid preparation at different timescales,” *Structure*, vol. 28, no. 11, pp. 1238–1248.e4, 2020. doi: [10.1016/j.str.2020.07.018](https://doi.org/10.1016/j.str.2020.07.018).
- [53] D. Cresta, D. C. Warren, C. Quirouette, A. P. Smith, L. C. Lane, A. M. Smith, and C. A. A. Beauchemin, “Time to revisit the endpoint dilution assay and to replace the TCID₅₀ as a measure of a virus sample’s infection concentration,” *PLOS Computational Biology*, vol. 17, no. 10, e1009480, 2021. doi: [10.1371/journal.pcbi.1009480](https://doi.org/10.1371/journal.pcbi.1009480).
- [54] D. Cresta, D. C. Warren, C. Quirouette, A. P. Smith, L. C. Lane, A. M. Smith, and C. A. A. Beauchemin, “Correction: Time to revisit the endpoint dilution assay and to replace the TCID₅₀ as a measure of a virus sample’s infection concentration,” *PLOS Computational Biology*, vol. 19, no. 1, e1010877, 2023. doi: [10.1371/journal.pcbi.1010877](https://doi.org/10.1371/journal.pcbi.1010877).
- [55] C. Lei, J. Yang, J. Hu, and X. Sun, “On the calculation of TCID₅₀ for quantitation of virus infectivity,” *Virologica Sinica*, vol. 36, no. 1, pp. 141–144, 2021. doi: [10.1007/s12250-020-00230-5](https://doi.org/10.1007/s12250-020-00230-5).
- [56] A. M. Stuart, “Inverse problems: A Bayesian perspective,” *Acta Numerica*, vol. 19, pp. 451–559, 2010. doi: [10.1017/S0962492910000061](https://doi.org/10.1017/S0962492910000061).
- [57] Y.-C. Hsieh, M. Delarue, H. Orland, and P. Koehl, “Analyzing the geometry and dynamics of viral structures: A review of computational approaches based on alpha shape theory, normal mode analysis, and Poisson–Boltzmann theories,” *Viruses*, vol. 15, no. 6, article 1366, 2023. doi: [10.3390/v15061366](https://doi.org/10.3390/v15061366).
- [58] J. R. Perilla and K. Schulten, “Physical properties of the HIV-1 capsid from all-atom molecular dynamics simulations,” *Nature Communications*, vol. 8, article 15959, 2017. doi: [10.1038/ncomms15959](https://doi.org/10.1038/ncomms15959).
- [59] R. F. Bruinsma, G. J. L. Wuite, and W. H. Roos, “Physics of viral dynamics,” *Nature Reviews Physics*, vol. 3, no. 2, pp. 76–91, 2021. doi: [10.1038/s42254-020-00267-1](https://doi.org/10.1038/s42254-020-00267-1).
- [60] E. J. Mendoza, K. Manguiat, H. Wood, and M. Drebot, “Two detailed plaque assay protocols for the quantification of infectious SARS-CoV-2,” *Current Protocols in Microbiology*, vol. 57, no. 1, e105, 2020. doi: [10.1002/cpmc.105](https://doi.org/10.1002/cpmc.105).